

**WA School of Mines: Minerals, Energy and Chemical
Engineering**

**Formation of Sugars and Organic Acids
from Hydrothermal Conversion
of Biomass and Biomass-Derived Sugars**

Gelareh Nazeri

0000-0001-6477-1152

This thesis is presented for the degree of

Doctor of Philosophy

Of

Curtin University

October 2022

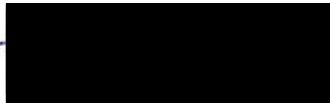
Declaration

To the best of my knowledge and belief this thesis contains no material previously published by any other person except where due acknowledgment has been made. This thesis contains no material which has been accepted for the award of any other degree or diploma in any university.

Name:



Signature:



Date: 12/10/2022

To my beloved family

Abstract

Mallee biomass is considered as an important feedstock for renewable biofuels and biochemicals production. Therefore, a study is required to understand the mechanism of hydrothermal conversion of mallee biomass for sustainable production of biofuels and value-added biochemicals (i.e., sugars and organic acids), and also potential applications for the production of renewable biofuels. Among the available technologies for biomass utilization, hydrothermal processing in hot-compressed water (HCW) has received increasing interest for sustainable production of biofuels and value-added biochemicals (i.e., sugars and organic acids) from biomass, due to the unique properties of HCW. However, the mechanism of biomass hydrothermal decomposition in HCW has not been clearly understood, due to complex components of biomass and complicated reaction pathways of biomass decomposition.

Therefore, this thesis aims to understand the hydrothermal decomposition behaviour of mallee biomass and its main components in HCW, and the subsequent conversion of various sugar products into organic acids as value-added biochemicals. The main objectives are to (1) investigate the liquid products from hydrothermal decomposition of mallee biomass and its main components (i.e., wood, leaf and bark) using a semi-continuous reactor, focusing on the sugar recovery and the release of inorganic species; (2) understand the formation mechanism of organic acids from hydrothermal decomposition of cellobiose (as a model compound of glucose oligomers); (3) elucidate the formation pathways of various organic acids from hydrothermal decomposition of glucose and fructose (as key sugar monomers from cellulose decomposition); (4) reveal the decomposition mechanism and formation pathways of various organic acids from hydrothermal decomposition of mannose (as a model compound of hemicellulose-derived sugars).

The main experiments conducted in this work included hydrothermal conversion of mallee biomass and the main components of mallee biomass in HCW. The total organic carbon, pH value, sugar and organic acids content of the liquid products were analysed after each experiment. The concentrations of sugars were analysed by higher performance anion exchange chromatography with pulsed amperometric detection (HPAEC-PAD, model: Dionex ICS-3000, and CarboPac PA20 analytical

column), and the concentrations of organic acids in the liquid were analysed by high performance anion exchange chromatography with conductivity detection and mass spectrometry (HPAEC-CD-MS, model: Dionex ICS-5000) equipped with a Dionex IonPac AS11-HC analytical column and a Dionex AERS 500 suppressor.

The following work has been conducted to achieve mentioned goals.

Firstly, systematic experiments have been conducted to understand the compositions of liquid products from hydrothermal decomposition of mallee biomass and its main components (wood, leaf and bark), as well as the leaching characteristics of Ca and Mg species for each mallee component. The results suggest that the recovery of arabinose, galactose, glucose, and xylose are different for wood, leaf and bark, due to different sugar compositions of mallee components. The recovery of arabinose, galactose and xylose achieves >80% for all components at 270 °C, much higher than the glucose recovery. For example, the maximum glucose recovery is 62% for wood, compared to 30% and 40% for leaf and bark, respectively. The low glucose recovery for all components is more likely due to the in situ structural changes of cellulose in biomass during hydrothermal processing. The liquid products from wood samples at different temperatures are analysed, and the results show that the formation of oligosaccharides is more favoured compared to monosaccharides. Further results suggest that the recovery of oligosaccharides is almost complete at high temperatures, which confirms that the solubility of large oligomers increase with temperature. Moreover, the contribution of saccharides to the total converted carbon in wood sample decreases by increasing temperature, as more lignin participates in hydrothermal conversion at higher temperatures. Also, the leaching of the water-insoluble Ca from leaf and bark is slow as the majority of these water-insoluble Ca is only soluble in acid.

Secondly, this thesis further reports the formation mechanism of organic acids as important value-added chemicals from hydrothermal conversion of biomass under non-catalytic condition. Since oligosaccharides are major sugar products from biomass processing in HCW, cellobiose as the simplest glucose oligomer has been used to understand the formation mechanism of organic acids using a continuous reactor system. The liquid products produced during cellobiose decomposition in HCW at 200–275 °C and a residence time of 8–66 s were collected and characterised by high-performance anion exchange chromatography with conductivity detection

and mass spectrometry (HPAEC-CD-MS). Various organic acids including saccharinic, formic, lactic and glycolic acids were identified and quantified. The yields of all organic acids increase with temperature. The selectivities of organic acids are almost zero at early conversion, suggesting that these organic acids are not primary products from cellobiose decomposition in HCW. Among the identified organic acids, saccharinic acid, which is reported for the first time in the field under non-catalytic conditions, has the highest yield (i.e., ~5.8% at 275 °C and ~66 s) on a carbon basis, but formic acid has the highest contribution to total hydrogen ion in the liquid product due to its high molar concentration and high dissociation constant. The results also show that the hydrogen ion concentrations contributed by the identified organic acids agree well with those calculated from the measured pH of the solutions after the reaction, especially at cellobiose conversions <80%. The reaction pathways for the production of these organic acids during cellobiose decomposition in HCW are also summarised and discussed.

Thirdly, since organic acids are not primary products from cellobiose decomposition, hydrothermal decomposition experiments of glucose and fructose have been conducted to better understand the formation mechanism of organic acids during biomass hydrothermal processing. Five organic acids including metasaccharinic, formic, lactic, glycolic and 2,4-dihydroxybutyric acids were identified and quantified via HPAEC-CD-MS. The yield and selectivities of all quantified organic acids from fructose decomposition are higher than that of glucose decomposition. Metasaccharinic acid (MSA) is the major organic acid in the liquid products with maximal selectivities of ~12% and ~9.5% from fructose and glucose decomposition in HCW, respectively. For the first time in the field, MSA is confirmed as a minor primary product from fructose decomposition under non-catalytic conditions, but only a secondary product from glucose decomposition. Lactic acid can be produced from glyceraldehyde, a primary product of fructose decomposition, which explains the higher selectivity of lactic acid from fructose decomposition compared to that from glucose decomposition. Further analysis demonstrate that formic acid contributes the highest to the total hydrogen ion dissociated during fructose and glucose decomposition under all conditions, followed by MSA as the second contributor. Since MSA can be directly produced from fructose decomposition, it is suggested that the formation mechanism of MSA may be different from that proposed under alkaline conditions (i.e., via diketo intermediates).

Fourthly, hydrothermal decomposition of mannose has also been investigated to understand the formation of major products under non-catalytic conditions. Mannose is an important monosaccharide due to two reasons. First, mannose can be produced as a primary product from hydrothermal decomposition of glucose and fructose. Second, mannose can be derived from hemicellulose, which is the second most abundant component in biomass. The data clearly show that isomerisation reactions to produce fructose and glucose are two primary reactions identified during mannose hydrothermal decomposition, which contribute to ~82% and ~18% of mannose primary decomposition reactions. Other products such as 5-HMF, glycolaldehyde, glyceraldehyde and organic acids are also detected, but those products are all secondary products during mannose decomposition in HCW. It can be clearly seen that the pH value decreases substantially as mannose conversion increases under current experimental conditions. Similar to glucose and fructose, formic acid has the highest contribution to the hydrogen ion in the liquid product from mannose decomposition, while MSA has the highest yield and selectivity on a carbon basis. A close match between $[H^+]$ from quantified organic acid and pH measurement directly after each experiment suggests that majority of organic acids produced during mannose decomposition in HCW are identified. Reaction pathways for the production of key compounds during mannose decomposition in HCW are also summarised.

Overall, this study provides new understandings on the hydrothermal decomposition behaviour of biomass and the main components under non-catalytic conditions. More importantly, systematic research has been undertaken to understand the formation mechanisms of various organic acids from key intermediates including cellobiose, glucose, fructose and mannose. As the first time in this field, metasaccharinic acid is identified as a minor primary product from fructose decomposition in HCW. The reaction pathways for other key organic acids from various sugar model compounds are revealed.

Based on the findings in this study, further research is required to understand the mechanism of mallee biomass and its components during hydrothermal conversion in HCW:

- Further development of kinetic model from biomass decomposition in HCW, which can be used for proper reactor design,

- The decomposition behaviour from other key components of mallee biomass such as lignin and hemicellulose in HCW,
- Since glucosyl-fructose (GF) and glucosyl-mannose (GM) are important isomers of cellobiose decomposition in HCW, further studies are required to understand the mechanism and primary products of those isomers during hydrothermal conversion in HCW.

Acknowledgements

I am very grateful for Australian Postgraduate Awards (APA) from Curtin University to support my PhD stud and partial support from Australian Research Council through its Discovery Projects Program.

I would like to express my deep gratitude to my supervisors, Professor Hongwei Wu and Dr. Yun Yu for giving me this opportunity to join their research group. I also greatly appreciate for their continued guidance, training, inspiration and invaluable support during my PhD study. It would be impossible for me to complete my PhD without their supervision and advice.

I am particularly grateful to Ms. Karen Haynes, Mr. Jason Wright, Ms. Roshanak Doroushi, Mr. Andrew Chan, Ms. Melina Miralles, Ms. Ann Carroll and Mr. Araya Abera for their help and technical support in the lab. I would also like to offer my special thanks to Dr. Sui Boon Liaw for his continued advice and help, and also other members of our research group, Mr. Rashedul Khondakar, Dr. Bing Song, Mr. Zhiliang Wu, Dr. Wenran Gao, Mr. Yu Long, Ms. Jinxiu Cao for all their help in various ways.

Most importantly, I would like to thank my family and friends for their moral support, encouragement and understanding during my PhD study. Special thanks to my husband, Amir, and my daughter, Delsa, for their constant support and understanding during my study.

List of Publication

Journal Papers

- **Gelareh Nazeri**, Yun Yu, Hongwei Wu. Formation of Organic acids during glucose and fructose decomposition in hot-compressed water, to be submitted to *Industrial & Engineering Chemistry Research*.
- **Gelareh Nazeri**, Yun Yu, Hongwei Wu. Formation of Sugar Products and Organic acids during mannose decomposition in hot-compressed water, to be submitted to *Fuel*.
- **Gelareh Nazeri**, Sui Boon L, Yun Yu, Hongwei Wu. Formation of Organic acids during cellobiose decomposition in hot-compressed water. *Fuel*, **2018**, 218, 174-178.
- Sui Boon Liaw, **Gelareh Nazeri**, Yun Yu, Hongwei Wu. Differences in Leaching Characteristics of Mg and Ca from Various Biomass Components of Mallee Tree in Hot-Compressed Water. *Energy & Fuels*, **2016**, 30 (10), 7851-7857.

Peer-Reviewed Conference Papers

- **Gelareh Nazeri** Sui Boon Liaw, Yun Yu, Hongwei Wu. Hydrothermal Processing of Different Biomass Components of Mallee Tree in Hot-Compressed Water. Bioenergy Australia 2016 Conference, 14-16 November 2016.
- Sui Boon Liaw, **Gelareh Nazeri**, Yun Yu, Hongwei Wu. Recovery of Sugar Products from Hydrothermal Decomposition of Mallee Biomass. Bioenergy Australia 2015 Conference, 30 November-2 October 2015.

Table of Contents

Declaration.....	i
Abstract.....	iii
Acknowledgements.....	viii
List of Publication.....	ix
Table of Contents.....	x
List of Figures.....	xv
List of Tables.....	xxi
Chapter 1 : Introduction	1
1.1 Background and Motives.....	1
1.2 Scope and Objectives.....	4
1.3 Thesis Outline.....	5
Chapter 2 : Background and Literature Review	7
2.1 Introduction	7
2.2 Common Biomass Components	8
2.2.1 Cellulose.....	9
2.2.2 Hemicellulose.....	11
2.2.3 Lignin.....	12
2.2.4 Other Components	14
2.3 Biomass Conversion.....	16
2.3.1 Pyrolysis of Biomass.....	17
2.3.2 Gasification of Biomass	18
2.3.3 Biological Pre-Treatment of Biomass.....	19
2.3.4 Hydrothermal Conversion of Biomass.....	19
2.3.4.1 Properties of Hot Compressed Water (HCW)	21

2.4	Lignocellulosic Biomass Hydrolysis in HCW	23
2.5	Cellulose Hydrolysis in HCW	26
2.5.1	Factors Influencing the Reaction Pathway of Cellulose Hydrolysis in HCW.....	29
2.5.1.1	Type of Feedstock	30
2.5.1.2	Reactor Configuration.....	30
2.5.1.3	Temperature	31
2.5.1.4	Catalysts.....	31
2.6	Hemicellulose Hydrolysis in HCW	32
2.7	Lignin Hydrolysis in HCW.....	33
2.8	Hydrothermal Decomposition of Dimers in HCW.....	35
2.8.1	Hydrothermal Decomposition of Cellobiose in HCW.....	35
2.8.2	Hydrothermal Decomposition of Cellobiulose in HCW	38
2.9	Hydrothermal Decomposition of Mono-Compounds in HCW	38
2.9.1	Hydrothermal Decomposition of Glucose and Fructose in HCW ...	40
2.9.2	Hydrothermal Decomposition of Xylose in HCW.....	51
2.10	Hydrothermal Decomposition of Other Compounds in HCW	52
2.10.1	Hydrothermal Decomposition of Glyceraldehyde and Dihydroxyacetone	52
2.10.2	Hydrothermal Decomposition of 5-Hydroxymethylfurfural (5-HMF)	54
2.11	Reaction Kinetics of Biomass Decomposition in HCW.....	55
2.11.1	Global Reaction Kinetics of Biomass and Model Compounds Decomposition in HCW.....	55
2.11.2	Kinetic Modelling of Monocompounds Decomposition in Hot Compressed Water	60
2.12	Conclusion and Research Gap.....	62
2.13	Research Objectives of Present Study	63
	Chapter 3 : Experimental Set-up and Methods	64

3.1	Introduction	64
3.2	Methodology.....	64
3.2.1	Hydrothermal Processing of Mallee Biomass and the Main Components in HCW	66
3.2.2	Cellobiose, Glucose, Fructose and Mannose Decomposition in HCW	66
3.3	Experimental.....	67
3.3.1	Raw Material and Chemicals	67
3.3.2	Reactor System.....	67
3.4	Sample Analysis	69
3.4.1	Total Organic Carbon Analysis.....	69
3.4.2	Quantification of Biomass Structural Carbohydrate, Sugar Content and Monosaccharides in Liquid Products	70
3.4.3	Quantification of Inorganic Species in Liquid Products	71
3.4.4	Quantification of Organic Acids in Liquid Products	71
3.5	Data Acquisition and Processing.....	73
3.5.1	Conversion, Yield and Selectivity.....	73
3.5.2	Kinetics	74
3.5.3	Calculation of Total Hydrogen Ion Concentration [H ⁺] from the Quantified Organic Acids Concentration.....	75
3.6	Summary.....	76
Chapter 4 : Hydrothermal Processing of Different Biomass Components of Mallee Tree in Hot-Compressed Water		77
4.1	Introduction	77
4.2	Sugar Recovery in Various Mallee Biomass Components.....	78
4.3	Leaching of Mg and Ca in Various Mallee Biomass Components	84
4.4	Further Discussion.....	86
4.5	Conclusions	89

Chapter 5 : Formation of Organic Acids During Cellobiose Decomposition in HCW.....	91
5.1 Introduction	91
5.2 Typical HPAEC-CD-MS Chromatogram of the Liquid Sample.....	92
5.3 Yields and Selectivities of Organic Acids from Cellobiose Decomposition	94
5.4 Comparisons Between $[H^+]$ Calculated from Quantified Organic Acids and Measured pH.....	97
5.5 Reaction Pathways of Organic Acids During Cellobiose Decomposition	98
5.6 Conclusions	100
Chapter 6 : Formation of Organic Acids During Glucose and Fructose Decomposition in HCW	101
6.1 Introduction	101
6.2 Yields and Selectivities of Organic Acids from Glucose and Fructose Decomposition in HCW.....	102
6.3 Comparisons Between $[H^+]$ Calculated from Quantified Organic Acids and Measured pH.....	105
6.4 Reaction Pathways of Organic Acids During Glucose and Fructose Decomposition	108
6.5 Conclusions	110
Chapter 7 : Reaction Mechanism and Pathways of Mannose Decomposition in HCW.....	112
7.1 Introduction	112
7.2 Mannose Conversion and Yields of Major Products During Mannose Decomposition in HCW.....	113
7.3 Selectivities of Major Products During Mannose Decomposition in HCW	116
7.4 Kinetics of Mannose Decomposition in HCW.....	118
7.5 Formation of Organic Acids During Mannose Decomposition in HCW.	120

7.6	Mechanism and Reaction Pathways of Mannose Decomposition in HCW.	123
7.7	Conclusions	125
Chapter 8 : Conclusions and Recommendations		126
8.1	Introduction	126
8.2	Conclusions	126
8.2.1	Hydrothermal Processing of Different Biomass Components of Mallee Tree in Hot-Compressed Water	126
8.2.2	Formation of Organic Acids During Cellobiose Decomposition in HCW	127
8.2.3	Formation of Organic Acids During Glucose and Fructose Decomposition in HCW	128
8.2.4	Mechanism and Reaction Pathways of Mannose Decomposition in HCW	128
8.3	Recommendations	129
References		130
Appendix 1: Copyright Permission Statements		147
Appendix 2: Attribution Tables		149

List of Figures

Figure 1-1: Schematic diagram of biomass decomposition in HCW to organic acid formation.....	3
Figure 1-2: Thesis Map.....	6
Figure 2-1: Typical plant cell wall arrangement ⁴⁴	8
Figure 2-2: Chemical structure of Cellulose with intrachain and interchain hydrogen-bonded bridging ⁴⁸	10
Figure 2-3: Main Components of hemicellulose ⁴⁸	11
Figure 2-4: Schematic of the basic structure of hemicellulose. A: Arabinose; FeA: Ferulic acid; G: Galactose; Glc: Glucuronic acid; X: Xylose ⁵⁶	12
Figure 2-5: <i>p</i> -coumaryl, coniferyl and sinapyl Structures ⁴⁸	13
Figure 2-6: Partial structure of a hardwood lignin molecule ⁴⁸	14
Figure 2-7: Pathways of biomass conversion to bio-oil production using biochemical, hydrothermal and thermochemical routes ⁶⁶	17
Figure 2-8: schematic overview of hydrothermal conversion of biomass ⁷⁸	20
Figure 2-9: Properties of water at different temperatures. (A): Density, (B): Dielectric Constant, (C): Ion product. Dashed line: 25 MPa; solid line: 50 MPa; dotted line: 100 MPa ⁸⁵	23
Figure 2-10: summary reaction routes for the degradation of main components of lignocellulosic biomass during hydrothermal conversion ⁹⁶	24
Figure 2-11: Proposed reaction pathway of cellulose hydrolysis at subcritical and supercritical region ²⁰	28
Figure 2-12: Proposed scheme for lignin decomposition in subcritical water ¹⁴⁵	34
Figure 2-13: Main reaction pathway of cellobiose degradation in HCW ¹⁵⁰	36
Figure 2-14: Main reaction pathway of GF decomposition in HCW. ISM: Isomerization; DHD: dehydration; RAC: retro-aldol condensation; BHE: β -hydroxycarbonyl elimination; BAR: benzylic acid rearrangement; ADC: α -dicarbonyl cleavage ¹⁵⁷	38
Figure 2-15: Lobry de Bruyn-Alberda van Ekenstein rearrangement during hydrothermal decomposition of monomers ¹⁴³	39
Figure 2-16: Decomposition of biomass derived monomers and their products in HCW ⁸⁹	40
Figure 2-17: Mechanism of hydrothermal decomposition of glucose in HCW ¹⁵⁹	42

Figure 2-18: Reaction pathway of glucose decomposition under supercritical condition ¹⁷⁵	43
Figure 2-19: Proposed reaction pathway of lactic acid formation from hydrothermal conversion of glucose ¹⁸⁵	44
Figure 2-20: Reaction pathway of fructose in water at high temperature and high pressure ¹⁸⁸	45
Figure 2-21: Proposed reaction pathway from pyrovaldehyde to lactic acid ¹⁸⁸	46
Figure 2-22: Proposed reaction pathway of formic acid from hydrothermal conversion of fructose ¹⁹⁰	46
Figure 2-23: Proposed Reaction pathway of formic acid production from oxidation of monosaccharides in HCW in the presence of an alkali ¹⁹⁷	47
Figure 2-24: Three isomers of Saccharinic acid, (a): Metasaccharinic acid, (b): Isosaccharinic acid, (c): Saccharinic acid.	48
Figure 2-25: Alkaline degradation of glucose to produce saccharinic acids ¹⁵²	49
Figure 2-26: Alkaline Degradation of Polysaccharides to produce saccharinic acids ²⁰⁶	50
Figure 2-27: Dehydration reaction of xylose to furfural in HCW ²¹¹	51
Figure 2-28: Retro-aldol reaction of xylose to glycolaldehyde and glyceraldehyde in HCW ²¹¹	51
Figure 2-29: Series of reaction from glyceraldehyde to lactic acid during hydrothermal decomposition of xylose ²¹¹	52
Figure 2-30: Proposed pathway from 5-MHF to 1,2,4-Benzotriol ¹⁴³	55
Figure 2-31: Proposed cellobiose decomposition in HCW ¹⁵⁵	60
Figure 3-1: Overall research and methodology.....	65
Figure 3-2: Schematic representation of the continues reactor system used: (1) feedstock Solution Container; (2) deionised water container; (3,4) HPLC pump; (4) sample chamber; (5) fluidized sand bath; (6) preheating tube; (7) continuous reactor; (8) cooling bath; (9) back pressure regulator; (10) sample collection ¹⁷³	68
Figure 3-3: Schematic representation of the semi continues reactor system used in this study. (1) water reservoir; (2) HPLC pump; (3) infrared image furnace; (4) sample chamber; (5) stinted stainless steel filter; (6) thermocouple; (7) ice water bath; (8) pressure regulator; (9) liquid product collector ¹⁷	69
Figure 3-4: Calibration curves for all organic acids with available standards by HPAEC-CD for formic acid and HPAEC-CD-MS for other identified organic acids using gradient method.	72

Figure 3-5: Schematic diagram of MSQ detector system ²²⁸	73
Figure 4-1: Recovery of arabinose, galactose, glucose and xylose recovery from wood, leaf and bark as a function of time during hydrothermal processing at 100–270 °C.	80
Figure 4-2: Specific reactivity of wood biomass as a function of biomass conversion (on a carbon basis) during hydrothermal processing at various reaction temperatures: (a) 150 °C, (b) 180 °C, (c) 230 °C and (d) 270 °C.....	81
Figure 4-3: Carbon conversion as a function of reaction time during hydrothermal processing at various reaction temperatures: (a) 150 °C, (b) 180 °C, (c) 230 °C and (d) 270 °C, expressed as % of total C in mallee wood.....	83
Figure 4-4: Total mono- and oligosaccharides recovered in liquid products collected from hydrothermal processing of wood sample for 70 min at (a) 150 °C, (b) 180 °C, (c) 230 °C and (d) 270 °C, expressed as % of the respective total saccharides in mallee wood. The light gray bars indicate the total oligosaccharides quantified via the post-hydrolysis of the liquid products while the dark gray bars indicate the total monosaccharides in the liquid products.	84
Figure 4-5: Leaching of water-insoluble Mg and Ca as a function of time from wood, leaf and bark during hydrothermal processing at 100–270 °C.....	86
Figure 4-6: Recovery and yield of (a) arabinose, (b) galactose, (c) glucose, (d) xylose oligomers from the hydrothermal processing of the whole mallee biomass at 120–270 °C.	87
Figure 4-7: Overall recovery and yield of sugars from the hydrothermal processing of whole mallee biomass at 120–270 °C.....	88
Figure 4-8: Leaching of (a) Mg and (b) Ca in biomass during hydrothermal processing at 120–270 °C.	88
Figure 5-1: HPAEC-CD-MS chromatogram of a typical sample from cellobiose decomposition at 275 °C and a residence time of 66 s. MS detection mode: negative ion; needle voltage: –4 kV; ESI probe temperature: 450 °C; cone voltage: 45 V.....	93
Figure 5-2: Identification of organic acids from cellobiose decomposition using available standards. 1: unidentified saccharinic acid; 2: metasaccharinic acid (α and β); 3: unidentified organic acid with molecular weight of 120 g/mol; 4: lactic Acid; 5: glycolic Acid and 6: formic acid.....	94
Figure 5-3: Yield and selectivity of organic acids produced from cellobiose decomposition at 200 – 275 °C. (a) Formic acid yield, (b) MSA yield, (c) Lactic acid	

yield, (d) Glycolic acid yield, (e) Formic acid selectivity, (f) ISA selectivity, (g) Lactic acid selectivity, (h) Glycolic acid selectivity.	95
Figure 5-4: Contribution of MSA, formic acid, lactic acid and glycolic acid to total hydrogen ion dissociated by four quantified organic acids during cellobiose decomposition in HCW at 200 – 275 °C. (a) 200 °C, (b) 225 °C, (c) 250 °C, (d) 275 °C.	96
Figure 5-5: Comparisons of the hydrogen ion concentrations calculated from total concentrations of the quantified organic acids and the measured pH after cellobiose decomposition in HCW at various conversions.	97
Figure 5-6: Summarised reaction pathways for saccharinic, formic, lactic and glycolic acids during cellobiose decomposition in HCW based on the reports in the literature ^{143, 151, 152, 205, 206} and this study. R1: Isomerisation, R2: Hydrolysis, R3: Keto-enol tautomerisation, R4: β-hydroxycarbonyl elimination, R5: Benzilic acid rearrangement, R6: α-dicarbonyl cleavage, R7: Retro-aldol condensation, R8: Lobry de Bruyn-Alberda van Ekenstein transformation (LBAE), R9: Aldol condensation and R10: Dehydration. Compound (1): Cellobiose; (2): Glucosylmannose; (3): Cellobiulose; (4): Glucose; (5): Mannose; (6): Fructose; (7): Diketones Intermediate; (8): Glyceraldehyde; (9): Dihydroxyacetone; (10): Glycolaldehyde; (11): Erythrose and (12): Pyruvaldehyde; (13): Diketones Intermediate.	99
Figure 6-1: Yields and selectivities of organic acids produced from glucose (hollow) and fructose (solid) decomposition in HCW at 225–275 °C. (a) Formic acid yield, (b) MSA yield, (c) Glycolic acid yield, (d) Lactic acid yield, (e) DHBA yield, (f) Formic acid selectivity, (g) MSA selectivity, (h) Glycolic acid selectivity, (i) Lactic acid selectivity, (j) DHBA selectivity.	104
Figure 6-2: Comparisons of the hydrogen ion concentrations calculated from total concentrations of the quantified organic acids and the measured pH of the liquid products after (a) glucose and (b) fructose decomposition in HCW at various temperatures.	106
Figure 6-3: Contributions of formic acid, MSA, glycolic acid, DHBA and lactic acid to the total [H ⁺] dissociated calculated by the quantified organic acids from glucose and fructose decomposition in HCW at 225–275 °C. (a) glucose at 225 °C, (b) glucose at 250 °C, (c) glucose at 275 °C, (d) fructose at 225 °C, (e) fructose at 250 °C, (f) fructose at 275 °C.	107
Figure 6-4: Summarised reaction pathways for saccharinic, formic, lactic, glycolic and 2,4 dihydroxy butyric acids during glucose and fructose decomposition in HCW	

based on the previous literatures^{143, 151, 152, 205, 206, 245, 259-261} and this study. (1): Glucose; (2): fructose; (3): erythrose; (4): glyceraldehyde; (5): dihydroxyacetone; (6): pyruvaldehyde; (7): glycolaldehyde; (8): formic acid; (9): lactic Acid; (10): 2,4 dihydroxy butyric acid; (11) metasaccharinic acid; (12) glycolic acid. R1: Isomerisation; R2: Retro-aldol condensation; R3: Rehydration; R4: Dehydration; R5: α -dicarbonyl cleavage; R6: Benzilic acid rearrangement; R7: aldol condensation. 110

Figure 7-1: Mannose conversion during decomposition in HCW at 200 – 275 °C. 114

Figure 7-2: Yields of major products during mannose conversion during decomposition in HCW at 200 – 275 °C. (a) Yield of glucose; (b) yield of fructose; (c) yield of GCA; (d) yield of 5-HMF; (e) yield of GA; (f) yield of formic acid; (g) yield of saccharinic acid; (h) yield of glycolic acid; (i) yield of lactic acid and (j) yield of DHBA..... 116

Figure 7-3: Selectivities of major products during mannose conversion during decomposition in HCW at 200 – 275 °C. (a) Selectivity of glucose; (b) selectivity of fructose; (c) selectivity of GCA; (d) selectivity of 5-HMF; (e) selectivity of GA; (f) selectivity of formic acid; (g) selectivity of saccharinic acid; (h) selectivity of glycolic acid; (i) selectivity of lactic acid and (j) selectivity of DHBA..... 118

Figure 7-4: Correlations between $-\ln[C(t)/C(0)]$ and residence time during mannose decomposition in HCW at 200 – 275 °C..... 119

Figure 7-5: Arrhenius plots during mannose decomposition in HCW at 200 – 275 °C. 120

Figure 7-6: Contribution of organic acids to the total $[H^+]$ dissociated calculated by the quantified organic acids from mannose decomposition in HCW at 200 – 275 °C. (a) 200 °C, (b) 225 °C, (c) 250 °C, (d) 275 °C. 121

Figure 7-7: pH value of liquid product as a function of mannose conversion during mannose decomposition in HCW at 200 – 275 °C 122

Figure 7-8: Comparisons of the hydrogen ion concentrations calculated from total concentrations of the quantified organic acids and the measured pH of the liquid products during mannose decomposition in HCW at 200 – 275 °C. 123

Figure 7-9: Reaction pathways of mannose decomposition in HCW based on the previous literatures^{130, 147, 148, 200, 201, 240, 253-255} and this study. (1): Mannose; (2): Glucose; (3): Fructose; (4): Erythrose; (5): Glycolaldehyde; (6) Glyceraldehyde; (7): Dihydroxyacetone; (8): Pyrovaldehyde ; (9): Formic Acid; (10) 2,4 dihydroxy butyric acid; (11): Lactic Acid; (12): Glycolic Acid; (13): Meta saccharinic Acid; (14): 5-HMF; R1: Isomerisation; R2: Retro-aldol condensation; R3: Rehydration;

R4: Dehydration, R5: α -dicarbonyl cleavage; R6: Benzilic acid rearrangement;
R7:Aldol condensation..... 124

List of Tables

Table 2-1: The content of cellulose, hemicellulose, lignin and ash in various lignocellulosic biomass ⁴⁵⁻⁴⁷	9
Table 2-2: Inorganic species content in different biomass component (Na, K, Mg, Ca, Fe, Si, Al, and P in wt% db; wt% daf for S, Cl and N) ²⁹	15
Table 2-3: The operation condition for pyrolysis processes ⁶⁸	18
Table 2-4: Different properties of ambient water, subcritical and supercritical water ^{9, 10}	22
Table 2-5: Kinetic parameters of various reaction pathways of cellobiose decomposition in HCW ¹⁵⁵	37
Table 2-6: Kinetics parameters of dihydroxyacetone decomposition under Subcritical Condition, DHA: dihydroxyacetone; GCA: glyceraldehyde; MGX: methylglyoxal; GLYA: glycolic acid; MEOH: methanol; AA: acetic acid; FAD: formaldehyde ²¹³ ..	54
Table 2-7: Kinetic parameters of various reaction pathways of glucose decomposition in HCW ²¹⁶	56
Table 2-8: Summary of Kinetic parameters of glucose, cellulose and cellobiose decomposition in HCW under different reaction condition.....	58
Table 2-9: Summary of kinetic parameters from previous literature.....	59
Table 2-10: Detailed reactions kinetic data from cellobiose decomposition in HCW, the numbers listed are in accordance with the reaction numbers in Figure 2-31 ¹⁵⁵ ...	61
Table 3-1: HPAEC-PAD gradient program for monosaccharides separation.	71
Table 4-1: Proximate and ultimate analysis of mallee tree components used in this study.....	78
Table 4-2: Sugar and inorganic species content (wt% in dry basis) of mallee tree components.	78

Chapter 1 : Introduction

1.1 Background and Motives

The main source of energy production and chemical synthesis relies on fossil fuels feedstock such as petroleum, oil, coal and natural gas¹. The increasing global demand for using fossil fuels causes the environmental issues and significant rise in carbon dioxide emission, which has the main contribution to the global warming and climate change issues². Additionally, the shortage of fossil fuel resources creates the energy security concern. Therefore, it becomes increasingly important to find new technologies for energy supply and sustainable development.

Biomass as a pivotal source of renewable energy, has attracted increasing attention to address issues such as shortage of fossil fuels and its environmental problems arisen from fossil fuel using. Recycle of carbon dioxide is a great advantage of using biomass, which leads to little increase to greenhouse gases³. Another important advantage of using biomass is to produce green chemicals and value-added chemicals such as 5- hydroxymethylfurfural (5-HMF), lactic acid, formic acid^{4, 5}. National Renewable Energy Laboratory (NREL) National Renewable Energy Laboratory listed organic acids as the top value chemicals from biomass^{4, 6}, and sustainable production of these platform chemicals from biomass is highly attractive. Therefore, a fundamental study is of great importance to understand the formation mechanisms of organic acids as the high-value biochemicals from biomass.

Main components of lignocellulosic biomass are cellulose, hemicellulose and lignin, which contribute to 40-60%, 20-40% and 10-25% of whole biomass, respectively⁷. Hydrothermal processing of biomass in HCW has been identified as one of the promising technologies to convert biomass and biomass components to biochemicals⁸. Due to unique properties of HCW such as low dielectric constant and high ion products, HCW can promote both acidic and alkaline reactions in biomass conversion⁹⁻¹¹. Hydrothermal conversion of biomass in HCW leads to the breakdown of polymer components in biomass to sugars, followed by further conversion into value-added chemicals such as organic acids¹², or subsequently into bioethanol¹³⁻¹⁶.

This thesis aims to understand the formation mechanisms of organic acids during biomass hydrothermal conversion. Organic acids are considered as the value-added biochemicals which are obtained as the end-products or sometimes as the intermediate components of a particular biochemical cycle. Generally, they are produced commercially by chemical synthesis or fermentation^{1,2}.

It has been widely reported that sugar oligomers with a wide range of degrees of polymerization (DPs) were identified in the liquid products from hydrothermal processing of biomass using a semi-continuous reactor system¹⁷⁻¹⁹. The subsequent conversion of high-DP oligomers produces low-DP oligomers and monomers such as glucose and fructose, which can be further converted into value-added chemicals such as organic acids²⁰. In order to better understand the formation mechanism of organic acids from biomass conversion in HCW, it is of great importance to study hydrothermal conversion of sugar intermediates such as sugar oligomers and monomers. Figure 1-1 shows schematic diagram of biomass conversion in HCW to organic acids formation. Most of the previous studies conducted under catalytic condition, and there are limited studies on the decomposition of biomass and its derived sugars decomposition under non-catalytic conditions. Thus, further insights on hydrothermal conversion of model compounds under non-catalytic conditions are of significance.

In Australia, mallee biomass is a by-product from dryland salinity management and considered as a potential second-generation feedstock. To date, approximately 15,000 hectare of mallee trees have been planted by over 1,000 farmers in Western Australia.²¹⁻²³ With its near carbon-neutral plantation, high energy output, short harvesting cycle and potential for large scale production^{24, 25}, mallee biomass is considered to be an important second-generation bioenergy feedstock^{26,27}.

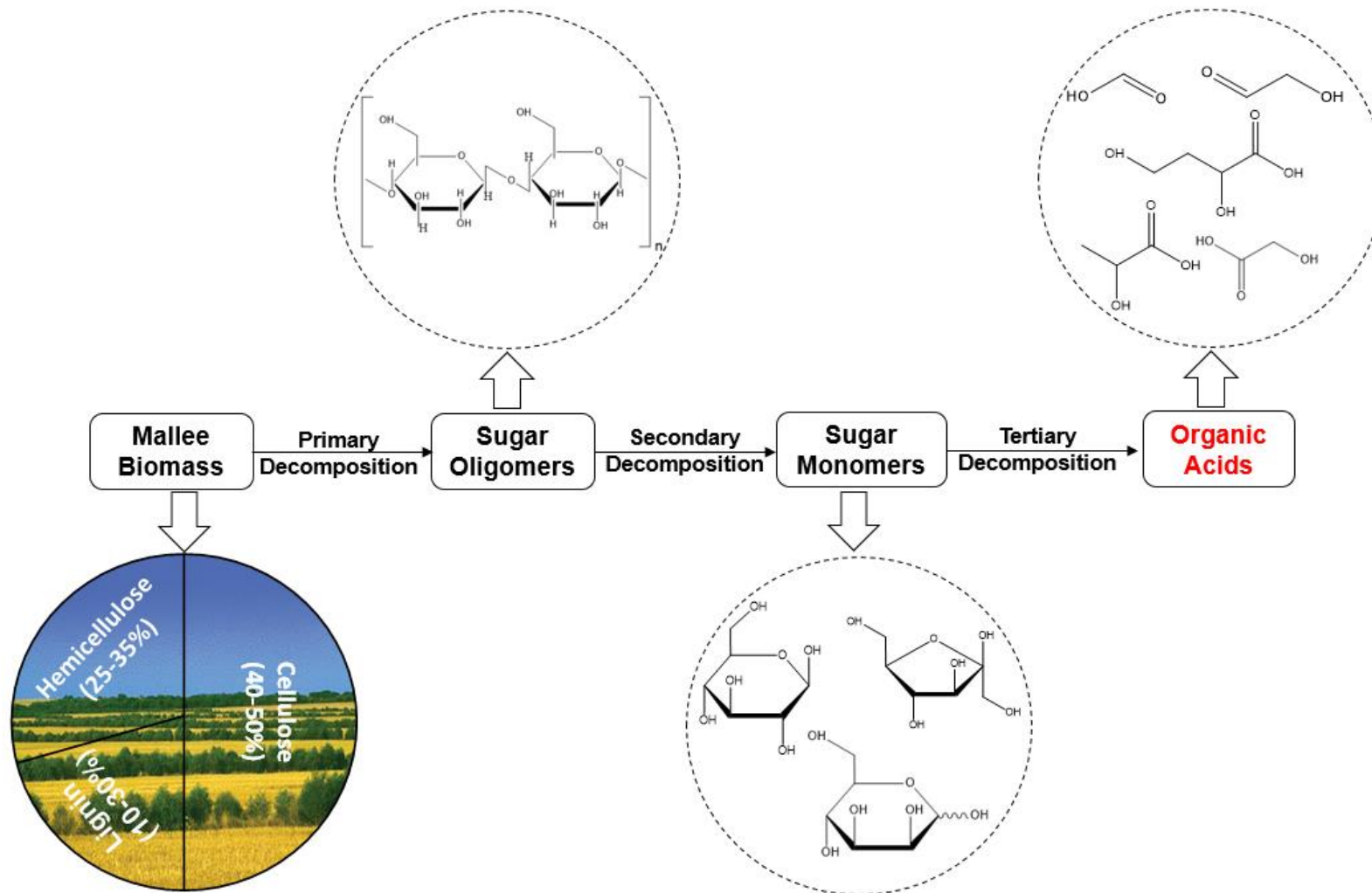


Figure 1-1: Schematic diagram of biomass decomposition in HCW to organic acid formation

Wood, leaf and bark are the main components of mallee tree, while decomposition behaviour of various sugar components (e.g., arabinan, galactan, xylan, glucan) from mallee wood, leaf and bark is still poorly understood²⁸. Furthermore, biomass contains alkali and alkaline earth metallic (AAEM) species which the content and leaching characteristic are different for each component²⁹. Therefore, an investigation is of great importance to understand the sugar recovery and leaching characteristics of AAEM species from mallee wood, leaf and bark.

1.2 Scope and Objectives

The new findings provide some insights into the kinetics and reaction mechanism of mallee biomass hydrolysis in HCW to achieve a proper reactor design and consequently produce desired extracts and value-added chemicals (e.g. sugar and organic acids products).

The main purpose of this study is to understand the hydrothermal decomposition behaviour of mallee biomass and its main components in HCW, and the subsequent conversion of various sugar products into organic acids as value-added biochemicals, including the following works.

- To investigate the liquid products from hydrothermal decomposition of mallee biomass and its main components (i.e., wood, leaf and bark) using a semi-continuous reactor, focusing on the sugar recovery and the release of inorganic species;
- To understand the formation mechanism of organic acids from hydrothermal decomposition of cellobiose (as a model compound of glucose oligomers);
- To elucidate the formation pathways of various organic acids from hydrothermal decomposition of glucose and fructose (as key sugar monomers from cellulose decomposition);
- To reveal the decomposition mechanism and formation pathways of various organic acids from hydrothermal decomposition of mannose (as both a key sugar

from glucose decomposition and a model compound of hemicellulose-derived sugars).

1.3 Thesis Outline

This thesis consists of 8 chapters including the current chapter. The thesis structure is schematically presented in the thesis map (Figure 1-1):

- Chapter 1 introduces the background and objectives of present study;
- Chapter 2 reviews the existing literatures on the fundamental chemistry of biomass, hydrothermal processing, the reaction mechanism of dimers, mesocompounds and other compounds under hydrothermal condition. This chapter identifies research gaps and specific objectives of this thesis;
- Chapter 3 provides an overview on the methodology employed to achieve the research objectives and provided the details on the sample preparation, experimental setup and analytical instrumentations and methods;
- Chapter 4 reveals sugar recovery and Mg and Ca leaching characteristics from mallee wood, leaf and bark in HCW under non-catalytic condition;
- Chapter 5 reports organic acids formation and mechanism on cellobiose decomposition in HCW;
- Chapter 6 explores the organic acids formation and identifies the primary and non-primary organic acids produced on glucose and fructose decomposition in HCW;
- Chapter 7 identify the major products during mannose conversion and investigates the decomposition mechanism of mannose in HCW;
- Chapter 8 presents the conclusion obtained from current study and outlines recommendations for future research.

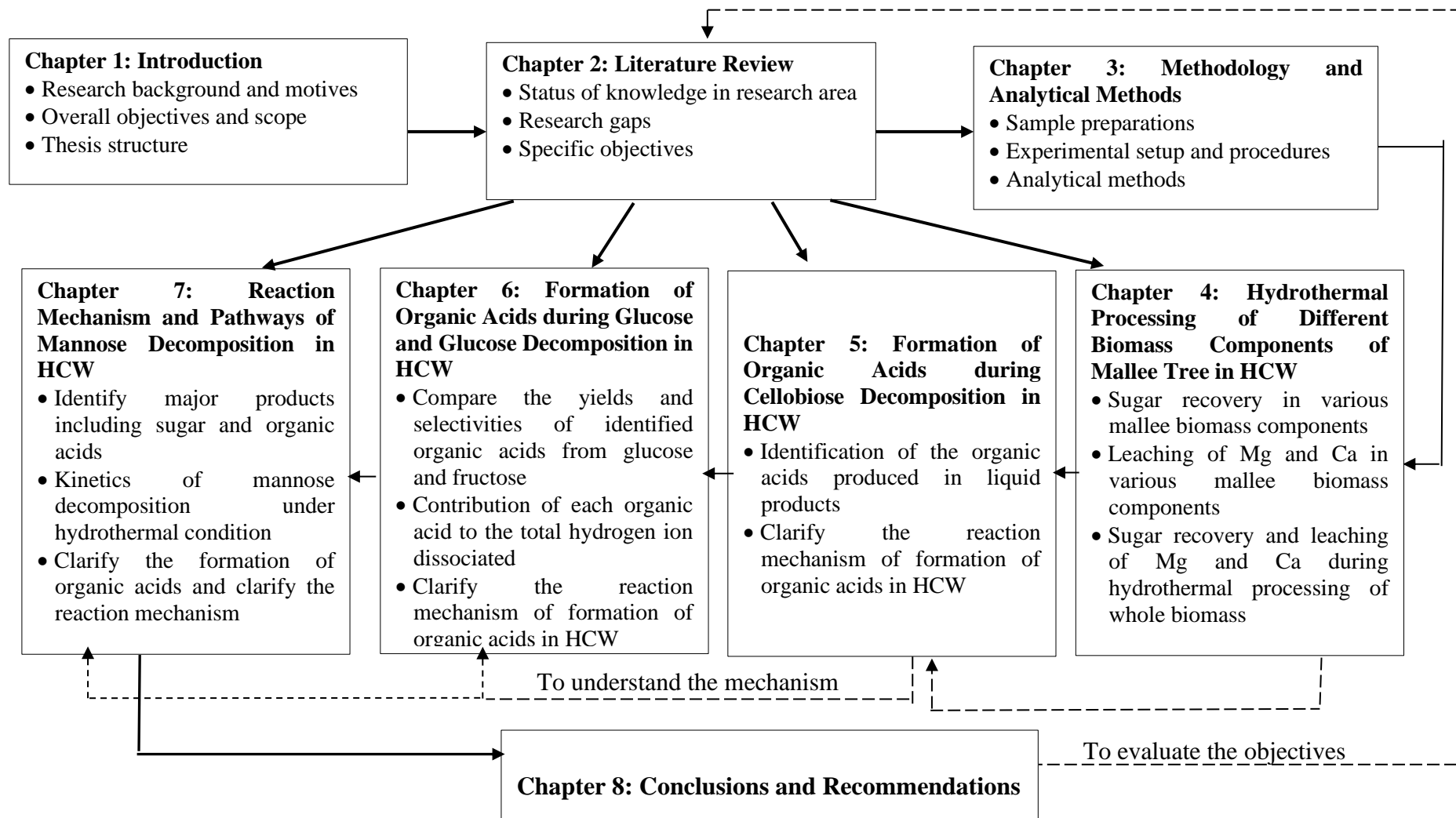


Figure 1-2: Thesis Map.

Chapter 2: Background and Literature Review

2.1 Introduction

Significant problems arising from fossil fuels to produce energy lead countries to find alternative resources for supplying energy and valuable chemicals^{5, 16}. Renewable energy is becoming an important option to address fossil fuel shortage and environmental issues related to their usage. Lignocellulosic Biomass, one of the main abundant sources of the renewable energy, is a promising feedstock for sustainable production of biofuels and platform biochemicals such as sugars, furans, polyols, and organic acids^{16, 30, 31}. In Western Australia, plantation of mallee tree was introduced as a strategy for managing the serious dryland salinity issue in the wheatbelt region.²³ With its near carbon-neutral plantation, high energy output, short harvesting cycle and potential for large scale production, mallee biomass is considered to be an important second-generation bioenergy feedstock.³² Hydrothermal processing is an important technical route for biomass conversion.^{33, 34} It can be deployed to effectively pretreat lignocellulosic biomass for subsequent enzymatic hydrolysis to produce fermentable saccharides,^{11, 35} or directly produce some value-added chemicals such as furfural³⁶ and hydroxymethylfurfural.³⁷ Various reactor systems including batch,^{34, 38, 39} semi-continuous flow^{34, 40} and continuous-flow reactors^{41, 42} may be employed for hydrothermal processing of biomass or its model compounds, depending on experimental conditions.

As discussed earlier, mallee biomass is considered to be an important second-generation bioenergy feedstock in WA. So far, there has been a lack of fundamental understanding of its hydrothermal conversion in HCW. Therefore, a study is required to understand the mechanism and primary products from mallee biomass hydrolysis as a whole in HCW to provide new insights for sustainable production of biofuels and value-added biochemicals (i.e., sugars and organic acids).

This chapter reviews the current literatures on hydrothermal decomposition of biomass and various model compounds in HCW. It gives a brief structure of mallee biomass and its main components, following by properties of hot compressed water and overview of biomass and its components conversion in HCW. This chapter then reviews the hydrothermal processing of monomers, dimers and some other compounds in HCW. At the end, the main research gaps are identified, assisting in the present study objectives.

2.2 Common Biomass Components

Common sources of biomass classified into four main categories including forest, agriculture, municipal solid wastes and other sources like fast growing plants, herbage plants and ocean biomass^{43, 44}. Key components for all types of biomass are cellulose (consists of long chain of the 6-carbon sugar), hemicellulose (mainly 5-carbon sugars and xylose) and lignin that the distribution of each component varies in different types of biomass^{45, 46}. A typical plant cell wall is shown in Figure 2-1. A common wood biomass consists of ~40-50% cellulose, ~20-30% hemicellulose, ~20-28% lignin and less percentage for other components such as organic and inorganic extractives⁴⁵⁻⁴⁷. Table 2-1 summarized the content of each component in various biomass types based on the literatures.

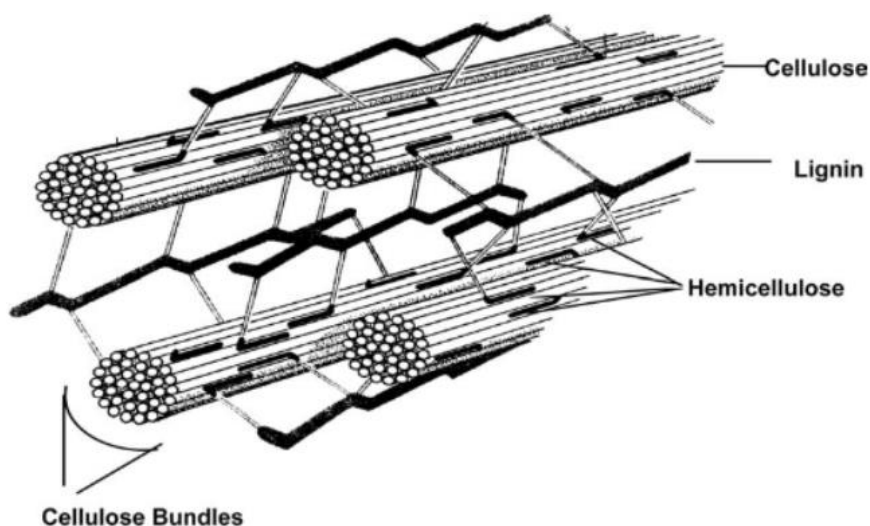


Figure 2-1: Typical plant cell wall arrangement⁴⁴.

2.2.1 Cellulose

Cellulose comprises ~35-50% of total dry mass of lignocellulosic biomass. As shown in figure 2-2, it is a polysaccharide consisting of glucose units attached to each other by β -1,4-glycosidic bonds⁴⁸. The number of glucose units in the cellulose chain determines DP which indicates many properties of cellulose. The simplest model of cellulose is Cellobiose consists of two bound glucose units. In nature, the value of DP varies between approximately 7000-10000 glucose units in wood cellulose and around 15000 in cotton cellulose^{46, 49}.

Table 2-1: The content of cellulose, hemicellulose, lignin and ash in various lignocellulosic biomass ⁴⁵⁻⁴⁷.

Lignocellulosic	Cellulose	Hemicellulose	Lignin	Ash
Hard Woods				
White poplar	49.0	25.6	23.1	0.2
European birch	48.5	25.1	19.4	0.3
White willow	49.6	26.7	22.7	0.3
Soft woods				
White spruce	44.8	30.9	27.1	0.3
Europ. Spruce	40.4	31.1	28.2	0.3
Douglas fir	42.0	23.5	27.8	0.4
Agricultural				
Corn Stover	37.1	24.2	18.2	5.2
Sugarcane	39.0	24.9	23.1	3.7
Wheat straw	44.5	24.3	21.3	3.1
Other wastes				
Maize stalk	38.0	26.0	11.0	3.0
Newspaper	40-55	25-40	18-30	NA
Primary wastewater solids	8-15	NA	24-29	NA

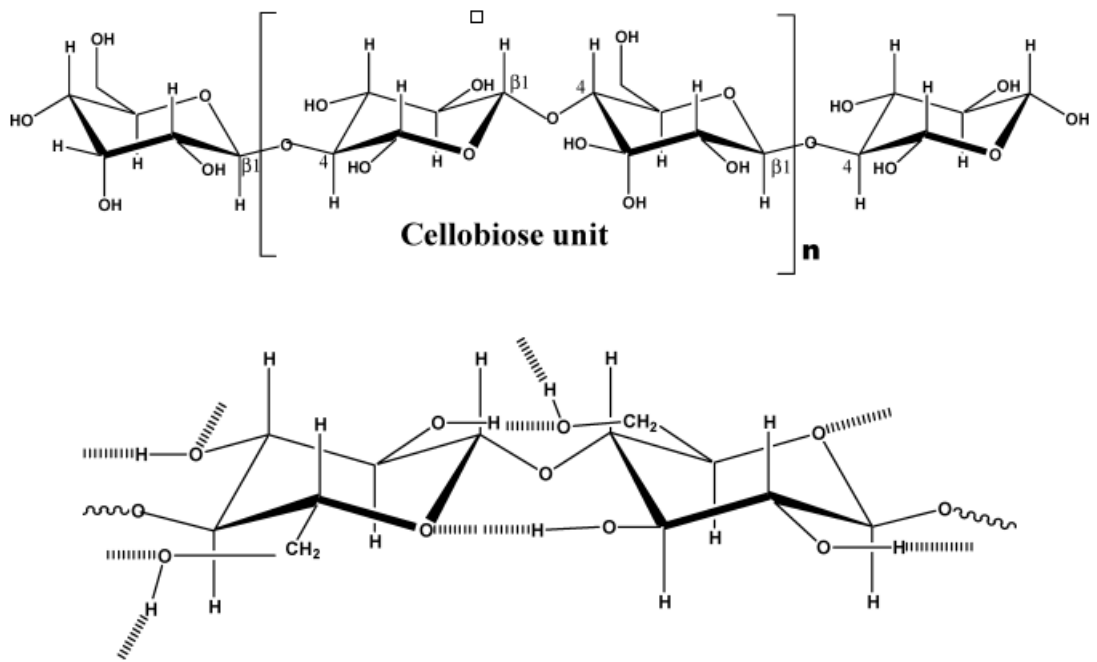


Figure 2-2: Chemical structure of Cellulose with intrachain and interchain hydrogen-bonded bridging⁴⁸.

Cellulose comprises of two fractions, (1) crystalline structure which is portion of cellulose bound together by hydrogen network formed by hydroxyl groups in glucose, (2) amorphous cellulose which is less ordered portion. While crystalline cellulose is water insoluble due to the low surface area, amorphous part is more easily degraded under hydrolysis and other biomass pretreatment due to having more accessible surface area⁵⁰⁻⁵². However, strong acids and bases are required to swell or dissolve the cellulose with high portion of crystalline fraction. The proportion of each part in cellulose depends on its origin and treatment. The percentage of crystalline part in cotton (70%) is more than of wood (40%) which is consequently less ordered⁵³.

2.2.2 Hemicellulose

Hemicellulose consists approximately 35% of total mass of lignocellulosic biomass. Different types of hemicellulose normally account for 25%-35% of mass of dry wood, 28% in softwood and 35% in hardwood. It comprises of various aldopentoses (mainly xylose and arabinose), aldohexoses (glucose, mannose and galactose), 4-O-methyl glucuronic acid and galacturonic acid residues^{48, 54}. Main components of various types of hemicellulose is shown in Figure 2-3.

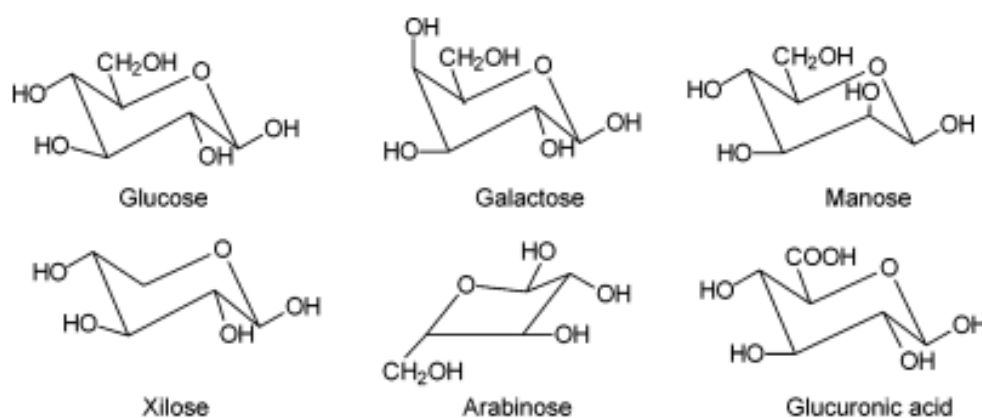


Figure 2-3: Main Components of hemicellulose⁴⁸

The structure of hemicellulose in hardwood consists of mainly xylan and small amount of glucomannan as a backbone chain which is usually branched with various saccharides. Different monomer units at the backbone position, variety of monosaccharides or oligosaccharides in sidechains and variety of linkages contribute

to the construction of various types of hemicellulose which may result in different properties and decomposition behaviour. The structure of softwood contains a small amount of xylan and large quantity of galactoglucomannan⁴⁸. Figure 2-4 illustrates an example of hemicellulose structure.

Due to its branched structure and lower molecular weight, hemicellulose is relatively more easily to decompose than cellulose under treatment of lignocellulosic biomass and its hydrolysis starts at lower temperature compared to cellulose^{48, 55, 56}. It is water-insoluble at low temperature, but by increasing temperature becomes soluble and the presence the acids significantly improve the solubility of hemicellulose in water.

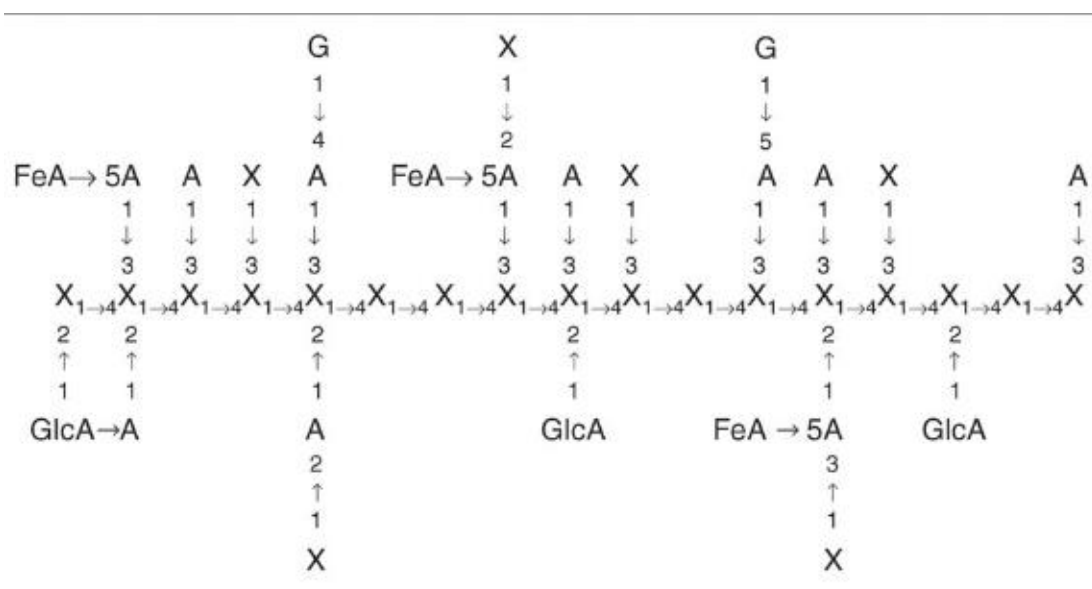


Figure 2-4: Schematic of the basic structure of hemicellulose. A: Arabinose; FeA: Ferulic acid; G: Galactose; Glc: Glucuronic acid; X: Xylose⁵⁶.

2.2.3 Lignin

Lignin by filling the spaces between cellulose and hemicellulose is cross-linked polymer of the cell wall formation, and accounts for 23%-33% of the mass of softwood and 16%-25% of hardwood. Its amorphous structure leads to a large number of possible interkages between individual unit. Lignin units linked together with ether bonds, unlike cellulose and hemicellulose with acetal functions⁴⁸.

Lignin is an amorphous cross-linked resin, provides a shield that preserves cellulosic fibres against microbial and fungal attacks^{48, 57}. Lignin is branched aromatic phenolic polymer, comprises of phenylpropane units, which main building blocks as shown in Figure 2-5 are *p*-coumaryl, coniferyl and sinapyl with various types of interlinkages^{48, 57, 58}. The structure of lignin is different in hardwood and softwood. Generally, softwood lignin is rich in coniferyl units while hardwoods lignin is a copolymer of both the coniferyl and sinapyl units with higher fraction of sinapyl units compared than that in softwood⁴⁸.

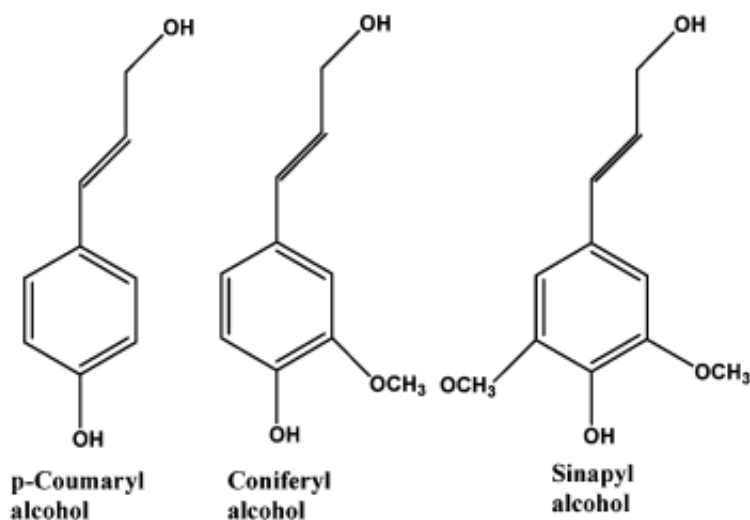


Figure 2-5: *p*-coumaryl, coniferyl and sinapyl Structures⁴⁸.

The linkages of Lignin is broken down before cellulose and hemicellulose become accessible while lignocellulosic biomass is subjected to decomposition or hydrolysis⁵⁴. Figure 2-6 presents chemical linkages in a small section of the lignin polymer.

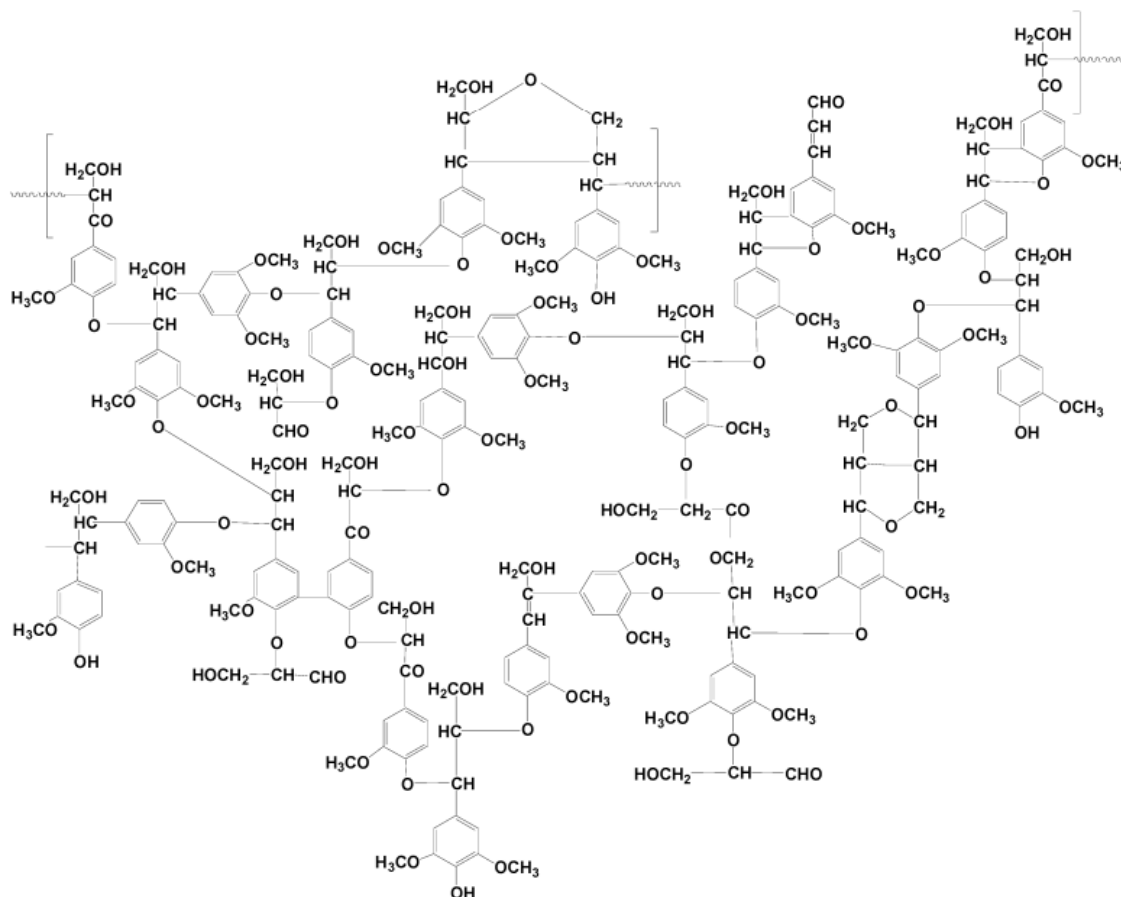


Figure 2-6: Partial structure of a hardwood lignin molecule⁴⁸.

2.2.4 Other Components

Organic Extractives

Other components of biomass include minor low-molar-mass extraneous species mostly organic extractives and inorganic minerals. These organic extractives mostly include fats, phenolics, waxes, alkaloids, proteins, fatty acids, simple sugars, pectins, gums, glycosides, terpenes, starches, resin, saponins, and essential oils^{48, 53, 59}. Organic extractives can be extracted with polar solvents (such as water, methylene chloride, or alcohol) or nonpolar solvents (such as toluene or hexane). Extractives have several roles in biomass structure, it acts as intermediates in metabolism, reserve the energy, and protect the biomass against microbial and insect attack. The amount of extractives varies between different components of biomass⁵³. Depending on biomass species, the ash content of biomass is typically < 1% for wood, while it is ~3.8% and ~5.5% for leaf and bark respectively and as high as ~20% for agriculture residue²⁹.

Biomass Inorganic Species

Another component of biomass is inorganic species. Biomass contains various inorganic species include AAEM species (Na, K, Mg and Ca), Si, Fe, Al, Cl, P, Ti and other elements which are up taken during growth. The amount of these elements is different depending on the type of biomass and environmental condition^{48, 60}. Table 2-2 shows amount of these elements in mallee biomass used in this study²⁹.

Table 2-2: Inorganic species content in different biomass component (Na, K, Mg, Ca, Fe, Si, Al, and P in wt% db; wt% daf for S, Cl and N)²⁹.

Element (wt%)	Wood	Leaf	Bark
Na	0.0212	0.5537	0.2094
K	0.0744	0.3797	0.1105
Mg	0.0364	0.1447	0.0796
Ca	0.1236	0.7652	2.6591
Si	0.0026	0.0550	0.0099
Al	0.0025	0.0192	0.0028
Fe	0.0001	0.0142	0.0019
P	0.0182	0.1075	0.0235
S	0.0183	0.1181	0.0509
N	0.1910	1.4574	0.3918
Cl	0.0323	0.1839	0.2601

The inorganic species may also be present in very different occurrence forms (e.g. dissolved salts, organically-bound species that are ion-exchangeable or others such acid-soluble but not ion exchangeable). The dissolved salts typically consist ions such as K^+ , Na^+ , Ca^{2+} , Cl^- and SO_4^{2-} while organically-bound species consist of cations (e.g. Na^+ , K^+ , Mg^{2+} and Ca^{2+}) bound to organic functional groups within biomass^{60, 61}.

Wu et al.²⁹ studied mallee biomass and found out while the majority of Na, K and Cl is water soluble, the amount of water-soluble form of Mg, P and S is less and varies between different components of biomass. Some part of these water soluble AAEM species is in the form of water-soluble salt with Cl^- , SO_4^{2-} and PO_4^{3-} . They also appear as the cation of water-soluble organic compounds like carboxylates^{29, 61}. They also reported the occurrence of Mg and Ca in the form of carboxylate is mainly water-insoluble.

They also reported that most of the water-insoluble Mg in wood and bark is organically bounded and ion exchangeable form and only part of the water-insoluble form of Mg is acid soluble. Conversely, the majority of water-insoluble form of Mg in leaf is acid soluble which is not ion exchangeable²⁹.

On the other hand, small part of Ca in mallee biomass is water soluble, the majority of water insoluble Ca in the wood is in the form of ion exchangeable via ammonium acetate, but those in leaf and bark are acid soluble and not ion exchangeable which are likely to be in various forms of calcium oxalate (i.e. calcium oxalate monohydrate or dehydrate)^{61, 62}.

Chlorine mainly present in the form of chloride of AAEM species like NaCl and KCl in biomass, and it is water-soluble⁶¹. The water-soluble part of P and S is mainly in the form of sulphate and phosphate of AAEM species. However, the source of some part of P is organic compound that contains phosphorous like phytic acids⁶¹ and some part of P and S presented in the form of sulphate and phosphate leachable by ammonium acetate and acid⁶³.

2.3 Biomass Conversion

Several technologies are deployed to pretreat lignocellulosic biomass for subsequent enzymatic hydrolysis and produce fermentable saccharides,^{11, 35} or directly produce some value-added chemicals such as furfural³⁶ and 5-hydroxymethylfurfural (5-HMF)⁵. Pretreatment step is a way to make the components of lignocellulosic biomass more accessible to the enzymes through altering the biomass structure and break down the available carbohydrate as cellulose or hemicellulose to desired biomass products^{46, 64, 65}.

Biomass can be used as the energy source for production of biofuels. The main pretreatment techniques for overcoming biomass recalcitrance are divided into three categories: (1) thermochemical include pyrolysis and gasification technologies (based on operating temperature), which produce a synthesis gas (CO+H₂) and then leading to reforming of various types of long carbon chain biofuels such as bio-oils, (2) hydrothermal, where water at high temperature such as supercritical water acts as a medium to convert biomass to fermentable sugars and (3) biochemical, which uses

enzymes and microorganisms to convert cellulose and hemicellulose parts of biomass to alcohols^{66, 67}. Figure 2-7 shows the pathway for biomass conversion to biofuels.

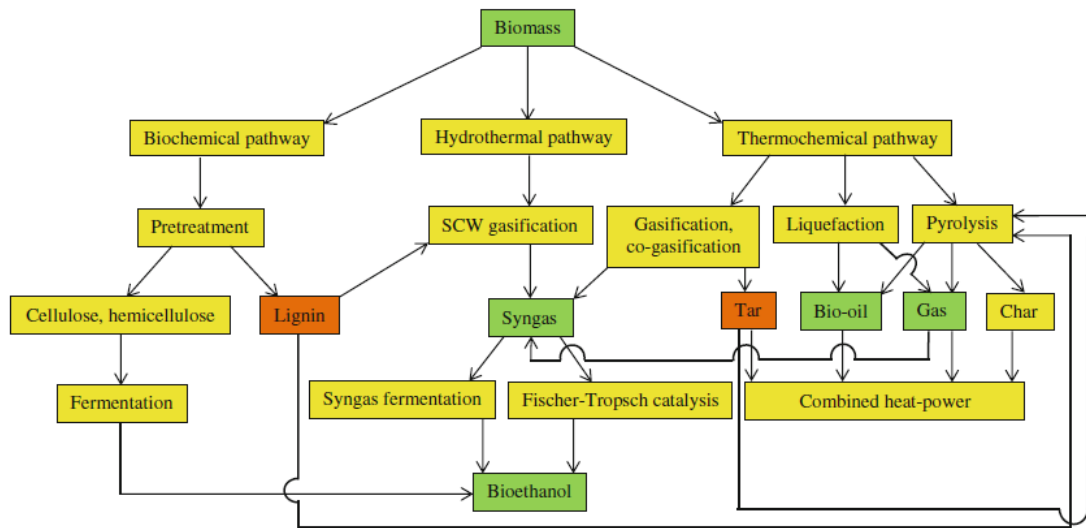


Figure 2-7: Pathways of biomass conversion to bio-oil production using biochemical, hydrothermal and thermochemical routes ⁶⁶.

2.3.1 Pyrolysis of Biomass

Pyrolysis of biomass is a thermal degradation process which biomass heated at high temperature (generally 500°C -800°C) under oxygen depleted environment. At this high temperature, cellulose part of biomass decomposes to produce pyrolysis oil, biochar and gaseous substances ⁶⁸. Mild acid hydrolysis (1 N sulfuric acid, 97°C and 2.5 h) on residue of biomass after pyrolysis resulted ~85% cellulose conversion and >5% glucose ⁶⁹.

Pyrolysis process is categorised to (1) conventional pyrolysis (slow pyrolysis), (2) fast pyrolysis and (3) flash pyrolysis. Slow-pyrolysis produces 35% biochar, 30% bio-oil and 35% fuel gas which generally favours biochar production. In fast pyrolysis, bio-oil is the desired product. In this reactor system, thermal decomposition of biomass to produce vapour, aerosols and light gases occurs due to the high heating rate. short vapour residence time (<1s) and rapid cooling of vapour product, produces higher yield of bio-oil compared to slow pyrolysis (50-70% bio-oil, 10-30% biochar and 15-20% gas product by mass) ^{70 71}. Flash pyrolysis requires

biomass with fine particles compared to fast and slow pyrolysis, and gaseous compound is the major product under this pyrolysis condition. Generally, the products distribution depends on the type of pyrolysis, characteristics of biomass and reaction parameters ^{67 72 68}. Table 2-3 listed the range of operating condition for slow, fast and flash pyrolysis.

Table 2-3: The operation condition for pyrolysis processes ⁶⁸.

	Slow Pyrolysis	Fast Pyrolysis	Flash Pyrolysis
Pyrolysis Temperature (K)	550-950	850-1250	1050-1300
Heating Rate (K/s)	0.1-1	10-200	>1000
Particle Size (mm)	5-50	<1	<0.2
Solid Residence Time (s)	450-550	0.5-1.0	<0.5

2.3.2 Gasification of Biomass

Gasification is a technology which converted solid and liquid into useful gaseous fuels or chemicals that can be used as feedstock to release energy by burning, or used for value-added chemicals formation. Gasification converts biomass into high quantities of mixture of gaseous products (carbon dioxide, carbon monoxide, hydrogen, water and gaseous hydrocarbons), small amounts of char and condensable compounds (tars and oils) through partial thermal oxidation. It involves a variety of chemical reactions, heat and mass transfer processes and pressure changes ^{73 74 75}.

Oxidizing agent or gasifying agent are generally air, steam, oxygen, nitrogen, carbon dioxide or combination of these. Gasifier exposed to high temperature directly or indirectly leads to increasing the gasification temperature to reach 600-1000°C, then in the presence of oxidizing agent molecular structure of biomass rearrange to lighter molecules and eventually convert to permanent gaseous fuel with higher hydrogen-to-carbon (H/C) ratio ⁷⁴.

The main steps involved in gasification process are drying, pyrolysis, oxidation (combustion) and reduction (char gasification). In a typical gasifier, drying undergoes at lower temperature (<150 °C), pyrolysis occurs at temperature range of 150-170 °C, oxidation occurs at 700-1500 °C and reduction takes place at 800-1100 °C. In the drying step, steam is released by evaporating the moisture of the fuel. The pyrolysis step involves volatile component of feedstock which is vaporized while heated. The

volatile vapour produced and main components are hydrogen, carbon monoxide, carbon dioxide, methane, hydrocarbon gases, tar and water vapour. As biomass feedstock has high quantities of volatile components (70-86% on a dry basis), pyrolysis step plays an important role in biomass gasification. Then oxygen supplied to the gasifier reacts with the available combustible substances and CO₂ is formed. Hydrogen component of biomass also undergoes oxidation to produce water, leading to release of large amount of heat produced by oxidation of carbon and hydrogen. Partial oxidation of carbon also may occur and carbon monoxide produced. H₂O and CO₂ subsequently undergo reduction through contact with the char (product from pyrolysis) in the absence of oxygen^{74 75 73}. The temperature ranges of each step and the kinetics parameters of the degradation products, depend on the characterisation of biomass, the heat transfer rate and the degree of the oxidizing environment.

2.3.3 Biological Pre-Treatment of Biomass

Biological pretreatment of biomass employed microorganism such as brown, white and soft rot-fungi to degraded hemicellulose, lignin and small part of cellulose. Although this pretreatment requires low energy and mild operation condition, the hydrolysis rate is very slow and long residence time is required^{67, 76}. The ability of Microorganisms for ethanol fermentation categorised based on the process parameters, compatibility with existing products, type of fermentation and equipment. Wide range of microorganisms used in the fermentation of biomass to bioethanol. For example, fungi can decompose cellulose, hemicellulose and lignin through series of enzymatic reactions⁶⁶.

2.3.4 Hydrothermal Conversion of Biomass

Hydrothermal conversion of biomass is defined as an effective pathway to decompose biomass, whether wet or dry, into renewable fuels⁷⁷. Among the available technologies for biomass conversion, hydrothermal liquification of biomass is reported a suitable process that tackle the wet biomass conversion to fuels. The major difference between wet biomass (such as microalgae and forest biomass residues) and dry biomass treatments is pre-treatment step elimination⁷⁸. Hydrothermal

conversion operated by two ways: (a) biomass first converted to syngas and then subsequently produce fuels, (b) biomass converted to liquid fuels directly through using solvents such as sub/supercritical water, alcohols and ionic liquid. The second option has the priority due to the mild operational condition, higher yield of products and outstanding characteristics⁷⁸.

Hydrothermal conversion of biomass in water has numerous advantages (over other technologies) such as being eco-friendly technology, additionally natural occurrence of water in biomass eliminates pre-treatment step⁷⁹. Moreover, the consumption of water is less and the efficiency is more compared to pyrolysis, due to the fact that bio-oil produced from hydrothermal conversion which has lower content of oxygen, smaller molecular weight and higher heating value, has higher quality and better chemical and physical characteristics^{80, 81}. However the key factors such as temperature, solvent, pressure, time and catalyst affect significantly the yield of products⁷⁸. Figure 2-8 presented the schematic overview of hydrothermal conversion of biomass.

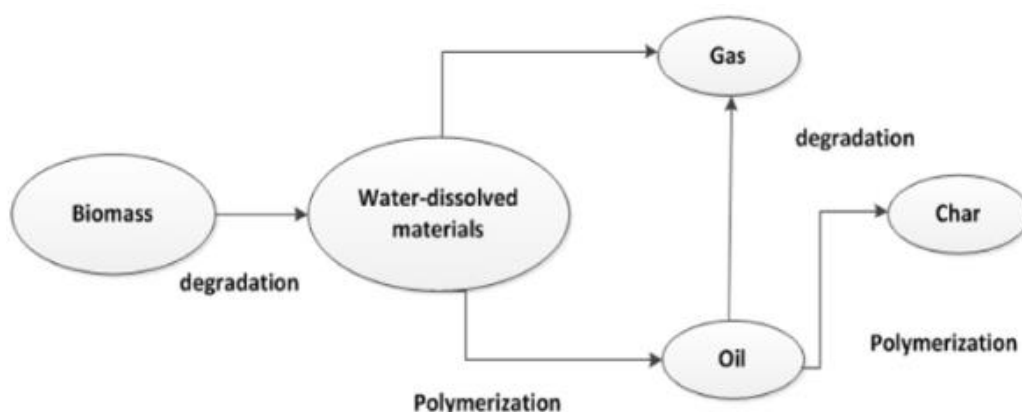


Figure 2-8: schematic overview of hydrothermal conversion of biomass⁷⁸

Acid hydrolysis, alkaline hydrolysis and hydrolysis in HCW are used to convert biomass component such as cellulose to its monomer or oligomers and make biomass ready for enzymic hydrolysis. Although dilute acid hydrolysis resulted in high glucose yield, the degradation rate is also massive and there is a limitation of heat transfer at higher temperature^{82, 83}. On the other hand, concentrated acid hydrolysis produces high glucose yield and minimal glucose degradation, but it has some disadvantages such as cost, environmental and corrosion issues that makes this technology economically unviable^{53, 84}. Similarly, in alkaline hydrolysis the yield of

sugar is low particularly at temperature lower than 100 °C due to the degradation. Additionally, organic acids produced during hydrolysis consume the alkali^{46, 53}.

Hydrolysis in HCW is a pretreatment with water at high temperature and pressure. Unlike acid hydrolysis and alkaline hydrolysis, environmental and corrosion problems can be avoided as no catalyst or chemicals involve in hydrothermal conversion in HCW⁵³.

2.3.4.1 Properties of Hot Compressed Water (HCW)

At condition near the critical point, water has attractive properties that make it as a promising reaction medium^{85, 86}. The main properties of water that can determine the identity of the reaction medium are density, ion product (K_w), dielectric constant and miscibility⁸⁷. These properties can be modified by variations in temperature and pressure of water near critical point which consequently provide different reaction conditions to produce desired products⁸⁸. HCW is defined as water above 150 °C and at sufficiently high pressure⁸⁹. By changing the temperature, the nature of reactions governed by HCW changed. Regarding the critical point of water ($T_c = 374$ °C, $p_c = 22.1$ MPa, $\rho_c = 320$ kg/m³), HCW is divided to subcritical (below its critical point) and supercritical (above the critical point) water. Table 2.4 summarizes the properties of normal water, subcritical and supercritical water. Subcritical water is pressurized water in condition below at critical point, above its boiling point temperature and at ambient pressure (>100°C and 0.1 MPa)⁸⁹. The ion product of water, K_w , (self-ionization constant) increases by three orders of magnitude from $K_w = 10^{-14}$ mol²/Kg² at 25°C to approximately $K_w \sim 10^{-11}$ mol²/Kg² at 300°C which has the decreasing trend by increasing temperature above the critical point^{88, 89}. High ionic products lead to high concentration of H⁺ and OH⁻ ions which convert water to excellent reaction medium that can act as an acid or base catalyst for homogenous reactions such as biomass hydrolysis⁹⁰. In subcritical region, dielectric constant decreases by increasing temperature from 78.5 (normal water) to 27.1 at 250 °C which gives rise to solubility for organic compounds^{86, 89, 91}. Generally ionic reactions such as dehydration of carbohydrates, are favoured at subcritical region due to the high density and high dissociation constant of water⁸⁶.

Table 2-4: Different properties of ambient water, subcritical and supercritical water^{9, 10}.

Properties	Normal water	Subcritical Water	Supercritical Water	
Temperature T (°C)	25	250	400	400
Pressure p (MPa)	0.1	5	25	50
Density ρ (gcm ⁻³)	0.997	0.80	0.17	0.58
pK _w	78.5	27.1	5.9	10.5
Dielectric constant ϵ	14.0	11.2	19.4	11.9
Heat capacity C_P (kJ kg ⁻¹ K ⁻¹)	4.22	4.86	13.0	6.8
Dynamic viscosity η (mPas)	0.89	0.11	0.03	0.07
Heat conductivity λ (mWm ⁻¹ K ⁻¹)	608	620	160	438

On the other hand, supercritical water is above the critical point and the dielectric constant varies in the range of 3.7~19^{92, 93}. Density of water at this range varies continuously, changing from the liquid phase values to gas phase values without any transition occurred between phases⁸⁸. From macroscopic point of view, supercritical water has non-polar solvent properties and supports free radical reactions, On the other hand, the single water molecule is still available which makes water act as polar solvent and interact with ionic compounds^{88, 90}. In addition, gases are complete miscible in supercritical water, makes water to be considered as a good solvent in the reactions involved organic compounds and gases⁹⁰. By variation of the temperature and pressure and consequently the density in supercritical region, supercritical water can cover a wide range of reaction of free radical to ionic reactions due to the different ionic product values⁸⁸. Figure 2-9 shows the properties of water as a function of temperature⁸⁵.

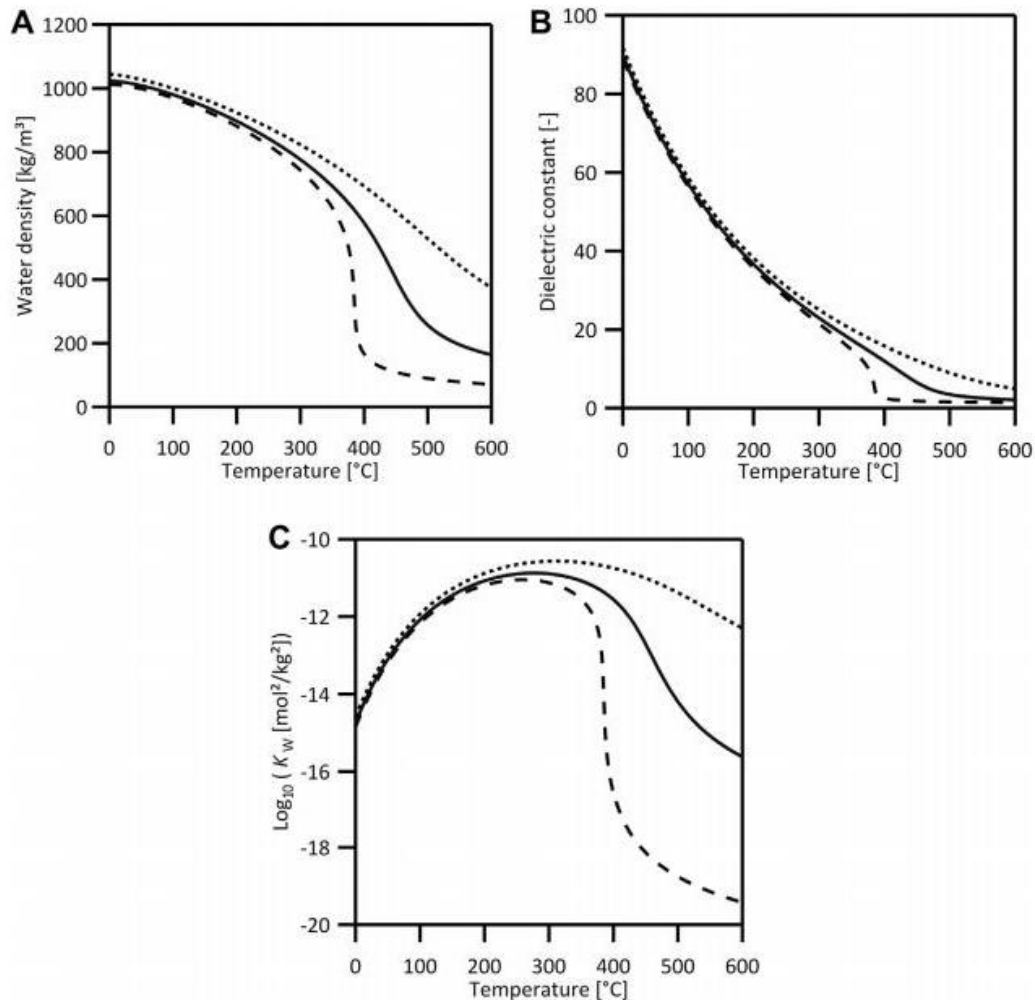


Figure 2-9: Properties of water at different temperatures. (A): Density, (B): Dielectric Constant, (C): Ion product. Dashed line: 25 MPa; solid line: 50 MPa; dotted line: 100 MPa⁸⁵.

2.4 Lignocellulosic Biomass Hydrolysis in HCW

The large volume of previous studies have witnessed significant research efforts in Lignocellulosic biomass hydrolysis in HCW^{19, 33, 65, 92, 94, 95}. The main objective of hydrothermal degradation of biomass is production of platform chemicals and a pretreatment step for fermentation process to produce ethanol⁹⁴. Generally, the hydrothermal conversion of biomass comprises three major steps: (i) depolymerisation of the biomass, (ii) decomposition of biomass monomers (iii) recombination of reactive fragments^{78, 86}.

As lignocellulosic biomass consists of different components (cellulose, hydrocellulose and lignin) with different hydrolysis behaviour, finding the optimised

condition with the high yield of target products would be difficult. Figure 2-10 shows some of the products from degradation of lignocellulosic biomass main components during hydrothermal conversion.

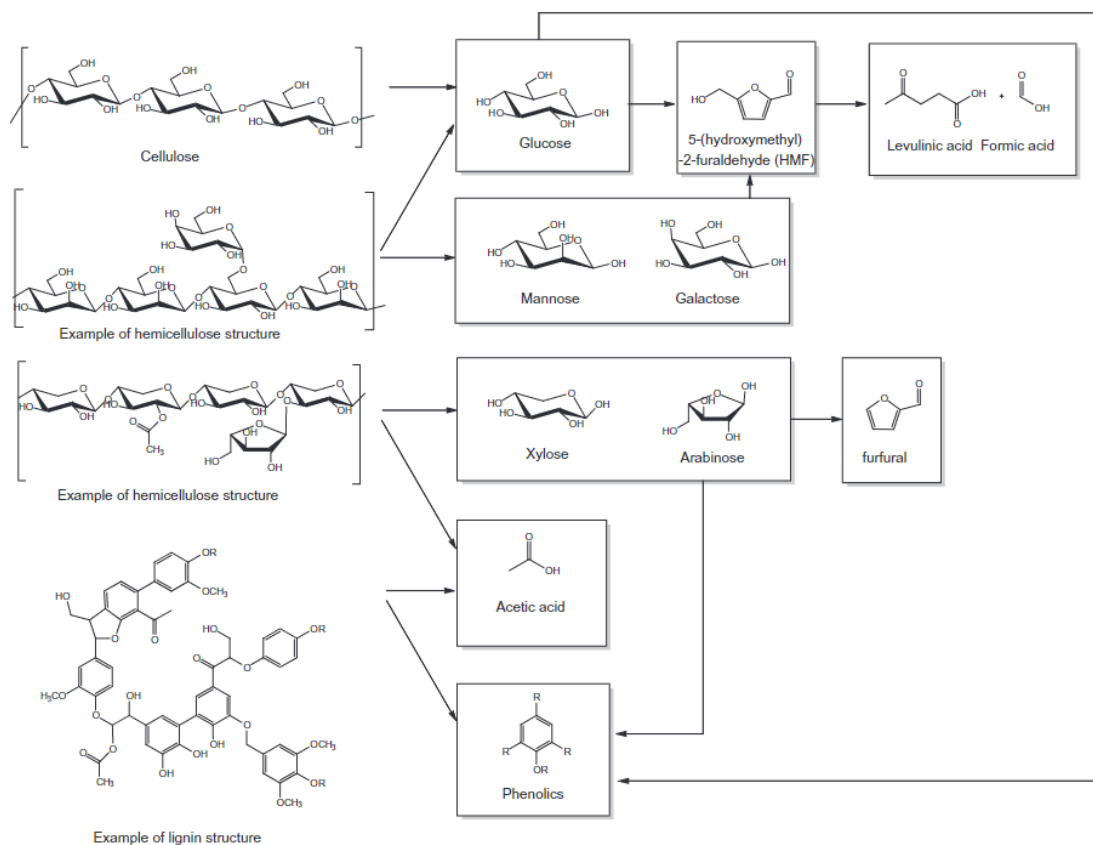


Figure 2-10: summary reaction routes for the degradation of main components of lignocellulosic biomass during hydrothermal conversion⁹⁶.

Hydrothermal degradation of biomass can be carried out in batch^{34, 97-99}, semicontinuous^{11, 19, 34, 100-102} and continuous reactor systems^{20, 41, 65, 103}. In batch system^{34, 97-99}, biomass particles are mixed with HCW in the reactor and hold at desired pressure and temperature, the reaction residence time is long leading to degradation of liquid products, low sugar yields and high yields of oil and char. In semicontinuous reactor system^{11, 19, 34, 100-102}, the feedstock is charged in a reactor and a stream of HCW is fed and flows through the bed of feedstock. In continuous reactor system^{20, 41, 65, 103}, the slurry of feedstock particles and HCW is fed to the reactor at the same time. In both semicontinuous and continuous reactor systems, the reaction effluent is rapidly quenched to stop the reactions immediately and the liquid products are collected to analyse. The residence time is short compared to batch reactor system, leads to less degradation and higher yield of sugar products^{41, 65}.

Bobleter et al.^{46, 104} reported that semi continuous reactor system produce more digestible cellulose, hemicellulose with higher sugar content and higher lignin removal.

To understand the hydrolysis behaviour of lignocellulosic biomass and optimize the experimental condition to increase the yield of target products, component fractionation of biomass provides great knowledge. Various biomass model compounds^{33, 34, 94} studied to investigate the reaction mechanism of biomass hydrolysis and liquid product characterisation. Ando et al.³³ studied decomposition of three biomass model compounds in HCW and found out that most of hemicellulose solubilized and flow out at 180°C, whereas cellulose starts to decompose at temperature above 230°C. It is also reported that lignin removal depends on the amount of lignin available in biomass, relatively moderate lignin content results the extraction of lignin at low temperature with hemicellulose. Another study⁹⁴ reported the degradation of willow as a biomass model compound at 200-350°C and found out that hemicellulose and lignin dissolve at 200°C, while cellulose decomposes at 280-320°C. On the other hand, part of the cellulose that available in amorphous form dissolve at 215-230°C. It is noteworthy to say that at temperature >230°C, precipitation formed as a result of the re-condensation reactions of primary products from lignin and hemicellulose. Therefore, cellulose blocked in the reactor and become inaccessible for the hydrolysis, leading to cellulose dehydration reactions and char-like solids form inside the reactor.

Several attempts have been made to separate biomass components using two step hydrolysis process in HCW. Previous studies^{34, 105-109} conducted two step hydrolysis by semicontinuous reactor system in HCW and found that while hemicellulose and lignin solubilised in a recoverable form in the first step at 230°C, crystalline cellulose decomposed in the second step at 270°C. Lu et al.¹⁰⁶ analysed the liquid products at both steps, concluded that products from first step comprise xylose, xylo-oligosaccharides, glucuronic and acetic acid from hemicellulose and also lignin products including guaiacyl and syringyl units and the second step accounted for cellulose hydrolysis products, glucose and cello-oligosaccharides.

Treating of lignocellulosic biomass in combined supercritical and subcritical condition studied by Zhao et al.^{110, 111} to increase the yield of fermentable hexoses

and production of valuable chemicals including furfural and 5-HMF. At the first step in supercritical water, lignin removed from lignocellulosic biomass and cellulose decomposed into oligomers, followed by second step in subcritical water which oligomers turned to fermentable hexose¹¹². On the other hand, this method has adverse effect on fermentable sugars production such as xylose in hemicellulose which were degraded when the glucose yield reached the maximum.

Sugar recovery varies between hydrolysis of different biomass model compounds in HCW. Sugar recovery is low from hydrothermal decomposition of lignocellulosic biomass in HCW, mainly due to its complex structure. Additionally, most of the previous studies utilised batch reactor system to hydrolyse lignocellulosic biomass in HCW which resulted in sugar products degradation due to the long residence time during heating up and cooling down processes. On the other hand, hydrolysis in continuous and semi continuous reactor system resulted in higher amount of sugar products due to the shorter residence time which prohibits the degradation of sugar products. Sakaki reported 40% of glucose recovery from hydrolysis of cellulose under continuous reactor system. Hashaikeh studied hydrothermal dissolution of willow (with 50% cellulose content) at two stages under continuous reactor system and 20% glucose recovery obtained at 95% dissolution of willow.

Using continuous and semi continuous reactor system produce large amount of sugar oligomers in the liquid products, therefore it is preferable to combine HCW with another treatment i.e. enzymes to convert sugar oligomers to monomers as the fermentable sugars.

2.5 Cellulose Hydrolysis in HCW

The mechanism and temperature of decomposition of cellulose, hemicellulose and lignin are different due to the difference in their structures. Lü and Saka studied the hydrolysis of lignocellulosic at 170-290°C treated by semi flow and batch hot compressed water, the maximum saccharides production (16.1%) reported from cellulose obtained at 270°C when treated by semi flow hot compressed water which was much higher than 2.1% obtained from batch type reactor at 230°C³⁴.

Series of studies carried out by Yu and Wu^{19, 113, 114} to investigate the primary reactions of cellulose in HCW and evolution of cellulose structure at 180-270°C and 10M Pa. They used the semi continuous reactor system to minimize the secondary reactions of primary liquid products. The results suggested that glucose oligomers with high DP (>25) produced from primary reactions of cellulose. It is also observed that reactive components are consumed at 180-200°C and 230°C at amorphous and microcrystalline part of cellulose respectively. Other parallel reactions including breaking the hydrogen bond, degradation reactions and cross-linking reactions are also involved in hydrolysis of cellulose at HCW. It has also been inferred that glucose oligomers accounted for 31-34% (on a carbon basis) of the liquid products and post hydrolysis of the primary liquid product resulting in ~80% glucose recovery during hydrolysis of cellulose at 270°C under HCW. It is important to note that the amount of hydrolysis reaction can be influenced by some cross linking reactions which occur during hydrolysis¹⁹. Monosaccharides or oligosaccharides in liquid products are prone to decompose through dehydration or fragmentation reactions and form compounds such as furfural, 5-HMF, levoglucosan, glycoaldehyde and erythrose³⁴.

Sasaki et al.^{20, 98, 115-118} carried out a comprehensive research on hydrothermal conversion of cellulose at higher temperature at subcritical and supercritical water, 290-400°C and a pressure of 25 MPa. The main degradation products are hydrolysis products including oligomers (cellohexaose, cellopentaose,...) and monomers (glucose and fructose), degradation products including furfural, 5-HMF, erythrose, glycoaldehyde, dihydroxyacetone, glyceraldehyde, pyruvaldehyde, 1,6-anhydroglucose and organic acids^{98, 117, 119}. Figure 2-11 illustrated the proposed reaction mechanism of cellulose at subcritical and supercritical region²⁰.

The distribution of products is different at various temperatures. At 320°C, with retention time at around 10 s, all the cellulose converted, along with pH value reduction, and most of the products are glucose degradation products. At 350°C, the retention time is shorter and it took 2-4 s for complete degradation of cellulose but the products are similar, mainly degradation products. At supercritical region, at 400°C and 35 MPa, cellulose was completely converted at 0.05 s and hydrolysis products including oligosaccharides and monosaccharides accounted for most of the

products. It has also been shown that at lower range of temperatures, the decomposition rate of hydrolysis products (oligomers and glucose) is faster than cellulose hydrolysis rate, while at supercritical region the cellulose conversion rate is higher leading to higher yield of hydrolysis products^{20, 65, 103, 118, 120}.

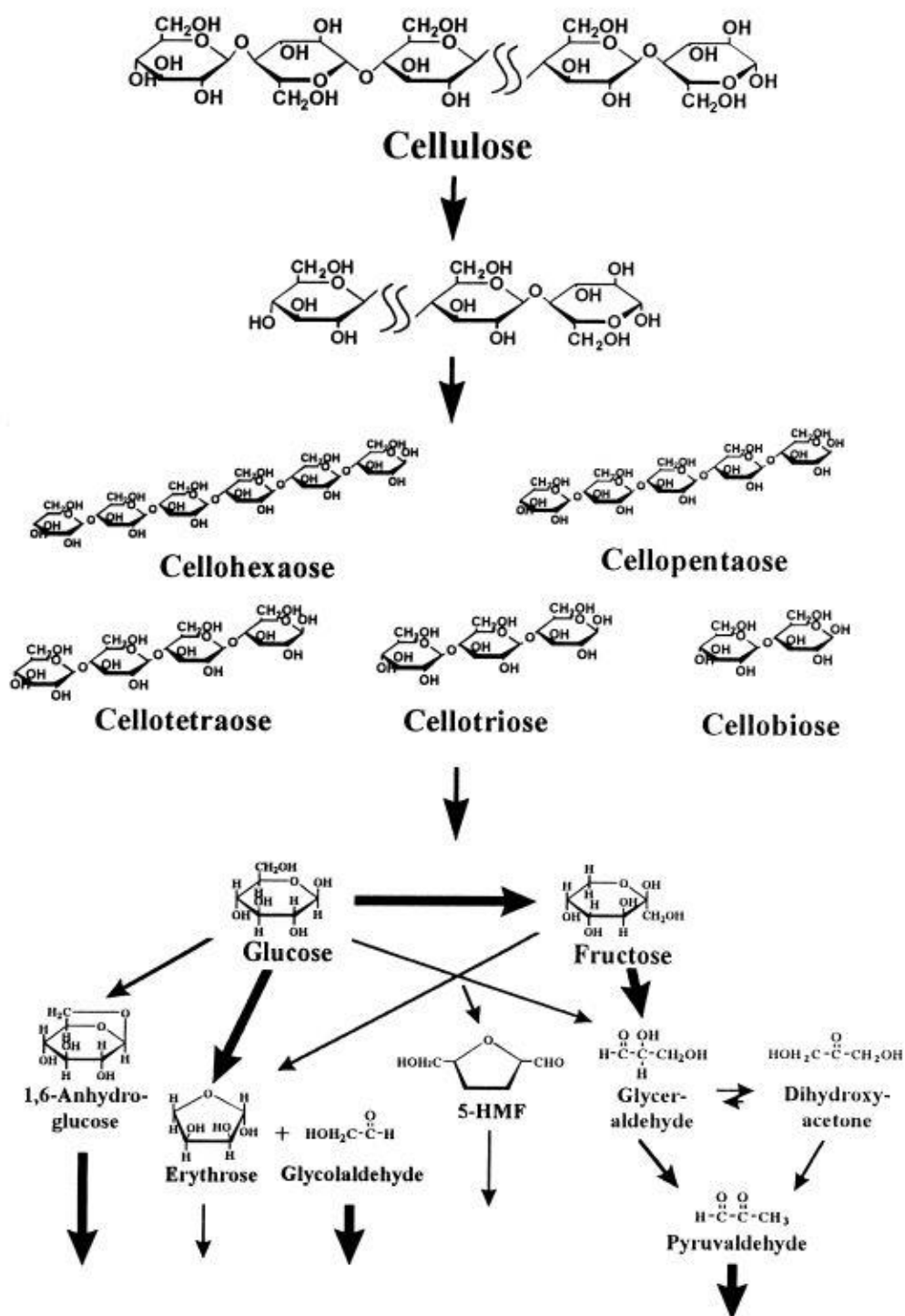


Figure 2-11: Proposed reaction pathway of cellulose hydrolysis at subcritical and supercritical region²⁰.

It can be inferred that the contribution of hydrolysis products to the overall cellulose conversion rate increased at higher temperature and pressure^{65, 103, 118, 120}. These results suggest that the reaction atmosphere is different at subcritical and supercritical water. Although the liquid products obtained after the reaction is clear transplant, precipitation occurred after a while, when the solution is maintained at room temperature and the detailed analysis prove that structure of solid residue is the same as cellulose¹¹⁵. At subcritical region cellulose I crystal appeared, while at near and supercritical condition the formation of cellulose II crystal approved which suggested the dissolution and swelling of microcrystalline structure of cellulose at high temperature. This dissolution takes place at surface area of cellulose leads to the formation of amorphous part which easily hydrolyse to low DP oligosaccharides and high formation rate of hydrolysis products at supercritical region¹¹⁵. On the other hand, hydrolysis of cellulose takes place at the surface area without dissolution and swelling at subcritical region resulted the formation of higher DP sugar oligomers^{98, 115, 116}.

While production of fermentable sugars is more favoured from cellulose hydrolysis in supercritical water, these sugars turned to degradation products faster compared to subcritical water. On the other hand, the degradation rate of fermentation sugars is lower in subcritical water, however hydrolysis of cellulose is more difficult¹²¹. Therefore, Enhara and Saka⁶⁵ treated cellulose in the combination of subcritical and supercritical water to take advantage of both conditions.

2.5.1 Factors Influencing the Reaction Pathway of Cellulose Hydrolysis in HCW

Different products from cellulose hydrolysis in HCW produce through various reaction pathways, and it is necessary to control these reaction pathways to have desired products. Therefore, it is worthwhile to understand the factors influence the reaction pathway under hydrothermal condition. The following sections summarize the major factors from hydrothermal decomposition of model compounds in HCW.

2.5.1.1 Type of Feedstock

Microcrystalline cellulose contains both amorphous and crystalline parts with various compositions, leading to different water accessibilities. Saka et al.¹²² studied hydrolysis of cellulose with different compositions and the degree of crystallinity under supercritical condition at 500 °C and pressure of 35 MPa in semi batch type reactor system. They found out although the proportion of amorphous and crystallinity parts are not the same for various types of cellulose, the hydrolysis pattern is similar. However, the glucose yield achieved is higher in cellulose II (48%) compared to cellulose I (32%) after 10 s. Hydrolysis reaction of starch under supercritical water occurs faster than cellulose, due to the fact that starch is rich in amorphous structure compared to cellulose which composes mainly of crystalline microfibrils.

Another study reported the different hydrolysis behaviour of cellulose and chitin in HCW at 300-400 °C and pressure of 15-30 MPa, and explained it due to the different intra and intermolecular hydrogen bonding structure¹²³.

2.5.1.2 Reactor Configuration

Cellulose and/or biomass hydrolysis in HCW studied under different reactor system, including batch, semicontinuous and continuous^{20, 33, 94, 101, 124-127}. In batch reactor system, the hydrolysis products exposed to long residence time, therefore glucose undergoes decomposition reactions^{39, 124, 128}. On the other hand, under continuous and semi-continuous reactor system conditions, the heating, treating and cooling times are short leads to less degradation of sugar products. Another study⁴¹ compared cellulose hydrolysis under batch-type and flow type (continuous and semi-continuous) reactor systems condition. It is reported that after settling, higher yield of hydrolysis products including sugar oligomers precipitate from fresh liquid product under flow type reactor system.

As batch-type reactor system is not sufficient to decrystallized crystalline structure of cellulose under subcritical condition, a two-steps water treatment that consists both supercritical (i.e. 0.1 s) and subsequent subcritical (i.e. 30 s) conditions using flow-

type reactor system was used. By this method, higher yield of hydrolysis products (66.8%) achieved at 30.1 s⁶⁵.

Therefore, the type of the reactor system significantly influences the characteristics of the biomass products. For example, high amounts of secondary products produced in batch reactor system, leads to low yield of sugar products. On the other hand, flow-type reactor system generally reduces the intermediates degradation in the liquid phase^{18, 124}.

2.5.1.3 Temperature

Changes in temperature leads to changes in reaction pathway, distribution of products and consequently reaction rates which follows Arrhenius equation [$k = Ae^{-E_a/(RT)}$]. Generally cellulose conversion increased at higher temperatures, such as several hours in subcritical condition accelerates to a few seconds in the supercritical condition.

Sasaki^{20, 103} reported that the hydrolysis products are higher at temperature above critical point and declared supercritical water promotes the dissolution of cellulose compared to subcritical water. Another study¹²⁹ showed the cellulose particle dissolution dependence on temperature and water density, which minimum temperature of cellulose dissolution occurs at water densities around 800 kg/m³. Cellulose particles swelled by increasing the temperatures at densities from 600-800 kg/m³. The accessibility of water to cellulose particles increased by swelling. High water densities (>900 kg/m³) causes higher dissolution temperature and reached those at the lower densities (500 kg/m³).

2.5.1.4 Catalysts

Catalysts are generally used to promote the formation of desired products and enhance the reaction rate of biomass or model compounds in HCW⁸⁹. Typically, two types of catalysts are used, homogenous catalysts and heterogenous catalysts. Wide range of homogenous catalysts, including Bronsted acids^{130, 131}, organic acids^{132, 133}, Lewis acids¹³⁴⁻¹³⁷ and bases¹³⁶, are used in hydrothermal conversion of cellulose in HCW. On the other hand, the most common heterogenous catalysts used for cellulose conversion are solid acid/based catalysts, because the solid catalysts are

environmentally friendly and it can be easily separated from solvent and reactant⁸⁵. Additionally, solid catalysts tackled the corrosion issues arising from using homogenous acid/base catalysts^{85, 138}.

It is reported that solid acid catalyst such as sulfonated activated carbon (AC-SO₃H) was used for cellulose hydrolysis, and more than 90% glucose selectivity on a carbon basis achieved at 423K.

2.6 Hemicellulose Hydrolysis in HCW

Hemicellulose demonstrates lower thermal stability than cellulose. Hydrothermal degradation of xylan, as a model substance of hemicellulose, in subcritical water was studied by Pinkowska et al¹³⁹. Liquid product fraction includes saccharides (xylose is dominant), carboxylic acids (formic and acetic acid are dominants), furfurals (2-FA is dominant), aldehydes and dihydroxyacetone. By increasing the reaction time, the yield of furfural and other degradation products increased. The reaction pathway started with depolymerisation of xylan and cleavage of acetyl group leading to formation of xylose, arabinose and acetic acid. At the next step, pentoses subjected to dehydration and retro-aldol condensation. While furfural is a product of dehydration which consequently form other intermediates like formic acid, glycoaldehyde and glyceraldehyde are the products of retro-aldol condensation of xylose and arabinose. Glyceraldehyde further converted to dihydroxyacetone through keto-enol tautomerism which in turn dehydrated to pyruvaldehyde by dehydration which can produce lactic acid^{139, 140}.

In another report, Sasaki conducted xylose degradation in the range of subcritical and supercritical temperature (360-420°C and 25-40 MPa) in the continuous flow-type reactor and concluded that retro-aldol condensation and dehydration reactions are the main primary decomposition reactions. The results suggested that retro-aldol condensation is the dominant reaction and the contribution of dehydration reaction is very small. By increasing the temperature and decreasing the pressure in the supercritical range, the rate of retro-aldol reaction become higher, while it has a little effect on the rate of dehydration reaction to produce furfural, on the other hand furfural formation is promoted at lower temperature¹⁴⁰.

Another study, treated different biomass species in hot compressed water at 200-230°C for 0-15 min and observed that 40-60% of the mass of all the sample species solubilized, considering that 100% of hemicellulose component for all of them solubilised and ~90% of that is recovered in the form of monomeric sugars¹⁴¹.

The effect of hemicellulose with different xylan structures on hydrolysis behaviour at 179°C studied by Nabarlantz et al¹⁴². It has been inferred that however all of the substrates produce xylo-oligomers, the yield and composition of oligomers are different due to the various contents of xylan and acetyl groups in the raw material. It is important to note that acetic acid produced from cleavage of acetyl group and capable to catalyse the depolymerisation of xylan in to xylo-oligomers as the primary products and subsequent secondary products, as a result, higher content of acetyl group leads to higher yield of xylose oligomers¹⁴².

Hemicellulose is a copolymer of pentoses (arabinose and xylose) and hexoses (galactose and mannose) units. Srokol et al.¹⁴³ conducted hydrothermal reaction of some pentoses and hexoses monosaccharides model compounds at 340°C and 27.7 MPa during 25-204 s. However, there are some differences on the amount and the formation rates of products, the nature of compounds formed from the studied model samples are the same. The main acid-catalyzed product is 5-HMF and base catalyzed reaction result in glycoaldehyde and glyceraldehyde and other lower molecular compounds such as organic acids are the products of fragmentation and dehydration reactions^{143, 144}. Therefore it has been concluded that the reaction pathways of hemicellulose with five-carbon sugars and six-carbon sugars structures are similar under HCW¹⁴³.

2.7 Lignin Hydrolysis in HCW

Lignin decomposes into three main monomeric parts in HCW, syringyl (S), guaiacyl (G) and p-hydroxyphenyl (H) units¹⁴⁵. Various phenols and methoxy phenols can be produced through lignin decomposition in HCW via cleavage of ether-bond⁸⁶. Guaiacol was studied as the model compound of lignin in HCW at 380-400°C and various pressures¹⁴⁶. The production of phenolic compounds including catechol, phenol and o-cresol was observed which their amounts increase by increasing time

and pressure. Additionally, by increasing the reaction time, the production of guaiacol oligomers and low-molecular-weight compounds increased¹⁴⁶.

The products yield clearly depends on the nature of the lignin and its structure. Zhang et al.¹⁴⁷ studied hydrothermal decomposition of five types of lignin at 300-374°C and found out ~33-79 wt% of liquids and ~12-49% of solids produced from hydrothermal decomposition of different types of lignin.

Figure 2-12 presents the simplified hydrothermal degradation of lignin in subcritical water into methanol soluble (MS) fraction including catechol, phenol and cresol compounds and methanol soluble (MI) fraction including residual solid.¹⁴⁵.

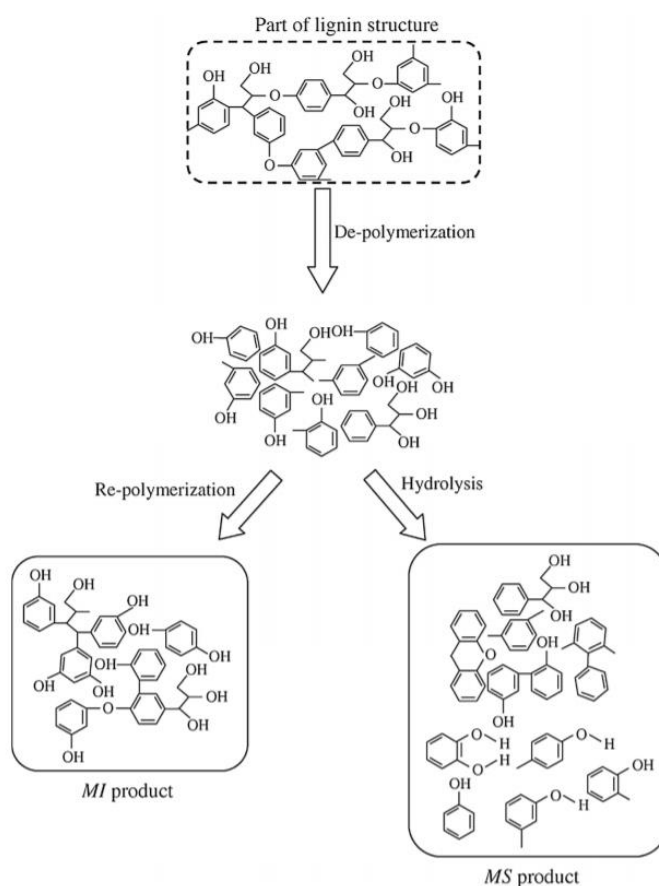


Figure 2-12: Proposed scheme for lignin decomposition in subcritical water¹⁴⁵.

2.8 Hydrothermal Decomposition of Dimers in HCW

As it mentioned in 2.5, hydrothermal decomposition of cellulose in HCW primarily produce glucose oligomers with a wide range DPs, which further decompose to glucose and other monomers. The monomers subsequently undergo secondary reactions and produce smaller molecules and value added chemicals^{19, 113}.

Due to the complexity of biomass structure, a broad range of starting materials were employed to investigate the mechanism of cellulose and biomass decomposition in hot compressed water under different conditions. In this section, hydrothermal decomposition of dimers, as the simplest sugar oligomer, studied to understand the decomposition mechanism of sugar oligomers.

2.8.1 Hydrothermal Decomposition of Cellobiose in HCW

Hydrothermal decomposition of cellobiose, as the simplest glucose oligomer with the glycosidic bond, studied significantly. Bobleter and Bonn¹⁴⁸ conducted one of the first studies on cellobiose in batch reactor at 180-249 °C. They found out that glucose is the main product with the high yield (~60%) from cellobiose decomposition in HCW but the reaction pathway and mechanism were still unclear. Investigation of mechanism and reaction rate of cellobiose at 300-420 °C conducted by Kabyemela et al.¹¹⁷ and Sasaki et al.¹⁴⁹ using a continuous reactor. They suggested hydrolysis reaction to form two molecules of glucose and retro-aldol condensation reaction to produce glucosyl-erythrose (GE) and glycolaldehyde are the main degradation reactions of cellobiose decomposition. Glucose and erythrose formed from GE by hydrolysis reaction which subsequently turn into glucosyl-glycolaldehyde (GG) through retro-aldol condensation reaction. GG is also transformed into glucose and glycolaldehyde via the hydrolysis reaction. As the decomposition proceeds, glucose (the product of hydrolysis reaction of cellobiose, GE and GG) turns into fructose, glycolaldehyde and other degradation products¹⁴⁹.

Yun Yu et al.¹⁵⁰ studied cellobiose decomposition in HCW at 200-275°C using continuous reactor system. They found out that isomerisation is the main primary reaction under experimental condition and cellobiulose (GF) and glucosyl mannose (GM) are the primary products of isomerisation reaction and small portion of

cellobiose hydrolysis into glucose in HCW. The isomerisation reaction to produce GF and GM account for 64-76% and 8-11% respectively and hydrolysis reaction to produce glucose account for 10-20% of cellobiose decomposition reactions depending on temperature. Glucosyl erythrose (GE) and glycolaldehyde are also primary products from retro aldol condensation reaction, but their contribution is very small (only <5%) compared to the isomerisation and even hydrolysis reactions of cellobiose under non-catalytic condition in HCW. The maximum selectivity of these products reach ~10% and ~ 3% for glycolaldehyde and erythrose respectively at 275°C. The study also reported the formation of organic acids as the reaction proceeds, leading to acidic condition (pH~4) which is subsequently promotes the acid-catalysed reactions like dehydration reaction to produce 5-HMF particularly at the middle and later stages of hydrothermal decomposition of cellobiose. The main reaction pathways of cellobiose decomposition at 200-275 °C shown in Figure 2-13.

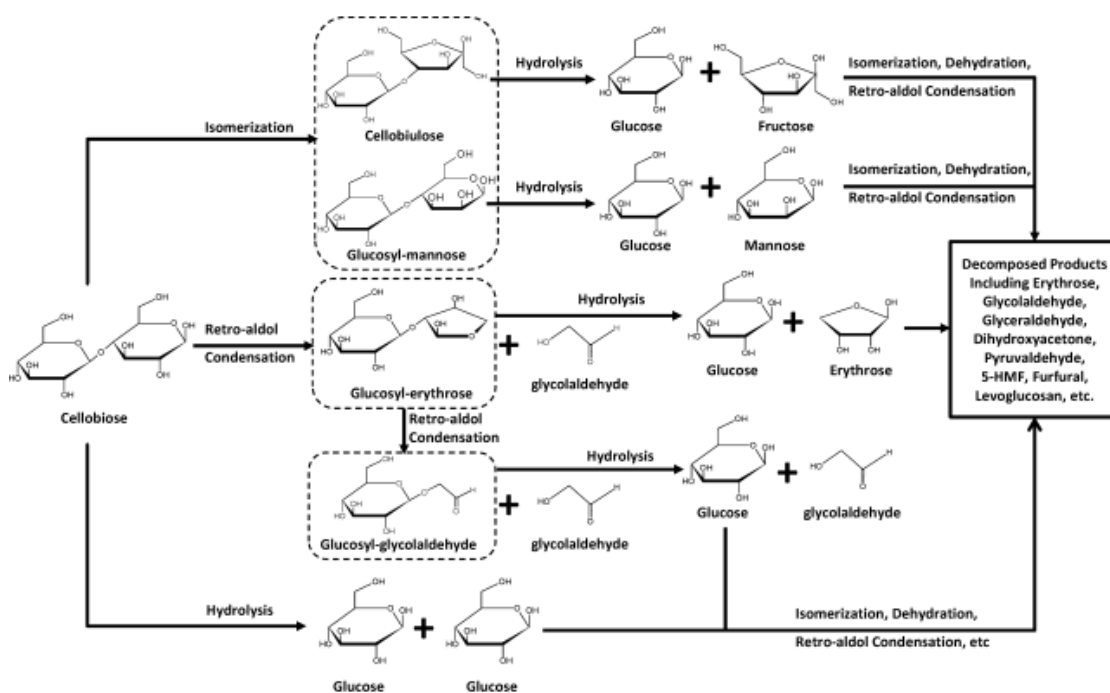


Figure 2-13: Main reaction pathway of cellobiose degradation in HCW¹⁵⁰.

As discussed earlier, saccharinic acids are the products from alkaline degradation of carbohydrates through peeling and stopping reactions, so they are also reported to produce from di- and poly-saccharides treatment in HCW. In a case of alkaline degradation of 1,4-linked polysaccharides, β -alkoxy-carbonyl elimination leads to splitting off the reducing end group and generates ISA. Additionally, 1,4-linked

polysaccharides undergoes stopping reaction leading to the formation of α and β forms of MSA, via β -hydroxycarbonyl elimination at C₃ atom at reducing end group and subsequent rearrangement of the enol through keto-enol tautomerism (figure 2-16)¹⁵¹⁻¹⁵⁴.

Xiao et al¹⁵⁵ also reported the proposed reaction mechanism and kinetics data of cellobiose decomposition in HCW. The main products are glucose, GF, GM and glucosyl-erythrose from hydrolysis, isomerisation and retro-aldol condensation, and further products produced from retro-aldol reaction of these products and intermediates. Table 2-5 presents the kinetic data of main products from cellobiose reactions in HCW¹⁵⁵

Table 2-5: Kinetic parameters of various reaction pathways of cellobiose decomposition in HCW¹⁵⁵.

Products	Reaction Pathway	Activation Energy (Kcal/mol)	Frequency Factor (s ⁻¹)
GF	Isomerisation	16.5	3.95 x 10 ⁵
GM	Isomerisation	28.3	2.27 x 10 ⁹
Glucose	Hydrolysis	25.0	1.26 x 10 ⁷
glucosyl-erythrose	Retro-aldol condensation	29.3	1.26 x 10 ¹⁰

The effect of initial pH is also investigated on hydrothermal decomposition of cellobiose in HCW by Zainun Mohd Shafie et al.¹⁵⁶. However, Isomerisation and hydrolysis reactions to produce GF, GM and glucose are the main reactions similar to non-catalytic condition, acidic condition promoted the glucose formation and suppressed isomerisation reaction to produce GF and GM.

2.8.2 Hydrothermal Decomposition of Cellobiulose in HCW

As mentioned earlier, GF is the main primary product from isomerisation reaction of cellobiose in HCW. Rashedul et al.¹⁵⁷ investigated the hydrothermal decomposition of Cellobiulose at 200-275 °C using continuous reactor system in HCW. They found out primary reactions are hydrolysis reaction to produce glucose and fructose, isomerisation reaction to produce cellobiose and GM, and retro aldol condensation reaction to produce glucosyl-erythrose and glycolaldehyde. In contrast to cellobiose decomposition in HCW that isomerisation reaction to GF and GM has the highest contribution among other primary products, for GF decomposition hydrolysis reaction to glucose and fructose contributes to ~60% at 200 °C^{150, 157}. Figure 2-14 presents the main reaction pathways of GF decomposition in HCW.

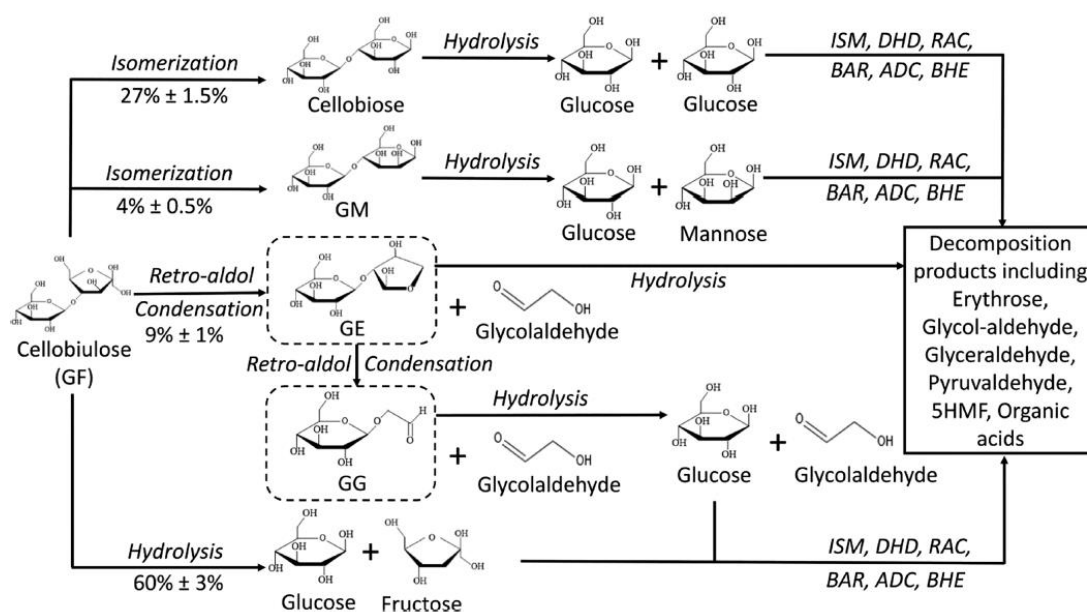


Figure 2-14: Main reaction pathway of GF decomposition in HCW. ISM: Isomerization; DHD: dehydration; RAC: retro-aldol condensation; BHE: β -hydroxycarbonyl elimination; BAR: benzilic acid rearrangement; ADC: α -dicarbonyl cleavage¹⁵⁷.

2.9 Hydrothermal Decomposition of Mono-Compounds in HCW

A number of researches have studied the detailed analysis of products from hydrothermal decomposition of different model compounds including monomers in

HCW under various catalytic or non-catalytic conditions^{143, 158-161}. The major products from hydrothermal decomposition of monomers under HCW are: 5-HMF, furfural, glycolaldehyde, glyceraldehyde, pyrovaldehyde, dihydroxyacetone, erythrose and organic acids^{89, 143, 162-164}. The contribution of each product and their rates of formation depend on the nature of starting monomer. The similarity of the products from hydrothermal decomposition of monomers can be explained by base catalysed Lobry de Bruyn-Alberda van Ekenstein rearrangement, resulting in interconversion of glucose, mannose and fructose through 1,2 enediol anion¹⁴³ (see Figure 2-15). Generally, in monosaccharides isomerization, the yield of ketoses is higher than the yield of aldoses. While mannose is isomerized to both glucose and fructose, in glucose isomerization no mannose or very little is produced compared to fructose¹⁶⁵.

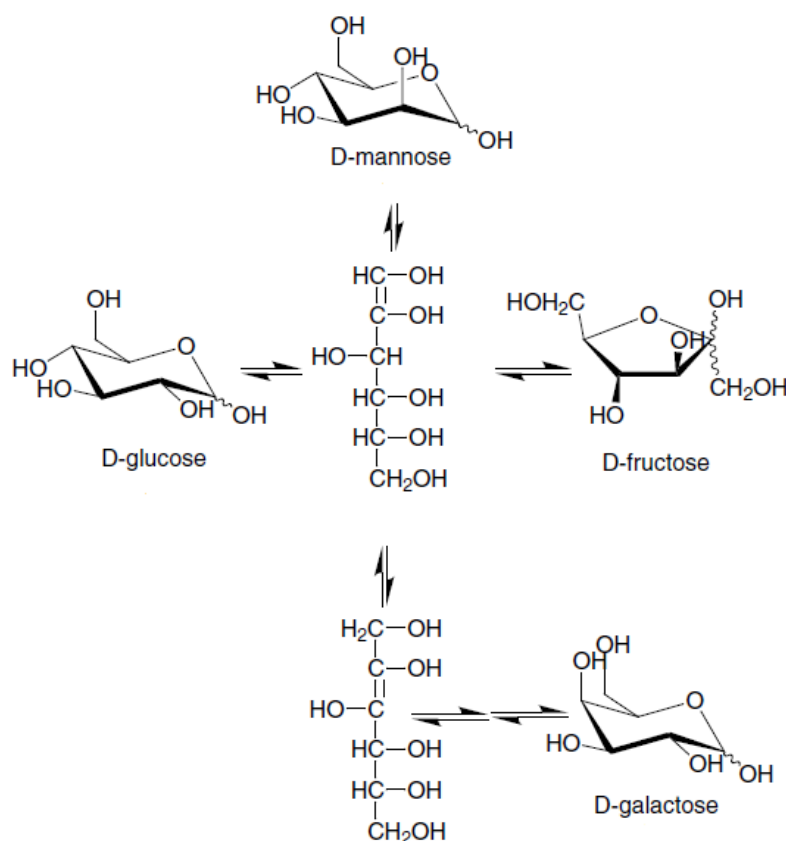


Figure 2-15: Lobry de Bruyn-Alberda van Ekenstein rearrangement during hydrothermal decomposition of monomers¹⁴³.

The general reaction mechanism of the monomeric sugars in HCW is summarised in Figure 2-16.

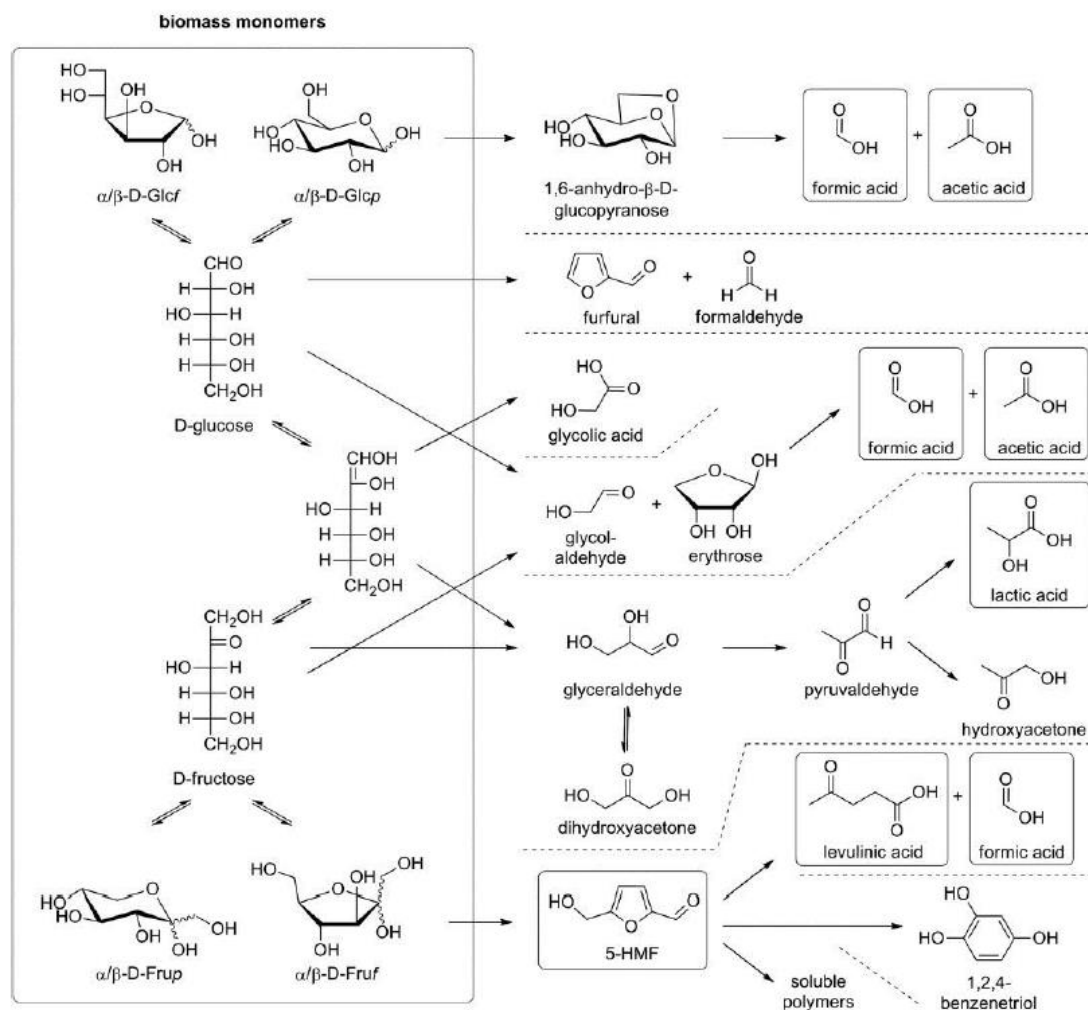


Figure 2-16: Decomposition of biomass derived monomers and their products in HCW⁸⁹.

2.9.1 Hydrothermal Decomposition of Glucose and Fructose in HCW

Most of the previous literatures studied the decomposition of glucose, as the most abundant biomass derived monomeric sugars, under subcritical and supercritical conditions with and without any catalyst to understand the reaction mechanism in order to increase the yield of target products^{119, 149, 150, 166-169}. Fructose, mannose¹⁶⁸, erythrose¹⁷⁰, glyceraldehyde, glycolaldehyde, dihydroxyacetone, levoglucosan, pyruvaldehyde, 5-HMF¹⁶²⁻¹⁶⁴, levulinic¹⁷¹ and formic acids are the main products from hydrothermal decomposition of glucose in HCW^{159, 172}. Figure 2-17 presents the main reaction pathways of hydrothermal decomposition of glucose in HCW¹⁵⁹. Generally, glucose decomposes through the following major reactions in HCW:

a) Glucose isomerises to fructose and mannose by Lobry-de Bruyn-van Ekenstein transformation^{159, 164}. It is found out that the rate of fructose into glucose formation is slower compared to glucose to fructose at 300-400°C and 25-40 MPa¹¹⁹. Yu and Wu¹⁷³ also reported the isomerisation to fructose as one of the main primary reactions with the highest selectivity (>90%) of glucose decomposition at 175-275 °C and pressure of 10 MPa. Additionally, by increasing the temperature and pressure to 350 °C and 25 MPa, the isomerisation reaction is contributing >50% of the primary reactions.

b) Dehydration reaction to produce levoglucosan by losing one molecule of water¹¹⁹. Kabyemela et al.¹⁵⁹ studied fructose decomposition at 300-400 °C and 25-40 MPa and no levoglucosan reported in the liquid products suggesting it is not the decomposition product of fructose, but only glucose. On the other hand, dehydration of fructose produces 5-HMF by losing three molecules of water which further decomposes to levulinic and formic acids by rehydration¹⁷⁴ and furfural is also reported as decomposition product of 5-HMF.

Glucose undergoes retro-aldol condensation reaction to produce aldehyde and ketones including glycolaldehyde, erythrose, glyceraldehyde and dihydroxyacetone¹⁷⁵. Erythrose consequently decomposes to glycolaldehyde via retro-aldol condensation¹⁷⁰ and glyceraldehyde form dihydroxyacetone by reversible isomerisation which both turn to pyrovaldehyde by dehydration¹⁷⁶.

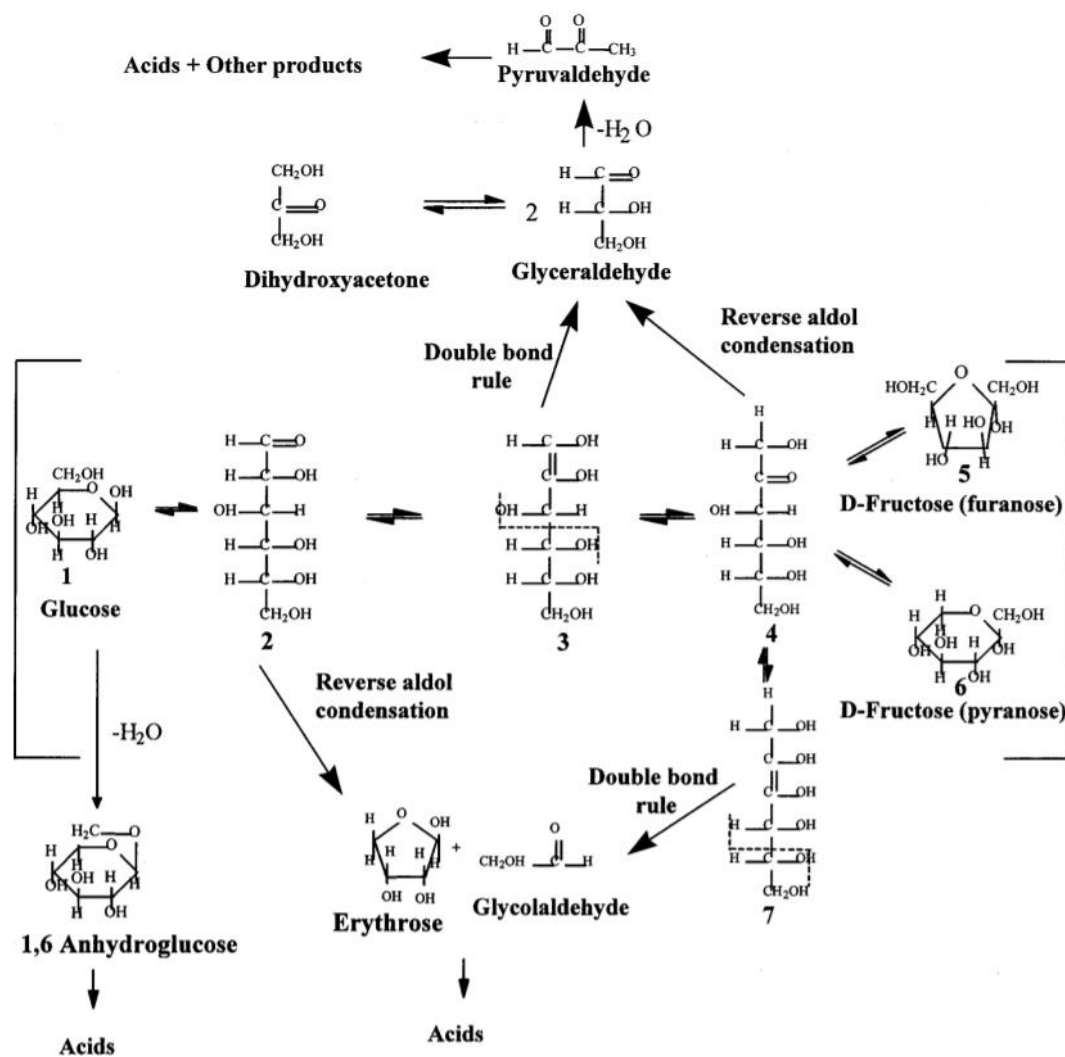


Figure 2-17: Mechanism of hydrothermal decomposition of glucose in HCW¹⁵⁹.

The formation of furfural from glucose treatment in HCW is also reported through fragmentation to pentoses and formaldehyde via retro-aldol condensation of glucose and consequently pentoses dehydrated to furfural¹⁶⁵. It is also reported that furfural is also produced when hexoses such as glucose treated in hot compressed water.

Decomposition of glucose at higher temperature (400-500 °C) and pressure (40MPa) studied by Sinag et al.^{177, 178} and they presented the simplified reaction pathway for glucose decomposition under this condition as shown in Figure 2-18. They reported two reactions mainly contribute to the total glucose decomposition: (a) glucose first dehydrated via C-O breakage to produce furfural which further undergoes dehydration into phenols, (b) C-C bond breaking via different reactions such as retro-aldol condensation to produce acids and aldehydes^{138, 178} which further decomposed to gases such as CO₂, H₂ and CH₄^{175, 178}.

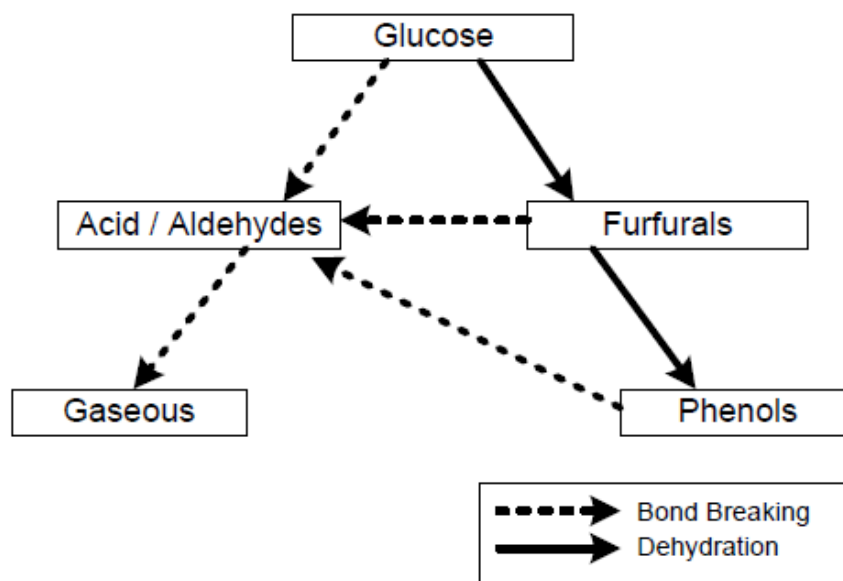


Figure 2-18: Reaction pathway of glucose decomposition under supercritical condition¹⁷⁵.

Significant studies reported hydrothermal degradation of glucose under acidic conditions^{138, 179-182}. It is found out that while the production of 5-HMF and levoglucosan is more favourable under acidic condition, the isomerisation reaction forming fructose is suppressed^{138, 143}. On the other hand, degradation of 5-HMF catalysed under acidic condition resulting to other products including levulinic acid and formic acid^{143, 183}. The effect of acid concentration studied by McKibbins et al.¹⁸³ by treating glucose with different concentration of sulphuric acid (0.025-8 N) at 140-250 °C. It is shown that the yield of 5-HMF and levulinic acid increased by increasing the acid concentration¹⁸³. Xiang et al.¹⁸⁰ and Kupiainen et al.¹⁷⁹ treated glucose under acidic condition in HCW. Both studies found out the concentration of acid which determines the hydrogen ion concentration has the important effect on the reaction pathway of glucose decomposition since protonation (adding proton to the hydroxyl group on the glucose ring from water) is the important reaction of glucose decomposition¹⁸⁴.

Hydrothermal decomposition of glucose also studied under alkaline condition. In contrast to the acidic condition, while 5-HMF and levoglucosan formation is suppressed, isomerisation reaction to produce fructose and mannose and retro-aldol condensation reaction into glycolaldehyde, erythrose and glyceraldehyde become the

important reactions^{89, 138, 143}. The formation of pyrovaldehyde, lactic and acetic acids also promote under alkaline condition.

lactic acid is reported to produce from glycolaldehyde (the degradation product of glucose by retro aldol condensation) via the formation of pyrovaldehyde through series of reaction. The possible reaction pathway of lactic acid formation from glucose can be proposed as shown in Figure 2-19.

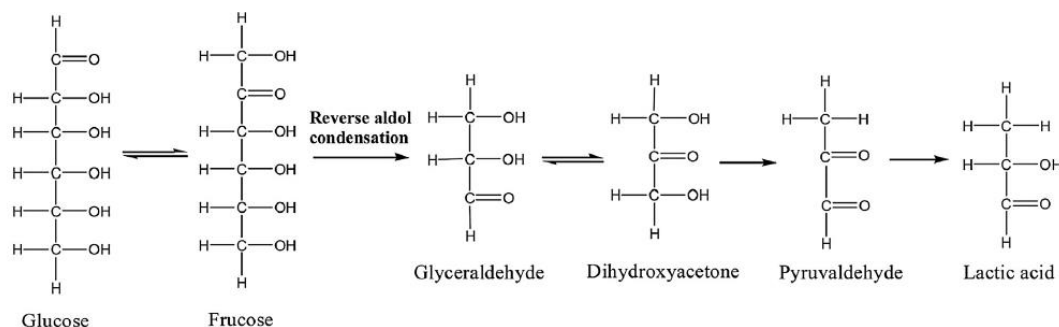


Figure 2-19: Proposed reaction pathway of lactic acid formation from hydrothermal conversion of glucose¹⁸⁵.

Turning to fructose decomposition, it is reported that glucose, mannose, 5-HMF and glyceraldehyde are the major products in hot compressed water through isomerisation, dehydration and reverse aldol reactions^{186, 187}. Figure 2-20 illustrates the reaction pathway of fructose and the main products in water at high temperature and high pressure based on previous literatures.

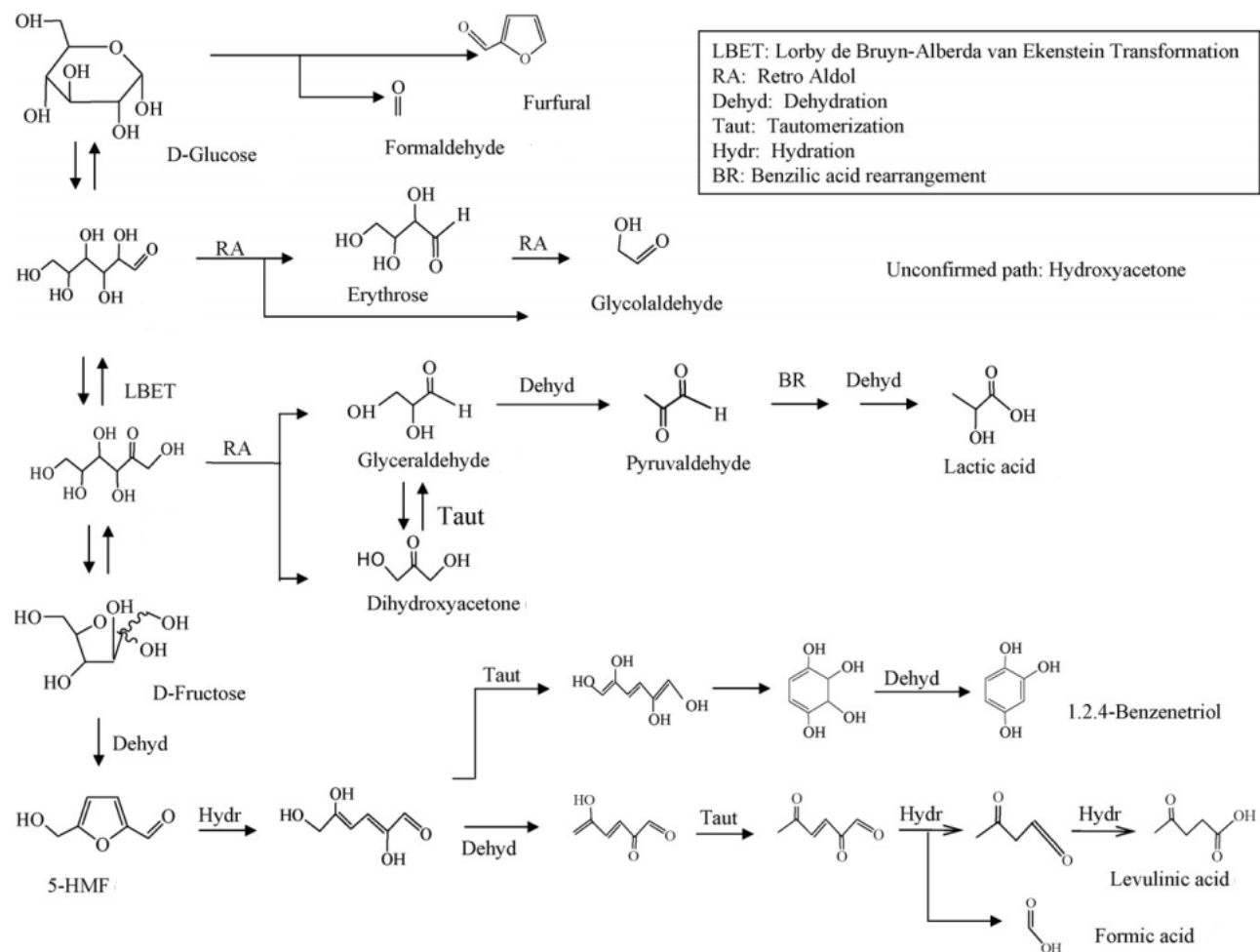


Figure 2-20: Reaction pathway of fructose in water at high temperature and high pressure¹⁸⁸.

Dihydroxyacetone and glyceraldehyde are produced from reverse aldol reaction of fructose decomposition, and pyrovaldehyde is the dehydration product of glyceraldehyde leading to formation of lactic acid through benzilic acid rearrangement^{185, 187}. Figure 2-21 shows the proposed reaction mechanism from pyrovaldehyde to lactic acid via benzilic acid-rearrangement in water at high temperature and high pressure.

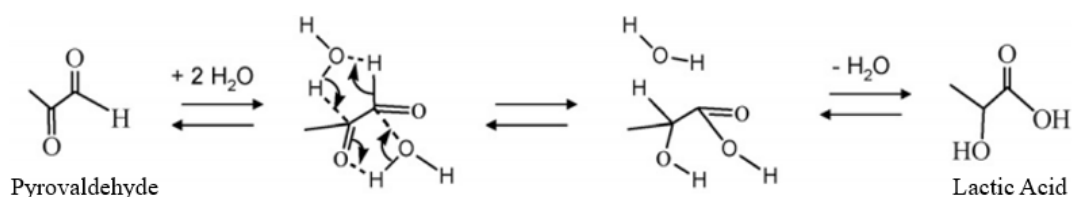


Figure 2-21: Proposed reaction pathway from pyrovaldehyde to lactic acid¹⁸⁸.

Kobayashi et al. reported the formation of glucose and mannose is not observed in the treatment of fructose in the salty subcritical water condition, due to the formation of organic acids that prohibits the base-catalysed reaction like LEAB transformation¹⁸⁹. It is also reported that the value of pH decreases as temperature and pressure increase in fructose decomposition in HCW which is attributed to the formation of organic acids such as lactic acid and levulinic acid, additionally high values of water density and longer residence time can possibly promote organic acids formation¹⁸⁸.

As it can be seen in Figure 2-22, It is generally reported that formic acid and levulinic acid are rehydration products of 5-HMF in acid catalysed reactions of fructose¹⁹⁰⁻¹⁹².

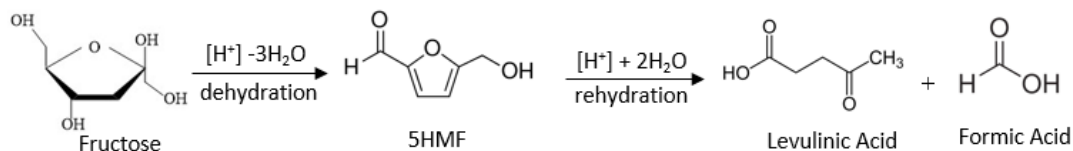


Figure 2-22: Proposed reaction pathway of formic acid from hydrothermal conversion of fructose¹⁹⁰.

It is also reported that the presence of acid significantly improve the yield of 5-HMF under identical condition, while fructofuranosyl cation is an important intermediate in the formation of 5-HMF from fructose¹⁸⁷. Kuster and van der Baan¹⁹¹ concluded

that the reaction rate of fructose decomposition and 5-HMF production is first order in fructose concentration.

Formic acid is also reported as the basic product from hydrothermal oxidation of carbohydrates including glucose and fructose in hot compressed water which involves some reactions including thermal degradation, oxidation and hydrolysis¹⁹³⁻¹⁹⁶. It has been found that yield and purity of formic acid improved by addition the alkali. The addition of alkali can prevent the decomposition of formed formic acid and also has the catalytic role in facilitating oxidation¹⁹⁷.

The proposed reaction pathway of production of formic acid from monosaccharides oxidation in the presence of an alkali is shown in Figure 2-23. At first, H₂O₂ and OH⁻ react to produce active species of HOO⁻. Then HOO⁻ attacks the carbon on the carbonyl group of the aldose (glucose) to form formic acid and H-C(O)-R by breaking C1-C2 bond. On the other hand, HOO⁻ attacks the carbon on the carbonyl group of the ketose (fructose) and form glycolic acid, H-C(O)-R' and OH⁻ by breaking C2-C3 bond. Both H-C(O)-R and H-C(O)-R' from aldose and ketose respectively, react with reactive HOO⁻ again via Root (I) until all the carbon transformed to formic acid. It is reported that 1 mol of glucose (aldose) and fructose (ketose) could generate 6 mol and 4 mol of formic acid respectively.^{194, 198-202}

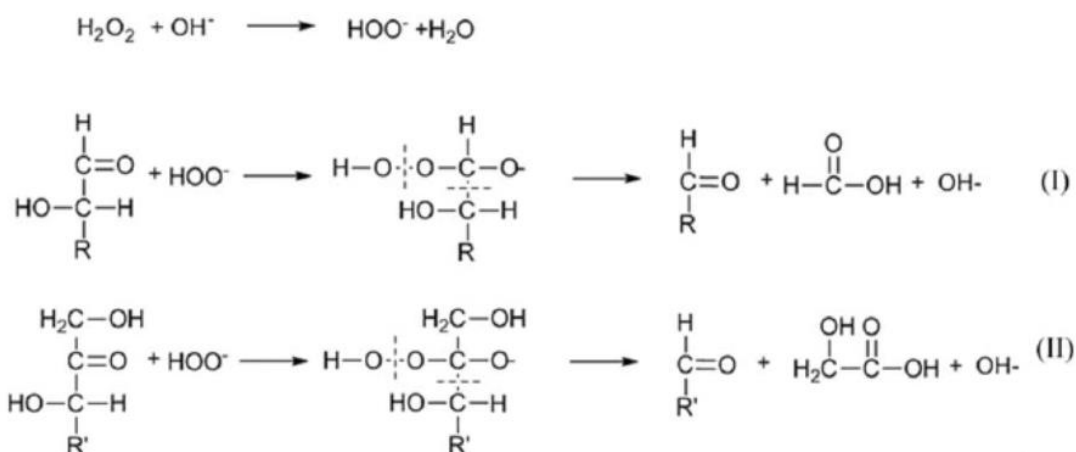


Figure 2-23: Proposed Reaction pathway of formic acid production from oxidation of monosaccharides in HCW in the presence of an alkali¹⁹⁷.

Previous literatures^{151, 152, 154, 203, 204} also reported the formation of saccharinic acids from carbohydrates including monosaccharides degradation in HCW which is the characteristic of alkaline condition. Three structurally isomeric forms have been established for saccharinic acids: saccharinic or 2-methylpentonic acids,

isosaccharinic or 3-deoxy-2-hydroxymethylpentonic acids, metasaccharinic or 3-deoxyhexonic acids (Figure 2-24).

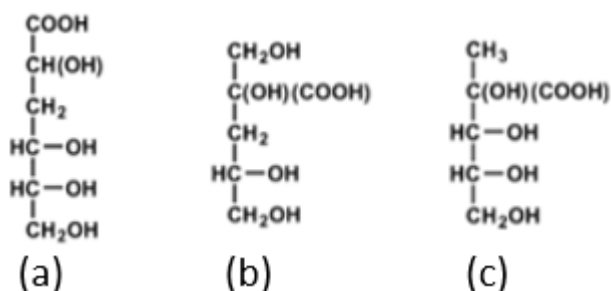


Figure 2-24: Three isomers of Saccharinic acid, (a): Metasaccharinic acid, (b): Isosaccharinic acid, (c): Saccharinic acid.

The Nef-Isbell mechanism for the saccharinic acids formation in alkali involve following steps: (a) the formation of enediol via keto-enol tautomerism followed by production and isomerisation of anion, (b) β -hydroxycarbonyl elimination to form diketo intermediate, (c) dicarbonyl intermediate formation via keto-enol tautomerism (d) benzylic acid rearrangement of the intermediate to produce the corresponding saccharinic acid (Figure 2-25)^{151, 152, 203, 204}.

On the other hand, it is widely reported that two types of reaction compete during low temperature alkaline degradation of cellulose, end-wise degradation (peeling) and termination (stopping) reactions (Figure 2-26). Isosaccharinic acid (ISA) and metasaccharinic acid (MSA) are the most important products of peeling and stopping reactions respectively^{151-153, 205, 206}. 3-deoxy-D-arabino-hexonic acid and 3-deoxy-D-ribo-hexonic acid (α , β metasaccharinic acids) are well known products from alkaline degradation of monosaccharides and di- and polysaccharides¹⁵⁴.

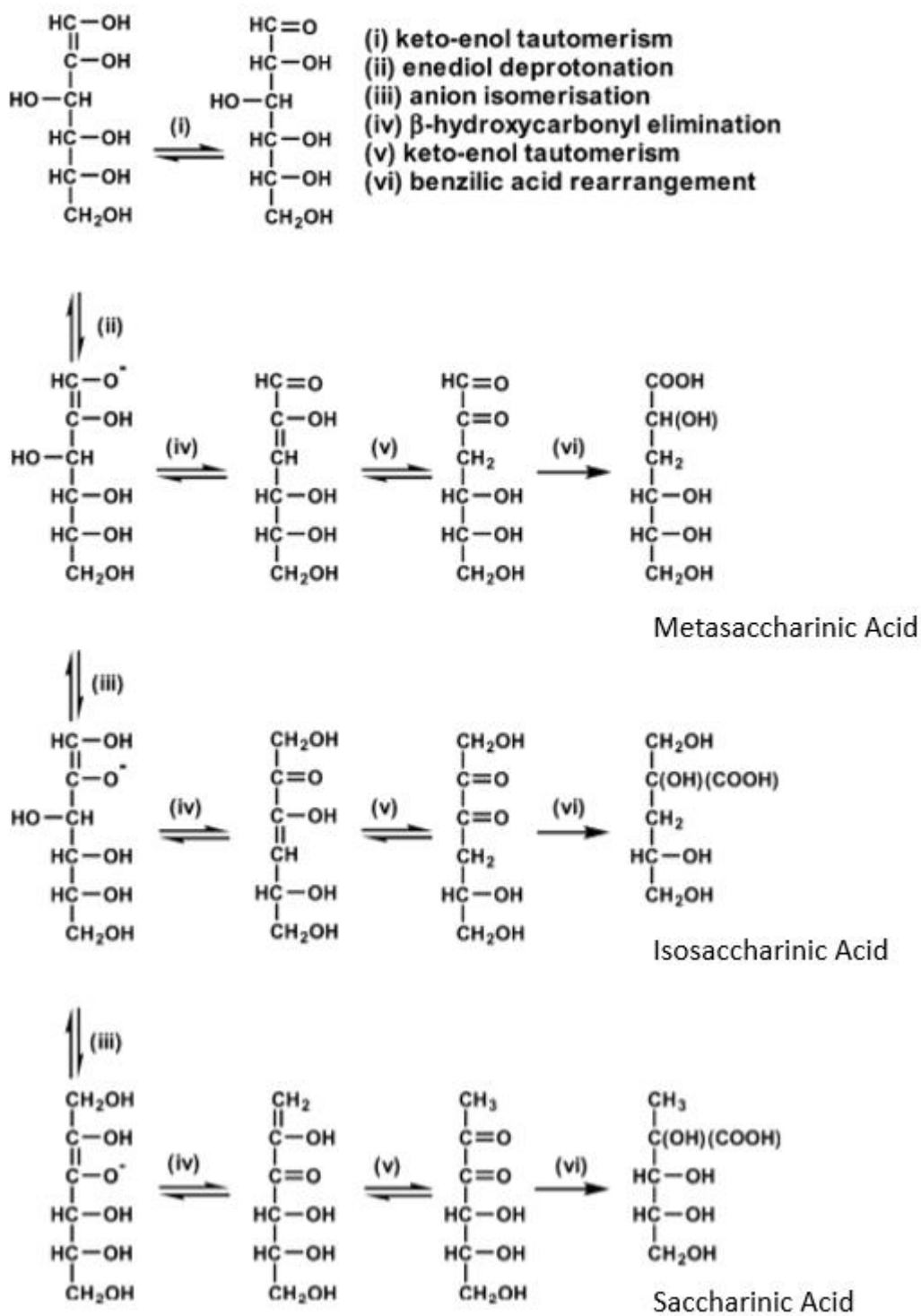


Figure 2-25: Alkaline degradation of glucose to produce saccharinic acids¹⁵².

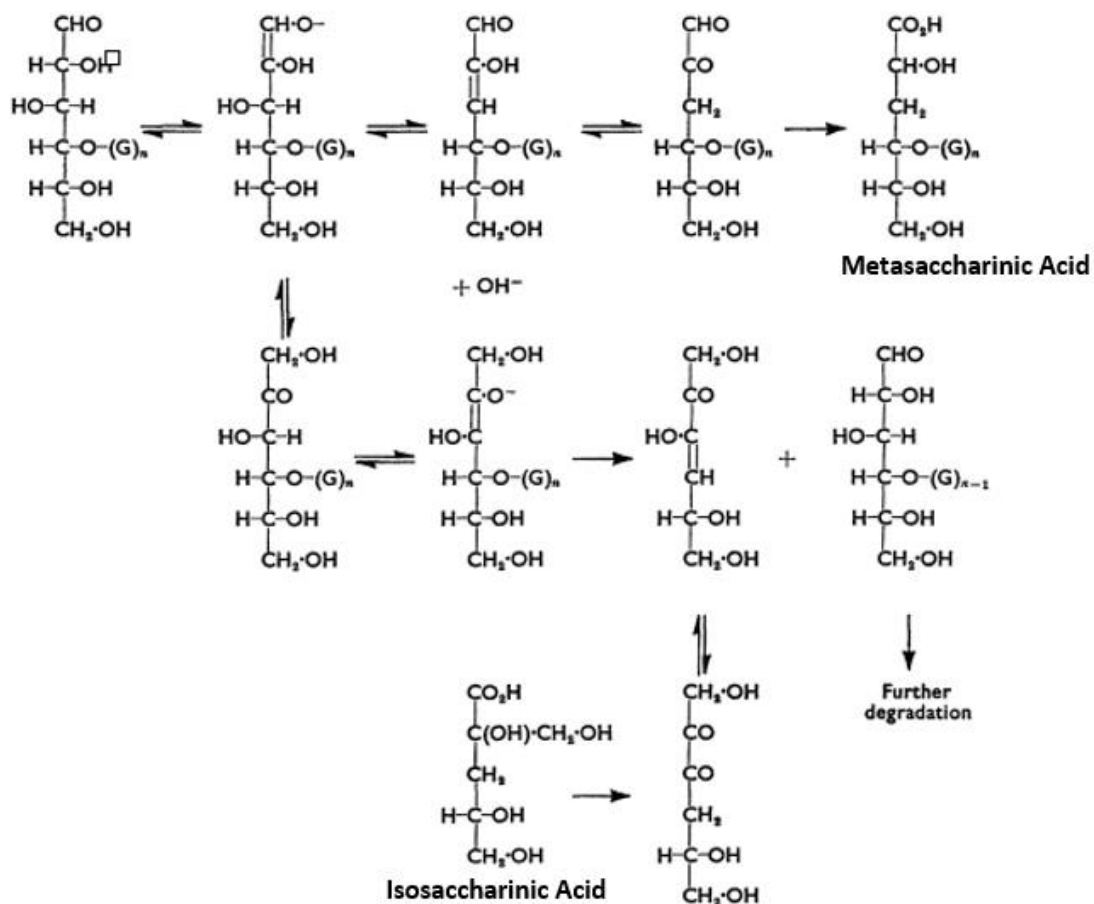


Figure 2-26: Alkaline Degradation of Polysaccharides to produce saccharinic acids²⁰⁶.

De Bruijn et al.²⁰⁷⁻²⁰⁹ investigated the effect of reaction variables on the hydrothermal degradation of monomers including glucose, fructose and mannose under alkaline condition. They found out that enediol anion intermediates produced which involved in isomerisation and other degradation products of monomers. By increasing the hydroxyl anion concentration, the rate of enolization is increased which promotes isomerisation and degradation reactions, and subsequently increase the overall decomposition of sugar monomers²⁰⁷. Maclaurin and Green²¹⁰ studied the glucose, fructose and mannose decomposition at 22 °C and 1M sodium hydroxide. They found out that isomerisation reaction of glucose, fructose and mannose is a reversible reaction.

2.9.2 Hydrothermal Decomposition of Xylose in HCW

Previous literatures^{139, 211} studied the hydrothermal decomposition of xylose as the main building block monomer of hemicellulose. The degradation of xylose at 200-300 °C and 200 bar studied and identified a range of acidic and base catalysed reactions leading to fragmentation products including formic acid, glyceraldehyde, glycolaldehyde, dihydroxyacetone, formic acid, glycolic acid and lactic acid.

The dehydration reaction of xylose to furfural illustrated in Figure 2-27, which the yield of furfural increased by residence time and temperature up to 260°C.

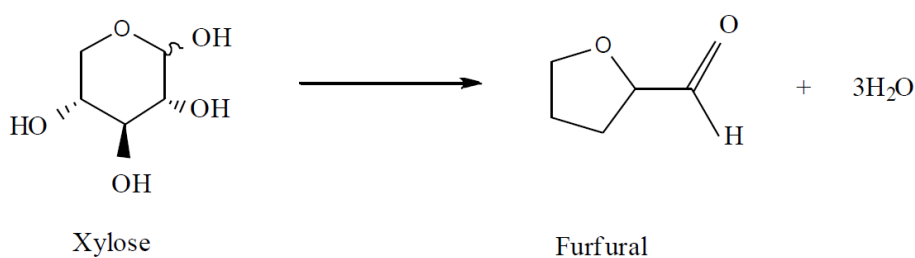


Figure 2-27: Dehydration reaction of xylose to furfural in HCW²¹¹.

Glycolaldehyde and glyceraldehyde are produced from retro-aldol reaction of xylose which is observed in Figure 2-28, minor amounts of glyceraldehyde isomerised to dihydroxyacetone at temperatures < 240°C²¹¹.

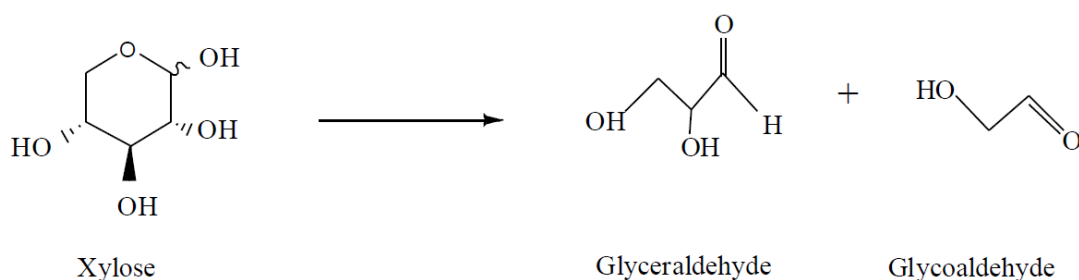


Figure 2-28: Retro-aldol reaction of xylose to glycolaldehyde and glyceraldehyde in HCW²¹¹.

At temperatures > 240°C, glyceraldehyde produces lactic acid through benzilic acid rearrangement (BR) and hydration via intermediate methylglyoxal (see Figure 2-29).

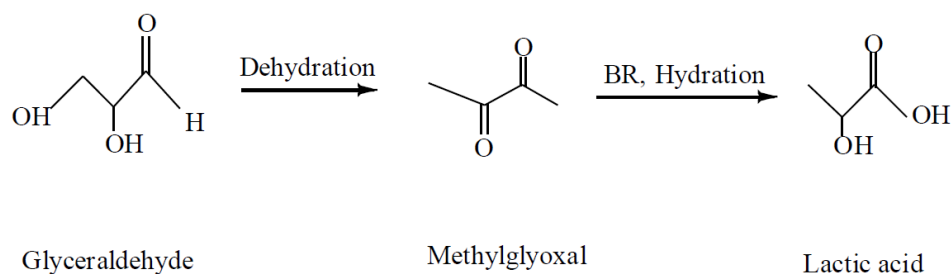


Figure 2-29: Series of reaction from glyceraldehyde to lactic acid during hydrothermal decomposition of xylose²¹¹.

Formation of formic acid is the main reason of pH reduction at all temperatures and residence times from xylose decomposition. At temperatures above 280°C and residence times ~10 seconds, formic acid decomposes to other products^{139, 211}.

Previous study reported that small amount of 5-HMF is also produced from xylose treatment in HCW, suggesting its formation passes through glyceraldehyde through cyclic intermediate.

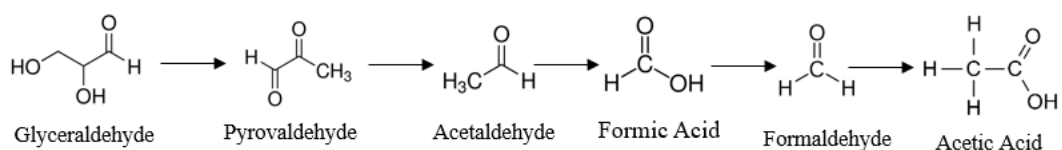
2.10 Hydrothermal Decomposition of Other Compounds in HCW

2.10.1 Hydrothermal Decomposition of Glyceraldehyde and Dihydroxyacetone

Many previous researches studied the decomposition of model compounds to understand the reaction characteristics of biomass. One of the important reactions of monomeric sugars decomposition in HCW, is retro-aldol condensation reaction. To better understand the nature of retro-aldol reaction undergoes during decomposition of sugars under hydrothermal decomposition, glyceraldehyde as the simple aldol sugar employed. It is elucidated that the nature of retro-aldol reaction of glyceraldehyde is a radical reaction under sub- and supercritical condition, and formic acid and acetaldehyde formed which are the products of the radical reaction²¹².

Kabyemela et al.¹⁷⁶ studied glyceraldehyde and dihydroxyacetone decomposition in subcritical and supercritical water condition, and found out that isomerization reaction between them occur and pyrovaldehyde produced through subsequent

dehydration. It was clearly indicated that the rate of dihydroxyacetone is higher than those of pyrovaldehyde in glyceraldehyde reaction, but the yield of pyrovaldehyde is higher than glyceraldehyde when dihydroxyacetone decomposed in HCW¹⁷⁶. Then on one hand, pyrovaldehyde undergoes benzilic rearrangements to form lactic acid, and on the other hand, formic acid, acetaldehyde and acetic acid produced through α -dicarbonyl cleavage of pyrovaldehyde. Formaldehyde with high reactivity also formed with acetic acid¹⁴³. The proposed pathway for glyceraldehyde decomposition in subcritical condition is summarized as below¹⁴³:



As discussed earlier in xylose decomposition, small quantity of 5-HMF is also reported to produce possibly through cyclic intermediate, when glyceraldehyde treated in hot compressed water¹⁶⁵.

A mixture of products contained low molecular weight acids and aldehydes including glyceraldehyde, glycolic acid, lactic acid, acetic acid and methylglyoxal identified from hydrothermal decomposition of dihydroxyacetone under subcritical water condition²¹³. A reduction of pH occurred as dihydroxyacetone decomposition progressed by increasing residence time and reaction temperature suggesting the formation of organic acids particularly lactic acid at more severe condition and higher residence time. The reaction pathway consists of isomerisation reaction to glyceraldehyde through keto-enol tautomerisation which plays an important role at higher temperatures, then dehydrated to methylglyoxal and fragmented to glycolic acid. Methylglyoxal further decomposed to lactic acid, acetic acid and formaldehyde²¹³. Table 2-6 presents the kinetics parameters of dihydroxyacetone decomposition under subcritical water condition.

Table 2-6: Kinetics parameters of dihydroxyacetone decomposition under Subcritical Condition, DHA: dihydroxyacetone; GCA: glyceraldehyde; MGX: methylglyoxal; GLYA: glycolic acid; MEOH: methanol; AA: acetic acid; FAD: formaldehyde²¹³.

Products	E_a	$\text{Ln}(A)$
$\text{DHA} \rightleftharpoons \text{GCA}$	87.3 ± 4.4	$14.93 \pm 1.10 \text{ s}^{-1}$
$\text{DHA} \rightleftharpoons \text{MGX} + \text{H}_2\text{O}$	72.5 ± 2.0	$13.20 \pm 0.47 \text{ s}^{-1}$
$\text{DHA} + \text{H}_2\text{O} \rightleftharpoons \text{GLYA} + \text{MEOH}$	72.3 ± 2.4	$7.69 \pm 0.54 \text{ s}^{-1} \text{ M}^{-1}$
$\text{GCA} \rightleftharpoons \text{MGX} + \text{H}_2\text{O}$	63.9 ± 0.1	$11.81 \pm 0.01 \text{ s}^{-1}$
$\text{MGX} + \text{H}_2\text{O} \rightleftharpoons \text{LA}$	64.3 ± 5.4	$6.87 \pm 0.48 \text{ s}^{-1} \text{ M}^{-1}$
$\text{MGX} + \text{H}_2\text{O} \rightleftharpoons \text{AA} + \text{FAD}$	139.8 ± 19.1	$22.52 \pm 4.40 \text{ s}^{-1} \text{ M}^{-1}$

2.10.2 Hydrothermal Decomposition of 5-Hydroxymethylfurfural (5-HMF)

Srokol et. al.¹⁴³ studied 5-HMF decomposition under subcritical condition and found out that the concentration of 5-HMF decreased by the reaction time. It is also reported that while the formation of several products reported, 1,2,4-Benzenetriol is the most abundant and major product which is stable under hydrothermal condition^{143, 154}. Figure 2-30 demonstrates the proposed pathway for the formation of 1,2,4-Benzenetriol from hydrothermal conversion of 5-HMF.

No 2-furaldehyde identified from 5-HMF decomposition, suggesting 2-furaldehyde formed through another pathway in hydrothermal decomposition of C6 monomers, most likely via C5 ketoses. 1,2 enediol is the intermediate from C6 monomers, which converted to 1,2 diketone via α -elimination and subsequently undergoes α -dicarbonyl cleavage to form formic acid and C5 monomers, then C5 monomers dehydrated to 2-furaldehyde^{143, 187}.

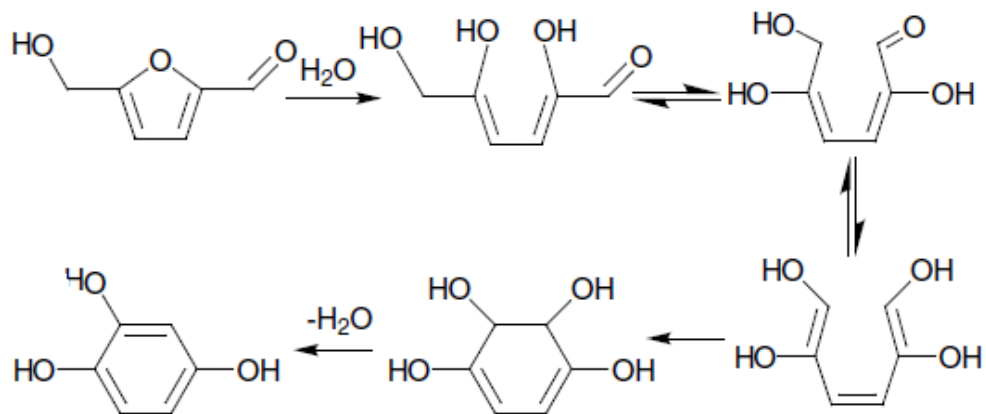


Figure 2-30: Proposed pathway from 5-MHF to 1,2,4-Benzentriol¹⁴³.

2.11 Reaction Kinetics of Biomass Decomposition in HCW

2.11.1 Global Reaction Kinetics of Biomass and Model Compounds Decomposition in HCW

Several studies^{117, 119, 125, 127, 149, 159, 161, 170, 176, 214, 215} reported the global reaction kinetics from hydrolysis of different model compounds and biomass in HCW. Matsumura et al.¹⁶¹ reported the reaction kinetics of glucose decomposition in HCW. Glucose decomposition reaction consists of parallel reactions at different temperatures and they found out that the reaction order of glucose decomposition decreases as temperature increases from 448 to 673 K, mainly due to the shifting of reaction mechanism from ionic to radicalic. Different Kinetic parameters are reported for the various reaction pathways of glucose decomposition as shown in table 2-7.

Sasaki et al. studied the kinetics of cellulose decomposition at 290-400 and 25 MPa. They revealed that the hydrolysis reaction rate is higher in supercritical water compared to subcritical water due to the swelling of cellulose. However higher sugar yield is obtained in supercritical water, they also decompose rapidly which makes the reaction difficult to control.

Table 2-7: Kinetic parameters of various reaction pathways of glucose decomposition in HCW²¹⁶.

Products	Reaction Pathway	Activation Energy (KJ/mol)	Frequency Factor (s ⁻¹)
Fructose	Isomerisation	78.6	5.71 x 10 ⁴
Erythrose	Retro-aldol condensation	96.2	2.7 x 10 ⁶
Glyceraldehyde	Retro-aldol condensation	95.6	6.59 x 10 ⁶
5-HMF	Dehydration	125.9	8.19 x 10 ⁸
Levoglucosan	Dehydration	193.2	1.21 x 10 ¹⁷

To better understand the reaction kinetics of cellulose hydrolysis, Sasaki and Kabyemela¹⁴⁹ employed cellobiose as the simplest cellulose oligomer. They considered hydrolysis and retro-aldol condensation as the main reactions. The contribution of hydrolysis reaction to the total decomposition of cellobiose decreased by decreasing of pressure at near and supercritical condition. Zainun Mohd Shafie et al.²¹⁷ investigated the kinetic parameters of cellobiose decomposition at lower temperatures (200-275°C) and different initial cellobiose concentration (10-10,000 mg L⁻¹). They reported that cellobiose decomposition is faster at lower initial concentration and the apparent activation energy of cellobiose decomposition increased (73-131 KJ mol⁻¹) at higher initial concentration (10-10,000 mg L⁻¹). Isomerisation reaction to GF production has the higher activation energy (68-133 KJ mol⁻¹) by increasing the initial cellobiose concentration compared to isomerisation reaction to produce GM (68-122 KJ mol⁻¹). Activation energy of hydrolysis reaction is higher (81-151 KJ mol⁻¹) compared to both isomerisation reactions at the same initial cellobiose concentration²¹⁷.

Sasaki et al.¹¹⁸ also studied the differences in decomposition rate between glucose and cellulose. In subcritical condition, the reaction rate constant of glucose decomposition is higher compared the value for cellulose decomposition which leads to low glucose yield from cellulose hydrolysis in this condition. In transition from subcritical to supercritical water, the cellulose decomposition rate exceeded the glucose decomposition rate, leading to a higher yield of glucose in supercritical water.

Several studies^{117, 119, 149, 159, 173, 218-220} investigated the kinetic parameters of glucose and cellobiose decomposition in HCW and reported that they follow the law of first order kinetic. The rate of decomposition reaction under non-catalytic condition of HCW can be controlled by changing the reaction parameters like pressure, temperature and the initial concentration of feedstock. Mochidzuki et al.^{220, 221} investigated the kinetic parameters of cellulose and hemicellulose from solid wastes with plant biomass source. They reported that activation energy of hemicellulose and cellulose decomposition are 85~150 kJ/mol and 130~220 kJ/mol respectively. Although it is a wide range depending on the source of the biomass, cellulose decomposition always has the higher activation energy compared to hemicellulose decomposition.

Several studies reported the kinetics data of various model compounds decomposition in HCW which follow the law of first order kinetic^{117, 119, 148, 149, 159, 161, 173, 218, 219, 222, 223}. The kinetics parameters can be controlled by reaction parameters like temperature, pressure, reactor type and initial concentration of the feedstock. Some of the results were concluded in table 2-8. Some studies report the kinetics of hemicellulose decomposition in HCW. Generally, the reaction rate of hemicellulose degradation is higher compared to cellulose degradation. The global activation energy for hemicellulose decomposition is 59-161 kJ mol⁻¹, however is 149-230 kJ mol⁻¹ for cellulose decomposition reaction^{115, 127, 139, 221, 224}. These wide range of activation energy probably due to the different reaction conditions and various origin of feedstock.

Few studies reported the kinetics of lignocellulosic biomass decomposition in HCW. The kinetics parameters studied for rice straw and palm shell decomposition in HCW at 160-220 °C and pressure of 4 MPa by Zhuang et al.²²⁴, and they found out the value is 68.76 and 95.15 kJ mol⁻¹ respectively. Lignocellulosic biomass composition and structure lead to different reaction rate and activation energy values. Table 2-9 collected some kinetics data for hemicellulose, lignin and lignocellulosic biomass decomposition in HCW.

Table 2-8: Summary of Kinetic parameters of glucose, cellulose and cellobiose decomposition in HCW under different reaction condition.

Feedstock	Reactor Type	Initial Concentration	Temperature (°C)	Pressure (MPa)	Residence Time	Activation Energy (KJ/mol)	Frequency Factor (s-1)	Reference
Glucose	Continuous	1.2 g/L	300-400	25-40	0.02-2s	96	N/A	Kabyemela et al. ¹¹⁹
Glucose	Continuous	3.6-21.6 g/L	175-400	25	< 350s	121	1.33×10 ¹⁰	Matsumara et al. ¹⁶¹
Glucose	Continuous	15 g/L	300-460	25	< 60s	95.5	6.9×10 ⁷	Promdej and Matsumara ²¹⁹
Glucose	Batch	10.8 g/L	180-220	10	< 180 min	118.8	1.4×10 ¹¹	Jing and Lu ²²³
Glucose	Continuous	0.00001-1 g/L	175-275	10	1-56s	90-109	2-10×10 ⁸	Yu et al. ¹⁷³
Cellulose	Continuous	100 g/L	290-400	30	0.02-13.1s	136	7.28×10 ⁶	Sasaki et al. ¹¹⁵
Cellulose	Continuous		240-310	25	0.5-1.6 min	147		Lv et al. ²²⁵
Cellulose	Semi-Batch		200-400	25		190		Adschiri et al. ¹⁰¹
Cellulose	Batch		250-300	10		215	2.33×10 ¹⁸	Mochidzuki et al. ²²⁰
Cellulose	Batch		250-300	10		180	5.9×10 ¹⁴	Mochidzuki et al. ²²¹
Cellulose	Batch		250-300	10		150	1.2×10 ¹²	Mochidzuki et al. ²²¹
Cellulose	Semi Continuous	10 g/L	240-310	20-25	0-3 min	147.9	5.32×10 ¹²	Rogalinski et al. ¹²⁷
Cellulose	Batch		250-300	10		230	1.6×10 ¹⁹	Mochidzuki et al. ²²¹
Cellobiose	Continuous	0.01-1.0 g/L	200-275	10	1-250s	73-131	N/A	Yu et al. ¹⁵⁰
Cellobiose	Continuous	9.8-24.4 g/L	325-400	25-40	0.01-0.54s	111.2	1×10 ^{9.4}	Sasaki et al. ¹⁴⁹
Cellobiose	Continuous	10 g/L	320-420	25-40	< 3s	51	N/A	Park et al. ²¹⁸

Cellobiose	Continuous	0.824 g/L	300-400	25	0.04-2 s	96.4	Kabyemela et al. ¹¹⁷
Cellobiose	Batch	10 g/L	180-249		< 14 min	136	Bobleter et al. ¹⁴⁸

Table 2-9: Summary of kinetic parameters from previous literature

Feedstock	Reactor Type	Reaction	Temperature (°C)	Pressure (MPa)	Residence Time	Activation Energy (KJ/mol)	Frequency Factor (s ⁻¹)	Reference
Beech wood xylan	Batch	Hemicellulose Decomposition	160-220	4	5-60 min	65.58	2.46×10 ⁶	Zhuang et al. ²²⁴
Beech wood xylan	Batch	Hemicellulose Decomposition	180-300		2-30 min	58.89	2.22×10 ³	Pinkowska et al. ¹³⁹
Spent Malt	Batch	Hemicellulose Decomposition	250-300	10		96	4.4×10 ⁸	Mochidzuki et al.
Rice Straw	Batch	Biomass Decomposition	160-220	4	5-60 min	68.76	6.89×10 ⁶	Zhuang et al. ²²⁴
Palm shell	Batch	Biomass Decomposition	160-220	4	5-60 min	95.19	3.13×10 ⁸	Zhuang et al. ²²⁴
Kraft pine lignin	Batch	Lignin Decomposition	300-374	10-22	Up to 30 min	37	70.2	Zhuang et al. ¹⁴⁷

2.11.2 Kinetic Modelling of Monocompounds Decomposition in Hot Compressed Water

The global kinetics data of biomass and model compounds fails to reveal the complexity of mechanism of feedstock decomposition and various products formation. Kinetic model of biomass decomposition in HCW is developed on the basis of numerous parameters including product analysed and global kinetic data. However, analysing of reaction pathways of biomass, main components and model compounds is difficult under hydrothermal condition, due to the intricacy of the reaction network, short lifetime of primary products and formation of various organic compounds which cause complex reaction environments¹⁵⁵.

Liang et al.¹⁵⁵ presented detailed kinetic data as shown in Table 2-10 for cellobiose decomposition in HCW based on the proposed mechanism shown in Figure 2-31. These data provided detailed insights into the mechanism of hydrothermal decomposition of cellobiose and formation of different products in HCW.

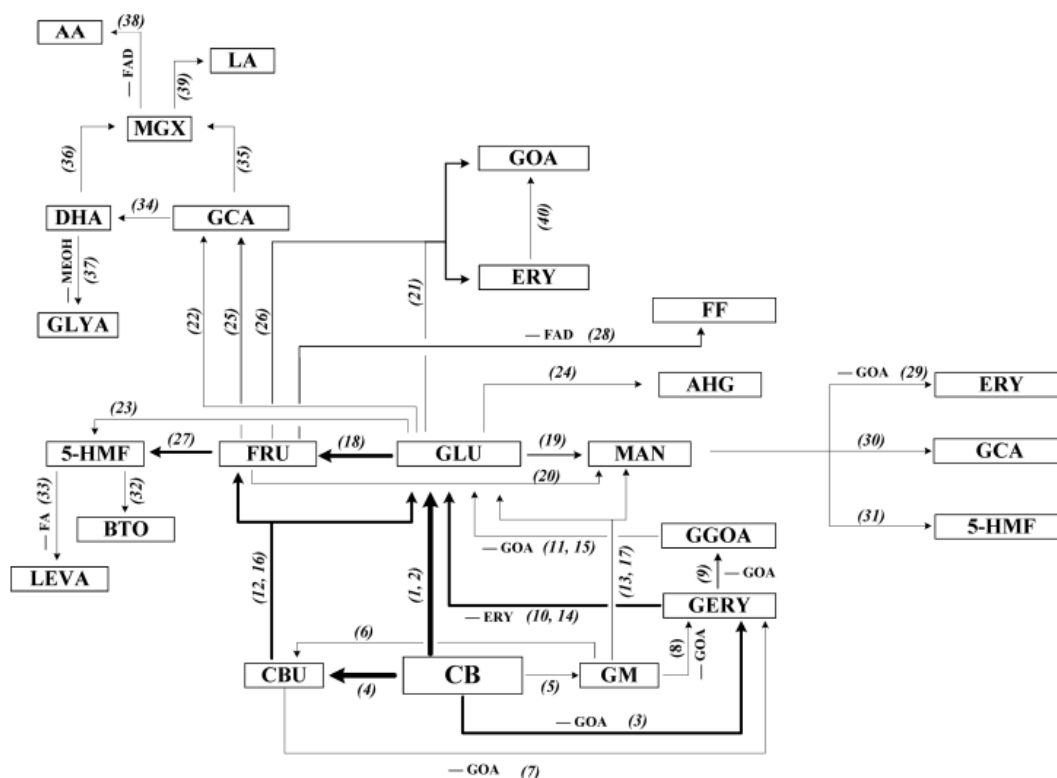


Figure 2-31: Proposed cellobiose decomposition in HCW¹⁵⁵.

Table 2-10: Detailed reactions kinetic data from cellobiose decomposition in HCW, the numbers listed are in accordance with the reaction numbers in Figure 2-31¹⁵⁵.

	Reaction	A_f	E_f	ΔG_{aq}
1	CB+H ₂ O+H ₃ O ⁺ ↔ 2GLU+H ₃ O ⁺		31.5/9.025.0	-3.8
2	CB+H ₂ O ↔ 2GLU	1.26 × 10 ⁷	25.0	-3.8
3	CB ↔ GERY+GOA	1.26 × 10 ¹⁰	29.3	11.3
4	CB ↔ CBU	3.95 × 10 ⁵	16.5	-0.7
5	GM ↔ CB	2.27 × 10 ⁹	28.3	-0.4
6	GM ↔ CBU	1.15 × 10 ⁹	25.3	-1.1
7	CBU ↔ GERY + GOA	1.26 × 10 ¹⁰	29.3	12.1
8	GM ↔ GERY + GOA	1.26 × 10 ¹⁰	29.3	11.0
9	GERY ↔ GGOA+GOA		29.3	10.3
10	GERY + H ₂ O + H ₃ O ⁺ ↔ GLU+ERY+H ₃ O ⁺		31.5/9.0	-3.2
11	GG + H ₂ O + H ₃ O ⁺ ↔ GLU+GOA+H ₃ O ⁺		31.5/9.0	-4.6
12	CBU + H ₂ O + H ₃ O ⁺ ↔ GLU+FRU+H ₃ O ⁺		31.5/9.0	-2.6
13	GM + H ₂ O + H ₃ O ⁺ ↔ GLU + MAN + H ₃ O ⁺		31.5/9.0	-3.4
14	GERY + H ₂ O ↔ GLU + ERY	1.26 × 10 ⁷	25.0	-3.2
15	GGOA + H ₂ O ↔ GLU + GOA	1.26 × 10 ⁷	25.0	-4.6
16	CBU + H ₂ O ↔ GLU + FRU	1.26 × 10 ⁷	25.0	-2.6
17	GM + H ₂ O ↔ GLU + MAN	1.26 × 10 ⁷	25.0	-3.4
18	GLU ↔ FRU	3.95 × 10 ⁵	16.5	0.5
19	MAN ↔ GLU	2.27 × 10 ⁹	28.3	0.8
20	MAN ↔ FRU	1.15 × 10 ⁹	25.3	0.3
21	GLU ↔ ERY + GOA	2.70 × 10 ⁶	23.0	11.9
22	GLU ↔ 2GCA	6.59 × 10 ⁶	22.8	14.4
23	GLU + H ₃ O ⁺ ↔ 5-HMF + 3H ₂ O + H ₃ O ⁺		30.0	-26.1
24	GLU ↔ AHG + H ₂ O	8.0 × 10 ⁷	28.9	-2.9
25	FRU ↔ 2GCA	4.90 × 10 ⁸	25.4	13.9
26	FRU ↔ ERY+GOA	1.80 × 10 ¹⁰	29.5	11.4
27	FRU + H ₃ O ⁺ ↔ 5-HMF+3H ₂ O+H ₃ O ⁺	8.4 × 10 ¹⁶	38.0	-26.6
28	FRU ↔ FF + FAD + 3H ₂ O	1.27 × 10 ¹¹	31.8	-23.2
29	MAN ↔ ERY + GOA	2.70 × 10 ⁶	23.0	11.1
30	MAN ↔ 2GCA	6.59 × 10 ⁶	22.8	13.6
31	MAN + H ₃ O ⁺ ↔ 5-HMF + 3H ₂ O + H ₃ O ⁺		30.0	-26.9
32	5-HMF ↔ BTO	3.41 × 10 ³	18.1	-24.5
33	5-HMF + 2H ₂ O ↔	1300+4.1 × 10 ⁶ C_H ₃ O ⁺	13.4	-26.9

	LEVA + FA			
34	DHA \leftrightarrow GCA	3.05×10^6	20.9	2.6
35	GCA \leftrightarrow MGX+H ₂ O	1.35×10^5	15.3	-12.7
36	DHA \leftrightarrow MGX + H ₂ O	5.40×10^5	17.3	-10.2
37	DHA + H ₂ O \leftrightarrow GLYA + ME	2.19×10^3	17.3	-3.3
38	MGX + H ₂ O \leftrightarrow AA+ FAD	6.03×10^9	33.4	-7.1
39	MGX + H ₂ O \leftrightarrow LA	1.00×10^3	15.4	-12.1
40	ERY \leftrightarrow 2GOA	2.70×10^{10}	30.1	8.9

Several studies have been conducted to investigate the reaction kinetics data of various biomass and model compounds. However, to the best of authors' knowledge, there is a research gap for the detailed kinetic modelling of other model compounds rather than cellobiose decomposition described in this section.

2.12 Conclusion and Research Gap

Hydrothermal conversion of biomass in HCW as one of the environmentally friendly technologies has received large research interest for the sustainable production of biofuels and value-added biochemicals such as organic acids. Due to the complexity of biomass structure, a series of model compounds were employed to investigate the mechanism of biomass decomposition in HCW. While hydrothermal conversion of various biomass had been carried out, little data is available for lignocellulosic biomass and main components of lignocellulosic biomass. Previous studies also reported the formation of organic acids during hydrothermal conversion of biomass which were mostly conducted under catalytic conditions, and little has been reported on the systematic study of the formation of organic acids during hydrothermal processing of monosaccharides or disaccharides under non-catalytic conditions. Therefore, further research is required to obtain fundamental understanding of lignocellulosic biomass and its components during hydrothermal decomposition in HCW, including:

- Understanding of the decomposition behavior of different components of lignocellulosic biomass in HCW under catalytic and non-catalytic conditions;

- The role of AAEM species on sugar recovery during hydrothermal decomposition of lignocellulosic biomass in HCW under catalytic and non-catalytic conditions;
- Formation mechanism of organic acids from key products of biomass decomposition in HCW including sugar oligomers and sugar monomers under non-catalytic condition;
- Fundamental studies on organic acids production from hydrothermal decomposition of hemicellulose and lignin in HCW.

2.13 Research Objectives of Present Study

From the literature review conducted in this study, several research gaps have been identified. However, it is impossible to address all identified research gaps in a PhD study. Therefore, this study focuses on hydrothermal conversion of lignocellulosic biomass and different components in HCW. Cellobiose, glucose, fructose and mannose as the model compounds employed to understand the mechanism for sugar and organic acid production from biomass in HCW under non-catalytic condition. The main objectives of this study are:

- To study the sugar recovery and role of AAEM species on sugar recovery from lignocellulosic biomass and different components of lignocellulosic biomass in HCW under non-catalytic condition
- To understand organic acid formation mechanism as the value-added chemicals from cellobiose (the simplest oligomer) decomposition under catalyst free condition of HCW using semi continuous reactor system
- To investigate the difference in glucose and fructose decomposition in HCW via quantification of produced organic acid with analytical tools
- To understand mannose decomposition mechanism in HCW under catalyst-free condition by quantification of sugar and organic acid products

Chapter 3: Experimental Set-up and Methods

3.1 Introduction

This chapter discusses the overall research methodology utilised to gain all of the thesis goals outlined in section 2.9. The experimental and analytical methods are also comprehensively explained in this chapter.

3.2 Methodology

To reach the principle objectives mentioned in section 2.8, a series of tests had been conducted. All of the experiments carried out in a semi continuous reactor system at different temperatures and pressure of 10MPa.

Experiments include:

- Hydrothermal Processing of Mallee biomass and the main components in hot compressed water
- Hydrothermal decomposition of cellobiose, as the simplest oligomer in primary products of biomass conversion in HCW, to study organic acids production mechanism.
- Hydrothermal decomposition of glucose and fructose, as the products of cellobiose conversion in HCW, to investigate the production of organic acids.
- Hydrothermal decomposition of mannose in Hot Compressed Water to study the sugar and organic acid produced.

In this research all of the experiments and analytical analysis were conducted at least in duplicates to ensure the repeatability of the results. The overall methodology used to attain the research goals in this thesis is illustrated in Figure 3-1.

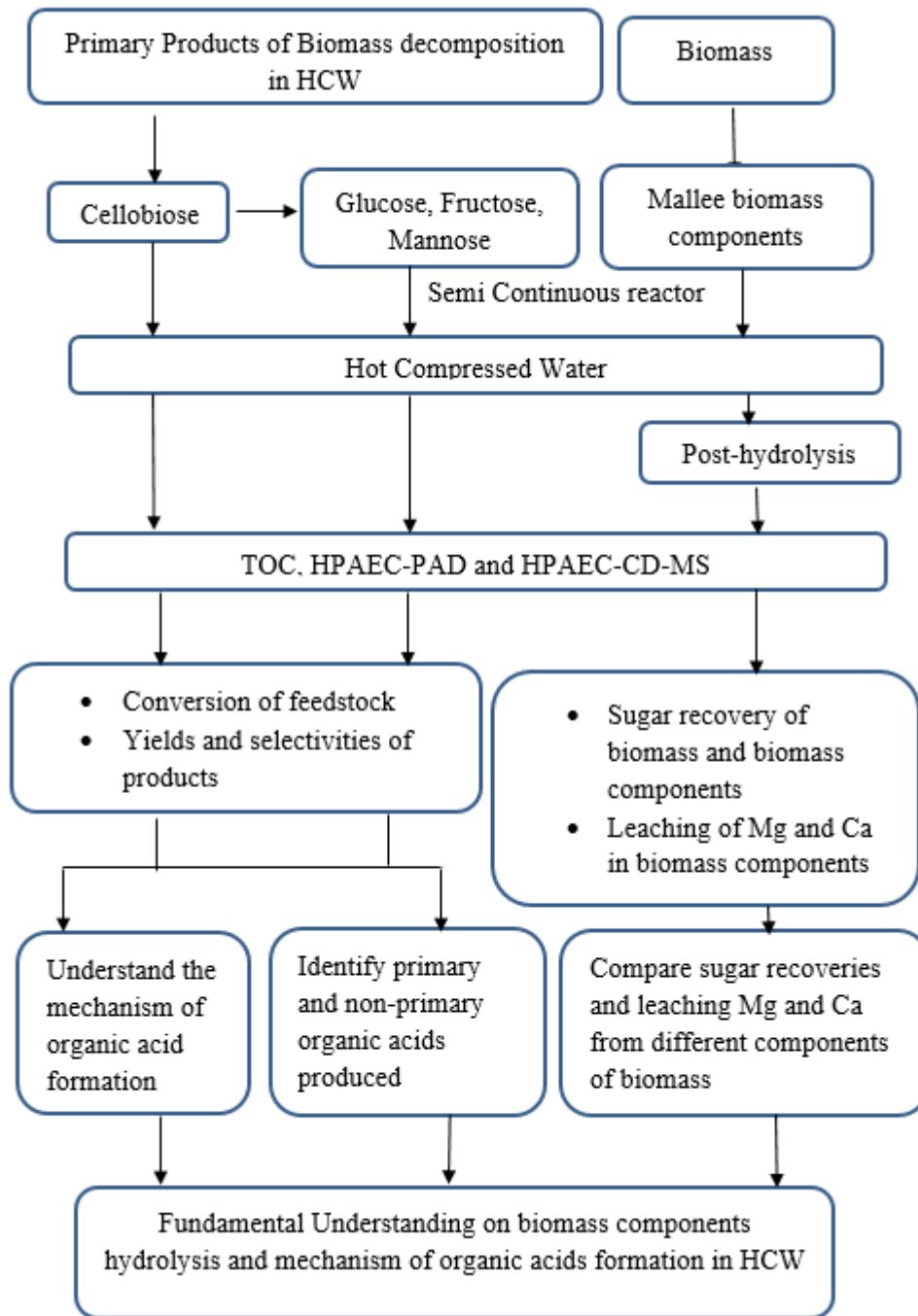


Figure 3-1: Overall research and methodology.

3.2.1 Hydrothermal Processing of Mallee Biomass and the Main Components in HCW

Mallee biomass Hydrothermal processing was performed utilising a semi-continuous flow reactor system to minimize the secondary reactions of liquid products. The components were separated from mallee trees (*Eucalyptus Loxophleba*, subspecies *Lissophoia*) harvested from Narrogin in Western Australia. The samples were cut using a cutting mill (model: Fritsch Pulverisette 15) and the size fraction of 150-250 μm were used in this study.

The reactor was filled in with ~80 mg of leaf and bark and ~50 mg of wood samples. Prior to heating-up the reactor system, the water-soluble compounds (both inorganic and organic) in biomass were leached at room temperature using ultrapure water for 30 min. Then the reactor system was rapidly heated to reaction temperature (150–270 °C) in 2 min and held at reaction temperature for 70 min. The pressure of the reactor system was controlled at 10 MPa for all experiments. The reactor effluent was immediately quenched in an ice water bath to minimise secondary reactions of the liquid product, and then sampled at designated time intervals. This study investigates the recovery of the sugars from mallee wood, leaf, and bark and the leaching characteristics of AAEM species (mainly Mg and Ca) from different biomass component at a wider range of temperatures (100–270 °C).

The total organic carbon (TOC), pH and sugar content of the liquid product were assed and examined immediately after each experiment.

3.2.2 Cellobiose, Glucose, Fructose and Mannose Decomposition in HCW

A continuous flow reactor system was used for cellobiose, glucose, fructose and mannose decomposition experiments in HCW at different temperatures, with the semi continues reactor system. The details of the reactor system are given in section 3.3.2.

To quantify the organic acids in the liquid products collected at different residence times, the liquid sample was analysed by high performance anion exchange

chromatography with conductivity detection and mass spectrometry (HPAEC-CD-MS, model: Dionex ICS-5000) equipped with a Dionex IonPac AS11-HC analytical column and a Dionex AERS 500 suppressor, using a gradient program developed in our previous study ²²⁶ to separate the organic acids. Selected ion monitoring (SIM) was used for quantification of organic acids in the liquid products. The yield and selectivity of each organic acid were calculated on a carbon basis, according to the method described in our previous study ²²⁶.

3.3 Experimental

3.3.1 Raw Material and Chemicals

Chemicals including cellobiose (purity $\geq 98\%$), D-(+)-mannose (purity $\geq 99\%$), glucose (purity $\geq 99\%$) fructose (purity $\geq 99\%$), together with other sugar standards used in this study (Glyceraldehyde, Glycolaldehyde, 5HMF) were obtained from Sigma-Aldrich. Organic acids standards including formic acid (purity $\geq 99\%$), glycolic acid (purity $\geq 99\%$), 2,4 dihydroxybutyric acid (Lithium Salt Hydrate) were obtained also from Sigma-Aldrich. Lactic acid stock standard solution (2 g/L) was sourced from Chem supply (Australia). The standards of α -metasaccharinic acid (3-deoxy-D-ribo-hexono-1,4-lactone), β -metasaccharinic acid (3-deoxy-D-arabino-hexonic acid, calcium salt), α -isosaccharinic acid ((2S,4S)-2,4,5-Trihydroxy-2-(hydroxymethyl) pentanoic acid, calcium salt) and β -isosaccharinic acid ((2R,4S)-2,4,5-Trihydroxy-2-(hydroxymethyl) pentanoic acid, calcium salt) were synthesized by Synthos Inc. (Canada).

3.3.2 Reactor System

Cellobiose, glucose, fructose and mannose solution with a concentration of 3 g/L and a waste stream were fed by two separate HPLC pumps at flow rates of 10 and 20 mL/min, respectively. Before the sugar solution and the water stream were mixed, the water stream was preheated in a sand bath so the sugar solution can be rapidly heated to a desired reaction temperature. The reaction temperature was monitored by a thermocouple placed at the inlet of the stainless steel tube reactor to ensure the

desired reaction temperature was reached before entering the reactor. After the reaction, the liquid product at the outlet of the reactor was quenched rapidly in an ice water bath, and then collected for further analysis. The reaction pressure of 10 MPa was maintained by a back-pressure regulator. The residence time (τ) was controlled by changing the tube length according to $\tau = V\rho/F$, where V is reactor volume (m^3), ρ is water density at the reaction temperature (kg/m^3), and F is total mass flow rate (kg/s). Figure 3-2 present the schematic diagram of continuous reactor used in the experiments¹⁷³.

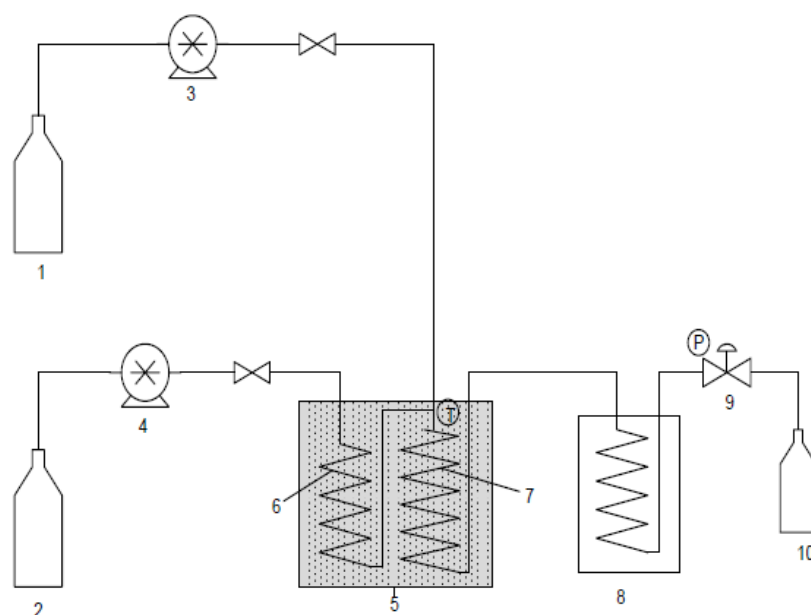


Figure 3-2: Schematic representation of the continues reactor system used: (1) Container of feedstock Solution; (2) container of deionised water; (3,4) HPLC pump; (4) sample chamber; (5) fluidized sand bath; (6) preheating tube; (7) continuous reactor; (8) cooling bath; (9) back pressure regulator; (10) sample collection¹⁷³.

Decomposition of Mallee biomass components occurred in HCW utilising semi-continuous reactor system which the contact between feedstock reaction particles and liquid product is continuous. All of the experiments were undertaken after the ageing of the reactor, so the effect of reactor walls can be neglected in our study during hydrothermal conversion of biomass and biomass-derived sugars in HCW.

The reactor system mainly consists of a HPLC pump (Alltech 627 HPLC pump) to provide water constant flow, an infrared gold image furnace (ULVAC-RIKO INC., Japan) to heat the reactor, ice water to rapidly quell the liquid products and back pressure regulator to regulate the reaction pressure (10 MPa). The biomass samples

retained in SUS316 stainless steel tubular reactor cell that sintered stainless still gasket filters placed at both ends of the reactor. The reactor cell was placed inside the gold furnace, and water was preheated in the furnace to the reaction temperature before entering to the reactor cell. Two thermocouples were used to monitor the reactor inlet and outlet temperatures. Figure 3-3 present the illustrative diagram of semi continuous reactor utilised in the experiments¹⁷.

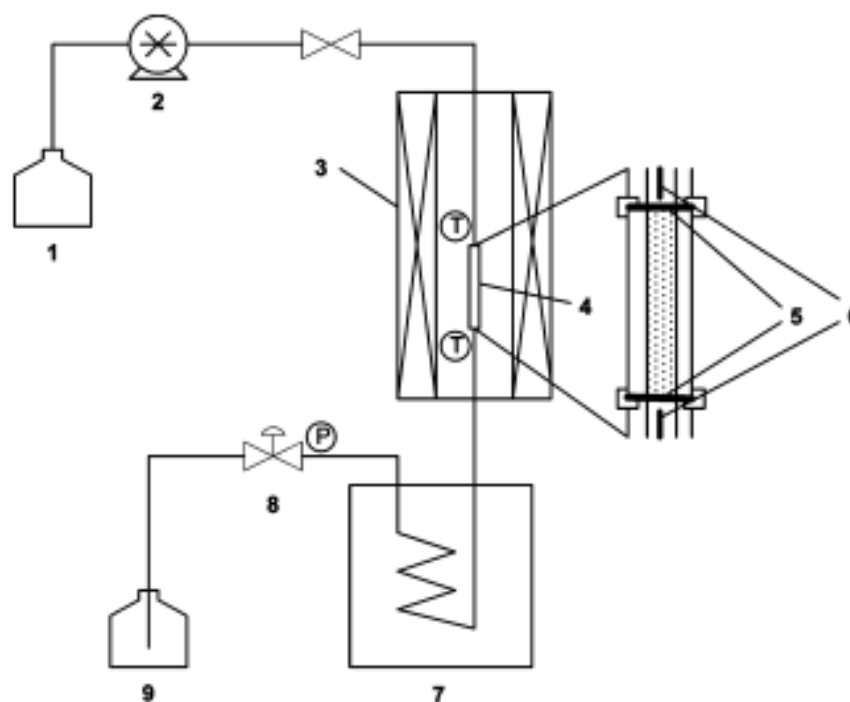


Figure 3-3: Schematic representation of the semi continues reactor system used in this study. (1) water reservoir; (2) HPLC pump; (3) infrared image furnace; (4) sample chamber; (5) stinted stainless steel filter; (6) thermocouple; (7) ice water bath; (8) pressure regulator; (9) liquid product collector¹⁷.

3.4 Sample Analysis

3.4.1 Total Organic Carbon Analysis

TOC Analyzer (Shimadzu TOC-V_{CPH}) was utilised to analyse total organic carbon of the liquid samples. TOC analyser performed oxidation by employing the powerful oxidation reagent (peroxodisulfuric acid) and also the ability to combine UV radiation and heating. Generally, the sample injected into the combustion tube

through sample injection system, then the carbon content in the test sample is oxidised to water and carbon dioxide. The moisture removes and the gas launch into the sample side of the non-dispersive infrared detector (NDIR) where can find carbon dioxide with a detection limit of 0.5 µg/L. The peak area can be calculated by converting NDIR signal to a peak profile.

3.4.2 Quantification of Biomass Structural Carbohydrate, Sugar Content and Monosaccharides in Liquid Products

The total sugars (i.e., arabinan, galactan, glucan, xylan, mannan) in the biomass sample and the liquid samples were examined via acid hydrolysis based on a NREL method.²²⁷ Briefly, about 100 mg of biomass was charged into a pressure tube which was then added 1 mL of 72% sulphuric acid. The content was plunged in 30 °C water bath for an hour. The concentration of acid was later calibrated to 4% by adding ultrapure water before it was autoclaved for 1 hour at 121 °C. For every round of analysis, a recovery standard containing arabinose, galactose, glucose, xylose and mannose was worked out to rectify the loss of saccharides throughout hydrolysis. The recovery standard was autoclaved along with the samples.

Post hydrolysis of liquid products conducted and the same method for the recovery standard was followed to decompose total saccharides to monosaccharides. After necessary dilution to reduce the sulfuric acid concentration < 0.8wt% in the acid hydrolysed samples, the concentrations of sugars were analysed by higher performance anion exchange chromatography with pulsed amperometric detection (HPAEC-PAD, model: Dionex ICS-3000, PAD with Au electrode and Ag/AgCl reference). A CarboPac PA20 analytical column was used to separate arabinose, galactose, glucose, xylose and mannose, with water at a flow rate of 0.5 mL/min used as the eluent. To achieve an adequate separation of monosaccharides, a gradient program was utilised as listed in Table 3-1. Post column addition of NaOH was required to ensure sufficient linearity of the PAD detector response. PEEK flow path HPLC pump was used to add 0.4 mL/min of 300 mM NaOH to analytical discharge column.

Table 3-1: HPAEC-PAD gradient program for monosaccharides separation.

Time	Eluent		
	A (%) 0.3 M NaAc in 0.1M NaOH	B (%) 0.3 M NaOH	C (%) Water
0.0	0	0	100
30.0	0	0	100
30.5	100	0	0
33.5	100	0	0
34.0	0	100	0
40.0	0	100	0
40.5	0	0	100
55.0	0	0	100

3.4.3 Quantification of Inorganic Species in Liquid Products

The AAEM Species (Mg and Ca) in the liquid products quantified by ion chromatography (IC, model Dionex ICS3000) with suppressed conductivity detection system. IonPac CS12A 4×250mm column and IonPac CS12AG 4×50 mm guard column with 0.02M methasulphonic acid as the eluent used to separate Mg and Ca ions.

3.4.4 Quantification of Organic Acids in Liquid Products

To quantify the organic acids in the liquid products collected at various residence times, the liquid sample was examined by high performance anion exchange chromatography with conductivity detection and mass spectrometry (HPAEC-CD-MS, model: Dionex ICS-5000) equipped with a Dionex IonPac AS11-HC analytical column and a Dionex AERS 500 suppressor. The system is equipped with Dionex ATC-3 trap column for removal of carbonate eluent, Dionex IonPac AS11-HC analytical column for separation and an AERS500 suppressor for removal of eluent prior to analysis by MS. A gradient program consists of initial elution of 1 mM NaOH for 8 min, followed by a linear increase of NaOH concentration to 60 mM for

20 min then holding at 60 mM NaOH for 20 min for adequate separation of organic acids.

For all identified organic acids with accessible standards, the calibration curves were drawn according to their peak areas as presented in Figure 3-4. For all standards, the detection limit was below 10 ppm, so various dilution factors applied for every sample to ensure all identified organic acids in the samples fall at detection limit.

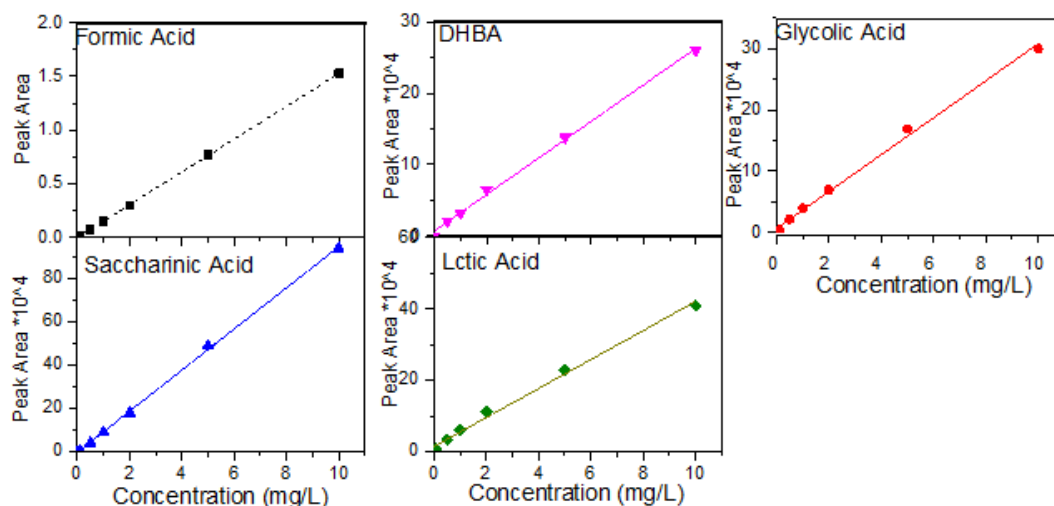


Figure 3-4: Calibration curves for all organic acids with available standards by HPAEC-CD for formic acid and HPAEC-CD-MS for other identified organic acids using gradient method.

MS detector is utilised to point out any unfamiliar peaks on the chromatogram according to the molecular weight to determine the chemical structure. SIM scanning mode is used for detection and quantification of organic acids. Figure 3-5 shows the schematic diagram of MSA detector system. Generally, the sample requires to be ionised after the column to be detectable by Mass detector and the ions in the liquid droplets turn into gas stage by Electrospray (ESI)²²⁸. Then the sample passes through stainless steel insert capillary at the high potential that can produce strong electric field by combining with nitrogen gas flow. Electric field forms highly charged droplets at the tip of the probe. The heated nitrogen gas evaporates the solvent, leads to increasing the charge density on the surface, until the droplets turn to smaller droplets by columbic explosion and only charged ions left²²⁹. The ions flow into the focusing region via the way in cone by the force through high electric field and the flow of gas. The quadrupole mass analyser is able to adjust the voltage of the four

rods in the quadrupole, to control the ions to pass through the detector based on the specific mass to charge ratio. Then electrons formed after hitting the ions from analyser with conversion dynode. The electrons go towards the channeltron electron multiplier and produce electron cascade. The formed current then converted in to the signal of voltage and more examined through data acquisition system^{228, 229}.

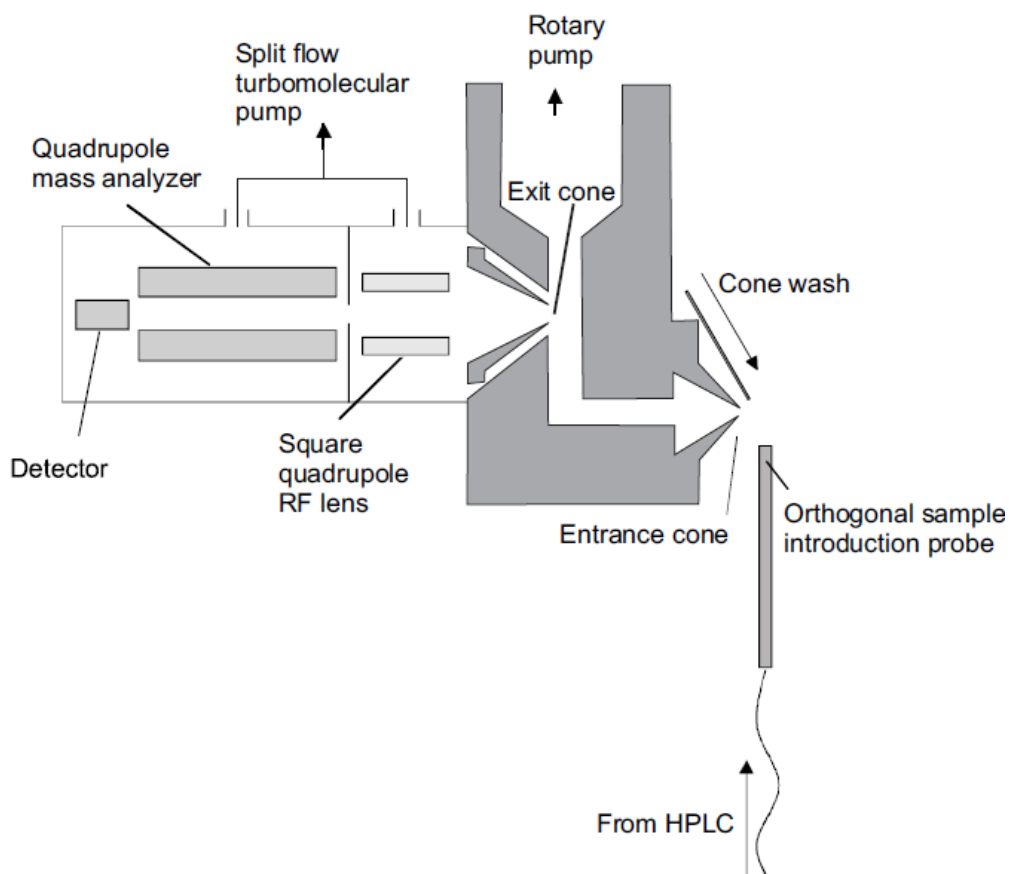


Figure 3-5: Schematic diagram of MSQ detector system²²⁸.

3.5 Data Acquisition and Processing

3.5.1 Conversion, Yield and Selectivity

The below equations were implemented to determine the conversion (X_i), yield (Y_i) and selectivity (S_i) of a compound (i) at a time of reaction (t):

$$X = \frac{(C_0 - C_t)}{C(0)} \quad (3.1)$$

$$Y_i = \frac{(C_i \times a_i)}{[C(0) \times a]} \quad (3.2)$$

$$S_i = \frac{(C_i \times a_i)}{[(C(0) - C(t)) \times a]} \quad (3.3)$$

where C_i is the compound concentration i in product, $C(0)$ is the initial concentration of compound (mgL^{-1}) in reactant, $C(t)$ is the compound concentration in product at reaction time t , a_i and a are the carbon content (mass fraction) of a compound i and the carbon content of the feedstock respectively.

All experiments were performed at least in duplicates to confirm the results repeatability. The average value of the data presented along with the error bar.

3.5.2 Kinetics

Assuming the decomposition of feedstock in this study follows the first-order kinetics, the reaction rate of feedstock decomposition was calculated using equation (3.4):

$$-\ln \frac{C(t)}{C(0)} = k\tau \quad (3.4)$$

where τ (s) is the reaction time.

The first rank delplot method determines the initial and non-initial products for each feedstock decomposition in HCW in current study. According to first rank delplot method, each product selectivity is plotted versus conversion and the intercept of product selectivity at $X \rightarrow 0$ determines if the product is a primary product (if the intercept is non-zero) or non-primary product (if the intercept is zero).

The rate of certain reaction calculated using the following equation:

$$\frac{k_i}{k} = \lim_{X \rightarrow 0} S_i = \lim_{n \rightarrow 0} \frac{Y_i}{X} \quad (3.5)$$

3.5.3 Calculation of Total Hydrogen Ion Concentration $[H^+]$ from the Quantified Organic Acids Concentration

To further understand if majority of organic acids were identified, the pH values of all liquid samples were also measured. Then, the hydrogen ion concentrations calculated from quantified organic acids were compared to the hydrogen ion concentrations calculated from measured pH of the liquid products. The total hydrogen ion concentration $[H^+]$ dissociated from all quantified organic acids in liquid products was calculated by considering the common ion (H^+) effect and the dissociation constants (K_a) of these organic acids, as detailed in our recent work²²⁶. In water, an organic acid, HA can ionise to form a hydrogen ion H^+ and an anion of the organic acid A^- , according to the reaction $HA \rightleftharpoons H^+ + A^-$. However, quantified organic acids do not fully ionise in water. The amount of organic acid i , dissociated at equilibrium can be defined the dissociation constant, $K_{a,i}$ in Eq. 3.6:

$$K_{a,i} = \frac{[H^+][A^-]_i}{[HA]_i} \quad (3.6)$$

where $[H^+]$, $[A^-]_i$ and $[HA]_i$ are the concentrations of the hydrogen ion, the organic acid i anion and the undissociated organic acid i in the solution at equilibrium, respectively. The $K_{a,i}$ is 1.8×10^{-4} for formic acid, 9.5×10^{-5} for saccharinic acid, 1.48×10^{-4} for glycolic acid, 1.99×10^{-4} for 2,4-dihydroxybutanoic acid and 1.38×10^{-4} for lactic acid²³⁰⁻²³². It is important to note that the self-ionisation of water is not considered due to its low dissociation constant ($K_a = 1 \times 10^{-14}$) compared to the organic acids quantified. In addition, $[HA]$ can also be expressed as, $[HA] = [HA]_T - [A^{-1}]$, where $[HA]_T$ is the concentration of the organic acid quantified. Therefore, Eq. (3.6) for each organic acid can be rewritten as Eq. (3.7) below:

$$K_{a,i} = \frac{([H^+][A^-]_i)}{([HA]_{T,i} - [A^-]_i)} \quad (3.7)$$

The total hydrogen ion in the solution can be calculated from Eq. (3.8):

$$[H^+] = \sum [A^-]_i \quad (3.8)$$

The concentration of the total dissociated H^+ from formic, saccharinic, glycolic, 2,4-dihydroxybutanoic and lactic acids can be obtained by solving Eq. 3.7 and Eq. 3.8 simultaneously.

3.6 Summary

Mallee biomass was used in this study to figure out the process of its decomposition in HCW in a semi-flow reactor system. This study investigated the recovery of sugar products and the leaching of some AAEM species from different components of mallee biomass (leaf, bark and wood) under hydrothermal condition at various temperatures and 10 MPa.

Furthermore, cellobiose, glucose, fructose and mannose were hydrothermally treated as model compounds, in order to figure out the mechanism of organic acids produced through decomposition of biomass in HCW at different temperatures and residence times. The liquid products gathered through the experiments, examined applying HPAEC-PAD and HPAEC-CD-MS for identifying and quantifying the desired compounds. The yield and selectivity of each product were calculated and discussed according to experimental results.

Chapter 4 : Hydrothermal Processing of Different Biomass Components of Mallee Tree in Hot-Compressed Water

4.1 Introduction

As introduced in Chapter 2, lignocellulosic biomass is recognised as a consequential alternative source for producing biofuels and green chemicals.¹⁶ Via the biomass hydrothermal conversion in HCW, different liquid products containing important chemicals such as sugars, furfural²³³ and organic acids can be directly synthesized.^{13, 14, 234, 235} As discussed, Organic acids considered as one of the value added chemicals from biomass decomposition in HCW, and it is important to understand the primary products produced from biomass to explore the mechanism of organic acids formation.

Mallee tree as a lignocellulosic biomass source, can be employed as a feedstock for hydrothermal processing. In despite of previous studies on the recovery of sugar product from different biomass,^{11, 33-35} thus far, no study has reported the recovery of sugar products from whole biomass or its various components. The sugar contents vary in different mallee biomass components (wood, leaf and bark), leading to their different decomposition behaviour in HCW. Also, the contents and occurrences of AAEM species vary in wood, leaf and bark²⁸. Therefore, an investigation is required to obtain better understanding of the recovery of sugar products and the leaching characteristics of AAEM species from hydrothermal conversion of mallee biomass in HCW. Also, it helps design a proper reactor to achieve higher yields of desired products. This chapter investigates the recovery of the sugars from mallee wood, leaf, and bark and the leaching characteristics of AAEM species (mainly Mg and Ca) from different biomass component at a wider range of temperatures (100–270 °C).

The characteristics of the wood, leaf and bark samples are noted in Tables 4-1 and 4-2.

Table 4-1: Proximate and ultimate analysis of mallee tree components used in this study.

Component	Moisture ^a (wt%)	Proximate (wt%, db)			Ultimate (wt%, daf ^d)			
		Ash	VM ^b	FC ^c	C	H	N	O ^e
Wood	4.0	0.5	83.6	15.9	47.7	6.2	0.51	45.6
Leaf	5.4	3.6	76.5	19.9	59.1	7.4	1.30	32.08
Bark	5.9	3.9	70.2	25.8	50.3	5.7	0.31	43.7

^a air dried; ^b VM–volatile matter; ^c FC–fixed carbon; ^d daf–dry ash free; ^e by difference

Table 4-2: Sugar and inorganic species content (wt% in dry basis) of mallee tree components.

Component	Structural carbohydrate content (wt%, db)					Inorganic species content (wt%, db)			
	Arabinan	Galactan	Glucan	Xylan	Manan	Na	K	Mg	Ca
Wood	0.93	1.99	36.60	15.80	0.34	0.024	0.066	0.033	0.128
Leaf	3.65	1.17	6.54	1.96	0.26	0.517	0.295	0.150	0.666
Bark	3.71	1.33	18.16	9.52	0.18	0.217	0.103	0.102	1.514
Whole Biomass ^a	2.58	1.54	21.47	9.39	0.27	0.245	0.155	0.091	0.663

^a The contents of sugar and inorganic species of whole biomass are estimated on the basis that the whole mallee tree consists of 40% wood, 35% leaf and 25% bark.

4.2 Sugar Recovery in Various Mallee Biomass Components

Figure 4-1 indicates the arabinose, galactose, glucose, and xylose recovery from leaf, bark and wood in the time of hydrothermal processing at 100–270 °C. As shown in the figure, slow but appreciable recovery of arabinose from leaf and bark is observed at 100 °C and wood at 120 °C. This suggested that the arabinan begin to decompose in HCW at a temperature as low as 100 °C for leaf and bark and 120 °C for wood. The arabinose recovery in leaf is close to its maximum recovery after 70 min reaction at 120 °C. For bark, >50% of arabinose can be recovered at 120 °C. On the other hand, only ~25% of arabinose is recovered from wood at this temperature. These observations also indicate that arabinan in leaf and bark are more susceptible to decomposition reaction compared to that in wood. The arabinan in all three components is found to be fully decomposed in 10 minutes at temperature ≥ 180 °C as little or no increase in arabinose recovery are observed. For galactan, small but appreciable galactose can be recovered from leaf and bark at 100–120 °C but its

recovery is <4% for wood. However, while a significant increase in recovery is observed at 150 °C for leaf and wood, its recovery from bark remained low. Likewise, >80% of the recoverable galactose is recovered within 20 min at reaction temperatures ≥ 180 °C. In addition, the data in Figure 4-1 also clearly shows that the decomposition of xylan in all three components started at 150 °C as negligible xylose is recovered at lower temperatures and can be fully recovered at 180°C except for xylan in leaf. On the other hand, while only around 10% of glucose can be recovered from leaf and bark at temperatures <230 °C, only <4% of glucose in wood is recovered at these temperatures. The glucose recovered at these temperatures is associated with the decomposition of glucan in hemicellulose as decomposition temperature of glucan in cellulose reported is ≥ 230 °C.¹⁹ A significant increase in glucose recovery from wood and bark is observed at 230 °C and 270 °C for leaf. The maximum recovery of glucose reaches ~30% and ~40% for leaf (~7% glucan content) and bark (~18% glucan content) respectively, compared to 62% for wood (~37% glucan content). Inorganic species such as Mg and Ca is known to promote the isomerisation reaction under hydrothermal condition.¹³⁴ The low glucose recovery from leaf and bark compared to wood might be due to a more severe structural changes possibly catalysed by higher Mg and Ca content in leaf and bark (see Table 4-2).

Such a glucose recovery is lower compared to that of ~80% attained from microcrystalline cellulose under the similar situation.¹⁹ A low recovery of glucose was also noted by Phaiboonsilpa and co-workers²³⁶ utilising a similar reactor system for Japanese cedar hydrothermal processing. The low glucose recovery is not promising expected because of the secondary reactions of initial liquid product, as the xylose recovery is about to 100% at 270 °C. It is very probable because of the in situ structural variations of cellulose in biomass during hydrothermal treatment,¹¹³ due to the decomposition of cellulose structure before conversion into the liquid product.

The observed differences in the decomposition of sugars (e.g., arabinan and galactan) between wood, leaf and bark might be due to significant difference in sugar content between these components as indicated in Table 4-2. Compared to wood (~56%), leaf (~14%) and bark (~22%) have significant lower sugar content. While xylan is

the dominant sugar component in wood hemicellulose (<5% arabinan), the hemicellulose in leaf and bark is rich in arabinan. This suggests the hemicellulose of wood is in the form of glucuronoxylans while hemicellulose in leaf and bark are likely to be in the form of high arabinose containing polysaccharides such as glucuronoarabinoxylan.

The different plateaus in recovery of arabinose and galactose in leaf and bark at different temperature might also indicate the hemicellulose in leaf and bark consists more than single type of hemicellulose.²³⁷

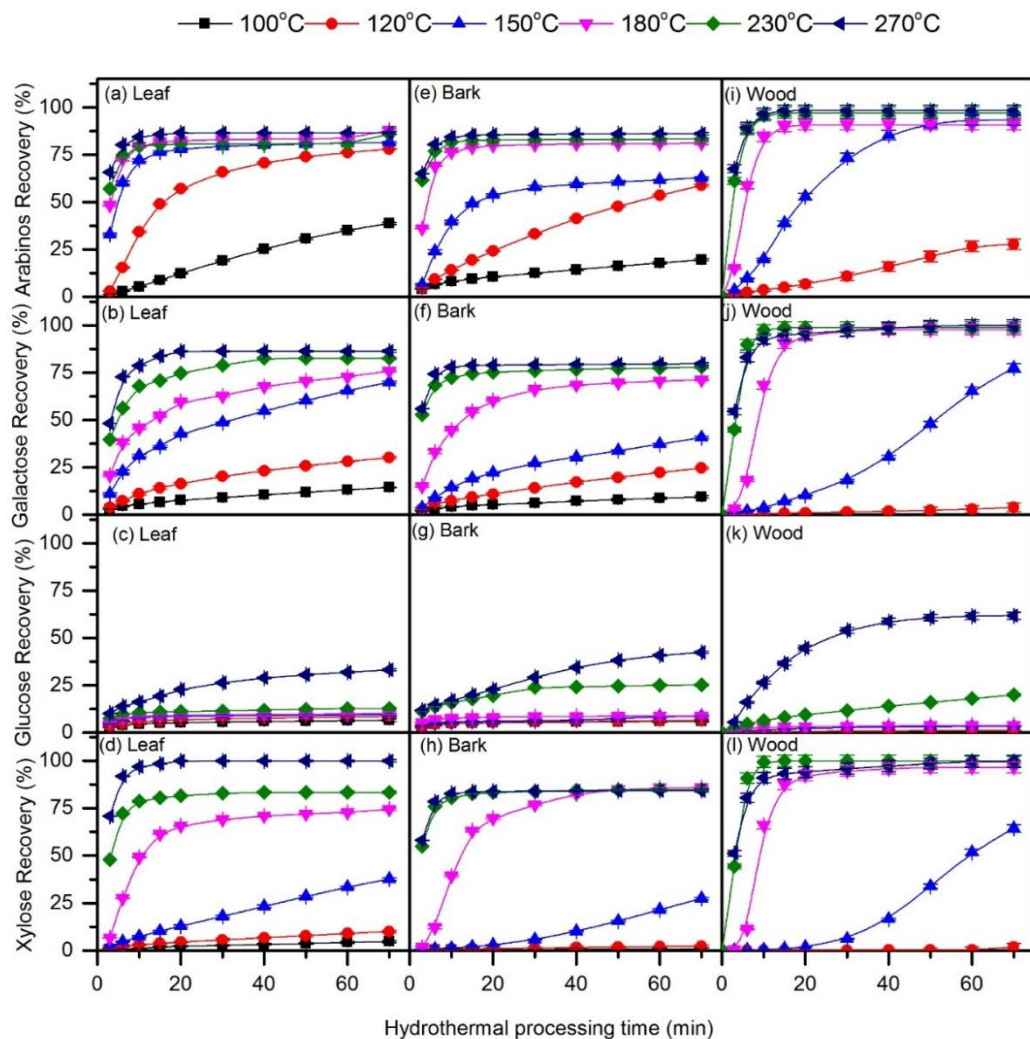


Figure 4-1: Recovery of arabinose, galactose, glucose and xylose recovery from wood, leaf and bark as a function of time during hydrothermal processing at 100–270 °C.

The specific reactivity of the organic matter (on a carbon basis) in wood biomass at different temperatures is shown in Figure 4-2. At 150 °C, the low specific reactivity

and its gradual growth with conversion of carbon display the slow decomposition of biomass organic matter. While reaction temperature increases to 180 °C, the specific reactivity and carbon conversion increases, denoting a more rapid decomposition of some reactive biomass components (such as hemicellulose and lignin). A further increase in temperature to 230 °C extends to speed up the decomposition of those reactive components in biomass. Nevertheless, the specific reactivity decreases outstandingly at biomass conversions of 40-60%, indicating the reactivity of the remaining biomass component (mostly cellulose) is slow at 230 °C. At 270 °C, although the specific reactivity also reduces at biomass conversions of 40-60%, but the particular reactivity is higher than that at 230 °C, approving the promotion of biomass conversion at increased temperatures.

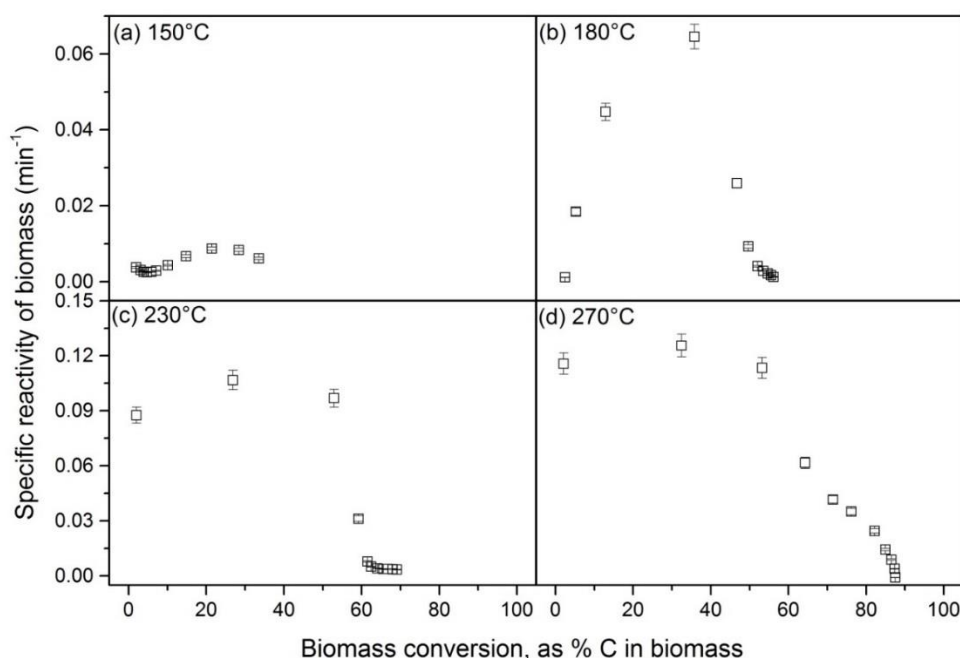


Figure 4-2: Specific reactivity of wood biomass as a function of biomass conversion (on a carbon basis) during hydrothermal processing at various reaction temperatures: (a) 150 °C, (b) 180 °C, (c) 230 °C and (d) 270 °C.

Figure 4-3 demonstrates the wood biomass hydrothermal conversion on a carbon basis at different temperatures. At 150 °C, the total carbon conversion increases marginally with reaction time, noting part of the biomass structure begins to decompose even at 150 °C. The carbon conversion is ~34% after 70 minutes. At 180 °C, there is a steep incline of carbon conversion at time < 15 minutes followed by a gradual increase to settle at ~56% after 70 min. The carbon conversion for hydrolysis

at 230°C and 270°C follows a similar trend with the conversion of ~69% at 230 °C and ~88% at 270 °C after 70 min.

Extra effort was taken to evaluate the contribution of saccharides to the total carbon converted from wood biomass during hydrothermal processing in the semi-continuous flow reactor. After hydrothermal processing of 70 min at 150 °C, over 30% of the total carbon in the biomass is recovered but less than half of the recovered carbon are contributed by sugar products (panel a). Under similar conditions at 180 °C, the recovery of total carbon in the biomass is close to 60%, in which about two-third (~60%) are non-sugar products (panel b). At 180 °C, the data wood in Figure 4-1 further shows that the recovery of sugar products in the biomass is almost complete (>90% for arabinan, galactan, and xylan), indicating that a considerable amount of lignin starts to hydrolyse under the prevailing conditions. Panel b also shows that at 180 °C there is a gradual increase in total carbon recovery after hydrothermal processing of 20 minutes, at which carbon recovery from saccharides have already levelled off, suggesting that an increasing amount of lignin participates in hydrothermal conversion with increasing reaction time. Similar observations can also be made at 230°C and 270 °C, albeit with increasing contribution of the reaction products from lignin.

Although almost all of the hemicellulose and significant amount of cellulose are recovered, only a small amount exists in their monosaccharides form. Figure 4-4 depicts the distribution of monosaccharides in the liquid product collected from wood biomass at various temperatures for 70 min. At 150 °C, ~12% of arabinan and galactan in mallee wood were recovered as arabinose and galactose. Only ~38% of xylan was recovered, and <1% is xylose. When the temperature increases to 180 °C, ~16-18% of arabinan, galactan and xylan were recovered as monomeric arabinose, galactose and xylose. At 230-270°C, ~20% of arabinan and galactan were recovered as arabinose and galactose. However, only ~2% of xylan in mallee wood was recovered as xylose. This indicates that xylan is more likely to be recovered as larger oligomers at higher temperatures under the current continuous-flow conditions. This is plausible due to the promoted formation of larger oligomers and/or the increased solubility of larger oligomers as a result of lower dielectric constant of hot-compressed water (HCW) at increased temperatures.^{90, 238}

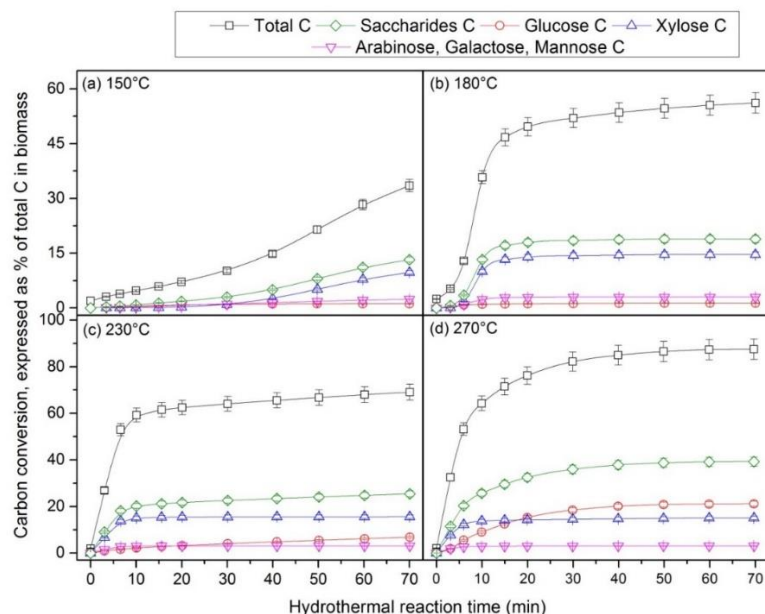


Figure 4-3: Carbon conversion as a function of reaction time during hydrothermal processing at different reaction temperatures: (a) 150 °C, (b) 180 °C, (c) 230 °C and (d) 270 °C, expressed as % of total C in mallee wood.

As opposed to reaction at lower temperatures, these oligomers have limited solubility in HCW thus remained in the reactor and further cleaved into smaller oligomers or xylose. As arabinan and galactan mostly present in hemicellulose as side chains to xylan backbone,^{56, 239} more arabinose and galactose can be produced as arabinose and galactose have lower degree of polymerisation (DP) compared to xylan. As cellulose only begins to decompose at ~230 °C,³³ only a small amount of glucose (~0.8%) was detected in liquid samples collected from wood sample at temperatures below 230 °C. Even at 230 °C and 270 °C, only ~6% of glucan in biomass was recovered as glucose. This might be due to the formation of high-DP glucose oligomers is favoured at high temperatures, similar as the formation of xylose oligomers.¹⁹

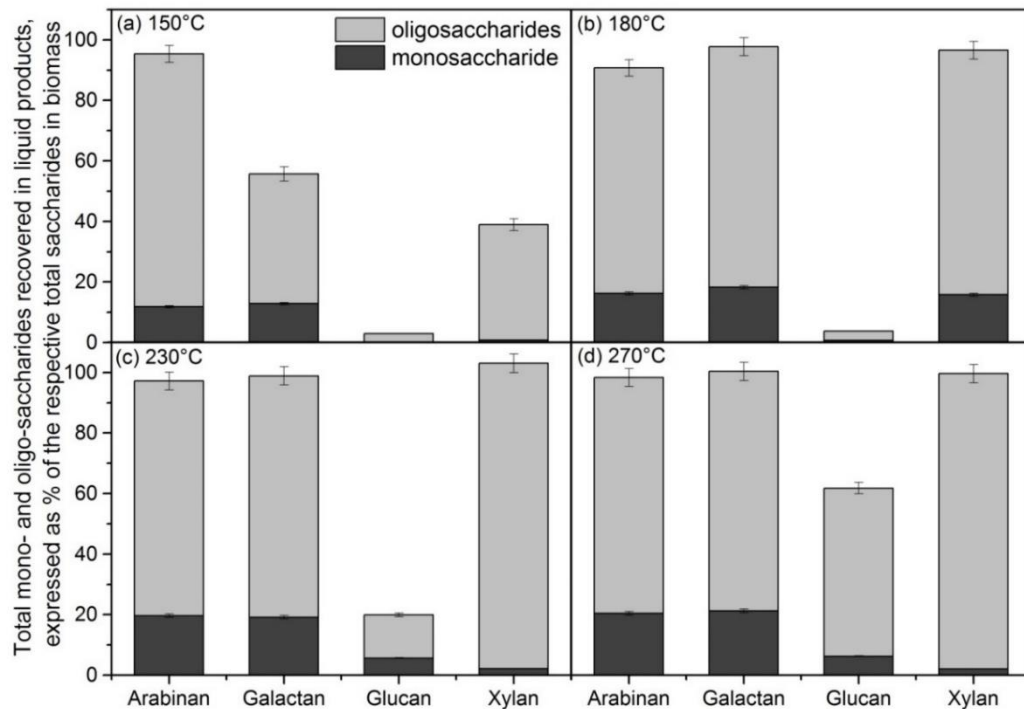


Figure 4-4: Total mono- and oligosaccharides recovered in liquid products collected from hydrothermal processing of wood sample for 70 min at (a) 150 °C, (b) 180 °C, (c) 230 °C and (d) 270 °C, expressed as % of the respective total saccharides in mallee wood. The light gray bars indicate the total oligosaccharides quantified via the post-hydrolysis of the liquid products while the dark gray bars indicate the total monosaccharides in the liquid products.

4.3 Leaching of Mg and Ca in Various Mallee Biomass Components

During hydrothermal processing of biomass, significant portion of the inherent inorganic species (mainly Na, K, Mg and Ca) in mallee biomass can be leached by HCW.^{28, 240} This work further investigated the leaching of the water-insoluble Mg and Ca from mallee leaf, bark and wood during hydrothermal processing at 150–270 °C. Figure 4-5 shows the release of the water-insoluble Mg and Ca in wood, leaf, and bark against reaction time at 100–270 °C. It is important to note that the concentrations of Mg and Ca in liquid samples collected from hydrothermal conversion of wood at 100 °C are too low to be quantified thus not reported. At 120 °C, only <15% of the water-insoluble Mg was leached from wood. However, it is interesting to observe that ~50% of the water-insoluble Mg in leaf was leached

during hydrothermal conversion even at 120 °C. Similarly, ~35% of water-insoluble Mg in bark can be leached even at 120 °C, doubled of that from wood. On the other hand, although Ca also can be leached from wood, leaf and bark at low temperature, no significant different is observed between these three components. Only about 25% of water-insoluble Ca was leached from wood, leaf and bark during hydrothermal conversion at 120 °C. The leaching of the water-insoluble but ion-exchangeable Mg and Ca in biomass during hydrothermal processing is known to be correlated to the decomposition of arabinan.^{28, 240} Therefore, it is not surprising that more water-insoluble Mg can be leached from leaf and bark and at a high rate compared to that in wood because the arabinan in leaf and bark is decomposed at lower temperatures and its decomposition is faster compared to that in wood. The decomposition of leaf and bark hemicellulose at lower temperatures removes the water-insoluble Mg bounded on hemicellulose acid functional groups, thus resulting in higher Mg leachability for leaf and bark at low temperatures.²⁸ This however, does not lead to more Ca being leached during hydrothermal processing of leaf and bark at low temperatures. This is might due majority of the water-insoluble Ca ($\geq 80\%$) in leaf and bark are only soluble in acid and the leaching of the water-insoluble but acid-soluble Ca does not correlate to the decomposition of arabinan.²⁸ Therefore, no significant difference is observed in leaching characteristic of water-insoluble Ca between wood, leaf and bark at low temperatures.

A further increase in the reaction temperature increases the leachability of water-insoluble Mg and Ca in biomass. At 180 °C, majority of the water-insoluble Mg from all three components and Ca from wood are leached within 20 min. A further increase in the reaction temperature to 270 °C only leads to a small increase in the amount of water-insoluble Mg leached from leaf and bark as majority of the hemicellulose sugars were decomposed at 180°C. On the contrary, the leaching of water-insoluble Ca ($\geq 80\%$ only soluble in acids) in leaf and bark is lower compared to that in wood. Substantial increase in the amount of water-insoluble Ca from leaf and bark is observed at 180°C and higher, possibly resulted from leaching of acid-soluble salt (e.g. calcium oxalate) present in cell cytoplasm as the cell wall structure was compromised with significant decomposition of hemicellulose at high temperatures.²⁸

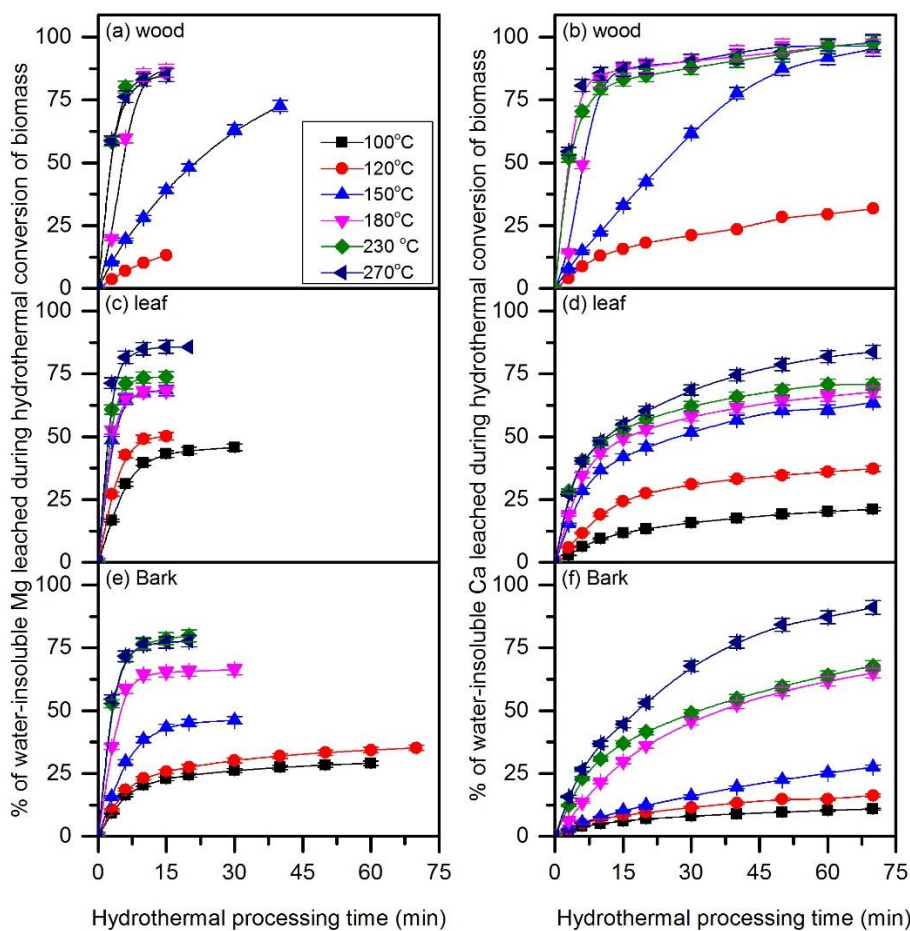


Figure 4-5: Leaching of water-insoluble Mg and Ca as a function of time from wood, leaf and bark during hydrothermal processing at 100–270 °C.

4.4 Further Discussion

The results presented thus far only confine to the recovery of sugar and the leaching of inorganic species during hydrothermal processing of each components in mallee biomass. Further calculation is also carried out to estimate the decomposition of sugars and the leaching of Mg and Ca during hydrothermal processing of whole mallee tree at temperatures of 120–270 °C. The result is presented in Figure 4-6, 4-7 and 4-8. The calculation is carried out based on the assumption that wood, bark and leaf contribute to 40%, 25% and 35% of a mallee tree, respectively,²³ and there are no interactions between each component during hydrothermal processing.

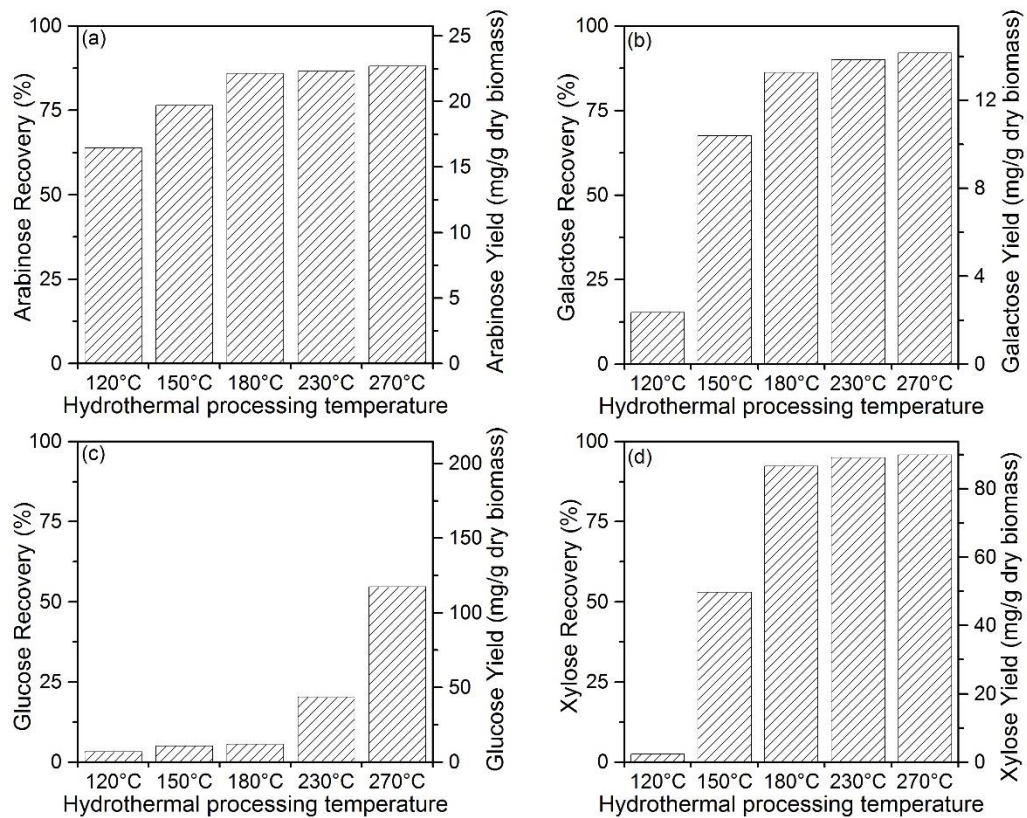


Figure 4-6: Recovery and yield of (a) arabinose, (b) galactose, (c) glucose, (d) xylose oligomers from the hydrothermal processing of the whole mallee biomass at 120–270 °C.

As shown in Figure 4-6, ~63% of arabinose can be recovered at 120 °C from mallee biomass, mainly due to the decomposition of arabinan especially in leaf and bark components. More than 85% of arabinose is recovered when temperature increase to ≥ 180 °C. On the other hand, only ~15% of galactose is recovered at 120 °C but the recovery increases to ~68% at 150 °C and reaches close to 90% at higher temperatures (≥ 180 °C). A similar trend is observed for xylose where the recovery increases from <3% at 120 °C to ~50% at 150 °C and reached its maximum conversion of approximately 95% at higher temperatures (≥ 180 °C). Likewise, as cellulose in all three components also decomposed at temperature around 230 °C, <6% glucose is recovered at temperatures ≤ 180 °C. As not all the glucose in all three components can be recovered, the maximum glucose recovery during hydrothermal conversion of whole mallee biomass at 270 °C is estimated to be around 55%. This data also demonstrates that ~70% of sugars in biomass (see Figure 4-7) can be recovered by hydrothermal processing of mallee tree in HCW, mainly in the form of sugar oligomers. Arabinose-oligomers are the major sugars in liquid product at 120

°C. Xylose oligomers are the major sugars in liquid product at 150 – 180 °C while xylose and glucose oligomers are the major sugars in liquid product for higher reaction temperatures (230–270 °C).

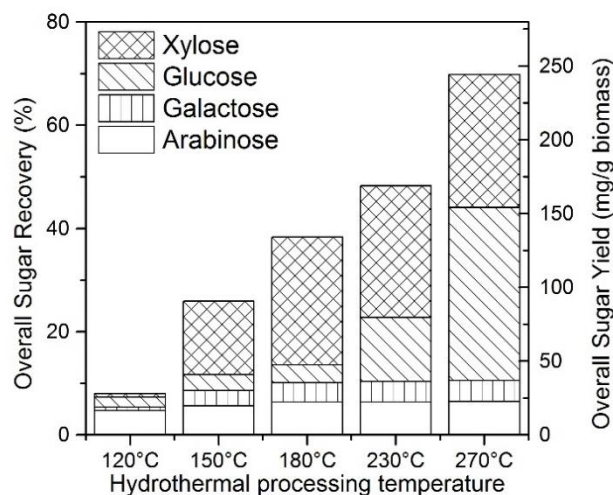


Figure 4-7: Overall recovery and yield of sugars from the hydrothermal processing of whole mallee biomass at 120–270 °C.

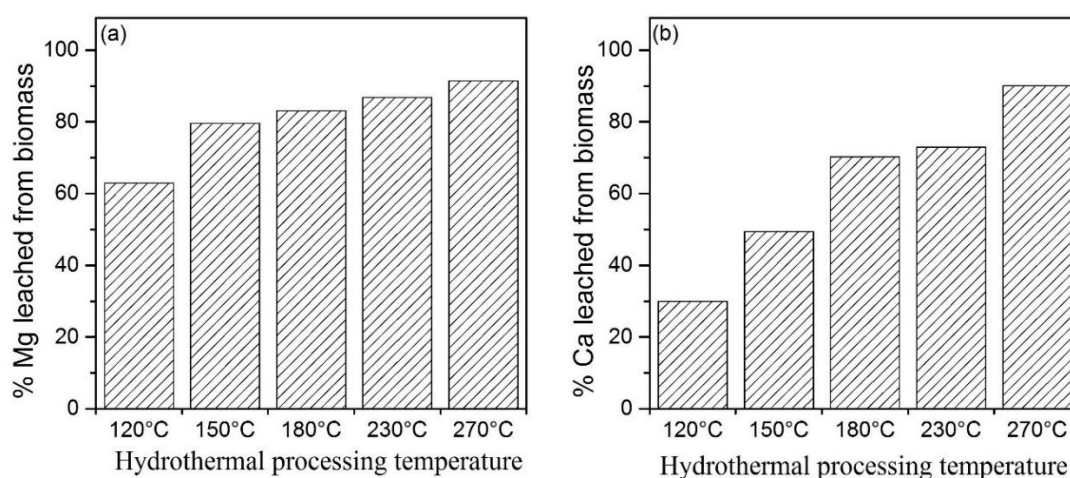


Figure 4-8: Leaching of (a) Mg and (b) Ca in biomass during hydrothermal processing at 120–270 °C.

The data in Figure 4-8 demonstrates that ~63% of Mg can be removed from biomass during hydrothermal processing at 120 °C but only ~30% of Ca are leached as majority of the Ca in mallee tree are acid-soluble fraction.²⁸ More than 80% and 70% of the Mg and Ca, respectively, are released during hydrothermal processing of

mallee tree at 180 °C. Nevertheless, there are ~10% of Mg and Ca in mallee tree that cannot be removed even at reaction temperature as high as 270 °C.

The results in Figure 4-6 and 4-8 also illustrated that hydrothermal processing at 180 °C can be effectively used as the pre-treatment strategy to remove hemicellulose sugars (e.g. arabinose, galactose and xylose) and inorganic species. The removal of hemicellulose can be crucial prior to hydrolysis of cellulose as pentose such as xylose and arabinose can inhibit the activity of some yeasts and bacteria used for bio-ethanol fermentation.²³⁹ The removal of inorganic species, especially Mg and Ca can be important when the pre-treated biomass are subjected to hydrothermal processing at higher temperature for glucose production as Mg and Ca are known to reduce the selectivity of glucose during hydrolysis process.¹³⁴

4.5 Conclusions

This study investigates sugar products and the leaching of water-insoluble Mg and Ca from malle wood, leaf and bark under hydrothermal condition in a semi-flow reactor at 100–270 °C and 10 MPa. The result indicates that arabinan and galactan in leaf and bark are more susceptible to decomposition at lower temperatures compared to those in wood, evident from higher arabinose and galactose recovery from leaf and bark compared to wood at 120 °C. Xylan in all three components only begins to decompose at 150 °C with the conversion of arabinan and galactan prior to xylan in wood sample, while significant glucan decomposition occurs at ≥ 230 °C.

The recovery of arabinan, galactan and xylan are close to 100% in wood sample at 270 °C, mainly in the form of oligomers as the formation of large xylose oligomers and solubility of these oligomers are increased at high temperatures. Although >80% of arabinose, galactose and xylose can be recovered from leaf, bark and wood, the recovery of glucose is between 30 – 62% in the order of wood > bark > leaf. The low recovery probably due to the significant in-situ structural changes during hydrothermal treatment. The lower glucose recovery in leaf and bark are likely due to its higher Mg and Ca content. This study also demonstrates that the leaching of the water-insoluble Mg and Ca during hydrothermal processing can start at 100 – 120 °C. About 50% and 35% of water-insoluble Mg in leaf and bark are released during

hydrothermal processing at 120 °C compared to just ~13% for wood. About 25% of water-insoluble Ca is leached from leaf, bark and wood at 120 °C. Majority of the water-insoluble Mg in wood, leaf and bark and water-insoluble Ca in wood are leached rapidly at 180°C and higher but the leaching of water-insoluble Ca from leaf and bark remained slow as >80% of these water-insoluble Ca is only soluble in acid. Further calculation considering decomposition of whole mallee tree shows that ~70% of sugar can be recovered at 270 °C. Hydrothermal processing of mallee biomass at 180 °C is shown to be an effective pre-treatment technique for hemicellulose and inorganic species removal prior to further processing.

This chapter explored the main products and sugar recovery from the main components of mallee biomass and also the whole biomass during hydrolysis in HCW, which is essential to understand the mechanism of organic acids formation as the value-added biochemicals from hydrothermal conversion of biomass in HCW as discussed in following chapters.

Chapter 5 : Formation of Organic Acids During Cellobiose Decomposition in HCW

5.1 Introduction

As concluded in chapter 2, Mallee biomass is an important alternative in WA for renewable biofuels and value added biochemicals (i.e. organic acids) production. Therefore, a study on kinetics and reaction pathways from primary products decomposition in HCW should be well understood to provide insights for proper reactor design and achieve desired products. In HCW, Biomass/cellulose is primarily decomposed into glucose oligomers with a wide range of degrees of polymerization (DPs), which are then converted into low-molecular-weight compounds via a series of reactions such as isomerization, hydrolysis, retro-aldol and dehydration reactions^{19, 42}. Furthermore, previous chapter demonstrated that sugar oligomers are more favoured to produce compared to sugar monomers from mallee biomass decomposition in HCW. Due to the complex structure of sugar oligomers, cellobiose as the simplest oligomer has been employed to understand the mechanism of organic acids formation from sugar oligomer decomposition in HCW. Previous studies conducted a series of systematic investigations to understand the primary reactions of cellobiose under various catalytic or non-catalytic hydrothermal conditions^{134, 150, 156, 217}. The pH value of the liquid product decreases substantially (i.e., from ~7 to ~4) as cellobiose conversion increases^{150, 156, 217, 241} and it was evident that some organic acids appears to be produced even at the early stage of cellobiose conversion^{156, 241}. Several studies investigated the formation of various organic acids (i.e., formic acid, acetic acid, glycolic acid, lactic acid, levulinic acid, saccharinic acid) from cellulose and glucose decomposition under alkaline hydrothermal conditions^{185, 203, 242, 243}. The composition of degradation products depends on the experimental condition, such as temperature, the nature and concentration of alkali is used. It is well known in the literature that saccharinic acids which has three isomeric forms, are one of the important organic acids produced under alkaline degradation of cellulose^{152, 153, 205,}

²⁴⁴⁻²⁴⁸. Furthermore, the reaction conditions such as alkali metal cation, pH and treatment affect which isomer of the saccharinic acid formed in the reaction. The previous studies outline that under alkaline degradation of cellulose, β -hydroxycarbonyl and β -alkoxycarbonyl elimination from reducing ends of the cellulose molecules take place, resulting in a rearrangement and formation of different types of saccharinic acids ^{151-153, 206, 245}. Until now, there has been no studies on the nature and quantity of organic acids produced during cellobiose decomposition under non-catalytic hydrothermal conditions. Yet, it is known that the initial pH can significantly influence the primary reactions of cellobiose decomposition in HCW ¹⁵⁶. Therefore, this chapter aims to identify and quantify the formation of various organic acids during cellobiose decomposition in HCW at 200 – 275 °C. It is noteworthy that this study has successfully identified the formation of metasaccharinic acid (MSA), which was seldom reported under non-catalytic conditions.

5.2 Typical HPAEC-CD-MS Chromatogram of the Liquid Sample

Figure 5-1 presents a typical HPAEC-CD-MS chromatogram of the liquid sample from cellobiose decomposition at 275 °C and a residence time of 66 s. Various organic acids including saccharinic ($m/z=179$), formic($m/z=45$), lactic ($m/z=89$) and glycolic ($m/z=75$) acids can be clearly detected in the liquid sample. It is noteworthy that two saccharinic acids are detected. To the authors' knowledge, this is the first time in the field that the formation of saccharinic acid is reported under non-catalytic conditions.

It is known that there are three types of saccharinic acids (i.e., isosaccharinic, metasaccharinic and parasaccharinic acid), but the formation of parasaccharinic acid is rarely reported from carbohydrate decomposition in HCW. To further identify the saccharinic acids from cellobiose decomposition, three different saccharinic acids tested: α -isosaccharinic, α -metasaccharinic and β -metasaccharinic acids.

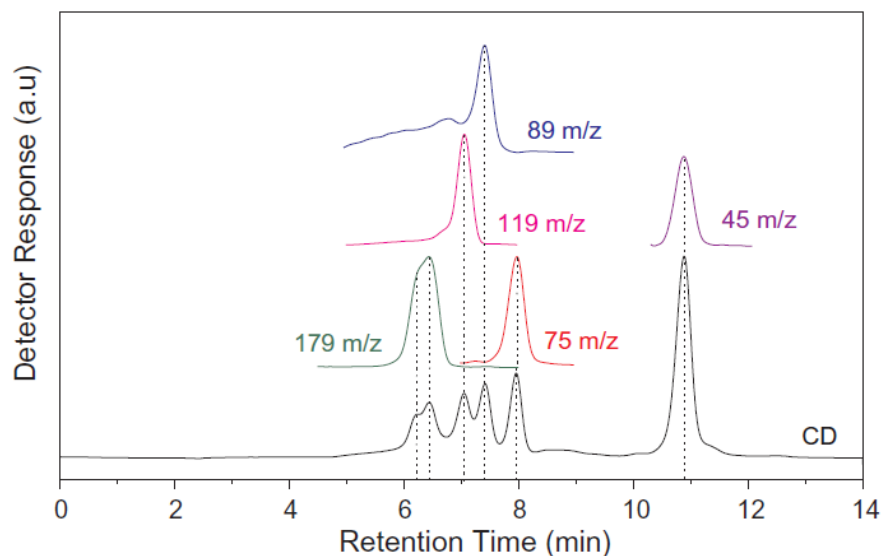


Figure 5-1: HPAEC-CD-MS chromatogram of a typical sample from cellobiose decomposition at 275 °C and a residence time of 66 s. MS detection mode: negative ion; needle voltage: -4 kV; ESI probe temperature: 450 °C; cone voltage: 45 V.

As shown in Figure 5-2, both α - and β -metasaccharinic acids match well with Peak 2, while α -isosaccharinic acid doesn't match with Peak1. Thus, it is very likely that Peak 1 is β -isosaccharinic acid. However, this study didn't identify Peak 1 due to the unavailability of standard. Further analysis of the calibration curves for the three saccharinic acids indicates that the saccharinic acids have almost same response for MS detection with SIM scan mode at $m/z=179$, so total saccharinic acid produced from cellobiose decomposition can be quantified.

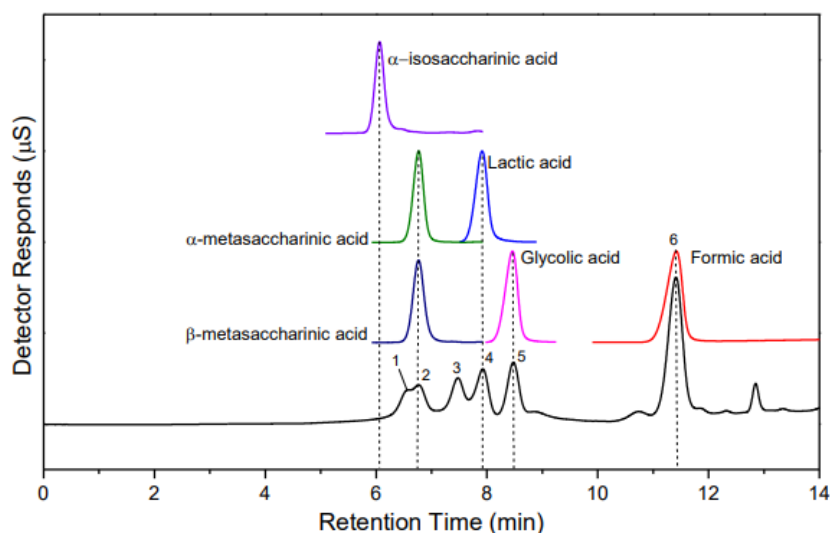


Figure 5-2: Identification of organic acids from cellobiose decomposition using available standards. 1: unidentified saccharinic acid; 2: metasaccharinic acid (α and β); 3: unidentified organic acid with molecular weight of 120 g/mol; 4: lactic Acid; 5: glycolic Acid and 6: formic acid.

5.3 Yields and Selectivities of Organic Acids from Cellobiose Decomposition

The concentrations of four major organic acids (i.e., saccharinic, formic, lactic and glycolic acids) in liquid products from cellobiose decomposition in HCW at 200–275 °C were quantified via HPAEC-CDMS. The yields and selectivities of those organic acids on a carbon basis are presented in Figure 5-3. The results clearly indicate that the yields of organic acids are low at 200 °C, i.e., ~0.53% for saccharinic acid, ~0.07% for formic acid, ~0.02% for glycolic acid and almost no lactic acid after a residence time of ~66 s. However, the yields of organic acids increase with reaction temperature. For example, the yields of saccharinic, formic, lactic and glycolic acids at 275 °C and ~66 s residence time substantially increase to ~5.8%, ~2.5%, ~0.8% and ~0.8%, respectively. Based on the concentrations of organic acids in the products, the selectivities of organic acids were further calculated and plotted as a function of cellobiose conversion in Figure 5-3. It can be seen that the selectivities of organic acids are initially zero and the organic acids only start to appear after a conversion of 5–10%, indicating that the organic acids are unlikely to be the primary products during cellobiose decomposition in HCW. The selectivities of organic acids

increase with cellobiose conversion, and the maximal selectivities achieved in this study are ~5.8% for saccharinic acid, ~2.0% for formic acid, ~1.0% for lactic acid and ~0.9% for glycolic acid at 275 °C and ~66 s. Among the organic acids quantified in this study, saccharinic acid has the highest yield and selectivity on a carbon basis. However, formic acid is the most abundant acid due to its high molar concentration, thus contributing significantly to the hydrogen ion in the liquid product.

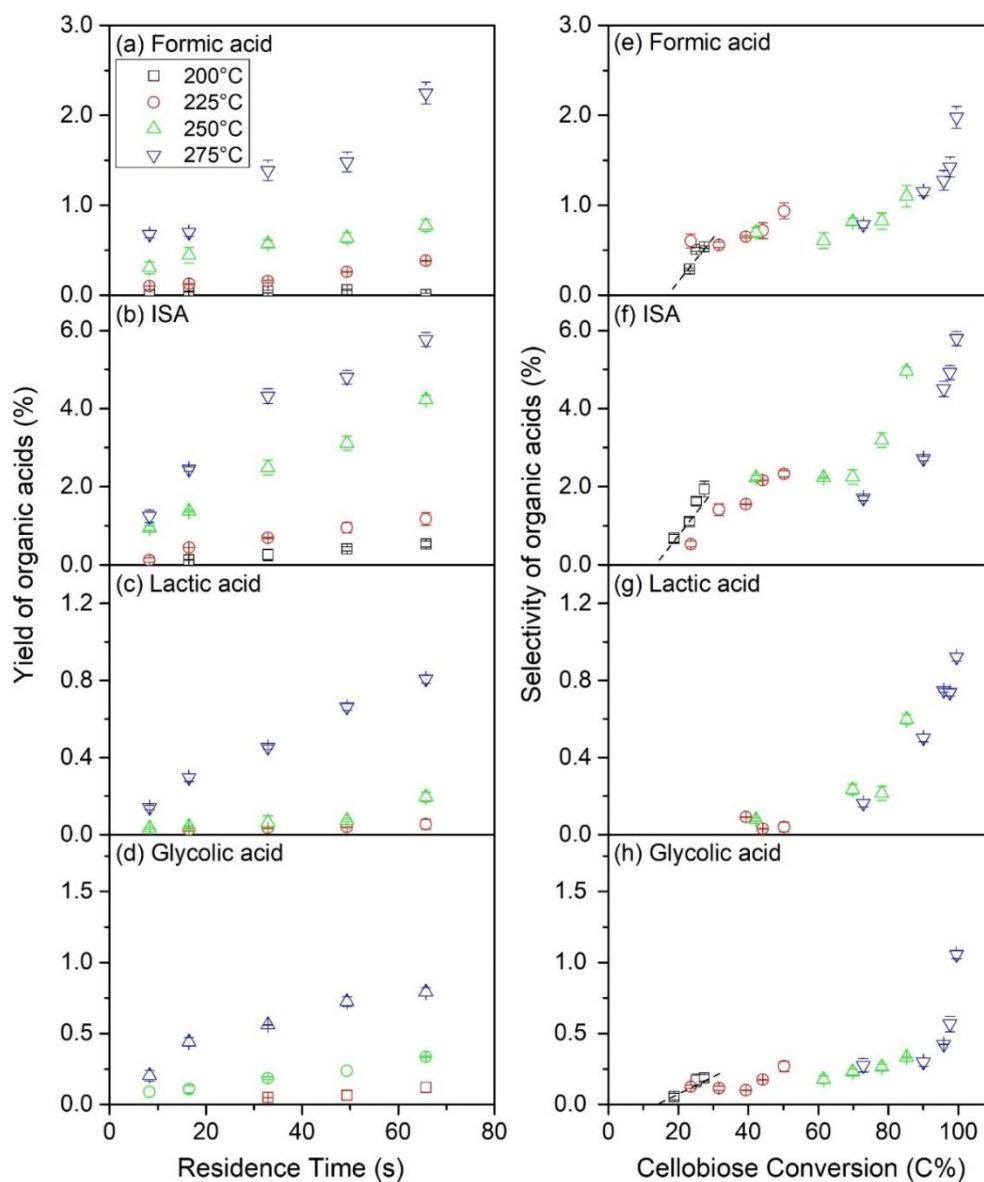


Figure 5-3: Yield and selectivity of organic acids produced from cellobiose decomposition at 200 – 275 °C. (a) Formic acid yield, (b) MSA yield, (c) Lactic acid yield, (d) Glycolic acid yield, (e) Formic acid selectivity, (f) ISA selectivity, (g) Lactic acid selectivity, (h) Glycolic acid selectivity.

Figure 5-4 shows the contributions of saccharinic, formic, lactic and glycolic acids to the total H^+ dissociated from the quantified organic acids at 200–275 °C. The total dissociated H^+ concentration was calculated based on the dissociation constants (K_a) of the acids at room temperature (see more details in section 3-5-3). The data indicate that the total dissociated H^+ is mainly contributed by formic acid especially at low cellobiose conversions, due to its higher molar concentration and higher dissociation constant compared to those for other organic acids. For example, formic acid contributes to ~90% of the total dissociated H^+ at ~12% cellobiose conversion, but its contribution decreases as cellobiose conversion increases and stabilises at ~50–60% at cellobiose conversions >40%. In contrast, the contribution of saccharinic acid is only ~8% of the total dissociated H^+ at ~12% cellobiose conversion, but increases to ~20–35% at cellobiose conversions >25%. The contributions of lactic acid and glycolic acid are < 10% under all conditions.

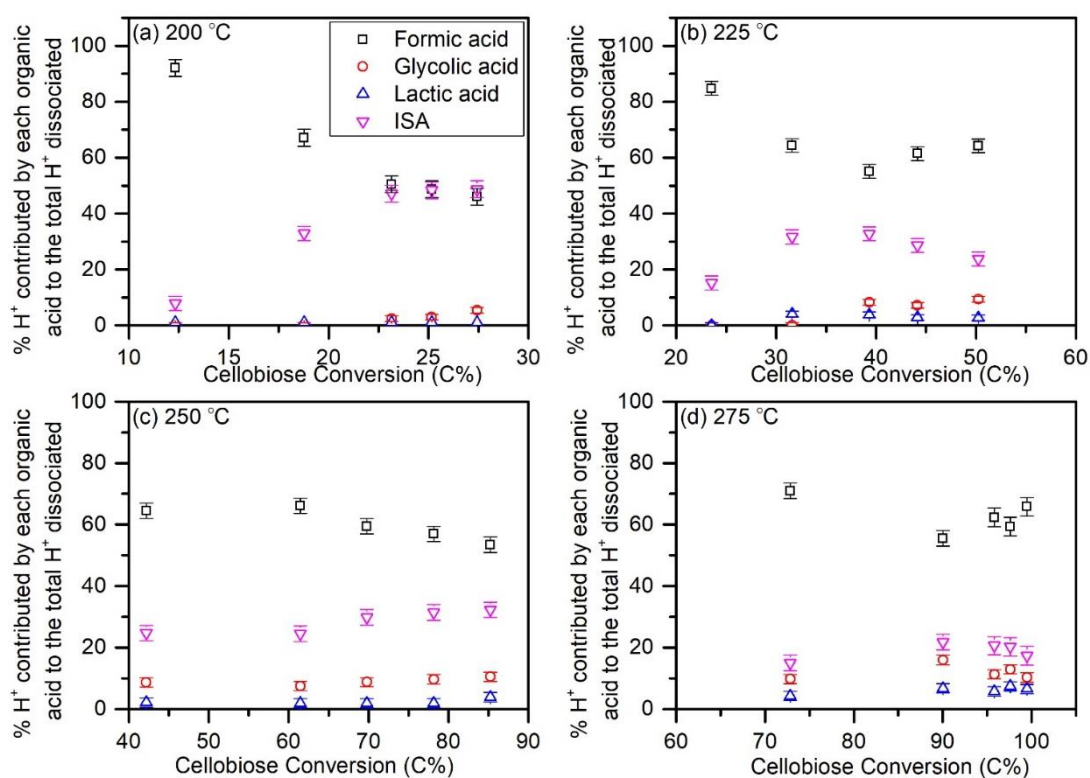


Figure 5-4: Contribution of MSA, formic acid, lactic acid and glycolic acid to total hydrogen ion dissociated by four quantified organic acids during cellobiose decomposition in HCW at 200 – 275 °C. (a) 200 °C, (b) 225 °C, (c) 250 °C, (d) 275 °C.

5.4 Comparisons Between $[H^+]$ Calculated from Quantified Organic Acids and Measured pH

Figure 5-5 further compares the hydrogen ion concentration ($[H^+]$) from the quantified organic acids with the $[H^+]$ from direct pH measurement of the liquid product right after the experiment at various conversions.

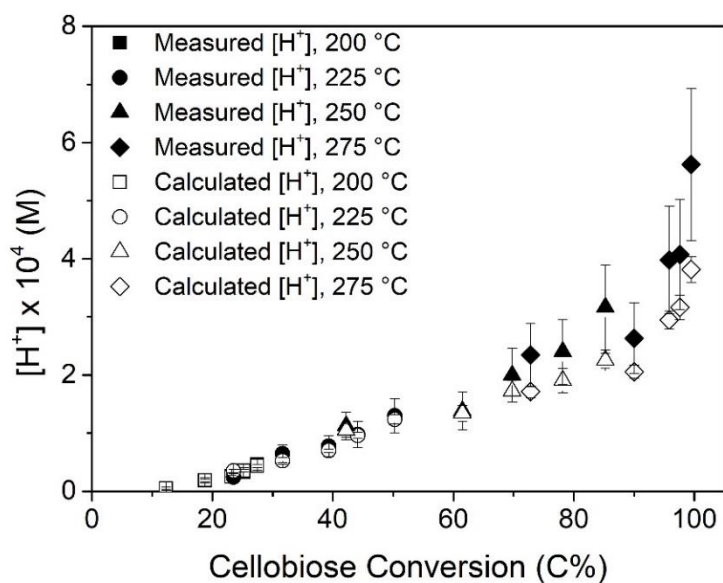


Figure 5-5: Comparisons of the hydrogen ion concentrations calculated from total concentrations of the quantified organic acids and the measured pH after cellobiose decomposition in HCW at various conversions.

A relatively close match between the calculated and measured $[H^+]$ (within experimental error) at cellobiose conversions $<80\%$ suggests that the quantified organic acids account for the majority of the organic acids produced during cellobiose decomposition in HCW. At a cellobiose conversion $>80\%$, the gaps between the calculated and measured $[H^+]$ widen, suggesting that other organic acids might be produced due to more pronounced secondary reactions at high cellobiose conversions. Nevertheless, other organic acids such as acetic and levulinic acids were not detected in the product under the current conditions. The above results indicate that small amount of organic acids can be produced even at low cellobiose conversions and become significant at increased cellobiose conversions. For example, the total hydrogen ion concentration increases from $\sim 0.018\text{mM}$ at $\sim 19\%$ cellobiose conversion to $\sim 0.56\text{mM}$ at $\sim 99\%$ cellobiose conversion, leading to the pH of the product reducing from 4.7 to 3.3. As pH can substantially alter the reaction

pathway of cellobiose decomposition in HCW, it is important to understand the reaction pathways leading to the formation of these organic acids.

5.5 Reaction Pathways of Organic Acids During Cellobiose Decomposition

Considering the new data in this study and those in the existing literature, Figure 5-6 presents the possible reaction pathways leading to the formation of these organic acids during cellobiose decomposition in HCW under non-catalytic conditions. Previous studies^{150, 156, 217} demonstrated that the primary reactions for decomposition of cellobiose in HCW are isomerisation of cellobiose to cellobiulose (glucosyl-fructose, GF) and glucosyl-mannose (GM) and hydrolysis of cellobiose to glucose. GF and GM are then further hydrolysed to monomeric sugars such as glucose, fructose and mannose. The monomeric sugars can also isomerise into each other in HCW via formation of 1,2-enediol anion²⁴⁹. As saccharinic acid, formic, lactic and glycolic acids are not the primary products, these organic acids are formed through the decomposition of monomeric sugars or its decomposed products. While saccharinic acid was reported to be formed during alkaline degradation of cellulose^{152, 205, 206, 245}, there was no report on the formation of saccharinic acid from the decomposition of cellobiose or cellulose under non-catalytic conditions. Based on the widely-accepted Nef-Isbell mechanism¹⁵², monomeric sugars (i.e., glucose, mannose or fructose) can form diketone intermediate (compound 7 and 13 in Figure 5-6) via a series of reactions including keto-enol tautomerisation, isomerisation and β -hydroxycarbonyl elimination, followed by benzilic acid rearrangement to form different types of saccharinic acids (i.e., isosaccharinic and metasaccharinic acids).

It is also noted that while benzilic acid rearrangement is widely regarded as a base-catalysed reaction, such reaction can also be catalysed by the hydroxyl ions in HCW. Furthermore, glycolic acid can also be produced from diketone intermediate (compound 7 in Figure 5-6) via α dicarbonyl cleavage.

Regarding the reaction pathway of formic acid formation, it is well known that 5-HMF can be rehydrated into formic and levulinic acid under acidic conditions^{192, 250}. However, in this study, no levulinic acid was detected in the products from

cellobiose decomposition under the current conditions. Regarding the reaction pathway of formic acid formation, it is well known that 5-HMF can be rehydrated into formic and levulinic acid under acidic conditions^{192, 250}. However, in this study, no levulinic acid was detected in the products from cellobiose decomposition under the current conditions.

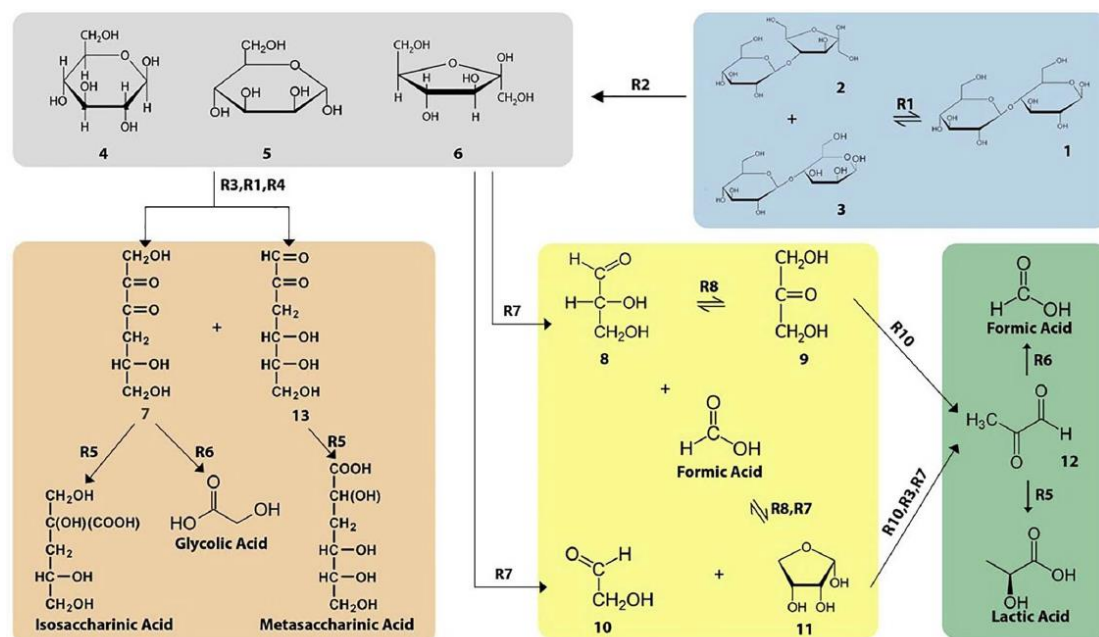


Figure 5-6: Summarised reaction pathways for saccharinic, formic, lactic and glycolic acids during cellobiose decomposition in HCW based on the reports in the literature^{143, 151, 152, 205, 206} and this study. R1: Isomerisation, R2: Hydrolysis, R3: Keto-enol tautomerisation, R4: β -hydroxycarbonyl elimination, R5: Benzilic acid rearrangement, R6: α -dicarbonyl cleavage, R7: Retro-aldol condensation, R8: Lobry de Bruyn-Alberda van Ekenstein transformation (LBAE), R9: Aldol condensation and R10: Dehydration. Compound (1): Cellobiose; (2): Glucosylmannose; (3): Cellobiulose; (4): Glucose; (5): Mannose; (6): Fructose; (7): Diketones Intermediate; (8): Glyceraldehyde; (9): Dihydroxyacetone; (10): Glycolaldehyde; (11): Erythrose and (12): Pyruvaldehyde; (13): Diketones Intermediate.

First, monomeric sugars (i.e., glucose, mannose and fructose) can easily decompose to glycolaldehyde, erythrose and glyceraldehyde through retro-aldol condensation reaction¹¹⁹. Erythrose is known to undergo Lobry de Bruyn-Alberda Van Ekenstein (LBAE) transformation to form glyceraldehyde and formic acid¹⁴⁴. Second, glyceraldehyde is also known to undergo LBAE transformation to form

dihydroxyacetone, which then produces pyrovaldehyde through dehydration, followed by the formation of formic acid via α -carbonyl cleavage¹⁴⁴. In addition, pyrovaldehyde is also known to undergo benzilic rearrangement to form lactic acid¹⁴³. Figure 5-1 shows substantial increases in the selectivities of formic and lactic acids at high temperatures (i.e., 275 °C), suggesting that these organic acids are likely to be formed from the products (i.e., glyceraldehyde, erythrose) from retro-aldol condensation reactions that are known to be more prevalent at high temperatures^{150, 159}.

5.6 Conclusions

This chapter provides direct evidences on the formation of organic acids during cellobiose decomposition in HCW at 200 – 275 °C. For the first time the formation of saccharinic acid as a major organic acid produced during cellobiose decomposition under non-catalytic conditions identified. Other organic acids such as formic acid, lactic acid and glycolic acid are also formed. The yields of organic acids increase with cellobiose conversion, i.e., from ~0.17% at ~18% conversion to ~9.6% at ~99% conversion. Among the four organic acids analysed, MSA has the highest yield on a carbon basis, but the low pH of liquid product is mainly contributed by formic acid due to its higher molar concentration and higher dissociation constant thus accounting for the majority of the dissociated hydrogen ions in the liquid product. A close match between the $[H^+]$ calculated from the quantified organic acids and the $[H^+]$ calculated from measured pH suggests that these acids are the majority organic acids produced during decomposition of cellobiose in HCW. However, the gaps between these two values become larger at higher conversions (i.e., >80%), indicating that other organics acids are produced due to more pronounced secondary reactions. Possible reaction pathways for those organic acids are also summarized and discussed.

This chapter demonstrates that organic acids are not the primary products from cellobiose decomposition in HCW, and they are more likely produced from monomeric sugars which are discussed in the following chapters.

Chapter 6 : Formation of Organic Acids During Glucose and Fructose Decomposition in HCW

6.1 Introduction

Hydrothermal conversion of biomass in hot-compressed water (HCW), as one of the environmentally friendly technologies, has received large research interest for the sustainable production of biofuels and value-added biochemicals such as sugars, alcohols and organic acids^{5, 16}. HCW as a reaction medium is capable of enhancing both acid- and base-catalysed reactions due to its unique properties^{94, 251}. Because of the complexity of biomass structure, a series of model compounds have been employed to investigate the mechanism of biomass decomposition in HCW, including polymeric sugars (i.e., cellulose and hemicellulose) and monomeric sugars (i.e., glucose and xylose) under various catalytic or non-catalytic conditions^{143, 158-161}. Previous studies also reported the formation of organic acids during hydrothermal conversion of biomass, which may influence the reaction mechanism of biomass decomposition and change the product distribution^{156, 190, 217, 252}.

As discussed in Chapter 2, Our recent study reported the formation of some organic acids (i.e., saccharinic, formic, glycolic and lactic acids) from hydrothermal decomposition of cellobiose (as the simplest glucose oligomer linked by glycosidic bond) under non-catalytic conditions²²⁶. It has been clearly shown that all organic acids are not the primary products from cellobiose hydrothermal decomposition. Instead, organic acids are more likely produced from monomeric sugars such as glucose and fructose²²⁶. Several previous studies^{144, 152, 192, 245} reported the formation of these organic acids from hydrothermal conversion of monosaccharides under catalytic conditions using various reactor systems. For example, saccharinic acid was mainly reported to form from carbohydrate decomposition under alkaline conditions, while formic acid could be produced from the rehydration of 5-hydroxymethylfurfural (5-HMF) under acidic conditions^{144, 152, 192, 245}.

Previous studies on the formation of organic acids from hydrothermal decomposition of monosaccharides were mostly conducted under catalytic conditions, and little has been reported on the formation of organic acids under non-catalytic conditions. However, the formation of organic acids can play a key role in the formation of some products (i.e., 5-HMF²⁵³) during monosaccharide decomposition under non-catalytic conditions.

As discussed earlier because of the complex structure of biomass, model compounds have been employed to understand the mechanism of organic acids formation from hydrothermal conversion of biomass in HCW. In chapter 5, it has been shown that organic acids are not the primary products from hydrothermal decomposition of cellobiose. Therefore, monomeric sugars (glucose and fructose) as the hydrolysis products from cellobiose are studied in chapter 6 to understand the mechanism of organic acids formation from hydrothermal conversion of biomass.

6.2 Yields and Selectivities of Organic Acids from Glucose and Fructose Decomposition in HCW

Various organic acids including saccharinic acid, formic acid, glycolic acid, lactic acid and 2,4-dihydroxy butyric acid (DHBA) can be identified from the liquid products from glucose and fructose decomposition in HCW via HPAEC-CD-MS. In our previous work²²⁶, two saccharinic acids ($m/z = 179$) have been identified from hydrothermal decomposition of cellobiose under non-catalytic condition. These are likely the isomers of saccharinic acid, since there are three different isomers of saccharinic acid as reported previously^{151, 254}. In this study, the similar method was used to detect the saccharides from glucose and fructose decomposition, but only one peak was identified for saccharinic acid ($m/z = 179$). Four isomer standards of saccharinic acids (α -isosaccharinic acid, β -isosaccharinic acid, α -metasaccharinic acid, β -metasaccharinic acid) were further tested to identify the type of saccharinic acid. It was confirmed that metasaccharinic acids (MSA) are the major saccharinic acids in the liquid products during hydrothermal decomposition of glucose and fructose under non-catalytic conditions.

Figure 6-1 presents the yields and selectivities (on a carbon basis) of organic acids during glucose and fructose decomposition in HCW at 225–275 °C. The yields of all quantified organic acids are low for both glucose and fructose at 225 °C, but their yields increase with temperature and residence time. Thus, the maximal organic acids are obtained at 275 °C and ~58s. Among all quantified organic acids from glucose decomposition, MSA has the maximal yield of ~8.4%, much higher than those for other organic acids, i.e., ~3.2% for formic acids, ~2.2% for glycolic acid, ~6.2% for lactic acid, and ~5.1% for DHBA. For fructose, the trends of organic acids are similar to those for glucose, but some differences can be found. For example, the yields of some organic acids (i.e., formic acid, MSA and lactic acid) from fructose decomposition are higher than those from glucose decomposition, indicating that those organic acids can be more easily produced from fructose. For example, the maximal yields of formic acid, MSA and lactic acid for fructose decomposition at 275 °C and ~58 s are ~4.6, ~10.1 and ~8.2 %, respectively, much higher those for glucose. While the maximal yields of other organic acids are similar, i.e., ~2.6% for glycolic acid, and ~4.9% for DHBA. This indicates that the formation pathways of organic acids may be quite different for glucose and fructose.

The selectivities of organic acids were further calculated, and the results are presented as function of conversion in Figure 2f-j. It can be see that the selectivities of all organic acids increase with conversion for both glucose and fructose. For glucose, the maximal selectivities of organic acids achieved under the current reaction conditions are ~3.5% for formic acid, ~9.5% for MSA, ~6.9% for lactic acid, ~5.7% for DHBA and ~2.5% for glycolic acid. For fructose, the maximal selectivities of organic acids achieved are ~4.8% for formic acid, ~11.5% for MSA, ~8.6% for lactic acid, ~5.1% for DHBA and ~2.7% for glycolic acid. While the selectivity trends of organic acids are similar for glucose and fructose, some differences can be observed. First, according to the Delplot method²⁵⁵, MSA is identified as a minor primary product from fructose decomposition (see Figure 2g) but not from glucose decomposition, which is an important finding of this study. This is reasonable since MSA is a saccharinic acid with 6 carbons, which can be only produced from some sugar compounds. However, the selectivity of MSA from fructose decomposition is very low, only ~3% based on the intercept at zero conversion. Other organic acids are all secondary products. Second, the selectivities

of formic acid and MSA for fructose are higher than those for glucose at the same conversion, indicating that formic acid and MSA can be easily formed from fructose. In comparison, the selectivities for other organic acids have similar trends as a function of conversion.

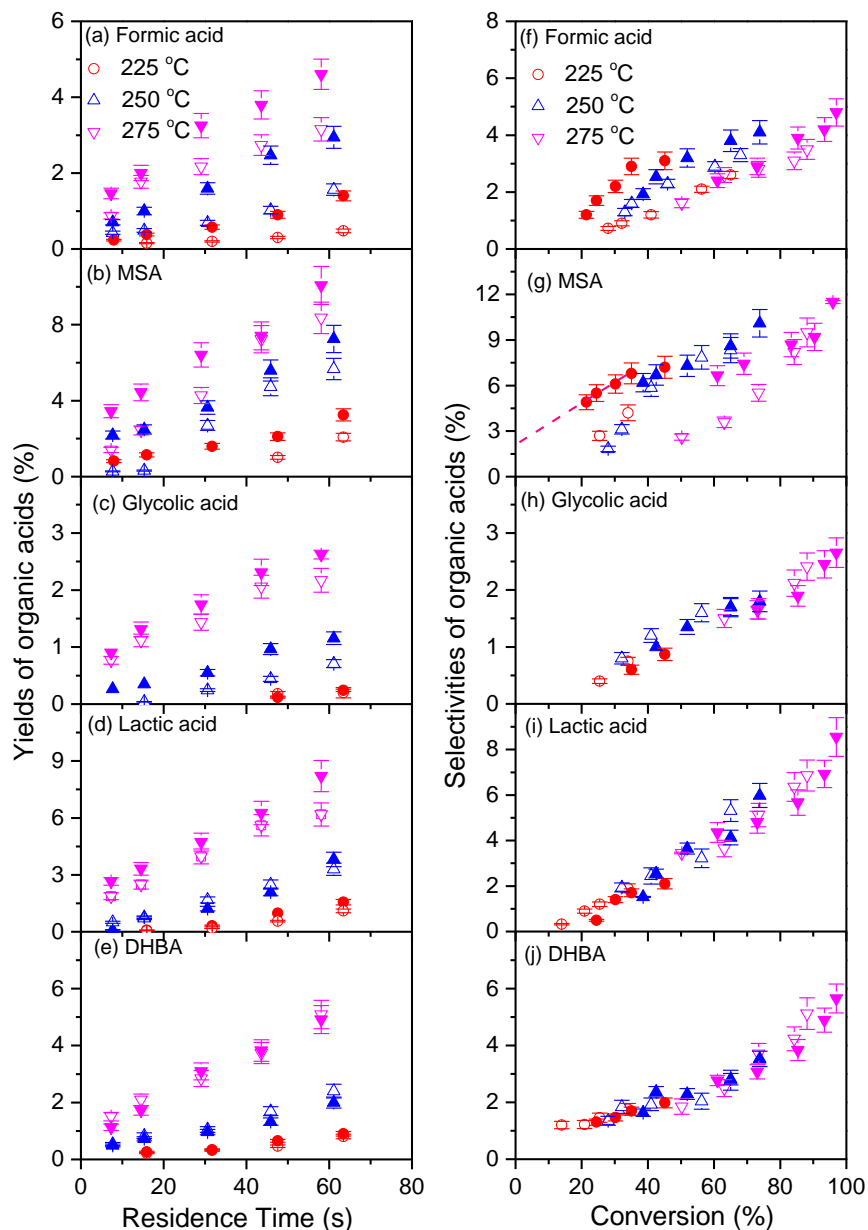


Figure 6-1: Yields and selectivities of organic acids produced from glucose (hollow) and fructose (solid) decomposition in HCW at 225–275 °C. (a) Formic acid yield, (b) MSA yield, (c) Glycolic acid yield, (d) Lactic acid yield, (e) DHBA yield, (f) Formic acid selectivity, (g) MSA selectivity, (h) Glycolic acid selectivity, (i) Lactic acid selectivity, (j) DHBA selectivity.

6.3 Comparisons Between $[H^+]$ Calculated from Quantified Organic Acids and Measured pH

The calculation of total hydrogen ion dissociated is based on the dissociation constant for each organic acid, with the detailed method presented in the Experimental Section. Figure 6-2 compares the hydrogen ion concentrations calculated from the quantified organic acids and the direct pH measurement of the product solution after each experiment for hydrothermal decomposition of glucose and fructose. It can be seen that the hydrogen ion concentration increases as sugar conversion increases, suggesting more organic acids are produced at increased conversions during hydrothermal decomposition of both glucose and fructose. For example, the concentration of hydrogen ion during glucose decomposition increases from ~0.02 mM at ~10% conversion to ~0.38 mM at ~93% conversion. While for fructose, the concentration of hydrogen ion increases from ~0.05 mM at ~20% conversion to ~0.45 mM at ~98% conversion. Although the hydrogen concentrations are similar at same conversion during hydrothermal decomposition of glucose and fructose, the hydrogen concentrations for fructose are slightly higher at higher conversions (i.e., >80%). Moreover, the data show that the differences between the calculated and measured $[H^+]$ are small during glucose and fructose decomposition in HCW, suggesting that majority of the organic acids produced are quantified in this study. At higher conversions, more secondary reactions lead to the formation of other organic acids which contribute to a small percentage of the total hydrogen concentration.

The calculation of total hydrogen ion dissociated is based on the dissociation constant for each organic acid, with the detailed method presented in Chapter 3.

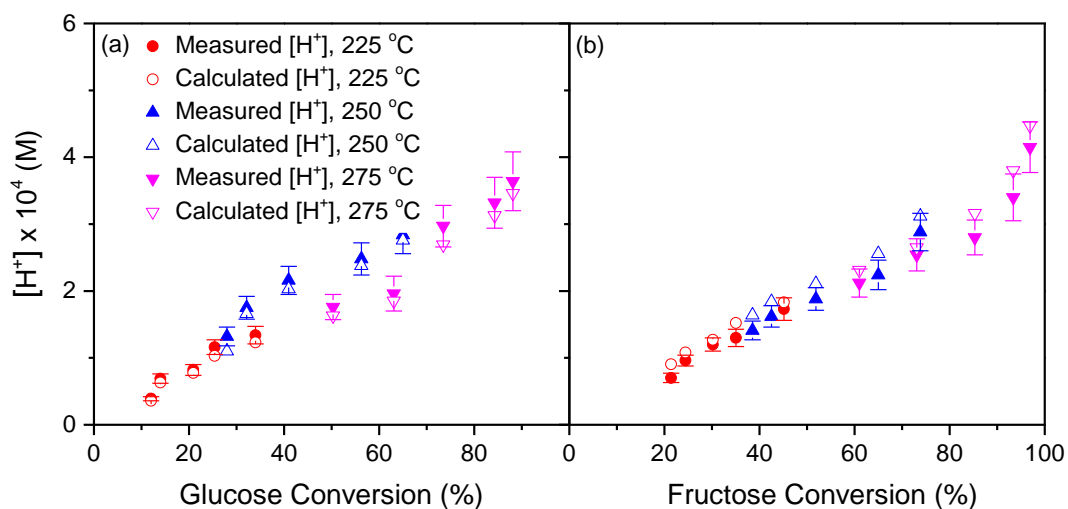


Figure 6-2: Comparisons of the hydrogen ion concentrations calculated from total concentrations of the quantified organic acids and the measured pH of the liquid products after (a) glucose and (b) fructose decomposition in HCW at various temperatures.

Further analysis was conducted to understand the contribution of each organic acid to the total $[H^+]$ concentration dissociated from the identified organic acids from glucose and fructose decomposition in HCW at 225–275 °C, as shown in Figure 6-3. It can be seen that formic acid contributes the highest to the total hydrogen ion dissociated for glucose decomposition. At 225 °C, the contribution of formic acid is ~75% at early conversions (i.e., at ~12% conversion), but decreases as conversion increases and stabilises at ~40-50% at conversions >40%. In contrast, the contribution of MSA to the total hydrogen ion dissociated stabilises at ~25% at 225 °C, but reduces to ~15% as glucose conversion further increases at higher temperatures. Another observation is that the contribution of lactic acid is ~20% at 225 °C, but increases to ~25% at 250 °C during glucose decomposition, making lactic acid the second largest contributor of the total hydrogen ion at temperatures >250 °C, followed by MSA, DHBA and glycolic acid. The contributions of DHBA and glycolic acid are generally low (<15%).

For fructose decomposition, the contributions of organic acids generally follow similar trends, but with some differences. While formic acid still contributes the highest to the total hydrogen ion dissociated, its contribution is slightly lower due to the increased contributions of MSA and lactic acid, especially at high temperatures.

For example, the contribution of MSA for fructose is ~22% and ~25% at 250 and 275 °C, slightly higher those of ~15% for glucose. This is due to that MSA becomes a primary product during fructose decomposition. For lactic acid, it contributes to ~27% and ~30% of total hydrogen ion at 250 and 275 °C, respectively, slightly higher those of ~25% for glucose. This is mainly because glyceraldehyde (as a precursor of lactic acid) becomes a primary product during fructose decomposition.

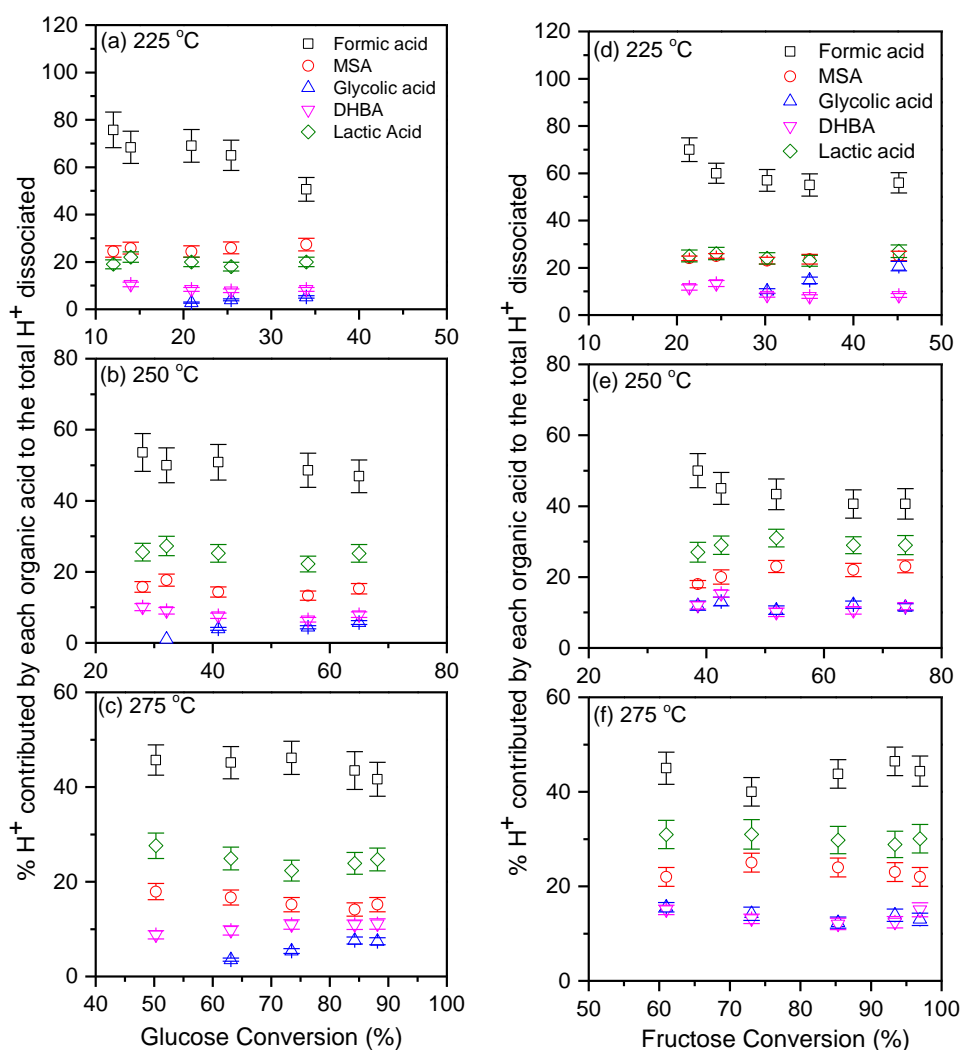


Figure 6-3: Contributions of formic acid, MSA, glycolic acid, DHBA and lactic acid to the total $[H^+]$ dissociated calculated by the quantified organic acids from glucose and fructose decomposition in HCW at 225–275 °C. (a) glucose at 225 °C, (b) glucose at 250 °C, (c) glucose at 275 °C, (d) fructose at 225 °C, (e) fructose at 250 °C, (f) fructose at 275 °C.

6.4 Reaction Pathways of Organic Acids During Glucose and Fructose Decomposition

The results in this study clearly show that various organic acids are generated during glucose and fructose decomposition in HCW. Considering the formation of organic acids can affect the products distribution, it is important to understand the reaction pathways of organic acids during hydrothermal decomposition of glucose and fructose. Based on our current data and previous literatures, Figure 6-4 presents the reaction pathways for identified organic acids during glucose and fructose decomposition in HCW under non-catalytic condition.

Formic acid is one of the most important organic acids produced from glucose and fructose, since it greatly contributes to the hydrogen ion in the liquid product. There are several reaction pathways for formic acid formation. First, it was mainly reported as a rehydration product of 5-hydroxymethylfurfural during acid hydrolysis of monosaccharides^{192, 202, 256}. Second, it can be also produced from hydrothermal oxidation by α -scission or alkaline hydrothermal treatment of monosaccharides¹⁹⁸⁻²⁰¹. Third, it can be produced through the Lobry de Bruyn–Albeda van Ekenstein transformation (LBAE) of erythrose to produce formic acid and glyceraldehyde under alkaline condition^{143, 144}. Fourth, formic acid can be formed through pyruvaldehyde via α -dicarbonyl cleavage. However, it is more likely that the last reaction pathway is responsible for the formic acid formation under current reaction conditions.

Saccharinic acid is also an important organic acid with high yields (on a carbon basis) from both glucose and fructose decomposition. However, its contribution to the hydrogen ion in the liquid product is much lower compared to formic acid, due to its lower molar concentration and lower dissociation constant. As discussed earlier, saccharinic acid is mainly produced during hydrothermal conversion of monosaccharides under alkaline conditions. Based on existing literature, three isomeric forms have been reported for saccharinic acids: saccharinic (or 2-methylpentonic) acids, isosaccharinic (or 3-deoxy-2-hydroxymethylpentonic) acids, metasaccharinic (or 3-deoxyhexonic) acids. This study is the first in the field to identify the formation of MSA during hydrothermal decomposition of glucose and

fructose under non-catalytic conditions. Under alkaline condition the Nef-Isbell mechanism for the saccharinic acid formation involves several key steps: (a) the formation of enediol via keto-enol tautomerism followed by production and isomerisation of anion, (b) β -hydroxycarbonyl elimination to form diketo intermediate, (c) dicarbonyl intermediate formation via keto-enol tautomerism (d) benzylic acid rearrangement of the intermediate to produce the saccharinic acid^{151, 152, 203, 204}. This study also clearly demonstrates that MSA is a minor primary product from fructose decomposition, but only a secondary product from glucose decomposition under non-catalytic HCW. Therefore, it is suggested that the mechanism of metasaccharinic acid formation may be different from Nef-Isbell mechanism via diketo intermediate under alkaline condition. It is more likely due to the similar structure of fructose to MSA or diketo intermediate as the important precursor for MSA formation.

Lactic acid also contributes largely to the hydrogen ion in the liquid product from both glucose and fructose decomposition. Lactic acid is generally formed via benzylic acid rearrangement of pyruvaldehyde^{144, 159, 202, 243, 257}, which can be easily produced from aldehydes (i.e., glyceraldehyde, erythrose). Particularly, glyceraldehyde is reported as a primary product from fructose decomposition¹⁸⁶, which explains a higher yield of lactic acid from fructose. Although lactic acid can also be formed from glycolaldehyde via the formation of pyruvaldehyde through series of reaction, glyceraldehyde can produce more lactic acid with a higher efficiency compared to glycolaldehyde and erythrose^{257, 258}. Previous literatures also reported DHBA produce from aldol condensation of glycolaldehyde²⁵⁹. The reaction pathway of Glycolic acid also consists of isomerisation between glyceraldehyde and dihydroxyacetone, which dihydroxyacetone undergoes C-C bond hydrolytic cleavage to produce glycolic acid²¹³.

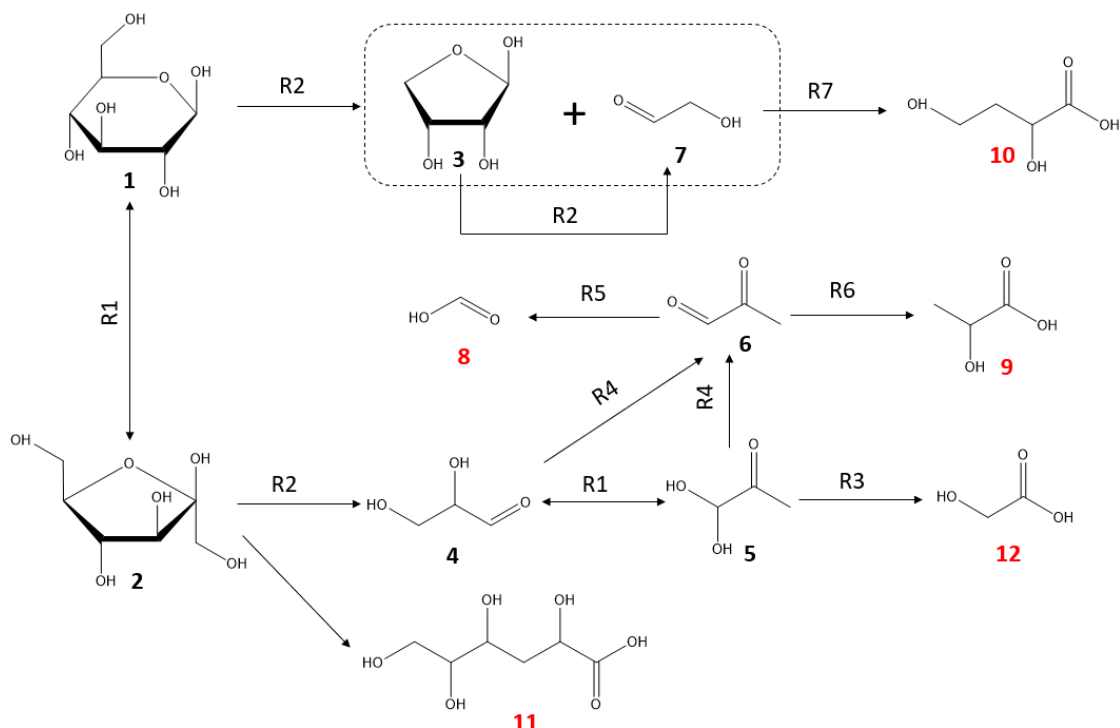


Figure 6-4: Summarised reaction pathways for saccharinic, formic, lactic, glycolic and 2,4 dihydroxy butyric acids during glucose and fructose decomposition in HCW based on the previous literatures^{143, 151, 152, 205, 206, 245, 259-261} and this study. (1): Glucose; (2): fructose; (3): erythrose; (4): glyceraldehyde; (5): dihydroxyacetone; (6): pyruvaldehyde; (7): glycolaldehyde; (8): formic acid; (9): lactic Acid; (10): 2,4 dihydroxy butyric acid; (11) metasaccharinic acid; (12) glycolic acid. R1: Isomerisation; R2: Retro-aldol condensation; R3: Rehydration; R4: Dehydration; R5: α -dicarbonyl cleavage; R6: Benzilic acid rearrangement; R7: aldol condensation.

6.5 Conclusions

This chapter reports the formation of organic acids during glucose and fructose decomposition in HCW under non-catalytic condition at 225–275 °C. Five organic acids including metasaccharinic, formic, lactic, glycolic and 2,4 dihydroxy butyric acids are identified from both glucose and fructose decomposition. As the first time in the field, MSA from glucose and fructose decomposition under non-catalytic condition is successfully identified and quantified. The data indicate that MSA is a minor primary product from fructose decomposition, but only a secondary product from glucose decomposition. Among the identified organic acids, MSA has the highest yield and selectivity on a carbon basis, i.e., with the selectivity of ~9.5% and

~11.5% at ~90-95% conversion for glucose and fructose, respectively. However, formic acid has the highest contribution to the total hydrogen ion dissociated, resulted in a reduction in the pH of the liquid product, due to its highest molar concentration and highest dissociation constant. The hydrogen ion concentrations calculated from the quantified organic acids are also compared with those calculated from pH directly measured after each experiment. A close match between the calculated and measured hydrogen ion concentration indicates that majority of organic acids produced during glucose and fructose decomposition have been identified. Possible reaction pathways of the identified organic acids during glucose and fructose decomposition in HCW are also summarised and discussed.

In next chapter, the decomposition behaviour of mannose, as an important monomeric sugar produced from cellobiose decomposition in HCW, will be investigated to better understand its decomposition mechanism and reaction pathways.

Chapter 7 : Reaction Mechanism and Pathways of Mannose Decomposition in HCW

7.1 Introduction

Lignocellulosic biomass as a renewable source of energy has attracted increasing attention to address the issues and concerns arise from fossil fuel using^{16, 30, 31}. Among the technologies for utilisation of biomass, hydrothermal processing of biomass HCW is a promising technology to convert biomass to biofuels and platform chemicals. Various reactor systems and different reaction conditions have been employed for studying hydrothermal conversion of biomass in HCW^{94, 251}. Lignocellulosic biomass consists of three major components: cellulose, hemicellulose and lignin. Cellulose and hemicellulose account for up to two thirds of lignocellulosic biomass^{262, 263}. Hemicellulose is the second most abundant component of plant biomass after cellulose and with its amorphous structure comprises 15-35% of plant biomass and consists of different sugars, mainly pentoses (xylose and arabinose) and hexoses (mannose, galactose and glucose)^{262, 263}. The structure of hemicellulose is complex as a result of different ratio of its monomers from various plant types. The sugars in hemicellulose may be converted to acids and furan derivatives which may act as inhibitors during biofuel production^{263, 264}. The proportion of hemicellulose is 10-15%, in softwood, 18-23% in hardwood and 20-25% in herbaceous plants. Compared to cellulose, hemicellulose with more amorphous structure, easily hydrolyse into its monomer sugars. The most abundant sugars in hemicellulose are xylose and mannose, and mannose (C-2 epimer of glucose) is the major component of hemicelluloses in soft wood^{263, 264}. While previous studies mainly focused on the hydrothermal conversion of cellulose, as part of lignocellulosic biomass, hemicellulose received far less attention^{173, 265}. Raisanen et al.²⁶⁶ reported the degradation products from mannose pyrolysis at 500 °C and 550 °C. Another study²⁶⁷ also investigated the catalytic gasification of mannose at 500-

700 °C and the obtained findings were in accordance with results of glucose and fructose gasification under supercritical water condition. Srokol¹⁴³ reported the hydrothermal treatment of dilute solution of some monosaccharides including mannose at 340 °C and 27.5 MPa. The identified products are quite similar due to the occurrence of Lobry de Bruyn-Alberda van Ekenstein rearrangement between studied monosaccharides.

As discussed in previous chapters, organic acids are one of the value-added chemicals from biomass decomposition. Oligomers as the primary products of hydrothermal conversion of biomass/cellulose, further decomposed into sugar monomers and other value-added compounds including organic acids. Previous chapter provided direct evidences on the formation of organic acids during glucose and fructose decomposition. So far, there is no fundamental study on the formation of degradation products from mannose decomposition under non-catalytic HCW. Therefore, a study of hydrothermal conversion of mannose (C-2 epimer of glucose) as one of the major components of hemicellulose is of great importance to better understand the hemicellulose behaviour. Consequently, this study focuses on hydrothermal conversion of mannose to provide new insights into all major mannose decomposition products in HCW under non-catalytic conditions.

7.2 Mannose Conversion and Yields of Major Products During Mannose Decomposition in HCW

The liquid samples were analysed by HPAEC-PAD-MS, and various products can be identified, including glucose and fructose produced via isomerization reactions, 5-HMF produced via dehydration reaction, glycolaldehyde (GA) and glyceraldehyde (GCA) produced via retro-aldol condensation reactions, as well as various organic acids such as formic acid, saccharinic acid, formic acid, glycolic acid, lactic acid and 2,4-dihydroxy butyric acid (DHBA). Since four isomer standards of saccharinic acids (α -isosaccharinic acid, β -isosaccharinic acid, α -metasaccharinic acid, β -metasaccharinic acid) are present, this study confirms that both isomers of MSA are the major saccharinic acids in the liquid products from mannose decomposition in HCW. Also, 1,6-anhydro- β -D-mannopyranose was identified in the liquid product

from mannose decomposition, but its yield is very low (max 0.1%) so its yield was not quantified in this study.

Figure 7-1 presents the conversions of mannose during its decomposition in HCW at 200 – 275 °C and various residence times. It can be seen that mannose decomposition is slow at 200 °C, with a conversion of ~15% at a residence time of ~66 s. However, the mannose conversion increases rapidly with temperature. At 275 °C, the mannose conversion increases from ~50% at ~7 s to ~95% at ~58 s.

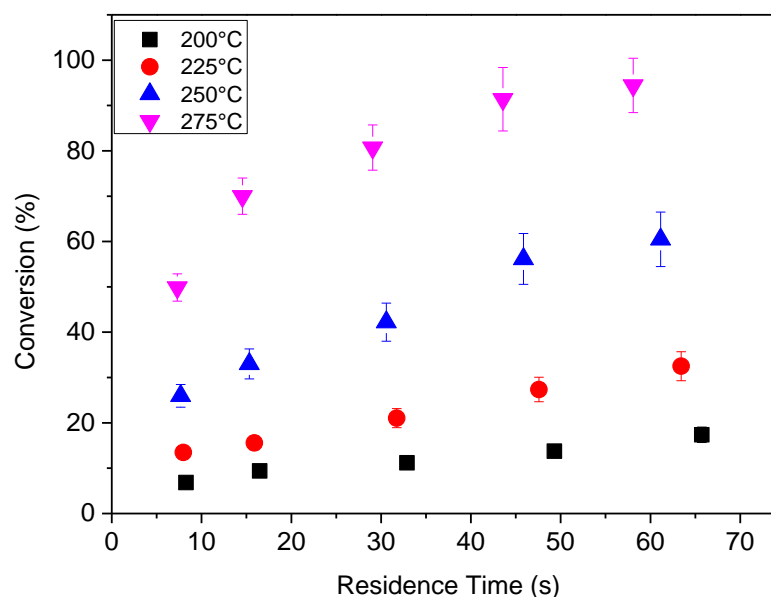


Figure 7-1: Mannose conversion during decomposition in HCW at 200 – 275 °C.

All major products from mannose decomposition in HCW at 200 – 275 °C were quantified, and their yields (on a carbon basis) are presented in Figure 7-2. For glucose and fructose, similar trends can be found but the yield of fructose is much higher than the yield of glucose. At 200 °C, both the glucose and fructose yields increase with residence time, i.e., from ~0.6 and ~3.4 % to ~1.5 and ~7.1% when the residence time increases from ~8 to ~66 s, respectively. At a higher temperature of 225 °C, the yields of glucose and fructose increase from ~1.4 and ~6.8% at 8 s to ~2.8 and ~11.4% at ~63 s, respectively. When the temperature increases to 250 °C, their yields first increase with residence time and then reach the maximal yields, followed by reductions when the residence time further increases. For example, the glucose and fructose yields increase from ~2.1 and ~9.4 % at 8 s to ~3.2 and ~12.5% at ~31 s, but reduces to ~2.8 and ~10.8% at ~61 s, respectively. At 275 °C, both the glucose and fructose yields decrease with increasing the residence time, i.e., from

~2.7 and ~11.3% to ~1.3 and ~3.7% when the residence time increases from ~7 to ~58 s, respectively. The data indicate that glucose and fructose are likely the primary products from mannose decomposition in HCW, but they can be easily decomposed at higher temperatures.

For other products, their yields all increase with residence time at all temperatures, indicating that those products are more likely the secondary products from mannose decomposition in HCW. Under the current conditions, the maximal yields are obtained at 275 °C and ~58 s, i.e., ~16 %, ~5% and ~23% for 5-HMF, GCA and GA, respectively. As for organic acids, their yields also increase with residence time at all temperatures, thus all organic acids are also the secondary products from mannose decomposition in HCW. Under the current conditions, the maximal yields are also obtained at 275 °C and ~58 s, i.e., ~3%, ~7.5%, ~1.5%, ~3.5% and ~4% for formic acid, MSA, glycolic acid, lactic acid and DHBA, respectively.

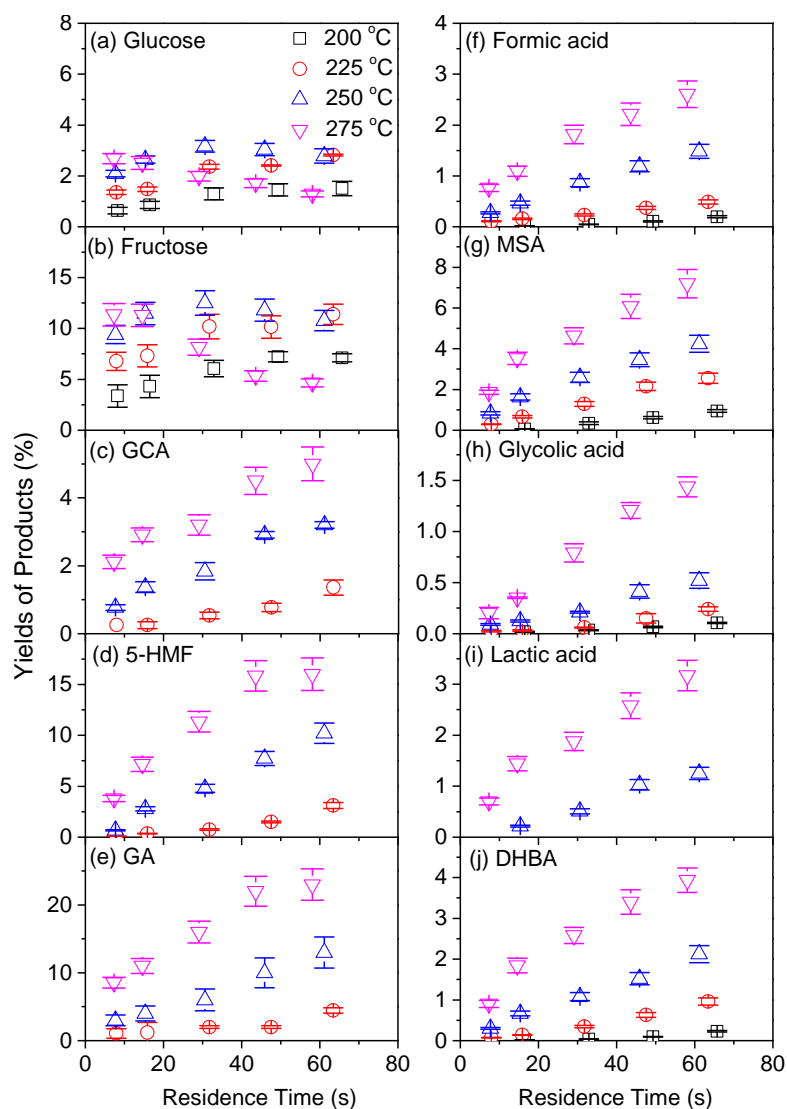


Figure 7-2: Yields of major products during mannose conversion during decomposition in HCW at 200 – 275 °C. (a) Yield of glucose; (b) yield of fructose; (c) yield of GCA; (d) yield of 5-HMF; (e) yield of GA; (f) yield of formic acid; (g) yield of saccharinic acid; (h) yield of glycolic acid; (i) yield of lactic acid and (j) yield of DHBA.

7.3 Selectivities of Major Products During Mannose Decomposition in HCW

Based on the above data, the selectivities of major products during mannose decomposition in HCW at 200 – 275 °C were further calculated on a carbon basis, and the selectivity results are presented as a function of mannose conversion in Figure 7-3. Clearly, the selectivities of glucose and fructose decrease continuously

with increasing the mannose conversion, confirming that glucose and fructose are indeed the primary products from mannose decomposition. The initial selectivity of fructose is ~80% at a low mannose conversion of 5%, much higher than that of glucose (~17%) under the same condition. This demonstrates that the isomerization reaction to produce fructose is a dominant primary reaction during mannose decomposition in HCW, while the isomerization reaction to produce glucose is only a minor primary reaction. Compared to those of glucose and fructose, the selectivities of other products are low at early conversions, but increase continuously with mannose conversion, demonstrating that all other products are indeed the secondary products from mannose decomposition in HCW. Under the current conditions, their maximal selectivities obtained are ~20%, ~40% and ~12% at ~90% mannose conversion for 5-HMF, GA and GCA, respectively. The results suggest that retro-aldol condensation reactions of mannose are difficult to take place, especially at low temperatures. GA and GCA are more likely produced from the primary products fructose¹⁸⁶. Similarly, the selectivities of organic acids also increase with mannose conversion. Under the current conditions, the maximal selectivity of MSA obtained is ~8.5%, much higher than those for other organic acids, i.e., by ~5%, ~4%, ~3%, ~1.6% for DHBA, lactic acid, formic acid and glycolic acid, respectively.

To further understand the contributions of two primary reactions during mannose decomposition in HCW, the delplot method^{255, 268} was employed to obtain the selectivities of glucose and fructose at mannose conversion $X \rightarrow 0$. According to the delplot method, the intercept of product selectivity at mannose conversion $X \rightarrow 0$ determines the ratio of primary reaction to overall mannose decomposition. It can be seen that the selectivities of glucose and fructose at mannose conversion $X \rightarrow 0$ are ~18% and ~82%, respectively. This clearly demonstrates that isomerization reactions to produce glucose and fructose are the only two primary reactions during mannose decomposition in HCW, since the total contribution of two isomerization reactions are close to 100%. Therefore, all other products (i.e., 5-HMF, GA, GCA and organic acids) cannot be directly produced from mannose under the current conditions. Rather, those products are more likely produced from glucose and fructose. The formation pathways of 5-HMF, GA and GCA can be found in our previous works^{173, 186}, while those of organic acids have been elucidated in previous chapters.

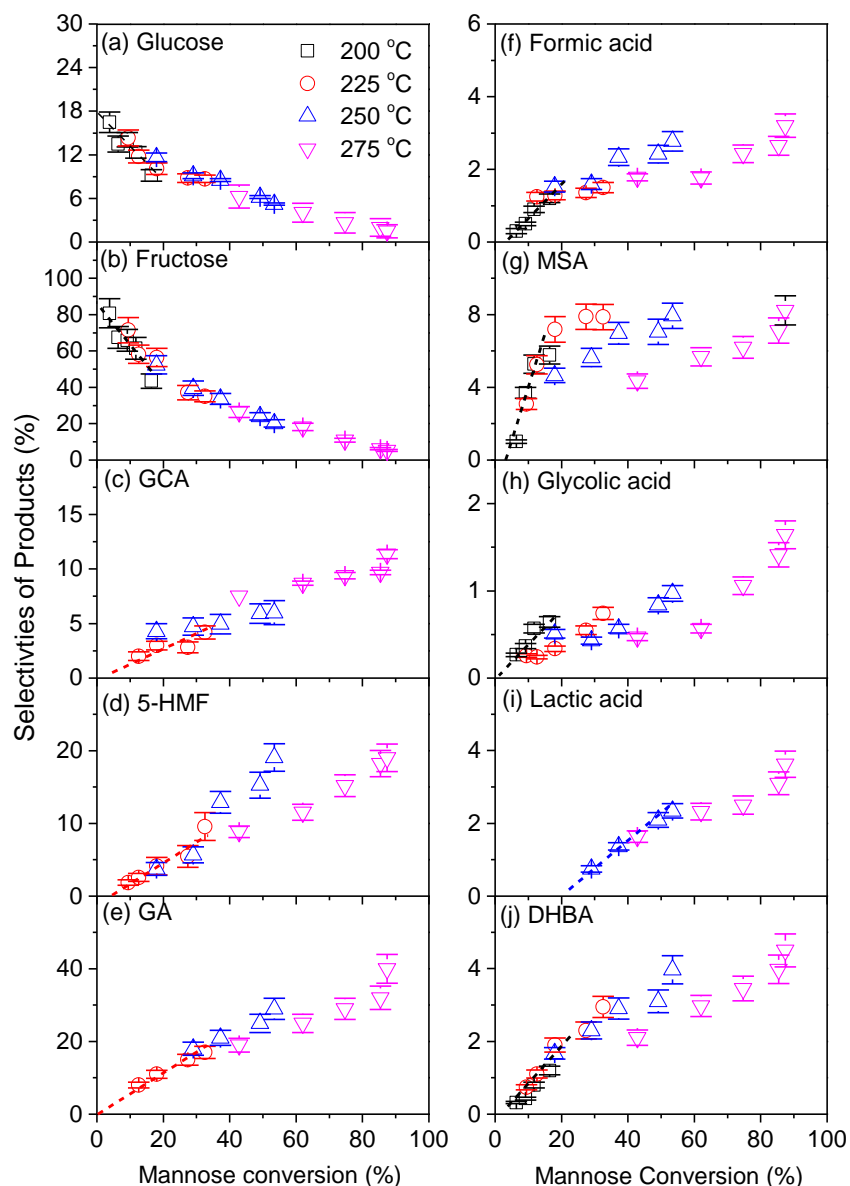


Figure 7-3: Selectivities of major products during mannose conversion during decomposition in HCW at 200 – 275 °C. (a) Selectivity of glucose; (b) selectivity of fructose; (c) selectivity of GCA; (d) selectivity of 5-HMF; (e) selectivity of GA; (f) selectivity of formic acid; (g) selectivity of saccharinic acid; (h) selectivity of glycolic acid; (i) selectivity of lactic acid and (j) selectivity of DHBA.

7.4 Kinetics of Mannose Decomposition in HCW

The reaction rate constants of mannose decomposition in HCW at 200-275 °C can be calculated based on the mannose conversion data. Assuming the mannose decomposition follows first-order kinetics, the reaction rate constant k (s^{-1}) can be determined using the following equation:

$$-\ln[C(t)/C(0)] = kt \quad (7.1)$$

where $C(t)$ and $C(0)$ (mg L^{-1}) are the mannose concentrations before and after decomposition, and t (s) is the residence time.

The correlations between $-\ln[C(t)/C(0)]$ and residence time t at different temperatures are plotted in Figure 7-4. Linear relationships between $-\ln[C(t)/C(0)]$ and residence time t can be observed for all temperatures, suggesting that mannose decomposition at HCW indeed follows first order kinetics. It can be found that the reaction rate constant increases with temperature, i.e., from 0.0018 at 200 °C to 0.0318 at 275 °C. According to the Arrhenius plots of mannose decomposition (see Figure 7-5), the activation energy and pre-exponential factor are further calculated to be 83 kJ/mol and $2.7 \times 10^6 \text{ s}^{-1}$, respectively.

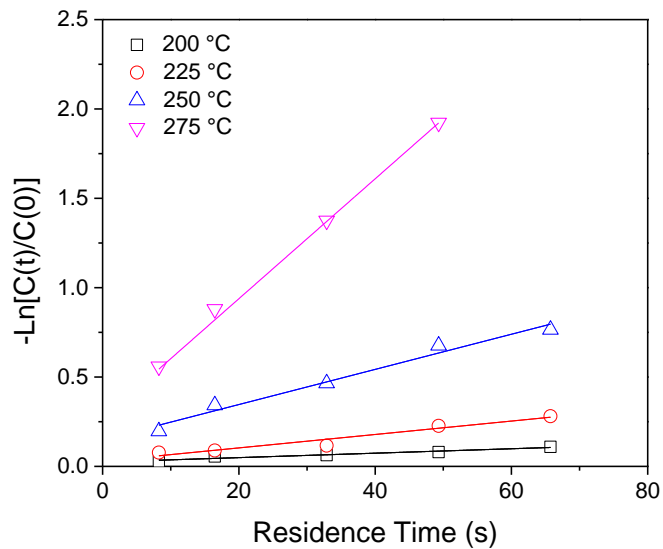


Figure 7-4: Correlations between $-\ln[C(t)/C(0)]$ and residence time during mannose decomposition in HCW at 200 – 275 °C.

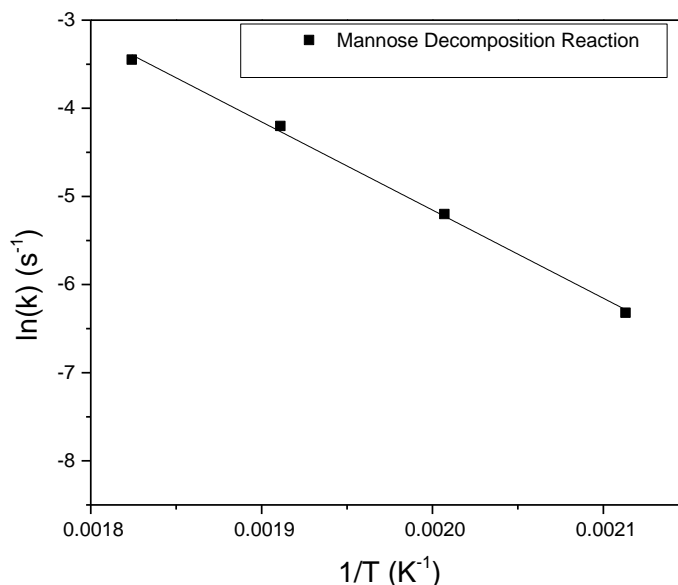


Figure 7-5: Arrhenius plots during mannose decomposition in HCW at 200 – 275 °C.

7.5 Formation of Organic Acids During Mannose Decomposition in HCW.

According to the yields of major organic acids, the contribution of each quantified organic acid to the total hydrogen ion dissociated from mannose decomposition in HCW at 200 – 275 °C were further estimated, and the results are presented in Figure 7-6. It can be seen that formic acid contributes to the most of the total hydrogen ion dissociated particularly at all conditions, which might be due to its high molar concentration and dissociation constant. For example, formic acid contributes to ~70% of the total [H⁺] dissociated at ~6% mannose conversion. However, its contribution decreases with mannose conversion, and becomes stable at ~40% at mannose conversions >15%. In contrast, the contribution of MSA increases with mannose conversion and reaches ~40% at ~17% conversion, followed by a decrease as the mannose conversion further increases and stabilises at ~20% at mannose conversions >40%. The contribution of other organic acids to the total hydrogen dissociated is low at all temperatures and the maximal value is <20% under all conditions.

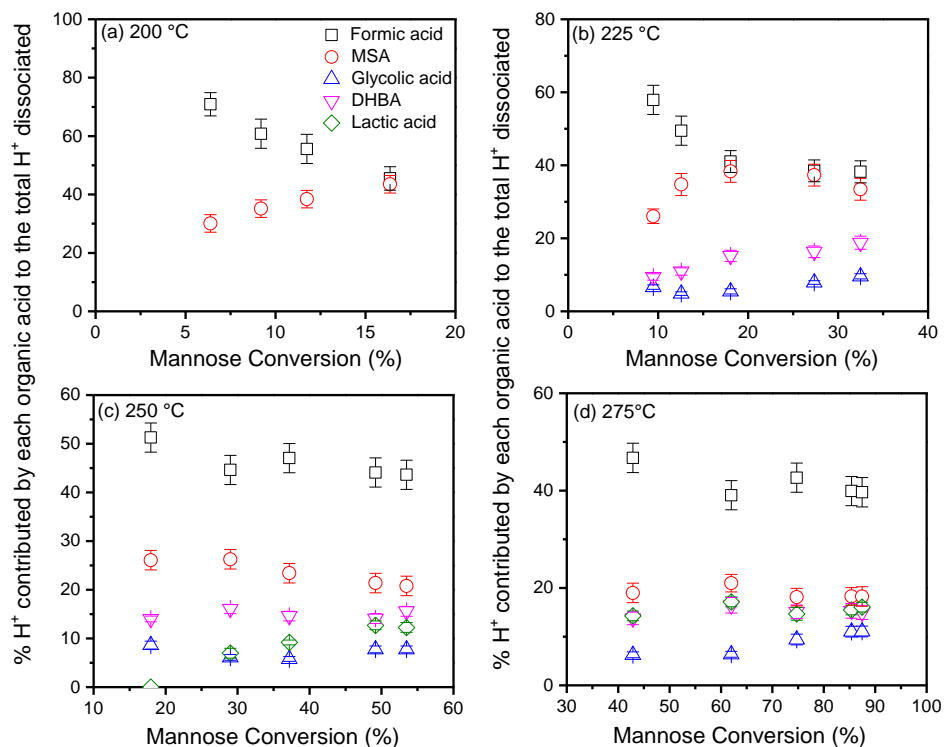


Figure 7-6: Contribution of organic acids to the total $[H^+]$ dissociated calculated by the quantified organic acids from mannose decomposition in HCW at 200 – 275 °C. (a) 200 °C, (b) 225 °C, (c) 250 °C, (d) 275 °C.

The pH value of the liquid product was also measured right after the experiments for all conditions and the results are presented as a function of mannose conversion in Figure 7-7. It can be clearly seen that the pH value decreases substantially as mannose conversion increases under current experimental conditions, i.e., from ~6 at ~10% conversions to ~3 at ~85% conversions. Such results are consistent with previous studies^{150, 217, 226}. The formation of organic acids can take place at the early stage of mannose decomposition, leading to a rapid reduction of pH in the product. The formation of organic acids may affect the reaction mechanism of mannose decomposition as well as the product distribution.

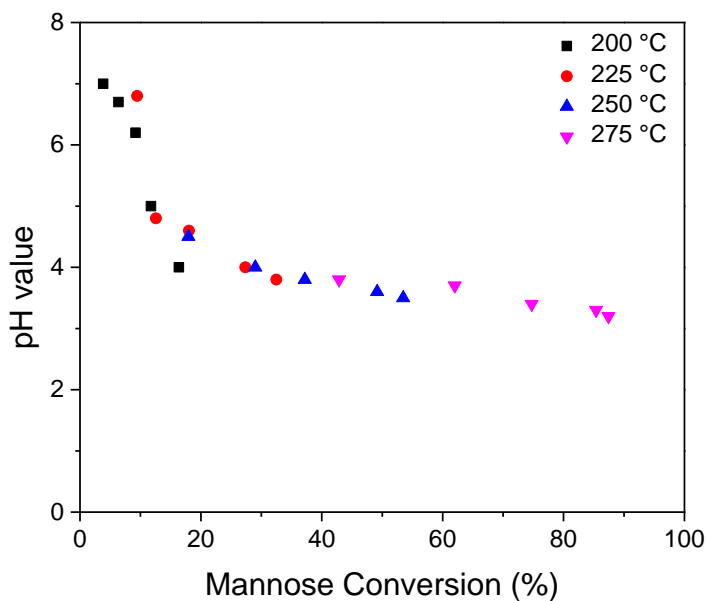


Figure 7-7: pH value of liquid product as a function of mannose conversion during mannose decomposition in HCW at 200 – 275 °C

Further comparisons between hydrogen ion concentrations calculated from the quantified organic acids and measured from direct pH measurement of the liquid product after each experiment are presented in Figure 7-8. It can be seen that the hydrogen ion concentration increases as mannose conversions increase, suggesting more organic acids are produced at increased conversions during mannose decomposition in HCW. For example, the concentration of hydrogen ion is ~0.05 mM at ~10% mannose conversion and increases to ~0.35 mM at ~90% mannose conversion. Moreover, the differences between the calculated and measured $[H^+]$ are small at low conversions, suggesting that majority of the organic acids produced during mannose decomposition in HCW are quantified in this study. At higher conversions, the gap between the calculated and measured $[H^+]$ becomes larger, indicating that other organic acids are formed due to enhanced secondary reactions. Overall, the contributions of unquantified organic acids are small.

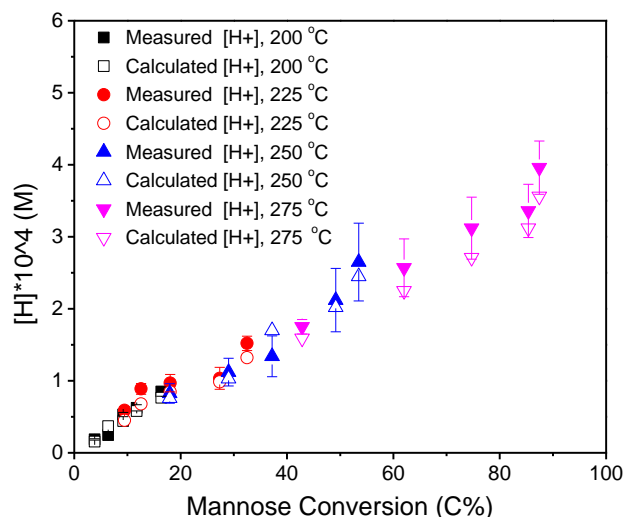


Figure 7-8: Comparisons of the hydrogen ion concentrations calculated from total concentrations of the quantified organic acids and the measured pH of the liquid products during mannose decomposition in HCW at 200 – 275 °C.

7.6 Mechanism and Reaction Pathways of Mannose Decomposition in HCW.

This study provides new insights into the primary decomposition mechanism of mannose in HCW. Our data clearly demonstrate that isomerization reactions to produce fructose and glucose are the only two primary reactions during mannose decomposition in HCW. According to the Delplot method, isomerization reactions to produce fructose and glucose are found to contribute to ~82% and ~18% of the primary decomposition reactions of mannose. Other products such as 5-HMF, GA, GCA and organic acids are also detected, but those products are all secondary products during mannose decomposition in HCW.

Based on the data in this study and previous literature, Figure 7-9 presents the reaction pathways of mannose decomposition in HCW, including the key compounds detected in this study. Mannose can be isomerised into glucose and fructose via Lobry de Bruyn-Alberda van Ekenstein transformation through enediol intermediate^{143, 165}. While the retro-aldol condensation reaction is not a primary reaction of mannose decomposition, it is a primary reaction of fructose decomposition to produce aldehydes such as GCA¹⁸⁶. Also, 5-HMF can be produced from fructose via dehydration¹⁷⁴, most likely catalysed by the formed organic acids. Previously,

formation of saccharinic acid was mainly reported under alkaline conditions, i.e., by the Nef-Isbell mechanism through a series of reactions^{151, 152, 203, 204}. In our experimental condition MSA produced through fructose decomposition, as demonstrated in previous chapter MSA is a minor primary product of fructose decomposition.

Formic acid is more likely formed through pyruvaldehyde (dehydration product of dihydroxyacetone) by α -carbonyl cleavage, while lactic acid is another product of pyruvaldehyde via benzilic acid rearrangement^{143, 144, 202, 257}. As mentioned in previous chapter, previous literatures reported DHBA produce from aldol condensation of glycolaldehyde²⁵⁹, and glycolic acid produced from glyceraldehyde via cleavage of C-C bond²¹³.

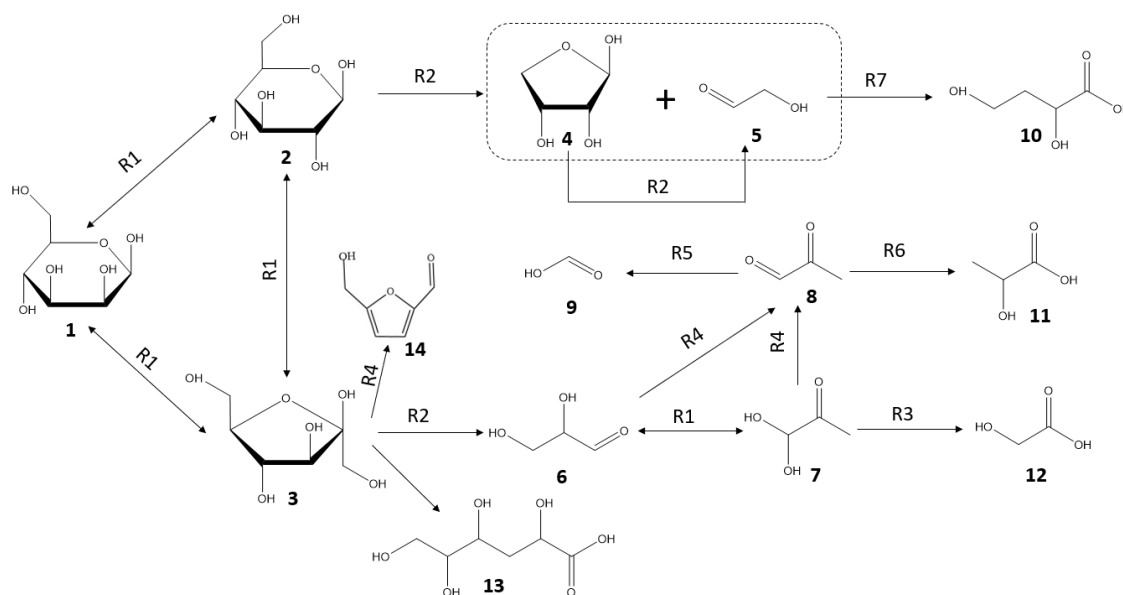


Figure 7-9: Reaction pathways of mannose decomposition in HCW based on the previous literatures^{130, 147, 148, 200, 201, 240, 253-255} and this study. (1): Mannose; (2): Glucose; (3): Fructose; (4): Erythrose; (5): Glycolaldehyde; (6) Glyceraldehyde; (7): Dihydroxyacetone; (8): Pyruvaldehyde ; (9): Formic Acid; (10) 2,4 dihydroxy butyric acid; (11): Lactic Acid; (12): Glycolic Acid; (13): Meta saccharinic Acid; (14): 5-HMF; R1: Isomerisation; R2: Retro-aldol condensation; R3: Rehydration; R4: Dehydration, R5: α -dicarbonyl cleavage; R6: Benzilic acid rearrangement; R7:Aldol condensation.

7.7 Conclusions

Chapter 7 studied mechanism, kinetics and reaction pathways of mannose decomposition in HCW, and all data can be used practically for proper reactor design and optimization of final products.

Isomerization reactions to produce fructose and glucose are the only two primary reactions during mannose decomposition in HCW, and contribute to ~82 and ~18% of the primary decomposition reactions of mannose, respectively. Other products including glyceraldehyde, glycolaldehyde, 5-HMF and organic acids (i.e., formic acid, MSA, lactic acid, glycolic acid and DHBA) are also identified, but they are all secondary products of mannose decomposition. Among all identified organic acids, formic acid has the highest contribution to the hydrogen ion in the liquid product from mannose decomposition, while MSA has the highest yield and selectivity on a carbon basis. A close match between $[H^+]$ from quantified organic acid and pH measurement directly after each experiment suggests that majority of organic acids produced during mannose decomposition in HCW are identified. Reaction pathways for the production of key compounds during mannose decomposition in HCW are also summarised.

Chapter 8: Conclusions and Recommendations

8.1 Introduction

Overall this PhD study provides new understanding in hydrothermal decomposition of biomass and its main components into various sugars, and the formation mechanisms of organic acids from key sugar products from biomass decomposition under non-catalytic condition. Decomposition behaviour of wood, leaf and bark as the main components of biomass have been studied, focusing on the recovery of different sugars and the leaching of Mg and Ca from each component. Moreover, the formation mechanisms of organic acids as the important platform biochemicals from key sugar products (i.e., cellobiose, glucose, fructose and mannose) are studied. This chapter summarises the main findings and suggests recommendations for future work.

8.2 Conclusions

8.2.1 Hydrothermal Processing of Different Biomass Components of Mallee Tree in Hot-Compressed Water

- The sugar recovery (arabinose, galactose, glucose xylose) between wood, leaf and bark is different due to the significant difference in sugar content between these components;
- Although >80% of arabinose, galactose and xylose can be recovered from leaf, bark and wood, the recovery of glucose is the lowest (30-62%) for all components in the order of wood > bark > leaf due to the significant in-situ structural changes during hydrothermal treatment. Decomposition temperature of glucan in cellulose started at ≥ 230 °C;

- Less than half of the recovered carbon are contributed by sugar products at different temperatures for three components, indicating that considerable amount of lignin hydrolysed under the prevailing conditions;
- As the leaching of water-insoluble Mg correlates to the decomposition of arabinan, only <15% water-insoluble Mg was leached from wood at 120°C, compared to ~35% and ~50% in bark and leaf respectively. In comparison to wood, arabinan in leaf and bark is decomposed at lower temperatures and its decomposition is faster;
- No significant difference is observed in leaching characteristic of water-insoluble Ca between wood, leaf and bark at low temperatures, as the majority of the water-insoluble Ca ($\geq 80\%$) are only soluble in acid.

8.2.2 Formation of Organic Acids During Cellobiose Decomposition in HCW

- Saccharinic, formic, lactic and glycolic acids were identified and quantified during cellobiose decomposition in HCW, and all identified organic acids are secondary products from cellobiose decomposition;
- Saccharinic acid is reported as the major organic acid produced from cellobiose decomposition under non-catalytic HCW, with the highest selectivity (~5.8% at 275 °C) compared to other identified organic acids;
- Although saccharinic acid has the highest yield and selectivity during cellobiose decomposition at different temperatures, formic acid is the main contributor to the total hydrogen ion dissociated due to its high molar concentration and higher dissociation constant;
- At cellobiose conversions <80%, a close match between the $[H^+]$ calculated from the quantified organic acids and the $[H^+]$ calculated from measured pH suggests that these acids are the majority organic acids produced during decomposition of cellobiose in HCW. At higher cellobiose conversions, other organic acids might be produced due to more pronounced secondary reactions.

8.2.3 Formation of Organic Acids During Glucose and Fructose Decomposition in HCW

- Various organic acids including metasaccharinic, formic, glycolic, lactic and 2,4-dihydroxy butyric acids were identified from hydrothermal decomposition of glucose and fructose under non-catalytic conditions;
- Metasaccharinic acid (MSA) has the highest yield and selectivity compared to other quantified organic acids. However, formic acid has the highest contribution to total organic acids during glucose and fructose decomposition.
- As the first time in the field, MSA has been identified as the minor primary product from fructose decomposition under non-catalytic conditions, but only a secondary product from glucose decomposition;
- At glucose and fructose conversions <80%, the calculated hydrogen ion concentrations from the quantified organic acids match well with the hydrogen ion concentrations from pH directly measured after each experiment, indicating that majority of organic acids produced during glucose and fructose decomposition have been identified. At higher conversions, more secondary reactions lead to the formation of other organic acids which contribute to a small percentage of the total hydrogen concentration;
- As MSA is the primary product from fructose decomposition, the formation mechanism of MSA under non-catalytic HCW may be different to that reported in previous literatures under alkaline conditions.

8.2.4 Mechanism and Reaction Pathways of Mannose Decomposition in HCW

- Isomerization reactions to produce fructose and glucose are the only two primary reactions during mannose decomposition in HCW, contributing to ~82 and ~18% of the primary decomposition reactions of mannose, respectively;
- Other products including glyceraldehyde, glycolaldehyde, 5-HMF and organic acids (i.e., formic acid, MSA, lactic acid, glycolic acid and DHBA) are identified, but they are all secondary products of mannose decomposition;

- Mannose decomposition at HCW follows first order kinetics, and the reaction rate constant increases with temperature;
- pH value decreases substantially from ~6 at ~10% mannose conversions to ~3 at ~85% conversions under current experimental conditions;
- MSA is the major organic acid identified with the highest yield and selectivity, and formic acids has the highest contribution to the total hydrogen oil concentration during mannose decomposition.

8.3 Recommendations

Based on the findings in this study, the following recommendations have been proposed for future research:

- In Chapter 4, the sugar products from biomass hydrolysis are mainly in the form of oligomers. It is important to develop advanced techniques to characterise the sugar oligomers from different components in lignocellulosic biomass.
- In Chapter 4, various non-sugar products are produced during biomass decomposition in HCW, including those products from lignin. It is critical to identify and characterise the lignin-derived compounds during lignocellulosic biomass decomposition in HCW;
- In Chapters 5-7, the formation of organic acids has been systematically investigated from cellobiose, glucose, fructose and mannose as the key compounds from cellulose decomposition in HCW. More works need to be carried out to understand the decomposition of other key compounds from hemicellulose decomposition in HCW.
- Since oligomers are the main sugar products from cellulose/hemicellulose decomposition, further studies are required for to understand the decomposition mechanisms of high-DP oligomers and their isomers. For example, glucosyl-fructose (GF) and glucosyl-mannose (GM) are important isomers produced during cellobiose decomposition.
- Further development of the kinetic model developed in chapter 7 and its applications in real reactor design.

References

1. Naik, S. N.; Goud, V. V.; Rout, P. K.; Dalai, A. K., Production of first and second generation biofuels: a comprehensive review. *Renewable and sustainable energy reviews* **2010**, 14, (2), 578-597.
2. Haines, A.; Wilkinson, P.; Tonne, C.; Roberts, I., Aligning climate change and public health policies. *The Lancet* **2009**, 374, (9707), 2035-2038.
3. Stöcker, M., Biofuels and biomass-to-liquid fuels in the biorefinery: Catalytic conversion of lignocellulosic biomass using porous materials. *Angewandte Chemie International Edition* **2008**, 47, (48), 9200-9211.
4. Werpy, T.; Petersen, G. *Top value added chemicals from biomass: volume I--results of screening for potential candidates from sugars and synthesis gas*; National Renewable Energy Lab., Golden, CO (US): 2004.
5. Bozell, J. J.; Petersen, G. R., Technology development for the production of biobased products from biorefinery carbohydrates—the US Department of Energy’s “Top 10” revisited. *Green chemistry* **2010**, 12, (4), 539-554.
6. Gómez Millán, G.; Hellsten, S.; Llorca Piqué, J.; Luque Álvarez de Sotomayor, R.; Sixta, H.; Balu Balu, A.-M., Recent advances in the catalytic production of platform chemicals from holocellulosic biomass. *ChemCatChem* **2019**, 11, (8), 2022-2042.
7. FitzPatrick, M.; Champagne, P.; Cunningham, M. F.; Whitney, R. A., A biorefinery processing perspective: treatment of lignocellulosic materials for the production of value-added products. *Bioresource technology* **2010**, 101, (23), 8915-8922.
8. Garrote, G.; Dominguez, H.; Parajo, J., Hydrothermal processing of lignocellulosic materials. *Holz als roh-und werkstoff* **1999**, 57, (3), 191-202.
9. Bröll, D.; Kaul, C.; Krämer, A.; Krammer, P.; Richter, T.; Jung, M.; Vogel, H.; Zehner, P., Chemistry in supercritical water. *Angewandte Chemie International Edition* **1999**, 38, (20), 2998-3014.
10. Krammer, P.; Vogel, H., Hydrolysis of esters in subcritical and supercritical water. *The Journal of Supercritical Fluids* **2000**, 16, (3), 189-206.
11. Liu, C.; Wyman, C. E., Partial flow of compressed-hot water through corn stover to enhance hemicellulose sugar recovery and enzymatic digestibility of cellulose. *Bioresource Technology* **2005**, 96, (18), 1978-1985.
12. Pang, J.; Zhang, B.; Jiang, Y.; Zhao, Y.; Li, C.; Zheng, M.; Zhang, T., Complete conversion of lignocellulosic biomass to mixed organic acids and ethylene glycol via cascade steps. *Green Chemistry* **2021**, 23, (6), 2427-2436.
13. Peterson, A. A.; Vogel, F.; Lachance, R. P.; Fröling, M.; Antal Jr, M. J.; Tester, J. W., Thermochemical biofuel production in hydrothermal media: a review of sub- and supercritical water technologies. *Energy & Environmental Science* **2008**, 1, (1), 32-65.
14. van Putten, R.-J.; van der Waal, J. C.; De Jong, E.; Rasrendra, C. B.; Heeres, H. J.; de Vries, J. G., Hydroxymethylfurfural, a versatile platform chemical made from renewable resources. *Chemical reviews* **2013**, 113, (3), 1499-1597.
15. Savage, P. E., Algae under pressure and in hot water. *Science* **2012**, 338, (6110), 1039-1040.

16. Ragauskas, A. J.; Williams, C. K.; Davison, B. H.; Britovsek, G.; Cairney, J.; Eckert, C. A.; Frederick, W. J.; Hallett, J. P.; Leak, D. J.; Liotta, C. L., The path forward for biofuels and biomaterials. *science* **2006**, 311, (5760), 484-489.
17. Yu, Y.; Wu, H., Characteristics and precipitation of glucose oligomers in the fresh liquid products obtained from the hydrolysis of cellulose in hot-compressed water. *Industrial & Engineering Chemistry Research* **2009**, 48, (23), 10682-10690.
18. Sakaki, T.; Shibata, M.; Sumi, T.; Yasuda, S., Saccharification of cellulose using a hot-compressed water-flow reactor. *Industrial & Engineering Chemistry Research* **2002**, 41, (4), 661-665.
19. Yu, Y.; Wu, H., Understanding the Primary Liquid Products of Cellulose Hydrolysis in Hot-Compressed Water at Various Reaction Temperatures. *Energy & Fuels* **2010**, 24, (3), 1963-1971.
20. Sasaki, M.; Kabyemela, B.; Malaluan, R.; Hirose, S.; Takeda, N.; Adschiri, T.; Arai, K., Cellulose hydrolysis in subcritical and supercritical water. *The Journal of Supercritical Fluids* **1998**, 13, (1), 261-268.
21. Stucley, C.; Schuck, S.; Sims, R.; Bland, J.; Marino, B.; Borowitzka, M.; Abadi, A.; Bartle, J.; Giles, R.; Thomas, Q. *Bioenergy In Australia: Status and Opportunities*; Bioenergy Australia: St Leonards NSW, 2012.
22. Cooper, D.; Olsen, G.; Bartle, J., Capture of agricultural surplus water determines the productivity and scale of new low-rainfall woody crop industries. *Australian Journal of Experimental Agriculture* **2005**, 45, (11), 1369-1388.
23. Bartle, J.; Olsen, G.; Cooper, D.; Hobbs, T., Scale of biomass production from new woody crops for salinity control in dryland agriculture in Australia. *International journal of global energy issues* **2007**, 27, (2), 115-137.
24. Wu, H.; Fu, Q.; Giles, R.; Bartle, J., Production of mallee biomass in Western Australia: energy balance analysis. *Energy & Fuels* **2008**, 22, (1), 190-198.
25. Yu, Y.; Bartle, J.; Li, C.-Z.; Wu, H., Mallee biomass as a key bioenergy source in Western Australia: importance of biomass supply chain. *Energy & Fuels* **2009**, 23, (6), 3290-3299.
26. Bartle, J. R.; Abadi, A., Toward sustainable production of second generation bioenergy feedstocks. *Energy & Fuels* **2010**, 24, (1), 2-9.
27. Harper, R.; Sochacki, S.; Smettem, K.; Robinson, N., Bioenergy feedstock potential from short-rotation woody crops in a dryland environment. *Energy & Fuels* **2010**, 24, (1), 225-231.
28. Liaw, S. B.; Nazeri, G.; Yu, Y.; Wu, H., Differences in Leaching Characteristics of Mg and Ca from Various Biomass Components of Mallee Tree in Hot-compressed Water. *Energy & Fuels* **2016**.
29. Wu, H.; Yip, K.; Kong, Z.; Li, C.-Z.; Liu, D.; Yu, Y.; Gao, X., Removal and recycling of inherent inorganic nutrient species in mallee biomass and derived biochars by water leaching. *Industrial & Engineering Chemistry Research* **2011**, 50, (21), 12143-12151.
30. Fushimi, C.; Kakimura, M.; Tomita, R.; Umeda, A.; Tanaka, T., Enhancement of nutrient recovery from microalgae in hydrothermal liquefaction using activated carbon. *Fuel Processing Technology* **2016**, 148, 282-288.
31. Huo, Y.; Zeng, H.; Zhang, Y., Integrating metabolic engineering and heterogeneous chemocatalysis: New opportunities for biomass to chemicals. **2016**.
32. Yu, Y.; Bartle, J.; Mendham, D.; Wu, H., Site Variation in Life Cycle Energy and Carbon Footprints of Mallee Biomass Production in Western Australia. *Energy & Fuels* **2015**.

33. Ando, H.; Sakaki, T.; Kokusho, T.; Shibata, M.; Uemura, Y.; Hatate, Y., Decomposition behavior of plant biomass in hot-compressed water. *Industrial & Engineering Chemistry Research* **2000**, 39, (10), 3688-3693.
34. Lü, X.; Saka, S., Hydrolysis of Japanese beech by batch and semi-flow water under subcritical temperatures and pressures. *Biomass and bioenergy* **2010**, 34, (8), 1089-1097.
35. Yu, G.; Yano, S.; Inoue, H.; Inoue, S.; Endo, T.; Sawayama, S., Pretreatment of rice straw by a hot-compressed water process for enzymatic hydrolysis. *Applied Biochemistry and Biotechnology* **2010**, 160, (2), 539-551.
36. Mamman, A. S.; Lee, J.-M.; Kim, Y.-C.; Hwang, I. T.; Park, N.-J.; Hwang, Y. K.; Chang, J.-S.; Hwang, J.-S., Furfural: Hemicellulose/xyloxy-derived biochemical. *Biofuels, Bioproducts and Biorefining* **2008**, 2, (5), 438-454.
37. Bozell, J. J.; Petersen, G. R., Technology development for the production of biobased products from biorefinery carbohydrates-the US Department of Energy's "Top 10" revisited. *Green Chemistry* **2010**, 12, (4), 539-554.
38. Sakaki, T.; Shibata, M.; Miki, T.; Hirose, H.; Hayashi, N., Decomposition of Cellulose in Near-Critical Water and Fermentability of the Products. *Energy & Fuels* **1996**, 10, (3), 684-688.
39. Minowa, T.; Zhen, F.; Ogi, T., Cellulose decomposition in hot-compressed water with alkali or nickel catalyst. *The Journal of Supercritical Fluids* **1998**, 13, (1-3), 253-259.
40. Liu, C.; Wyman, C. E., The Effect of Flow Rate of Compressed Hot Water on Xylan, Lignin, and Total Mass Removal from Corn Stover. *Industrial & Engineering Chemistry Research* **2003**, 42, (21), 5409-5416.
41. Ehara, K.; Saka, S., A comparative study on chemical conversion of cellulose between the batch-type and flow-type systems in supercritical water. *Cellulose* **2002**, 9, (3), 301-311.
42. Sasaki, M.; Kabyemela, B.; Malaluan, R.; Hirose, S.; Takeda, N.; Adschiri, T.; Arai, K., Cellulose hydrolysis in subcritical and supercritical water. *The Journal of Supercritical Fluids* **1998**, 13, (1-3), 261-268.
43. Liao, C.; Wu, C.; Huang, H., Study on the distribution and quantity of biomass residues resource in China. *Biomass and Bioenergy* **2004**, 27, (2), 111-117.
44. Murphy, J.; McCarthy, K., Ethanol production from energy crops and wastes for use as a transport fuel in Ireland. *Applied Energy* **2005**, 82, (2), 148-166.
45. Sun, Y.; Cheng, J., Hydrolysis of lignocellulosic materials for ethanol production: a review. *Bioresource technology* **2002**, 83, (1), 1-11.
46. Bobleter, O., Hydrothermal degradation of polymers derived from plants. *Progress in polymer science* **1994**, 19, (5), 797-841.
47. Hustvedt, G., Review of laundry energy efficiency studies conducted by the US Department of Energy. *International journal of consumer studies* **2011**, 35, (2), 228-236.
48. Mohan, D.; Pittman Jr, C. U.; Steele, P. H., Pyrolysis of wood/biomass for bio-oil: a critical review. *Energy & fuels* **2006**, 20, (3), 848-889.
49. Goswami, D. Y.; Kreith, F., *Energy efficiency and renewable energy handbook*. CRC Press: 2015.
50. Moon, R. J.; Martini, A.; Nairn, J.; Simonsen, J.; Youngblood, J., Cellulose nanomaterials review: structure, properties and nanocomposites. *Chemical Society Reviews* **2011**, 40, (7), 3941-3994.

51. Himmel, M. E.; Ding, S.-Y.; Johnson, D. K.; Adney, W. S.; Nimlos, M. R.; Brady, J. W.; Foust, T. D., Biomass recalcitrance: engineering plants and enzymes for biofuels production. *science* **2007**, 315, (5813), 804-807.
52. Kuhad, R. C.; Singh, A.; Eriksson, K.-E. L., Microorganisms and enzymes involved in the degradation of plant fiber cell walls. *Biotechnology in the pulp and paper industry* **1997**, 45-125.
53. Yu, Y.; Lou, X.; Wu, H., Some recent advances in hydrolysis of biomass in hot-compressed water and its comparisons with other hydrolysis methods. *Energy & Fuels* **2007**, 22, (1), 46-60.
54. Huber, G. W.; Dumesic, J. A., An overview of aqueous-phase catalytic processes for production of hydrogen and alkanes in a biorefinery. *Catalysis Today* **2006**, 111, (1-2), 119-132.
55. Pérez, J.; Munoz-Dorado, J.; De la Rubia, T.; Martinez, J., Biodegradation and biological treatments of cellulose, hemicellulose and lignin: an overview. *International microbiology* **2002**, 5, (2), 53-63.
56. Gray, K. A.; Zhao, L.; Emptage, M., Bioethanol. *Current opinion in chemical biology* **2006**, 10, (2), 141-146.
57. Hendriks, A.; Zeeman, G., Pretreatments to enhance the digestibility of lignocellulosic biomass. *Bioresource technology* **2009**, 100, (1), 10-18.
58. Sannigrahi, P.; Pu, Y.; Ragauskas, A., Cellulosic biorefineries—unleashing lignin opportunities. *Current Opinion in Environmental Sustainability* **2010**, 2, (5-6), 383-393.
59. Fengel, D.; Wegener, G., *Wood: chemistry, ultrastructure, reactions*. Walter de Gruyter: 2011.
60. Arvelakis, S.; Gehrman, H.; Beckmann, M.; Koukios, E. G., Agglomeration problems during fluidized bed gasification of olive-oil residue: evaluation of fractionation and leaching as pre-treatments☆. *Fuel* **2003**, 82, (10), 1261-1270.
61. Zevenhoven, M.; Yrjas, P.; Skrifvars, B.-J.; Hupa, M., Characterization of ash-forming matter in various solid fuels by selective leaching and its implications for fluidized-bed combustion. *Energy & Fuels* **2012**, 26, (10), 6366-6386.
62. Liaw, S. B.; Nazeri, G.; Yu, Y.; Wu, H., Differences in Leaching Characteristics of Mg and Ca from Various Biomass Components of Mallee Tree in Hot-Compressed Water. *Energy & Fuels* **2016**, 30, (10), 7851-7857.
63. Werkelin, J.; Skrifvars, B.-J.; Zevenhoven, M.; Holmbom, B.; Hupa, M., Chemical forms of ash-forming elements in woody biomass fuels. *Fuel* **2010**, 89, (2), 481-493.
64. Bobleter, O.; Niesner, R.; Röhr, M., The hydrothermal degradation of cellulosic matter to sugars and their fermentative conversion to protein. *Journal of Applied Polymer Science* **1976**, 20, (8), 2083-2093.
65. Ehara, K.; Saka, S., Decomposition behavior of cellulose in supercritical water, subcritical water, and their combined treatments. *Journal of wood science* **2005**, 51, (2), 148-153.
66. Nanda, S.; Mohammad, J.; Reddy, S. N.; Kozinski, J. A.; Dalai, A. K., Pathways of lignocellulosic biomass conversion to renewable fuels. *Biomass Conversion and Biorefinery* **2014**, 4, (2), 157-191.
67. Kumar, A. K.; Sharma, S., Recent updates on different methods of pretreatment of lignocellulosic feedstocks: a review. *Bioresources and bioprocessing* **2017**, 4, (1), 1-19.
68. Demirbas, A.; Arin, G., An overview of biomass pyrolysis. *Energy sources* **2002**, 24, (5), 471-482.

69. Fan, L.; Gharpuray, M.; Lee, Y., Biotechnology monographs. *Cellulose Hydrolysis* **1987**, 3.
70. Laird, D. A.; Brown, R. C.; Amonette, J. E.; Lehmann, J., Review of the pyrolysis platform for coproducing bio-oil and biochar. *Biofuels, bioproducts and biorefining* **2009**, 3, (5), 547-562.
71. Balat, M.; Balat, M.; Kirtay, E.; Balat, H., Main routes for the thermo-conversion of biomass into fuels and chemicals. Part 1: Pyrolysis systems. *Energy conversion and Management* **2009**, 50, (12), 3147-3157.
72. Babu, B., Biomass pyrolysis: a state-of-the-art review. *Biofuels, Bioproducts and Biorefining: Innovation for a sustainable economy* **2008**, 2, (5), 393-414.
73. Kumar, A.; Jones, D. D.; Hanna, M. A., Thermochemical biomass gasification: a review of the current status of the technology. *Energies* **2009**, 2, (3), 556-581.
74. Baruah, D.; Baruah, D., Modeling of biomass gasification: A review. *Renewable and Sustainable Energy Reviews* **2014**, 39, 806-815.
75. Puig-Arnabat, M.; Bruno, J. C.; Coronas, A., Review and analysis of biomass gasification models. *Renewable and sustainable energy reviews* **2010**, 14, (9), 2841-2851.
76. Harmsen, P. F.; Huijgen, W.; Bermudez, L.; Bakker, R., *Literature review of physical and chemical pretreatment processes for lignocellulosic biomass*. Wageningen UR-Food & Biobased Research: 2010.
77. Guo, Y.; Yeh, T.; Song, W.; Xu, D.; Wang, S., A review of bio-oil production from hydrothermal liquefaction of algae. *Renewable and Sustainable Energy Reviews* **2015**, 48, 776-790.
78. Gollakota, A.; Kishore, N.; Gu, S., A review on hydrothermal liquefaction of biomass. *Renewable and Sustainable Energy Reviews* **2018**, 81, 1378-1392.
79. Osman, A. I.; Mehta, N.; Elgarahy, A. M.; Al-Hinai, A.; Al-Muhtaseb, A. a. H.; Rooney, D. W., Conversion of biomass to biofuels and life cycle assessment: a review. *Environmental Chemistry Letters* **2021**, 19, (6), 4075-4118.
80. Guo, K.; Guan, Q.; Xu, J.; Tan, W., Mechanism of preparation of platform compounds from lignocellulosic biomass liquefaction catalyzed by Bronsted acid: A review. *Journal of Bioresources and Bioproducts* **2019**, 4, (4), 202-213.
81. Xu, C. C.; Shao, Y.; Yuan, Z.; Cheng, S.; Feng, S.; Nazari, L.; Tymchyshyn, M., Hydrothermal liquefaction of biomass in hot-compressed water, alcohols, and alcohol-water co-solvents for biocrude production. In *Application of hydrothermal reactions to biomass conversion*, Springer: 2014; pp 171-187.
82. Yu, Y.; Lou, X.; Wu, H., Some recent advances in hydrolysis of biomass in hot-compressed water and its comparisons with other hydrolysis methods. *Energy & fuels* **2008**, 22, (1), 46-60.
83. Goldstein, I. S., Chemicals from cellulose. In *Organic chemicals from biomass*, CRC Press: 2018; pp 101-124.
84. Duff, S. J.; Murray, W. D., Bioconversion of forest products industry waste cellulose to fuel ethanol: a review. *Bioresource technology* **1996**, 55, (1), 1-33.
85. Akizuki, M.; Fujii, T.; Hayashi, R.; Oshima, Y., Effects of water on reactions for waste treatment, organic synthesis, and bio-refinery in sub- and supercritical water. *Journal of bioscience and bioengineering* **2014**, 117, (1), 10-18.
86. Toor, S. S.; Rosendahl, L.; Rudolf, A., Hydrothermal liquefaction of biomass: a review of subcritical water technologies. *Energy* **2011**, 36, (5), 2328-2342.

87. Yedro, F. M.; Cantero, D. A.; Pascual, M.; García-Serna, J.; Cocero, M. J., Hydrothermal fractionation of woody biomass: Lignin effect on sugars recovery. *Bioresource technology* **2015**, 191, 124-132.
88. Watanabe, M.; Sato, T.; Inomata, H.; Smith Jr, R. L.; Arai Jr, K.; Kruse, A.; Dinjus, E., Chemical reactions of C1 compounds in near-critical and supercritical water. *Chemical Reviews* **2004**, 104, (12), 5803-5822.
89. Möller, M.; Nilges, P.; Harnisch, F.; Schröder, U., Subcritical water as reaction environment: fundamentals of hydrothermal biomass transformation. *ChemSusChem* **2011**, 4, (5), 566-579.
90. Kruse, A.; Dinjus, E., Hot compressed water as reaction medium and reactant: properties and synthesis reactions. *The Journal of supercritical fluids* **2007**, 39, (3), 362-380.
91. Jin, F.; Wang, Y.; Zeng, X.; Shen, Z.; Yao, G., Water under high temperature and pressure conditions and its applications to develop green technologies for biomass conversion. In *Application of Hydrothermal Reactions to Biomass Conversion*, Springer: 2014; pp 3-28.
92. Kruse, A.; Gawlik, A., Biomass conversion in water at 330– 410 C and 30– 50 MPa. Identification of key compounds for indicating different chemical reaction pathways. *Industrial & Engineering Chemistry Research* **2003**, 42, (2), 267-279.
93. Weingärtner, H.; Franck, E. U., Supercritical water as a solvent. *Angewandte Chemie International Edition* **2005**, 44, (18), 2672-2692.
94. Hashaikeh, R.; Fang, Z.; Butler, I.; Hawari, J.; Kozinski, J., Hydrothermal dissolution of willow in hot compressed water as a model for biomass conversion. *Fuel* **2007**, 86, (10), 1614-1622.
95. Goto, M.; Obuchi, R.; Hirose, T.; Sakaki, T.; Shibata, M., Hydrothermal conversion of municipal organic waste into resources. *Bioresource technology* **2004**, 93, (3), 279-284.
96. Rasmussen, H.; Sørensen, H. R.; Meyer, A. S., Formation of degradation compounds from lignocellulosic biomass in the biorefinery: sugar reaction mechanisms. *Carbohydrate research* **2014**, 385, 45-57.
97. Reza, M. T.; Lynam, J. G.; Uddin, M. H.; Coronella, C. J., Hydrothermal carbonization: fate of inorganics. *Biomass and Bioenergy* **2013**, 49, 86-94.
98. Matsumura, Y.; Sasaki, M.; Okuda, K.; Takami, S.; Ohara, S.; Umetsu, M.; Adschiri, T., Supercritical water treatment of biomass for energy and material recovery. *Combustion Science and Technology* **2006**, 178, (1-3), 509-536.
99. Kumar, S.; Gupta, R. B., Biocrude production from switchgrass using subcritical water. *Energy & Fuels* **2009**, 23, (10), 5151-5159.
100. Phaiboonsilpa, N.; Ogura, M.; Yamauchi, K.; Rabemanolontsoa, H.; Saka, S., Two-step hydrolysis of rice (*Oryza sativa*) husk as treated by semi-flow hot-compressed water. *Industrial crops and products* **2013**, 49, 484-491.
101. Adschiri, T.; Hirose, S.; Malaluan, R.; Arai, K., Noncatalytic conversion of cellulose in supercritical and subcritical water. *Journal of chemical engineering of Japan* **1993**, 26, (6), 676-680.
102. Matsunaga, M.; Matsui, H.; Otsuka, Y.; Yamamoto, S., Chemical conversion of wood by treatment in a semi-batch reactor with subcritical water. *The Journal of Supercritical Fluids* **2008**, 44, (3), 364-369.
103. Sasaki, M.; Fang, Z.; Fukushima, Y.; Adschiri, T.; Arai, K., Dissolution and hydrolysis of cellulose in subcritical and supercritical water. *Industrial & Engineering Chemistry Research* **2000**, 39, (8), 2883-2890.

104. Hörmeyer, H.; Schwald, W.; Bonn, G.; Bobleter, O., Hydrothermolysis of birch wood as pretreatment for enzymatic saccharification. **1988**.
105. Yu, Q.; Zhuang, X.; Yuan, Z.; Wang, Q.; Qi, W.; Wang, W.; Zhang, Y.; Xu, J.; Xu, H., Two-step liquid hot water pretreatment of *Eucalyptus grandis* to enhance sugar recovery and enzymatic digestibility of cellulose. *Bioresource Technology* **2010**, 101, (13), 4895-4899.
106. Lu, X.; Yamauchi, K.; Phaiboonsilpa, N.; Saka, S., Two-step hydrolysis of Japanese beech as treated by semi-flow hot-compressed water. *Journal of wood science* **2009**, 55, (5), 367-375.
107. Allen, S. G.; Kam, L. C.; Zemann, A. J.; Antal, M. J., Fractionation of sugar cane with hot, compressed, liquid water. *Industrial & Engineering Chemistry Research* **1996**, 35, (8), 2709-2715.
108. Sasaki, M.; Adschiri, T.; Arai, K., Fractionation of sugarcane bagasse by hydrothermal treatment. *Bioresource Technology* **2003**, 86, (3), 301-304.
109. Takada, M.; Minami, E.; Saka, S., Decomposition behaviors of the lignocellulosics as treated by semi-flow hot-compressed water. *The Journal of Supercritical Fluids* **2018**, 133, 566-572.
110. Zhao, Y.; Lu, W.-J.; Wu, H.-Y.; Liu, J.-W.; Wang, H.-T., Optimization of supercritical phase and combined supercritical/subcritical conversion of lignocellulose for hexose production by using a flow reaction system. *Bioresource technology* **2012**, 126, 391-396.
111. Zhao, Y.; Lu, W.-J.; Wang, H.-T.; Yang, J.-L., Fermentable hexose production from corn stalks and wheat straw with combined supercritical and subcritical hydrothermal technology. *Bioresource technology* **2009**, 100, (23), 5884-5889.
112. Zhao, Y.; Lu, W.; Chen, J.; Zhang, X.; Wang, H., Research progress on hydrothermal dissolution and hydrolysis of lignocellulose and lignocellulosic waste. *Frontiers of Environmental Science & Engineering* **2014**, 8, (2), 151-161.
113. Yu, Y.; Wu, H., Evolution of primary liquid products and evidence of in situ structural changes in cellulose with conversion during hydrolysis in hot-compressed water. *Industrial & Engineering Chemistry Research* **2010**, 49, (8), 3919-3925.
114. Yu, Y.; Wu, H., Significant differences in the hydrolysis behavior of amorphous and crystalline portions within microcrystalline cellulose in hot-compressed water. *Industrial & Engineering Chemistry Research* **2010**, 49, (8), 3902-3909.
115. Sasaki, M.; Adschiri, T.; Arai, K., Kinetics of cellulose conversion at 25 MPa in sub-and supercritical water. *AIChE Journal* **2004**, 50, (1), 192-202.
116. Sasaki, M.; Sekiguchi, G.; Adschiri, T.; Arai, K. In *Rapid and selective conversion of cellulose to valuable chemical intermediates with supercritical water*, Proceedings of the 6th International Symposium on Supercritical Fluids, 2003; 2003; pp 1417-1422.
117. Kabyemela, B.; Takigawa, M.; Adschiri, T.; Malaluan, R.; Arai, K., Mechanism and kinetics of cellobiose decomposition in sub-and supercritical water. *Industrial & Engineering Chemistry Research* **1998**, 37, (2), 357-361.
118. Sasaki, M.; Kabyemela, B.; Malaluan, R.; Hirose, S.; Takeda, N.; Adschiri, T.; Arai, K., Cellulose hydrolysis in subcritical and supercritical water. *The Journal of Supercritical Fluids* **1998**, 13, (1-3), 261-268.
119. Kabyemela, B. M.; Adschiri, T.; Malaluan, R. M.; Arai, K., Kinetics of glucose epimerization and decomposition in subcritical and supercritical water. *Industrial & engineering chemistry research* **1997**, 36, (5), 1552-1558.

120. Tolonen, L. K.; Penttilä, P. A.; Serimaa, R.; Kruse, A.; Sixta, H., The swelling and dissolution of cellulose crystallites in subcritical and supercritical water. *Cellulose* **2013**, 20, (6), 2731-2744.
121. Zhao, Y.; Lu, W.-J.; Wang, H.-T.; Li, D., Combined supercritical and subcritical process for cellulose hydrolysis to fermentable hexoses. *Environmental science & technology* **2009**, 43, (5), 1565-1570.
122. Saka, S.; Ueno, T., Chemical conversion of various celluloses to glucose and its derivatives in supercritical water. *Cellulose* **1999**, 6, (3), 177-191.
123. Sakanishi, K.; Ikeyama, N.; Sakaki, T.; Shibata, M.; Miki, T., Comparison of the hydrothermal decomposition reactivities of chitin and cellulose. *Industrial & engineering chemistry research* **1999**, 38, (6), 2177-2181.
124. Minowa, T.; Fang, Z.; Ogi, T.; Várhegyi, G., Decomposition of cellulose and glucose in hot-compressed water under catalyst-free conditions. *Journal of chemical engineering of Japan* **1998**, 31, (1), 131-134.
125. Rogalinski, T.; Ingram, T.; Brunner, G., Hydrolysis of lignocellulosic biomass in water under elevated temperatures and pressures. *The Journal of Supercritical Fluids* **2008**, 47, (1), 54-63.
126. Ingram, T.; Rogalinski, T.; Bockemühl, V.; Antranikian, G.; Brunner, G., Semi-continuous liquid hot water pretreatment of rye straw. *The journal of supercritical fluids* **2009**, 48, (3), 238-246.
127. Rogalinski, T.; Liu, K.; Albrecht, T.; Brunner, G., Hydrolysis kinetics of biopolymers in subcritical water. *The Journal of Supercritical Fluids* **2008**, 46, (3), 335-341.
128. Minowa, T.; Kondo, T.; Sudirjo, S. T., Thermochemical liquefaction of Indonesian biomass residues. *Biomass and Bioenergy* **1998**, 14, (5-6), 517-524.
129. Ogihara, Y.; Smith, R. L.; Inomata, H.; Arai, K., Direct observation of cellulose dissolution in subcritical and supercritical water over a wide range of water densities (550–1000 kg/m³). *Cellulose* **2005**, 12, (6), 595-606.
130. Jing, S.; Cao, X.; Zhong, L.; Peng, X.; Zhang, X.; Wang, S.; Sun, R., In situ carbonic acid from CO₂: a green acid for highly effective conversion of cellulose in the presence of Lewis acid. *ACS Sustainable Chemistry & Engineering* **2016**, 4, (8), 4146-4155.
131. Amarasekara, A. S.; Owereh, O. S., Hydrolysis and decomposition of cellulose in Bronsted acidic ionic liquids under mild conditions. *Industrial & Engineering Chemistry Research* **2009**, 48, (22), 10152-10155.
132. vom Stein, T.; Grande, P.; Sibilla, F.; Commandeur, U.; Fischer, R.; Leitner, W.; de María, P. D., Salt-assisted organic-acid-catalyzed depolymerization of cellulose. *Green Chemistry* **2010**, 12, (10), 1844-1849.
133. Mosier, N. S.; Ladisch, C. M.; Ladisch, M. R., Characterization of acid catalytic domains for cellulose hydrolysis and glucose degradation. *Biotechnology and bioengineering* **2002**, 79, (6), 610-618.
134. Yu, Y.; Mohd Shafie, Z.; Wu, H., Effect of Alkali and Alkaline Earth Metal Chlorides on Cellobiose Decomposition in Hot-Compressed Water. *Industrial & Engineering Chemistry Research* **2015**, 54, (20), 5450-5459.
135. Choudhary, V.; Mushrif, S. H.; Ho, C.; Anderko, A.; Nikolakis, V.; Marinkovic, N. S.; Frenkel, A. I.; Sandler, S. I.; Vlachos, D. G., Insights into the interplay of Lewis and Brønsted acid catalysts in glucose and fructose conversion to 5-(hydroxymethyl) furfural and levulinic acid in aqueous media. *Journal of the American Chemical Society* **2013**, 135, (10), 3997-4006.

136. Watanabe, M.; Aizawa, Y.; Iida, T.; Aida, T. M.; Levy, C.; Sue, K.; Inomata, H., Glucose reactions with acid and base catalysts in hot compressed water at 473 K. *Carbohydrate research* **2005**, 340, (12), 1925-1930.
137. Chambon, F.; Rataboul, F.; Pinel, C.; Cabiac, A.; Guillon, E.; Essayem, N., Cellulose hydrothermal conversion promoted by heterogeneous Brønsted and Lewis acids: remarkable efficiency of solid Lewis acids to produce lactic acid. *Applied Catalysis B: Environmental* **2011**, 105, (1-2), 171-181.
138. Watanabe, M.; Aizawa, Y.; Iida, T.; Nishimura, R.; Inomata, H., Catalytic glucose and fructose conversions with TiO₂ and ZrO₂ in water at 473 K: relationship between reactivity and acid–base property determined by TPD measurement. *Applied Catalysis A: General* **2005**, 295, (2), 150-156.
139. Pińkowska, H.; Wolak, P.; Złocińska, A., Hydrothermal decomposition of xylan as a model substance for plant biomass waste–hydrothermolysis in subcritical water. *Biomass and bioenergy* **2011**, 35, (9), 3902-3912.
140. Sasaki, M. In *MEASUREMENT OF THE RATE OF RETRO-ALDOL CONDENSATION OF*, Hydrothermal Reactions and Techniques: The Proceedings of the Seventh International Symposium on Hydrothermal Reactions, Changchun, China 14-18 December 2003, 2003; World Scientific: 2003; p 169.
141. Mok, W. S. L.; Antal Jr, M. J., Uncatalyzed solvolysis of whole biomass hemicellulose by hot compressed liquid water. *Industrial & Engineering Chemistry Research* **1992**, 31, (4), 1157-1161.
142. Nabarlatz, D.; Ebringerová, A.; Montané, D., Autohydrolysis of agricultural by-products for the production of xylo-oligosaccharides. *Carbohydrate Polymers* **2007**, 69, (1), 20-28.
143. Srokol, Z.; Bouche, A.-G.; van Estrik, A.; Strik, R. C.; Maschmeyer, T.; Peters, J. A., Hydrothermal upgrading of biomass to biofuel; studies on some monosaccharide model compounds. *Carbohydrate research* **2004**, 339, (10), 1717-1726.
144. Kishida, H.; Jin, F.; Yan, X.; Moriya, T.; Enomoto, H., Formation of lactic acid from glycolaldehyde by alkaline hydrothermal reaction. *Carbohydrate research* **2006**, 341, (15), 2619-2623.
145. Cocero, M. J.; Cabeza, A.; Abad, N.; Adamovic, T.; Vaquerizo, L.; Martinez, C. M.; Pazo-Cepeda, M. V., Understanding biomass fractionation in subcritical & supercritical water. *The Journal of Supercritical Fluids* **2018**, 133, 550-565.
146. Kanetake, T.; Sasaki, M.; Goto, M., Decomposition of a lignin model compound under hydrothermal conditions. *Chemical Engineering & Technology: Industrial Chemistry-Plant Equipment-Process Engineering-Biotechnology* **2007**, 30, (8), 1113-1122.
147. Zhang, B.; Huang, H.-J.; Ramaswamy, S., Reaction kinetics of the hydrothermal treatment of lignin. In *Biotechnology for Fuels and Chemicals*, Springer: 2007; pp 487-499.
148. Bobleter, O.; Bonn, G., The hydrothermolysis of cellobiose and its reaction-product D-glucose. *Carbohydrate research* **1983**, 124, (2), 185-193.
149. Sasaki, M.; Furukawa, M.; Minami, K.; Adschiri, T.; Arai, K., Kinetics and mechanism of cellobiose hydrolysis and retro-aldol condensation in subcritical and supercritical water. *Industrial & engineering chemistry research* **2002**, 41, (26), 6642-6649.
150. Yu, Y.; Shafie, Z. M.; Wu, H., Cellobiose decomposition in hot-compressed water: importance of isomerization reactions. *Industrial & Engineering Chemistry Research* **2013**, 52, (47), 17006-17014.

151. Gakhokidze, R. A., Saccharinic acids. *Russian Chemical Reviews* **1980**, 49, (3), 222.
152. Knill, C. J.; Kennedy, J. F., Degradation of cellulose under alkaline conditions. *Carbohydrate Polymers* **2003**, 51, (3), 281-300.
153. Van Loon, L.; Glaus, M.; Stallone, S.; Laube, A., THE DEGRADATION OF CELLULOSE: A PROBLEM FOR THE SAFETY OF A RADIOACTIVE WASTE REPOSITORY? *PSI Nuclear Energy*, 73.
154. Luijkx, G. C.; van Rantwijk, F.; van Bekkum, H.; Antal Jr, M. J., The role of deoxyhexonic acids in the hydrothermal decarboxylation of carbohydrates. *Carbohydrate research* **1995**, 272, (2), 191-202.
155. Liang, X.; Montoya, A.; Haynes, B. S., Mechanistic Insights and Kinetic Modeling of Cellobiose Decomposition in Hot Compressed Water. *Energy & Fuels* **2016**.
156. Shafie, Z. M.; Yu, Y.; Wu, H., Effect of initial pH on hydrothermal decomposition of cellobiose under weakly acidic conditions. *Fuel* **2015**, 158, 315-321.
157. Khondakar, R. H.; Yu, Y.; Wu, H., Cellobiulose as a Key Intermediate during Biomass Hydrothermal Conversion into Biofuels and Biochemicals: Fundamental Decomposition Mechanisms. *Energy & Fuels* **2021**.
158. Saito, T.; Sasaki, M.; Kawanabe, H.; Yoshino, Y.; Goto, M., Subcritical water reaction behavior of d-glucose as a model compound for biomass using two different continuous-flow reactor configurations. *Chemical Engineering & Technology: Industrial Chemistry-Plant Equipment-Process Engineering-Biotechnology* **2009**, 32, (4), 527-533.
159. Kabyemela, B. M.; Adschiri, T.; Malaluan, R. M.; Arai, K., Glucose and fructose decomposition in subcritical and supercritical water: detailed reaction pathway, mechanisms, and kinetics. *Industrial & Engineering Chemistry Research* **1999**, 38, (8), 2888-2895.
160. Klingler, D.; Vogel, H., Influence of process parameters on the hydrothermal decomposition and oxidation of glucose in sub-and supercritical water. *The Journal of Supercritical Fluids* **2010**, 55, (1), 259-270.
161. Matsumura, Y.; Yanachi, S.; Yoshida, T., Glucose decomposition kinetics in water at 25 MPa in the temperature range of 448– 673 K. *Industrial & engineering chemistry research* **2006**, 45, (6), 1875-1879.
162. Hu, S.; Zhang, Z.; Song, J.; Zhou, Y.; Han, B., Efficient conversion of glucose into 5-hydroxymethylfurfural catalyzed by a common Lewis acid SnCl₄ in an ionic liquid. *Green Chemistry* **2009**, 11, (11), 1746-1749.
163. Qi, X.; Watanabe, M.; Aida, T. M.; Smith Jr, R. L., Catalytical conversion of fructose and glucose into 5-hydroxymethylfurfural in hot compressed water by microwave heating. *Catalysis Communications* **2008**, 9, (13), 2244-2249.
164. Takagaki, A.; Ohara, M.; Nishimura, S.; Ebitani, K., A one-pot reaction for biorefinery: combination of solid acid and base catalysts for direct production of 5-hydroxymethylfurfural from saccharides. *Chemical Communications* **2009**, (41), 6276-6278.
165. Lü, X.; Saka, S., New insights on monosaccharides' isomerization, dehydration and fragmentation in hot-compressed water. *The Journal of Supercritical Fluids* **2012**, 61, 146-156.
166. Kimura, H.; Nakahara, M.; Matubayasi, N., Noncatalytic hydrothermal elimination of the terminal D-glucose unit from malto-and cello-oligosaccharides

through transformation to D-Fructose. *The Journal of Physical Chemistry A* **2012**, 116, (41), 10039-10049.

167. Mamleev, V.; Bourbigot, S.; Yvon, J., Kinetic analysis of the thermal decomposition of cellulose: the main step of mass loss. *Journal of analytical and applied pyrolysis* **2007**, 80, (1), 151-165.

168. Bermejo-Deval, R.; Orazov, M.; Gounder, R.; Hwang, S.-J.; Davis, M. E., Active sites in Sn-Beta for glucose isomerization to fructose and epimerization to mannose. *ACS Catalysis* **2014**, 4, (7), 2288-2297.

169. Pilath, H. M.; Nimlos, M. R.; Mittal, A.; Himmel, M. E.; Johnson, D. K., Glucose reversion reaction kinetics. *Journal of agricultural and food chemistry* **2010**, 58, (10), 6131-6140.

170. Kabyemela, B. M.; Adschiri, T.; Malaluan, R. M.; Arai, K.; Ohzeki, H., Rapid and selective conversion of glucose to erythrose in supercritical water. *Industrial & engineering chemistry research* **1997**, 36, (12), 5063-5067.

171. Weingarten, R.; Cho, J.; Xing, R.; Conner Jr, W. C.; Huber, G. W., Kinetics and reaction engineering of levulinic acid production from aqueous glucose solutions. *ChemSusChem* **2012**, 5, (7), 1280-1290.

172. Aida, T. M.; Sato, Y.; Watanabe, M.; Tajima, K.; Nonaka, T.; Hattori, H.; Arai, K., Dehydration of d-glucose in high temperature water at pressures up to 80 MPa. *The Journal of supercritical fluids* **2007**, 40, (3), 381-388.

173. Yu, Y.; Wu, H., Kinetics and mechanism of glucose decomposition in hot-compressed water: effect of initial glucose concentration. *Industrial & engineering chemistry research* **2011**, 50, (18), 10500-10508.

174. Yang, G.; Pidko, E. A.; Hensen, E. J., Mechanism of Brønsted acid-catalyzed conversion of carbohydrates. *Journal of catalysis* **2012**, 295, 122-132.

175. Watanabe, M.; Aizawa, Y.; Iida, T.; Levy, C.; Aida, T. M.; Inomata, H., Glucose reactions within the heating period and the effect of heating rate on the reactions in hot compressed water. *Carbohydrate research* **2005**, 340, (12), 1931-1939.

176. Kabyemela, B. M.; Adschiri, T.; Malaluan, R.; Arai, K., Degradation kinetics of dihydroxyacetone and glyceraldehyde in subcritical and supercritical water. *Industrial & engineering chemistry research* **1997**, 36, (6), 2025-2030.

177. Sinag, A.; Kruse, A.; Rathert, J., Influence of the heating rate and the type of catalyst on the formation of key intermediates and on the generation of gases during hydrolysis of glucose in supercritical water in a batch reactor. *Industrial & Engineering Chemistry Research* **2004**, 43, (2), 502-508.

178. Sinag, A.; Kruse, A.; Schwarzkopf, V., Formation and degradation pathways of intermediate products formed during the hydrolysis of glucose as a model substance for wet biomass in a tubular reactor. *Engineering in life sciences* **2003**, 3, (12), 469-473.

179. Kupiainen, L.; Ahola, J.; Tanskanen, J., Comparison of formic and sulfuric acids as a glucose decomposition catalyst. *Industrial & engineering chemistry research* **2010**, 49, (18), 8444-8449.

180. Xiang, Q.; Lee, Y. Y.; Torget, R. W. In *Kinetics of glucose decomposition during dilute-acid hydrolysis of lignocellulosic biomass*, Proceedings of the Twenty-Fifth Symposium on Biotechnology for Fuels and Chemicals Held May 4-7, 2003, in Breckenridge, CO, 2004; Springer: 2004; pp 1127-1138.

181. Daorattanachai, P.; Namuangruk, S.; Viriya-empikul, N.; Laosiripojana, N.; Faungnawakij, K., 5-Hydroxymethylfurfural production from sugars and cellulose in

- acid-and base-catalyzed conditions under hot compressed water. *Journal of Industrial and Engineering Chemistry* **2012**, 18, (6), 1893-1901.
182. Chang, C.; Xiaojian, M.; Peilin, C., Kinetics of levulinic acid formation from glucose decomposition at high temperature. *Chinese Journal of Chemical Engineering* **2006**, 14, (5), 708-712.
183. McKibbins, S. W., Kinetics of the acid catalyzed conversion of glucose to 5-hydroxymethyl-2-furaldehyde and levulinic acid. **1958**.
184. Qian, X.; Nimlos, M. R.; Johnson, D. K.; Himmel, M. E. In *Acidic sugar degradation pathways*, Twenty-Sixth Symposium on Biotechnology for Fuels and Chemicals, 2005; Springer: 2005; pp 989-997.
185. Gao, X.; Zhong, H.; Yao, G.; Guo, W.; Jin, F., Hydrothermal conversion of glucose into organic acids with bentonite as a solid-base catalyst. *Catalysis Today* **2016**, 274, 49-54.
186. Song, B.; Wu, Z.; Yu, Y.; Wu, H., Hydrothermal Reactions of Biomass-Derived Platform Molecules: Distinct Effect of Aprotic and Protic Solvents on Primary Decomposition of Glucose and Fructose in Hot-Compressed Solvent/Water Mixtures. *Industrial & Engineering Chemistry Research* **2020**, 59, (16), 7336-7345.
187. Antal Jr, M. J.; Mok, W. S.; Richards, G. N., Mechanism of formation of 5-(hydroxymethyl)-2-furaldehyde from D-fructose and sucrose. *Carbohydrate research* **1990**, 199, (1), 91-109.
188. Aida, T. M.; Tajima, K.; Watanabe, M.; Saito, Y.; Kuroda, K.; Nonaka, T.; Hattori, H.; Smith Jr, R. L.; Arai, K., Reactions of d-fructose in water at temperatures up to 400 C and pressures up to 100 MPa. *The Journal of supercritical fluids* **2007**, 42, (1), 110-119.
189. Kobayashi, T.; Khuwijitjaru, P.; Adachi, S., Decomposition kinetics of glucose and fructose in subcritical water containing sodium chloride. *Journal of Applied Glycoscience* **2016**, 63, (4), 99-104.
190. Yin, S.; Tan, Z., Hydrothermal liquefaction of cellulose to bio-oil under acidic, neutral and alkaline conditions. *Applied Energy* **2012**, 92, 234-239.
191. Kuster, B. F.; Temmink, H. M., The influence of pH and weak-acid anions on the dehydration of D-fructose. *Carbohydrate research* **1977**, 54, (2), 185-191.
192. Baugh, K. D.; McCarty, P. L., Thermochemical pretreatment of lignocellulose to enhance methane fermentation: I. Monosaccharide and furfurals hydrothermal decomposition and product formation rates. *Biotechnology and Bioengineering* **1988**, 31, (1), 50-61.
193. Jin, F.; Zhou, Z.; Kishita, A.; Enomoto, H., Hydrothermal conversion of biomass into acetic acid. *Journal of materials science* **2006**, 41, (5), 1495-1500.
194. Jin, F.; Zhou, Z.; Moriya, T.; Kishida, H.; Higashijima, H.; Enomoto, H., Controlling hydrothermal reaction pathways to improve acetic acid production from carbohydrate biomass. *Environmental science & technology* **2005**, 39, (6), 1893-1902.
195. Holgate, H. R.; Meyer, J. C.; Tester, J. W., Glucose hydrolysis and oxidation in supercritical water. *AIChE journal* **1995**, 41, (3), 637-648.
196. Calvo, L.; Vallejo, D., Formation of organic acids during the hydrolysis and oxidation of several wastes in sub-and supercritical water. *Industrial & engineering chemistry research* **2002**, 41, (25), 6503-6509.
197. Yun, J.; Yao, G.; Jin, F.; Zhong, H.; Kishita, A.; Tohji, K.; Enomoto, H.; Wang, L., Low-temperature and highly efficient conversion of saccharides into formic acid under hydrothermal conditions. *AIChE Journal* **2016**, 62, (10), 3657-3663.

198. NOVOTNÝ, O.; CEJPEK, K.; VELÍŠEK, J., Formation of carboxylic acids during degradation of monosaccharides. *Czech J. Food Sci* **2008**, 26, (2), 117-131.
199. Jin, F.; Yun, J.; Li, G.; Kishita, A.; Tohji, K.; Enomoto, H.; Tohji, K.; Tsuchiya, N.; Jeyadevan, B. In *Formation of formic acid by hydrothermal oxidation of carbohydrate biomass for producing hydrogen*, AIP Conference Proceedings, 2008; AIP: 2008; pp 139-142.
200. Yun, J.; Jin, F.; Kishita, A.; Tohji, K.; Enomoto, H. In *Formic acid production from carbohydrates biomass by hydrothermal reaction*, Journal of Physics: Conference Series, 2010; IOP Publishing: 2010; p 012126.
201. Song, J.; Fan, H.; Ma, J.; Han, B., Conversion of glucose and cellulose into value-added products in water and ionic liquids. *Green Chemistry* **2013**, 15, (10), 2619-2635.
202. Jin, F.; Enomoto, H., Rapid and highly selective conversion of biomass into value-added products in hydrothermal conditions: chemistry of acid/base-catalysed and oxidation reactions. *Energy & Environmental Science* **2011**, 4, (2), 382-397.
203. Yang, B. Y.; Montgomery, R., Alkaline degradation of glucose: effect of initial concentration of reactants. *Carbohydrate Research* **1996**, 280, (1), 27-45.
204. Reintjes, M.; Cooper, G. K., Polysaccharide alkaline degradation products as a source of organic chemicals. *Industrial & engineering chemistry product research and development* **1984**, 23, (1), 70-73.
205. Richards, G.; Sephton, H., 905. The alkaline degradation of polysaccharides. Part I. Soluble products of the action of sodium hydroxide on cellulose. *Journal of the Chemical Society (Resumed)* **1957**, 4492-4499.
206. Machell, G.; Richards, G., 906. The alkaline degradation of polysaccharides. Part II. The alkali-stable residue from the action of sodium hydroxide on cellulose. *Journal of the Chemical Society (Resumed)* **1957**, 4500-4506.
207. De Bruijn, J.; Kieboom, A.; Van Bekkum, H., Alkaline degradation of monosaccharides III. Influence of reaction parameters upon the final product composition. *Recueil des Travaux Chimiques des Pays-Bas* **1986**, 105, (6), 176-183.
208. De Bruijn, J.; Kieboom, A.; Van Bekkum, H., Alkaline degradation of monosaccharides V: Kinetics of the alkaline isomerization and degradation of monosaccharides. *Recueil des Travaux Chimiques des Pays-Bas* **1987**, 106, (2), 35-43.
209. De Bruijn, J.; Kieboom, A.; Van Bekkum, H., Alkaline degradation of monosaccharides Part VII. A mechanistic picture. *Starch-Stärke* **1987**, 39, (1), 23-28.
210. MacLaurin, D. J.; Green, J. W., Carbohydrates in alkaline systems. I. Kinetics of the transformation and degradation of d-glucose, d-fructose, and d-mannose in 1 M sodium hydroxide at 22 C. *Canadian Journal of Chemistry* **1969**, 47, (21), 3947-3955.
211. Rahubadda, A.; Montoya, A.; Haynes, B. S., C5 sugar decomposition products under hot compressed water conditions. *Chemeca 2011: Engineering a Better World: Sydney Hilton Hotel, NSW, Australia, 18-21 September 2011* **2011**, 698.
212. Mainil, R. I.; Paksung, N.; Matsumura, Y., Determination of retro-aldol reaction type for glyceraldehyde under hydrothermal conditions. *The Journal of Supercritical Fluids* **2019**, 143, 370-377.
213. Liang, X.; Rahubadda, A.; Haynes, B. S.; Montoya, A., Kinetic Insights into the Hydrothermal Decomposition of Dihydroxyacetone: A Combined Experimental and Modeling Study. *Industrial & Engineering Chemistry Research* **2015**, 54, (34), 8437-8447.

214. Antal Jr, M. J.; Allen, S. G.; Schulman, D.; Xu, X.; Divilio, R. J., Biomass gasification in supercritical water. *Industrial & Engineering Chemistry Research* **2000**, 39, (11), 4040-4053.
215. Khajavi, S. H.; Kimura, Y.; Oomori, T.; Matsuno, R.; Adachi, S., Degradation kinetics of monosaccharides in subcritical water. *Journal of Food Engineering* **2005**, 68, (3), 309-313.
216. Yoshida, T.; Yanachi, S.; Matsumura, Y., Glucose decomposition in water under supercritical pressure at 448-498 K. *Journal of the Japan Institute of Energy* **2007**, 86, (9), 700-706.
217. Mohd Shafie, Z.; Yu, Y.; Wu, H., Insights into the primary decomposition mechanism of cellobiose under hydrothermal conditions. *Industrial & Engineering Chemistry Research* **2014**, 53, (38), 14607-14616.
218. Park, J. H.; Do Park, S., Kinetics of cellobiose decomposition under subcritical and supercritical water in continuous flow system. *Korean Journal of Chemical Engineering* **2002**, 19, (6), 960-966.
219. Promdej, C.; Matsumura, Y., Temperature effect on hydrothermal decomposition of glucose in sub-and supercritical water. *Industrial & Engineering Chemistry Research* **2011**, 50, (14), 8492-8497.
220. Mochidzuki, K.; Sakoda, A.; Suzuki, M., Measurement of the hydrothermal reaction rate of cellulose using novel liquid-phase thermogravimetry. *Thermochimica Acta* **2000**, 348, (1-2), 69-76.
221. Mochidzuki, K.; Sakoda, A.; Suzuki, M., Liquid-phase thermogravimetric measurement of reaction kinetics of the conversion of biomass wastes in pressurized hot water: a kinetic study. *Advances in Environmental Research* **2003**, 7, (2), 421-428.
222. Knezevic, D.; van Swaaij, W. P. M.; Kersten, S. R., Hydrothermal conversion of biomass: I, glucose conversion in hot compressed water. *Industrial & Engineering Chemistry Research* **2009**, 48, (10), 4731-4743.
223. Qi, J.; Xiuyang, L., Kinetics of non-catalyzed decomposition of glucose in high-temperature liquid water. *Chinese Journal of Chemical Engineering* **2008**, 16, (6), 890-894.
224. Zhuang, X.; Yuan, Z.; Ma, L.; Wu, C.; Xu, M.; Xu, J.; Zhu, S.; Qi, W., Kinetic study of hydrolysis of xylan and agricultural wastes with hot liquid water. *Biotechnology advances* **2009**, 27, (5), 578-582.
225. Lv, X.; Sakoda, A.; Suzuki, M., Decomposition of cellulose by continuous near-critical water reaction. *Chin. J. chem. Eng* **2000**, 8, (4), 321-325.
226. Nazeri, G.; Liaw, S. B.; Yu, Y.; Wu, H., Formation of organic acids during cellobiose decomposition in hot-compressed water. *Fuel* **2018**, 218, 174-178.
227. Sluiter, A.; Hames, B.; Ruiz, R.; Scarlata, C.; Sluiter, J.; Templeton, D.; D., C., Laboratory Analytical Procedure (LAP). In *Determination of Structural Carbohydrates and Lignin in Biomass*, National Renewable Energy Laboratory Golden, Colorado, 2011; Vol. NREL/TP-510-42618.
228. Dionex, MSQ Hardware Manual. 2003.
229. Dionex, MS Application Guide.
230. Perrin, D. D., *Dissociation constants of organic bases in aqueous solution: supplement 1972*. Butterworths: 1972.
231. Ekberg, S.; Ekberg, C.; Albinsson, Y., Characterization of α -isosaccharinic acid: Lactone and carboxylic conformations. *Journal of solution chemistry* **2004**, 33, (5), 465-477.

232. Brown, P. L.; Allard, S.; Ekberg, C., Dissociation constants of α -D-isosaccharinic acid: “composite” and “intrinsic” values. *Journal of Chemical & Engineering Data* **2010**, *55*, (11), 5207-5213.
233. Mamman, A. S.; Lee, J. M.; Kim, Y. C.; Hwang, I. T.; Park, N. J.; Hwang, Y. K.; Chang, J. S.; Hwang, J. S., Furfural: Hemicellulose/xylose-derived biochemical. *Biofuels, Bioproducts and Biorefining* **2008**, *2*, (5), 438-454.
234. Binder, J. B.; Raines, R. T., Simple chemical transformation of lignocellulosic biomass into furans for fuels and chemicals. *Journal of the American Chemical Society* **2009**, *131*, (5), 1979-1985.
235. Karagöz, S.; Bhaskar, T.; Muto, A.; Sakata, Y., Comparative studies of oil compositions produced from sawdust, rice husk, lignin and cellulose by hydrothermal treatment. *Fuel* **2005**, *84*, (7-8), 875-884.
236. Phaiboonsilpa, N.; Yamauchi, K.; Lu, X.; Saka, S., Two-step hydrolysis of Japanese cedar as treated by semi-flow hot-compressed water. *J Wood Sci* **2010**, *56*, (4), 331-338.
237. Goldstein, I. S., *Organic chemicals from biomass*. CRC Press Boca Raton, FL: 1981; Vol. 310.
238. Yu, Y.; Lou, X.; Wu, H., Some Recent Advances in Hydrolysis of Biomass in Hot-Compressed Water and Its Comparisons with Other Hydrolysis Methods†. *Energy & Fuels* **2007**, *22*, (1), 46-60.
239. Gomez, L. D.; Steele-King, C. G.; McQueen-Mason, S. J., Sustainable liquid biofuels from biomass: the writing's on the walls. *New Phytologist* **2008**, *178*, (3), 473-485.
240. Liaw, S. B.; Yu, Y.; Wu, H., Association of inorganic species release with sugar recovery during wood hydrothermal processing. *Fuel* **2016**, *166*, 581-584.
241. Liang, X.; Montoya, A.; Haynes, B. S., Mechanistic Insights and Kinetic Modeling of Cellobiose Decomposition in Hot Compressed Water. *Energy & Fuels* **2017**, *31*, 2203-2216.
242. Yan, L.; Qi, X., Degradation of cellulose to organic acids in its homogeneous alkaline aqueous solution. *ACS Sustainable Chemistry & Engineering* **2014**, *2*, (4), 897-901.
243. Deng, W.; Zhang, Q.; Wang, Y., Catalytic transformations of cellulose and cellulose-derived carbohydrates into organic acids. *Catalysis Today* **2014**, *234*, 31-41.
244. Greenfield, B.; Holtom, G.; Hurdus, M.; O'Kelly, N.; Pilkington, N.; Rosevear, A.; Spindler, M.; Williams, S., The identification and degradation of isosaccharinic acid, a cellulose degradation product. *MRS Online Proceedings Library Archive* **1994**, 353.
245. Pavasars, I.; Hagberg, J.; Borén, H.; Allard, B., Alkaline degradation of cellulose: mechanisms and kinetics. *Journal of Polymers and the Environment* **2003**, *11*, (2), 39-47.
246. Glaus, M. A.; Van Loon, L. R.; Schwyn, B.; Vines, S.; Williams, S. J.; Larsson, P.; Puigdomenech, I., Long-Term Predictions of the Concentration of α -isosaccharinic Acid in Cement Pore Water. *MRS Online Proceedings Library Archive* **2008**, 1107.
247. Glaus, M.; Van Loon, L.; Achatz, S.; Chodura, A.; Fischer, K., Degradation of cellulosic materials under the alkaline conditions of a cementitious repository for low and intermediate level radioactive waste: Part I: Identification of degradation products. *Analytica Chimica Acta* **1999**, *398*, (1), 111-122.

248. Van Loon, L.; Glaus, M.; Laube, A.; Stallone, S., Degradation of cellulosic materials under the alkaline conditions of a cementitious repository for low-and intermediate level radioactive waste. Part III: effect of degradation products on the sorption of radionuclides on feldspar. *Radiochimica Acta* **1999**, 86, (3-4), 183-190.
249. De Bruyn, C. L.; Van Ekenstein, W. A., Action des alcalis sur les sucres, II. Transformation réciproque des uns dans les autres des sucres glucose, fructose et mannose. *Recueil des Travaux Chimiques des Pays-Bas* **1895**, 14, (7), 203-216.
250. Kuster, B. F. M.; Temmink, H. M. G., The influence of pH and weak-acid anions on the dehydration of d-fructose. *Carbohydrate Research* **1977**, 54, (2), 185-191.
251. Yu, Y.; Lou, X.; Wu, H., Some recent advances in hydrolysis of biomass in hot-compressed water and its comparisons with other hydrolysis methods. *synthesis* **2008**, 35, 36.
252. Bobleter, O.; Schwald, W.; Concini, R.; Binder, H., Hydrolysis of cellobiose in dilute sulphuric acid and under hydrothermal conditions. *Journal of Carbohydrate Chemistry* **1986**, 5, (3), 387-399.
253. Ranoux, A.; Djanashvili, K.; Arends, I. W. C. E.; Hanefeld, U., 5-Hydroxymethylfurfural Synthesis from Hexoses Is Autocatalytic. *ACS Catalysis* **2013**, 3, (4), 760-763.
254. Sowden, J. C., The saccharinic acids. *Advances in carbohydrate chemistry* **1957**, 12, 35-79.
255. Bhore, N. A.; Klein, M. T.; Bischoff, K. B., The delplot technique: a new method for reaction pathway analysis. *Industrial & engineering chemistry research* **1990**, 29, (2), 313-316.
256. Flannelly, T.; Lopes, M.; Kupiainen, L.; Dooley, S.; Leahy, J., Non-stoichiometric formation of formic and levulinic acids from the hydrolysis of biomass derived hexose carbohydrates. *RSC advances* **2016**, 6, (7), 5797-5804.
257. Yan, X.; Jin, F.; Tohji, K.; Kishita, A.; Enomoto, H., Hydrothermal conversion of carbohydrate biomass to lactic acid. *AIChE journal* **2010**, 56, (10), 2727-2733.
258. Cantero, D. A.; Álvarez, A.; Bermejo, M. D.; Cocero, M. J., Transformation of glucose into added value compounds in a hydrothermal reaction media. *The Journal of Supercritical Fluids* **2015**, 98, 204-210.
259. Niemelä, K.; Sjöström, E., The conversion of cellulose into carboxylic acids by a drastic alkali treatment. *Biomass* **1986**, 11, (3), 215-221.
260. Machell, G.; Richards, G., 384. Mechanism of saccharinic acid formation. Part I. Competing reactions in the alkaline degradation of 4-O-methyl-D-glucose, maltose, amylose, and cellulose. *Journal of the Chemical Society (Resumed)* **1960**, 1924-1931.
261. Machell, G.; Richards, G., 385. Mechanism of saccharinic acid formation. Part II. The $\alpha\beta$ -dicarbonyl intermediate in formation of D-glucoisaccharinic acid. *Journal of the Chemical Society (Resumed)* **1960**, 1932-1938.
262. Gírio, F. M.; Fonseca, C.; Carvalheiro, F.; Duarte, L. C.; Marques, S.; Bogel-Lukasik, R., Hemicelluloses for fuel ethanol: a review. *Bioresource technology* **2010**, 101, (13), 4775-4800.
263. Wang, S.; Zhou, Y.; Liang, T.; Guo, X., Catalytic pyrolysis of mannose as a model compound of hemicellulose over zeolites. *Biomass and bioenergy* **2013**, 57, 106-112.
264. Jia, S.; He, X.; Xu, Z., Valorization of an underused sugar derived from hemicellulose: efficient synthesis of 5-hydroxymethylfurfural from mannose with

aluminum salt catalyst in dimethyl sulfoxide/water mixed solvent. *RSC advances* **2017**, 7, (62), 39221-39227.

265. Yu, Y.; Song, B.; Long, Y.; Wu, H., Mass Spectrometry Analysis of Sugar and Anhydrosugar Oligomers from Biomass Thermochemical Processing. *Energy & Fuels* **2016**, 30, (10), 8787-8789.


266. Räisänen, U.; Pitkänen, I.; Halttunen, H.; Hurta, M., Formation of the main degradation compounds from arabinose, xylose, mannose and arabinitol during pyrolysis. *Journal of thermal analysis and calorimetry* **2003**, 72, (2), 481-488.


267. Madenoğlu, T. G.; Cengiz, N. Ü.; Sağlam, M.; Yüksel, M.; Ballice, L., Catalytic gasification of mannose for hydrogen production in near-and super-critical water. *The Journal of Supercritical Fluids* **2016**, 107, 153-162.

268. Klein, M. T.; Hou, Z.; Bennett, C., Reaction network elucidation: interpreting Delplots for mixed generation products. *Energy & fuels* **2012**, 26, (1), 52-54.

Appendix 1: Copyright Permission Statements

- A. Part of Chapter 4 reprinted with permission from (Sui Boon Liaw, Gelareh Nazeri, Yun Yu, Hongwei Wu. *Differences in Leaching Characteristics of Mg and Ca from Various Biomass Components of Mallee Tree in Hot-Compressed Water. Energy & Fuels*, 2016, 30 (10), 7851-7857). Copyright (2016) from American Chemical Society

Home Help ▾ Email Support GELAREH NAZERI ▾



Differences in Leaching Characteristics of Mg and Ca from Various Biomass Components of Mallee Tree in Hot-Compressed Water
Author: Sui Boon Liaw, Gelareh Nazeri, Yun Yu, et al
Publication: Energy & Fuels
Publisher: American Chemical Society
Date: Oct 1, 2016
Copyright © 2016, American Chemical Society

PERMISSION/LICENSE IS GRANTED FOR YOUR ORDER AT NO CHARGE

This type of permission/license, instead of the standard Terms and Conditions, is sent to you because no fee is being charged for your order. Please note the following:

- Permission is granted for your request in both print and electronic formats, and translations.
- If figures and/or tables were requested, they may be adapted or used in part.
- Please print this page for your records and send a copy of it to your publisher/graduate school.
- Appropriate credit for the requested material should be given as follows: "Reprinted (adapted) with permission from {COMPLETE REFERENCE CITATION}. Copyright {YEAR} American Chemical Society." Insert appropriate information in place of the capitalized words.
- One-time permission is granted only for the use specified in your RightsLink request. No additional uses are granted (such as derivative works or other editions). For any uses, please submit a new request.

If credit is given to another source for the material you requested from RightsLink, permission must be obtained from that source.

[BACK](#) [CLOSE WINDOW](#)

© 2022 Copyright - All Rights Reserved | [Copyright Clearance Center, Inc.](#) | [Privacy statement](#) | [Terms and Conditions](#)
Comments? We would like to hear from you. E-mail us at customer@copyright.com

B. Chapter 5, reprinted with permission from (Gelareh Nazeri, Sui Boon L, Yun Yu, Hongwei Wu. Formation of Organic acids during cellobiose decomposition in hot-compressed water. *Fuel*, 2018, 218, 174-178). Copyright (2018) from Elsevier



Formation of organic acids during cellobiose decomposition in hot-compressed water

Author: Gelareh Nazeri, Sui Boon Liaw, Yun Yu, Hongwei Wu

Publication: Fuel

Publisher: Elsevier

Date: 15 April 2018

© 2018 Elsevier Ltd. All rights reserved.

Journal Author Rights

Please note that, as the author of this Elsevier article, you retain the right to include it in a thesis or dissertation, provided it is not published commercially. Permission is not required, but please ensure that you reference the journal as the original source. For more information on this and on your other retained rights, please visit: <https://www.elsevier.com/about/our-business/policies/copyright#Author-rights>

BACK

CLOSE WINDOW